UNIVERSIDAD DE SANTIAGO DE COMPOSTELA

FACULTAD DE FARMACIA

Departamento de Farmacia y Tecnología Farmacéutica

"Microencapsulación de nanopartículas de quitosano para la administración pulmonar de macromoléculas terapéuticas"

Ana Margarida Moutinho Grenha

Santiago de Compostela, 2006

Agradecimientos

A veces, parece que el tiempo pasa tan rápido, que tiene la capacidad de hacernos olvidar todo lo que dejamos atrás, pero esto no fue exactamente lo que me sucedió.

Era yo muy jovencita, tendría unos 12 o 13 años, y siempre que venía a Santiago de Compostela (muchas veces lo hacía con motivo de la carrera pedestre organizada por "El Correo Gallego", que tiene lugar en Octubre) pensaba: "Un día, estudiaré aquí". Me fascinaba todo, desde el campus universitario a la ciudad en si misma.

Estábamos todavía en el siglo pasado, que gracioso resulta esto, en el año 1999, cuando por primera vez contacté con la profesora Begoña Seijo para informarme sobre la posibilidad de poder incorporarme en el programa de doctorado del departamento de Tecnología Farmacéutica. Ni me imaginaría que tres años más tarde estaría allí, lista para empezar un camino que cambiaría mi vida, o simplemente haría de ella aquello que yo siempre había soñado. En un contacto posterior, me entristecí cuando me comunicaron que, en general, solo aceptaban alumnos con beca, pero yo no disponía de ella; existía la posibilidad de conseguirla, pero no era segura. Y así, sin poder decirle nada más, le contesté simplemente que pasara lo que pasara, yo podría estar en el departamento hasta terminar la tesis, con financiación o sin ella. Afortunadamente, confió en mí, y por fin pude empezar mi tesis el 4 de noviembre de 2002, bajo la dirección de las profesoras Carmen Remuñán y Begoña Seijo. ¡Como recuerdo ese día! Al llegar, me indicaron una mesa en la que podría trabajar, y empecé a leer artículos sobre el tema al que me dedicaría en cuerpo y alma durante los cuatro años siguientes. ¡Dios mío! Todo me parecía chino y me preguntaba si algún día aquello me sería por fin familiar, si algún día podría entender todo lo que leía. Los días fueron pasando, primero lentamente y después más rápido, hasta que se tornaron meses y años.

Al inicio del segundo año, llegó la mejor noticia que podría haber recibido: ¡por fin me habían concedido una beca!, una beca del Gobierno Portugués. Eso me hizo muy feliz. Además, siempre dije que quería volver cuando terminara, poniendo al servicio de mi País los conocimientos adquiridos.

Ahora que finalizo esta tesis, me gustaría agradecer especialmente a mis dos directoras de tesis, las profesoras Carmen Remuñán y Begoña Seijo, a quienes debo el placer de haber aprendido esta labor, a veces tan ardua, de investigar,

descubrir y no desistir nunca. De corazón os digo que viví aquí una de las experiencias más gratificantes de mi vida, y me alegro mucho de haber tenido, además de dos profesoras, dos amigas con quién pude contar siempre. Por supuesto también quiero agradecer su apoyo constante a los otros profesores del grupo, Maria José Alonso, Dolores Torres, Alejandro Sánchez y José Luis Vila Jato.

También me gustaría agradecer su ayuda, paciencia, comprensión y sabios consejos a lo largo de estos años, a todos los compañeros con los que en algún momento he compartido el laboratorio, estudiantes, doctorandos y doctores. Especial mención merecen Edison, Dayamí y Rafa, que me han ayudado en incontables ocasiones. Edison que me guió en mis primeros pasos con las nanopartículas de quitosano. Dayamí que sin ella mi experiencia con los animales en vez de difícil, habría sido imposible, además de su ayuda constante a lo largo de toda mi tesis. Rafa que me ha enseñado la dinámica del laboratorio y me ha ayudado a trabajar tanto con los animales como con muchos equipos.

De igual forma, quisiera mencionar la ayuda prestada por la gente del servicio de microscopía, Miro, Merche y Raquel, que me han enseñado a trabajar con los distintos microscopios y han contribuido a obtener buenos resultados con sus consejos. También me gustaría agradecer a Carmen Serra, del CACTI de Vigo, por todo su empeño y paciencia en el trabajo de análisis de superficies.

Mi más sincero agradecimiento a los profesores Ben Forbes, Lea Ann Dailey y Gary Martin, del King's College London, por haberme acogido en su laboratorio y haberme brindado su ayuda y buena disposición a lo largo de mi estancia. A Chris Grainger, le agradeceré eternamente su paciencia, amistad y trabajo, que tanto ha contribuido a los buenos resultados obtenidos. Quisiera agradecer igualmente a todos con los que he compartido tantos momentos mientras estuve en Londres, especialmente a Cynthia Bosquillon y Marlise Santos.

Sin lugar a dudas, quiero agradecer profundamente el apoyo de Luis y el de mis padres, sin el cual no tendría el ánimo necesario para emprender este bonito (pero largo) camino.

Por fin, pero no menos importante: gracias Santiago y gracias España, por haberme recibido de una forma tan agradable y sin pedir nada a cambio, y por haberme transmitido una cultura y una forma de ser que hice y haré siempre un poco mías.

Dedicatória

Uma vez que sou uma portuguesa orgulhosa de o ser e que defendi e defendo sempre afincadamente o meu País, pareceu-me legítimo fazer constar desta memória umas poucas linhas nesta bonita língua de Camões.

Poder ter chegado a este momento, não deve ser entendido como o final de um caminho de apenas quatro anos, porque na realidade, o que contribuiu para este trajecto começou muito antes, quando eu era uma jovem em início de formação educacional, profissional e pessoal. Na verdade, em primeiro lugar quero dedicar esta tese aos meus PAIS, Carmen e João, que com o seu empenho e amor incondicional souberam fazer de mim uma jovem responsável, com espírito de sacrifício e, acima de tudo, disposta a ir até ao fim do mundo para conseguir alcançar os seus sonhos. Obrigada pelos vossos conselhos sempre amigos, obrigada por nunca pensarem em vocês senão em nós, obrigada pelo vossa presença constante. Além disso, se não fosse pelo apoio económico inicial que me prestaram, não poderia nunca ter empreendido este projecto.

Também gostaria de dedicar esta memória aos restantes membros da minha família, especialmente ao meu IRMÃO, João Pedro, que apesar da distância não deixou nunca de me dar um apoio constante.

Não poderia deixar de dedicá-la aos meus AVÓS, tanto ao avô Grenha, que já não se encontra entre nós, como à avó Rosa, à avó Lina e ao avô Moutinho, a quem agradeço do fundo do coração a sua preocupação constante e o terem podido entender a diminuição da frequência das minhas visitas.

A todos os meus AMIGOS de Famalicão e do Porto, que nunca deixaram de animar-me e que confiaram no sucesso deste projecto desde o primeiro momento. A ti, Isabel, companheira de tantos sorrisos e lágrimas, que acreditaste em mim mais do que eu própria. Obrigada pela tua cumplicidade e pela amizade sempre sincera.

Por último, mas obviamente no lugar de destaque, dedico esta tese ao LUIS, meu marido, melhor amigo, companheiro e grande amor, que soube entender desde sempre a minha necessidade de perseguir este sonho e soube dar-me o melhor de si mesmo. Sem ti, Amor, sem o teu apoio, sem a tua ilusão, não poderia ter chegado ao fim. Obrigada por tantos momentos vividos e sofridos, ridos e chorados. E como graças a ele ganhei uma segunda família, também a eles dedico esta tese.

MARÍA DEL CARMEN REMUÑÁN LÓPEZ y **BEGOÑA SEIJO REY**, PROFESORAS TITULARES DEL DEPARTAMENTO DE FARMACIA Y TECNOLOGÍA FARMACÉUTICA DE LA UNIVERSIDAD DE SANTIAGO DE COMPOSTELA

CERTIFICAN:

Que la presente memoria titulada **"Microencapsulación de nanopartículas de quitosano para la administración pulmonar de macromoléculas terapéuticas"** ha sido elaborada, bajo su dirección, por la Licenciada en Farmacia **Dña Ana Margarida Moutinho Grenha** en el Departamento de Farmacia y Tecnología Farmacéutica y, hallándose concluida, autorizan su presentación a fin de que pueda ser juzgada por el tribunal correspondiente.

Y para que así conste, expiden y firman al presente certificado en Santiago de Compostela, el 3 de Noviembre de 2006.

Fdo.: Maria del Carmen Remuñán López Fdo.: Begoña Seijo Rey

Resumen

El objetivo de esta tesis doctoral ha sido el diseño de sistemas microparticulares capaces de actuar como vehículos de nanopartículas de quitosano, obtenidas por gelificación iónica, y de complejos de lípidos y nanopartículas de quitosano hacía el pulmón, con el fin de conseguir una absorción pulmonar de la macromolécula terapéutica asociada a las nanopartículas. Para ello, se ha seleccionado como excipiente el manitol y como procedimiento de microencapsulación la técnica de atomización, optimizando las condiciones de este proceso para obtener microsferas con propiedades morfológicas y aerodinámicas adecuadas para su administración por vía pulmonar. Para la preparación de los sistemas complejos de lípidos y nanopartículas de quitosano, se han elegido dos lípidos endógenos del pulmón, la dipalmitoilfosfatidilcolina (DPPC) y el dimiristoilfosfatidilglicerol (DMPG), con carga neutra y negativa, respectivamente, y se ha comprobado que el recubrimiento lipídico de las nanopartículas es más eficaz cuando ambos fosfolípidos están presentes en la formulación. El análisis estructural de las microsferas conteniendo nanopartículas, ha demostrado que éstas se distribuyen uniformemente en la matriz de manitol. Utilizando la insulina y la albúmina bovina marcada con isotiocianato de fluoresceína (FITC-BSA) como modelos, se ha evidenciado el potencial de ambos sistemas para asociar péptidos y proteínas. Además, se ha observado que el proceso de atomización no produce ningún efecto negativo sobre las propiedades de los sistemas encapsulados, ni en el perfil de liberación de la insulina a partir de los mismos. Los estudios realizados con las microsferas conteniendo nanopartículas en dos líneas celulares del epitelio respiratorio (Calu-3 y A549), han demostrado la biocompatibilidad del sistema, evidenciando además fenómenos de mucoadhesión. Por otro lado, estudios preliminares *in vivo* realizados con este mismo sistema, tras la administración intratraqueal a ratas, han demostrado que las microsferas alcanzan el espacio alveolar, siendo más eficaces en la reducción de los niveles de glucosa que la disolución de insulina con una dosis equivalente. En definitiva, el conjunto de los resultados obtenidos en este trabajo experimental pone de manifiesto el interés de estos sistemas como vehículos para la administración pulmonar de péptidos y proteínas terapéuticos.

Índice

Página

Introducción

Artículo 1

NANO AND MICROPARTICULATE CARRIERS FOR PULMONARY DRUG DELIVERY

Ana Grenha, Dayamí Carrión-Recio, Desirée Teijeiro-Osorio, Begoña Seijo, Carmen Remuñán-López*

Dept. of Pharmacy and Pharmaceutical Technology, University of Santiago de Compostela, Faculty of Pharmacy, Campus Sur, 15782 Santiago de Compostela, Spain.

* Corresponding author: Phone: 0034 981 563100 – ext. 15405

Fax: 0034 981 547148

E-mail: ffcarelo@usc.es

Adaptado del capítulo del libro "Handbook of Particulate Drug Delivery" (R. Kumar (Ed.), American Scientific Publishers, en prensa, fecha prevista de publicación: Enero de 2007)

1. INTRODUCTION

Progress made in the field of drug delivery has accelerated enormously over the past two decades in parallel with major discoveries of new low molecular weight active molecules and, primarily, the introduction of the therapeutic products from biotechnology such as proteins and peptides, which pose particular physicochemical and biopharmaceutical challenges. Their usual bioavailability problems presented when administered by the oral route, always the first to consider due to its convenience [1], led to their administration by intravenous injection and to investigations to identify non-invasive alternative mucosal routes, like nasal, buccal and pulmonary routes, among others. Mucosal routes for systemic drug administration present a great advantage in comparison to the parenteral routes, since they are non-invasive. Thus, development of suitable non-injectable delivery systems for mucosal drug administration could significantly enhance patients' compliance, thereby leading to increased therapeutic benefits [2]. However, major barriers limit drug delivery via these unconventional routes, including poor permeability across epithelial barriers, enzymatic degradation at the site of administration, immune reactions at the delivery site and limitations in the available surface area for absorption [3]. Therefore, their application for drug administration and, in the end, the successful exploitation of the new generation of peptides and proteins as therapeutic agents, clearly depends on simultaneous progress in the development of new carriers for specific active molecules. These carriers should allow the molecules to remain stable in their specific biological environment and, ideally, enable them to cross mucosal barriers in order to reach their specific sites of action. Aside from this, the materials and technologies used to prepare these vehicles also seem to be relevant issues, the selection of which depends on the final goal of the administration [4].

Among the mucosal routes, lung drug delivery has attracted remarkable scientific and biomedical interest in recent years for the treatment of systemic diseases, such as diabetes mellitus. In fact, the lung mucosa has proved particularly attractive for systemic administration, given the large alveolar area exposed for drug absorption (approximately 100 m^2), and thin alveolar-vascular epithelium (0.1 – 0.2 μm) that permits rapid absorption, low proteolytic activity

compared to other mucosal routes and the possibility to avoid the first-pass effect [5-7].

The development of an inhaled therapy that is efficacious and safe depends on a well-designed administration device and drug carrier with appropriate particle size and density distribution to ensure optimal dose deposition in the desired region of the lung.

The main purpose of this chapter is to provide an overview of the advances in nano and microparticulate carriers aimed at improving the delivery of drugs, mainly peptides and proteins, to the lung. The most representative carriers are classified according to their particle size (microparticles and nanoparticles) and the nature of the materials used for their obtention. Special emphasis will be placed on the application of the new technologies developed for their preparation. In addition, delivery systems proposed for local and systemic effects as well as those intended for gene delivery will be discussed. *In vivo* and clinical studies, as well as marketed products will also be addressed. Over the last few years, our group has taken on the challenge of designing different types of nano- and microparticles mainly based on the polysaccharide chitosan. We have investigated their aerodynamic properties, their ability to associate peptides and proteins, and their biocompatibility with lung cells. Furthermore, we have administered them to rats and demonstrated their potential as insulin lung carriers. Therefore, the present chapter is also aimed at reviewing the characteristics and potential of these particles as protein carriers for lung delivery.

2. FACTORS AFFECTING DRUG DELIVERY TO THE LUNG

The lung performs complex functions at a metabolic and endocrine level, but also provides structural and immunologic protection against inhaled pathogens, preventing unwanted airborne particles from entering the body. Airway geometry, humidity and other drug clearance mechanisms contribute to this filtration process.

Comprised of a well organized structure, the lung can be divided in two main regions: the tracheobronchial region, from the larynx to the terminal bronchioles; and the alveolar region, comprising the respiratory bronchioles and

alveoli (in a number of 200-600 million). The former region is mainly formed by ciliated and goblet cells and presents *mucous*, which is a complex mixture of proteins, glycoproteins and lipids. This substance, together with the ciliated cells, forms a self-cleaning mechanism known as mucociliary escalator or mucociliary clearance, which consists of propelling the mucous blanket with all the entrapped materials by the coordinated movement of cilia. In contrast, the alveolar region is devoid of mucous and its epithelium is much thinner (0.1-0.5 μm), in order to permit efficacious gas exchange [7-9]. The alveoli include a dense capilar net supported by collagen and elastic fibres, covered by a thin epithelial layer composed of two different cell types: type I pneumocytes and type II pneumocytes [10]. Type I cells represent approximately 95% of the whole alveolar surface and form tight unions between them in order to prevent the passage of extracellular liquid to the alveolar lumen, thus maintaining the cellular structure and functional polarity [11]. Except for certain ions and very small solutes, these tight junctions are impermeable to hydrosoluble molecules. These type I cells are large, flat, and unable to divide. When damaged, they are replaced by type II cells that differentiate into type I cells [12-13]. Type II pneumocytes are small cells interposed between type I cells, with the ability to synthesize and secrete a tensioactive fluid usually referred to as the *pulmonary surfactant*. This substance, which remains stored in the cell inside lamellar bodies, covers the alveolar epithelial cells at the air-tissue interface, forming a 10-20 nm thick layer [2,7,11-12]. This surfactant has the important function of preventing the natural tendency of the lung to collapse and reducing the surface tension in the air-liquid interface. Surfactant is composed of a complex mixture of lipids and proteins, consisting of 80-90% lipids (mainly phosphatidylcholine and phosphatidylglycerol) and 5-10% proteins [10-13]. Being released by exocytosis, its continuous secretion creates a surface gradient that favours the flux from the alveoli to the bronchioles, until reaching the mucociliary escalator, thus playing a role in the elimination of exogenous substances, such as the drug-loaded nano- and microparticles reaching the alveoli [10]. The surfactant is eliminated by phagocytic mechanisms by macrophages, and is recycled by Type-II secretary cells [10-11]. Both types of cells constitute enzymatic and transport barriers to drug delivery

systems that might reach this area, although type I cells present lower proteolytic activity than type II cells [14].

Macrophages are the mononuclear phagocytes of the lung, representing its main defence mechanism. Derived from blood circulating monocytes, they differentiate in alveolar macrophages when they arrive at the lung [10-11]. These cells are not part of the alveolar wall, they form a suspension over the surface, therefore they move freely and by phagocytosis they eliminate the inhaled particles that manage to arrive at the alveolar surface after escaping the mucociliary clearance [10,15]. Macrophages have a size between 15 and 40 μm, contain many lysosomes rich in hydrolytic enzymes (acid phosphatase, glucuronidase and lysozyme), and have a life time of months or even years [10,16]. After phagocytosis, they usually migrate from the alveoli to the bronchial surface, where they integrate into the mucociliary escalator by being transported to the pharynx and swallowed afterwards. Macrophages are continuously eliminated and replaced and it is estimated that approximately 100 millions macrophages migrate to the bronchioles daily. Moreover, it is known that some are not eliminated, instead they migrate to the lymphatics [10-11,13,17].

Independent of the method used to produce the aerosol, before reaching the deep lung inhaled particles must overcome obstacles and lung defence mechanisms, essentially the effect of the airways structure and the mucus layer, which protect the epithelium in the tracheobronchial region. Particles targeted to the deep lung should be small enough to pass through the mouth, throat and conducting airways and reach the deep lung, but not so small that they fail to deposit and are breathed out again. Even so, a certain number of particles will be transported away from the lung by mucociliary clearance [6-7,18-19]. Once in the deep lung, particles will have to face at least two other defence mechanisms: the alveolar macrophages and the enzymatic activity. Therefore, the challenge in developing therapeutic aerosols is to produce an aerosol that eludes the lung's mechanisms of defence.

Table 1 depicts the most relevant advantages and limitations of the pulmonary drug delivery route. From the above mentioned comments and considering referred characteristics such as the provided large surface area, low

thickness of the alveolar epithelium and high vascularization, which could lead to rapid absorption, it is clear that drug administration through this route represents a very promising and alternative opportunity for some new macromolecules, as well as for some other drugs which did not gather good results through other routes. In spite of these advantages of pulmonary systemic administration, many challenges will have to be faced from now on and drugs will only be successfully administered by the pulmonary route when formulations have such properties that enable them to overcome the distinct barriers that oppose to drug absorption such as difficult accessibility, mucociliary clearance and safety concerns.

Table 1. Potential advantages and disadvantages of pulmonary systemic drug administration

Advantages	**Disadvantages**
Non-invasive route	Airway structure acts as a filter
Large alveolar surface area suitable for drug absorption (100 m^2)	Mucociliary clearance
Extensive vascularization	Alveolar macrophages
Low thickness epithelial barrier	Particles can be exhaled
Low proteolytic activity compared to other routes	Absorption affected by pathological conditions
Avoidance of first-pass metabolism and gastrointestinal degradation	Lungs are not readily accessible without design of adequate formulations
Rapid absorption and onset of action	Requires complex devices and particles with specific aerodynamic properties
Reduced systemic side effects	Difficulties associated with handling of inhalation device
Possibility of administering lower doses	Many factors affecting reproducibility

The specific characteristics of the lungs and the inherent issues to access the desired area implicate the achievement of satisfactory formulations into an appropriate aerosol device. Therefore, designing adequate carriers for local or

systemic effects has been a major concern for researchers in this area. This resulted in the appearance of novel liposome and nano- and microparticulate systems, which are gaining popularity due to their specific morphological and aerodynamic properties. In addition, using these recently developed systems, a more sustained release could be achieved, prolonging the therapeutic effect of the administered drugs, thus leading to a reduction of the dosage frequency and to increased patient compliance [5,7,9]. However, the great limitation will be tailoring these systems to reach the desired site of action.

Pulmonary delivery of pharmaceutics can be performed using three different types of devices: nebulizers, pressurized metered dose inhalers (pMDI) and dry powder inhalers (DPI). They all generate an aerosol of particles/droplets and differ in the technology used for aeorosol production. Nebulizers presented a disadvantage by not being portable, a limitation that was overcome by both pMDIs and DPIs, as well as by the recent introduction of new types of compact portable devices. Following the ratification of the Montreal Protocol, the production of clorofluorocarbonates (CFCs) has been banned, except for specific exemptions [20]. This has forced the introduction of non-ozone-depleting substitutes, such as the hydrofluoroalkanes (HFAs), and the reformulation of pMDI delivered formulations to suit the new propellants. In addition, the phasing out of CFCs has encouraged the development of alternative pulmonary drug delivery systems, such as the DPIs. The greatest difference between pMDIs and DPIs is that in the former the drug is dispersed in a liquid propellant under pressure, while the DPIs contain dry powders. Therefore, the latter avoids the stability problems usually presented by suspensions and, additionally, presents the advantage of avoiding the need for coordination between inhalation and device actuation required by the pMDIs. Furthermore, recent advances in MDI technology, such as the use of breath actuated instruments, solved the main limitation related to the DPIs, the necessity of a high inspiration capability, and generated increased interest in these devices [21]. Extensive reviews on inhalation devices are available elsewhere [9,22] and it is recognized that the technology of the aeorosol-producing device plays a very important role in the efficacy of the treatment, since it can influence aerosol distribution in the lung.

The success of inhaled aerosol particles for either a local or systemic effect depends on their aerodynamic properties. Particles intended to provide a local effect should have an aerodynamic diameter (diameter of a spherical particle with unit density that settles at the same rate as the particle in question) adequate to reach the specific site of action, usually the bronchial region (for local respiratory diseases, like asthma or cystic fibrosis, among others). This means that they should be small enough to pass the oropharyngeal region, but not too small that they pass the target region and reach the alveoli. On the contrary, particles aimed at systemic absorption should be small enough to pass through the mouth, throat and conducting airways into the alveoli, but not so small that they fail to deposit and are breathed out again [5-6,23]. Any particle arriving at the lungs will deposit and, depending on its size and density, different deposition mechanisms may occur. Three different mechanisms are known: impact, sedimentation and diffusion. Particles with an aerodynamic diameter higher than 6 μm and travelling with a high speed, will deposit by impact. This mechanism is more prone to occur in the extrathoracic and tracheobronchial area, where particle velocity is usually high. Sedimentation occurs in the smallest airways as well as in the alveolar region and it is particularly significant for particles of approximately 4-6 μm, although it can be observed with particles as small as 0.5 μm. Deposition by diffusion, occurring mainly in the alveolar region, is due to Brownian movements and, therefore, is more significant for particles smaller than 0.5 μm [24-25]. In this manner, it has been reported that particles intended for a local effect should possess an aerodynamic diameter between 5 and 10 μm, while particles intended to reach the deep lung for systemic action should be in the range of 1-5 μm, with the maximum effect achieved for particles of 2-3 μm [7,26]. For a broad review on the factors affecting the pulmonary delivery of drugs, the publications of *Courrier et al.*, *Labiris and Dolovich* and *Taylor and Kellaway* [7,9,27] can be consulted.

3. THERAPEUTIC APPLICATIONS

As it has been previously mentioned, pulmonary drug delivery offers the possibility of both local drug targeting for the treatment of specific respiratory diseases, and systemic absorption of therapeutic molecules and macromolecules. So far, the most common drugs administered by the pulmonary route are anti-

inflammatories and mucolytics intended to treat specific respiratory disorders, such as the asthma, bronchitis, chronic obstructive pulmonary disease, pulmonary emphysema and cystic fibrosis. This restriction was principally due to inefficiency of available inhalation devices which deposited only 10-15% of the emitted dose in the lungs; this is appropriate for local therapies but is not enough for systemic drugs [27].

Table 2 displays some relevant new molecules currently under study for a local effect [28-30]. From these molecules we can rebound macromolecules such as the protein B, the base of the pulmonary surfactant Surfaxin®, and rDNase (Pulmozyme®) which is a unique enzyme marketed for a local pulmonary effect in the treatment of cystic fibrosis. Several other molecules referred to in the table are presently in clinical trials, such as cyclosporin A as an immunosuppressive for lung transplants (submitted for FDA approval), alpha-1-antitrypsin for the treatment of emphysema (phase II), interferon-γ for the treatment of cystic fibrosis (phase II) and interferon-β for the treatement of asthma (phase I), among others.

Table 2. Examples of active molecules currently under investigation for local effect by inhalation

Active molecule	**Therapeutic indication**
Surfactant proteins (approved)	Adult Respiratory Distress Syndrome
rDNase (approved), Interferon- γ	Cystic Fibrosis
Succinyl peptide chloromethylketone, Alpha-1-antitrypsin	Emphysema
Cyclosporin A	Lung transplant
$Alpha_1$ proteinase inhibitor	Alpha-1-antitrypsin deficiency
Interferon-γ, Interleukin-2	Cancer
IL-1R, Anti-IgE Mab, Isoprenaline, Salbutamol sulphate, Albuterol sulphate, Beclometasone, Interferon-β	Asthma
Muramyl dipeptide, Rifampicin, Isoniazid	Antituberculosis vaccine
Catalase, Superoxide dismutase	Oxidative stress

The unique features of the pulmonary route are opening a way towards systemic delivery. Recent advances in aerosol and formulation technologies have led to the development of delivery systems that are more efficient and produce small particle aerosols, allowing higher drug doses to be deposited in the alveolar region of the lungs where they are available for systemic absorption [27]. In fact, there are already a few drugs in the market for systemic delivery through the lungs, as is the case for halothane, an anaesthetic, and ergotamine, available as an inhaler for the treatment of migraines. Furthermore, many peptides and proteins are undergoing clinical investigation for a range of clinical conditions. These include growth factors, hormones, monoclonal antibodies, cytokines and anti-infection agents.

It has been assumed that the lungs represent an ideal site for absorption of therapeutic macromolecules like peptides, proteins, plasmids, DNA and oligonucleotides, among others. The principal limitation presented by the majority of these molecules is their lack of activity when administered orally, a direct consequence of the intense degradation suffered in the gastrointestinal tract, their high molecular weight and hydrophilic character, all contributing to poor permeation across the intestinal epithelium. Consequently, these macromolecules are usually parenterally administered, resulting in inconvenience for the patients and limiting their applications. Recently a great interest has arisen to administer these macromolecules via the lung with the intention of achieving a systemic effect. This interest resides on the already mentioned high permeability of the alveolar epithelium [31] and its low enzymatic activity in comparison with other routes of administration, like oral and nasal routes [14,32].

It has been reported that macromolecules with a molecular weight (Mw) below 40 kDa and a diameter less than 5-6 nm, such as insulin (5.7 kDa, 2.2 nm), rapidly appear in the blood following inhalation into the airways. Macromolecules of Mw and diameter higher than 40 kDa and 5-6 nm, respectively, such as inhaled albumin (68kDa) and α_1-antitrypsin (45-51 kDa) are slowly absorbed over many hours [27]. Although the mechanism of absorption is unknown, it has been hypothesized that macromolecules either pass through cells via absorptive transcytosis (absorptive or receptor mediated), paracellular transport between

junctions or through large transitory pores in the epithelium caused by cell injury or apoptosis [8,33]. Thus, the high bioavailability of macromolecules deposited in the lung are likely due to its enormous surface area, very thin diffusion layer, slow surface clearance and antiprotease defence system [8].

Table 3 shows some of the active molecules currently under investigation for systemic administration via the lung [28-30]. Most of these molecules are peptides and proteins, including insulin which has been exhaustively investigated by many laboratories and is already approved for commercialization in Europe and United States in a formulation from Pfizer, Nektar and Aventis, called *Exubera*®. Furthermore, some of the molecules are currently in clinical trials, including parathyroid hormone which is in phase I for osteoporosis therapy and human growth hormone which is in phase I for the treatment of growth deficiency.

Table 3. Examples of active molecules currently under investigation for systemic effect by inhalation

Active molecule	**Therapeutic indication**
Calcitonin, Parathyroid hormone	Osteoporosis
Human growth hormone	Growth deficiency
Estradiol	Hormone replacement therapy
Interferon-β	Multiple sclerosis
Insulin (approved)	Diabetes
LH-RH analogs	Cancer
Ribavirin, Interferon-α	Viral infections
Gentamicin sulphate	Pneumonia
rhG-CSF	Neutropenia
Erythropoetin	Anemia
Heparin	Anticoagulation
dDAVP (1-diaminocystein-8-D-arginine vasopressin)	Diabetes insipidus

Attention should be paid to the fact that some of the molecules included in both Tables 2 and 3, although already available for pulmonary delivery, are currently under investigation for their incorporation into micro or nanoparticulate carriers, aimed to improve their aerosolization, lung deposition and therapeutic efficacy, as is the case of insulin, salbutamol, beclometasone and gentamicin, among others.

The application of the lung for gene therapy has been gaining interest in the last few years, especially concerning the therapy of specific lung disorders. Therefore, attention has been rising concerning its value for many acute and chronic diseases, including cancer, asthma, cystic fibrosis, alpha-1-antitrypsin deficiency and respiratory distress syndrome, among others. A variety of administration routes and delivery systems, viral and non-viral, have been investigated for this purpose. Administration routes include systemic administration, in which the gene carrier may become trapped in the capillary network of the lung, as well as intratracheal instillation of a gene suspension or even inhalation of aerosolized material carrying the therapeutic gene, either as droplets or dry powders (for further details, see *Hanes et al., 2004*) [25]. However, once in the lung, a gene transfer carrier can encounter highly effective defences that have evolved to protect the airways from particles of all sizes, including allergens, viruses and bacteria [34].

4. DRUG CARRIER SYSTEMS FOR PULMONARY DELIVERY

The therapeutic efficiency of numerous drugs, mainly peptides and proteins, is limited by their lack of specificity towards a given target and, as a result, a major portion of the dose remains unavailable for the intended therapeutic effect, increasing the occurrence of side effects. Therefore, a carrier system designed with a specific size, density or surface properties for drug delivery to the lung can play a key role in increasing the drug therapeutic index by the following mechanisms: (a) improving lung deposition and the amount of protein that reaches the site of action (either extracellular or intracellular) and, as a consequence, decreasing adverse effects due to non-specific drug delivery to non-target tissues; (b) protecting the protein and improving its *in vivo* stability;

and (c) reducing clearance and prolonging the drug residence time at its site of action. Furthermore, it can be employed to provide passive or active targeting. Topical delivery to the airways is itself a (passive) targeting approach for specific lung diseases, whereas active targeting refers more specifically to the use of a homing device like antibodies attached to the carrier to target specific tissues, cells or organelles. The choice of the appropriate carrier depends on several factors, including the nature of the drug to be delivered, the delivery device, the type of disease and site of action, and the nature and safety of the carrier.

Together with the development of new technologies for drug delivery capable of rendering efficacious administration of a selected drug, an investment in the improvement of the materials applied to the design of the systems has become a very important issue. The safety of the adjuvant used to develop lung carriers for protein delivery has to be determined and issues regarding local irritancy and toxicity, long-term accumulation and immunogenicity will all have to be addressed using suitable models [35]. While the safety of some carriers (e.g. conventional liposomes) has been examined [36], many others have not. For example, concerns have been raised about the use of excipients such as absorption enhancers and enzyme inhibitors [37-38].

Several different materials have been utilized in the production of nano and microparticulate carriers, such as polysaccharides, polyester derivatives, acrylates and lipids, among others. Concerning mucosal administration and, specifically, pulmonary delivery, one of the most promising strategies is the incorporation of polymers that prolong the residency time of drug carriers at the absorption sites, thus facilitating an increased uptake of the loaded molecule and resulting in higher absorption [4,39]. Approaches in this sense include the use of polymers that have mucoadhesive properties like cellulose derivatives or polysaccharides such as chitosan, either alone, in combination with a preformed particulate carrier or incorporated in the structure of the carrier itself [39-41].

Moreover, research has been focusing on the development of surface modified carriers, with the aim of improving their targeting properties, preventing the uptake by the mononuclear phagocytic system (MPS) or favoring their interaction with specific epithelial cells, thereby overcoming their biological

barriers [42]. For these purposes, strategies such as the application of wheat germ agglutinin (WGA), which is known to interact with specific WGA-receptors on cell membranes, or the inclusion of lipids in the formulations, which is known to reduce alveolar phagocytic activity [43-44], have been gaining popularity.

The bioavailability of macromolecular drugs by the pulmonary route is still poor when compared to parenteral routes, due to enzymatic degradation and clearance processes [7]. In an attempt to overcome these problems, the use of enzyme inhibitors and absorption enhancers has been punctually proposed in order to improve pulmonary drug absorption. Many reports have been published on the enhancement of pulmonary absorption of peptides and proteins, including reports on the introduction of bile acids, surfactants, phospholipids and enzyme inhibitors [23,45]. Although the addition of absorption enhancers is a promising method to increase the systemic bioavailability of inhaled macromolecules, long-term safety is an important issue that should be extensively examined. Therefore, the major challenge that remains is to find those enhancers that will reversibly increase membrane permeability without causing toxicity during long-term use. Actually, only a few studies have been performed on the local toxicity of these agents following administration and it was recently demonstrated that some of them, although efficient pulmonary absorption enhancers (i.e. *n*-lauryl *β-D*-maltopyranoside, laureth-9 and sodium glycocholate), induce lung damage [37,46], indicating that these substances should be used very cautiously. It is important to notice that the absorption enhancement effect can be dependent on the administered formulation, since some studies report a positive effect of the polymers in solution and an absence of effect when assayed as particulates [47]. An absorption enhancer of particular interest, given the absence of toxicity already demonstrated by several mucosal routes, is the mucoadhesive polymer chitosan. Our group demonstrated its absorption enhancement effect as a solution and in particulate form, in TR146 and Caco-2 cells, representative of buccal and intestinal mucosa, respectively [48-50]. The inclusion of enzyme inhibitors and, more specifically, protease inhibitors in formulations has also been reported. These substances enable the absorption enhancement of proteins and peptides by reducing the proteolytic activity of various enzymes which are responsible for degrading peptides and proteins. The degree of absorption

enhancement will rely on the enzyme to be inhibited. Investigated enzyme inhibitors include bacitracin, trypsin inhibitor, chymostatin, potato carboxypeptidase inhibitor, nafamostat mesilate, phosphoramidon, leupeptin, aprotonin and amastatin, among others [45,51]. For an extensive review on pulmonary absorption enhancers the *Hussain et al.* review can be consulted [45].

It is important to notice that phosphatidylcholine is the only excipient currently approved by the FDA for lung delivery; therefore, there is a long regulatory road ahead before the more sophisticated polymeric and targeted carriers may be used in clinics. This is an extremely important feature to have in consideration for the nano- and microparticulate carriers discussed below. Lactose is also approved as a carrier in dry powder products for pulmonary administration, but it is not intended to enter the lungs, rather its particle size limits deposition to the oropharynx.

In the following sections we will discuss the most representative nano- and microparticulate lung drug carriers. It should be noted that most of them are not yet licensed for use in humans, and many are only in the early stages of development. The limited number of products based on polymeric nano- and microparticles on the market can be justified by two main reasons: the polymers cytotoxicity and the lack of a suitable large-scale production method. Indeed, polymers accepted for use in other forms, such as implants for instance, are not necessarily well-tolerated in the particulate form. Presenting a size in the range of nano- or micrometers, the polymer can be internalized by macrophages, which can lead to cytotoxic effects.

5. MICROPARTICULATE LUNG DRUG DELIVERY CARRIERS

The majority of the inhalation systems currently available use the active drug in a micronised form by itself or together with an excipient like lactose (as was mentioned before, lactose is not inhaled in the case of dry powders, and is acting only as a vehicle to facilitate drug administration) or suspended or dissolved in a liquid propellant (as is the case with pressurized metered dose inhalers).

Recently, research work in this field has focused on the design and formulation of microspheres as an alternative system that can be tailored with the desired morphologic (shape and porosity) and aerodynamic (size and density) characteristics by simply modifying the composition and variables of the production process. The development of a microparticulate system, which enables the whole dose of loaded drug to reach the desired area, thus exhibiting a controlled release profile, will permit a decrease in the number of needed doses to achieve a determined effect, while reducing undesirable side effects and certainly increasing the therapeutic efficacy. In this manner, microspheres have been proposed as carriers for pulmonary administration, using a wide range of naturally occurring or synthetic polymers and materials, since they can offer efficient and controlled delivery, as well as protection of the encapsulated molecules.

Until the mid 90's, particles with a 1 to 3 μm geometric diameter and density around 1 g/cm^3 were thought to be the most suitable for lung delivery, since significant loss due to impact (large particles) and exhalation (small particles) would be avoided [29]. But, unfortunately, this range of size and density were responsible for aggregation and rapid phagocytosis by alveolar macrophages [5,52]. In an attempt to overcome these inconveniences, *Edwards et al.* introduced a new and promising concept based on the design of large porous particles [53]. These particles are lighter and larger than the typical dry powder particles with a mass density of approximately 0.1 g/cm^3 and geometric diameter of > 5 μm. By virtue of their hollow and porous characteristics, they give rise to an aerodynamic diameter which is smaller (< 5 μm) than their geometric diameter and, because of these features, particles can be aerosolized more efficiently (less aggregation) than smaller, nonporous particles, resulting in higher respirable fractions of the formulation. In addition, they can evade alveolar phagocytosis. Since the introduction of this new concept, a significant amount of research has addressed the development of new technologies to produce similar systems, achieving promising results that will be commented on later [54-57]. Interesting approaches in particle engineering technologies, such as hollow and porous microspheres, are the already registered PulmoSpheres™ (*Alliance Pharmaceutical)*, made of phosphatidylcholine, the primary component of human lung surfactant, and

AIR™ Microspheres (*Alkermes*), prepared with PLGA, which were proposed to deliver hIgG and insulin to the lung, respectively [53,58-60]. Technospheres™ (*Pharmaceutical Discovery Corporation*), based on diketopiperazine derivatives, have also been registered as a new drug delivery system for pulmonary administration, which captures and stabilizes peptides in small particles [61-62]. Special mention require the "Trojan" particles, prepared from different materials like polystyrene. Upon spray-drying, they assemble into microparticles with low density (< 0.1 g/cm^3), which are easily aerosolized from a dry powder inhaler and redisperse into nanoparticles once in solution. They are called "Trojan" particles because of their ability to escape both phagocytic and mucociliary clearance within the airways [63].

The fate of microspheres entering the lungs is dependent on the manufactured material and technique, the latter being selected according to the drug and polymer physicochemical properties, and on the delivery device.

An important part of microspheres developed for pulmonary delivery comprises the synthetic polymers polylactic acid (PLA) and polylactic–co-glycolic acid (PLGA) acid (PLGA) [53,64-71]. Other options include the use of natural polymers such as albumin, gelatine, chitosan, dextran, oligosaccharide derivatives or sodium hyaluronate among others [72-77]. Recently, a good deal of work has been presented on microspheres containing lipids, like dipalmitoylphosphatidylcholine (DPPC) [54-56,58,60,78-79], since it was reported that their presence avoids the adsorption of opsonic proteins, thereby reducing macrophagic phagocytosis in the alveoli [43,80]. Additionally, the biocompatibility of some lipids was demonstrated upon pulmonary administration of lipid particles, which did not induce any inflammatory response [81]. Lung-targeted microparticles based on these polymers can be elaborated using techniques such as spray-drying [40,54-56,67-68,74-75,78-79,82-85]; spray-congealing [86]; emulsion solvent evaporation [53,65,67-70,82] or solvent extraction/evaporation [66], supercritical fluid technology [71] and interfacial crosslinking [87]. When encapsulating labile molecules such as peptides/proteins, the effect of solvents, heat, moisture, pH oxygen and mechanical stresses must be assessed. Spray-drying is a very simple technique which consists in spraying a polymer drug

solution, suspension or emulsion into a drying air stream with such a temperature that allows the instantaneous evaporation of the solvent, leading to the formation of dried particulates of variable size [88]. Spray-congealing is a very similar technique, in which the solution, suspension or emulsion is sprayed into a cryogenic medium, such as liquid nitrogen. The frozen material is subsequently lyophilized and microparticles are obtained at the end of this process [89-90]. In the technique of emulsion solvent evaporation, an organic phase containing the drug and the polymer is generally incorporated in another aqueous phase containing a surfactant by means of sonication or homogenization. The solvent diffuses to the external phase and evaporates itself from the surface, leading to precipitation of the polymer, which results in the formation of particles [42]. In the so-called emulsion solvent extraction/evaporation, a solvent which is soluble in the polymer solvent is added to accelerate its evaporation. In the supercritical fluid technology, a solution of the drug material is fed with a stream of supercritical fluids (e.g. CO_2) through a specially designed nozzle under controlled temperature and pressure. The supercritical fluid disperses, mixes with and rapidly extracts the solvent from the drug solution, leading to the formation of particles which are retained in a particle formation vessel. Manipulation of the operating conditions enables accurate control of particle size, shape and morphology, which renders the process particularly attractive for use in pulmonary delivery [91-93]. Later in this section we will present an overview of the most recent studies aimed at developing microparticulate systems for pulmonary drug administration. Table 4 displays a summary of the polymers and materials used to produce the referred microparticulates. Tables 5 and 6, respectively, summarise aspects of the *in vitro* and *in vivo* research works described herein, indicating polymers, methods and major findings of the respective studies.

Table 4. Main excipients used to produce microparticulate lung drug delivery carriers

Synthetic hydrophobic excipients	
Polyester derivatives	Polylactic-co-glycolic acid (PLGA), polylactic acid (PLA), poly-ε-caprolactone (PCL)
Lipids	Egg phosphatidylcholine (EPC), dipalmitoylphosphatidylcholine (DPPC)
Natural hydrophilic excipients	
Proteins	Albumin, gelatin
Cellulose derivatives	Hydroxypropylcellulose (HPC)
Polysaccharides	Chitosan (CS), Hyaluronic acid (HA)
Others	
Sugars	Mannitol, oligosaccharide ester derivatives (OED)

5.1. Microparticles made of synthetic hydrophobic materials

5.1.1. Microparticles of polyester derivatives

Much attention has been given to the biodegradable and biocompatible polymers polylactic acid (PLA) (used in medical applications such as sutures, orthopaedic implants and medical dressings) and polylactic-co-glycolic acid (PLGA) for the production of lung-targeted microparticles, given their recognized safety by the parenteral route, which led to their FDA approval for this application [94]. Nevertheless, despite the knowledge of their safety by the parenteral route, it could not be discarded that the slow rate of PLGA degradation in the lung periphery, possibly due to the small area of contact between the polymer and lung fluid, could induce lung toxicity [95]. Therefore, concerns about this led to the development of some new polymers, derived from PLGA, such as polyvinyl alcohol (PVA) grafted PLGA (PVA-g-PLGA) or this same polymer grafted with diethylamino-propylamine (DEAPA) (DEAPA-PVA-g-PLGA), which are degraded in a shorter time [95-96]. Furthermore, oligolactic acid, an oligomer of lactic acid, has a shorter biological half-live than PLA and, therefore, may be better suited for pulmonary drug delivery [97].

Table 5. Description of *in vitro* studies performed with microparticulate systems developed for lung drug delivery

Main excipient	Associated molecule	Preparation method	Performed studies	Major findings	Ref.
PLA	Beclomethasone	Solvent evaporation	Aerosolization with a DPI, drug release	Particle size: approximately 1 µm, respirable fraction: 42%, sustained drug release during 6 days	[65]
PLA	Isoniazid + Rifampicin	Solvent extraction and evaporation	Cell culture (J774A.1)	Higher macrophage concentration of drug upon cellular incubation with microspheres when compared to free drug	[66]
PLA	THA-INHMS	Supercritical fluids	Drug release Cell culture (NR8383)	Initial burst effect (40%) and sustained release (60%) for 10 days. Higher macrophage concentrations of isoniazid upon incubation with microspheres when compared to free drug	[71]
PLGA	Rifampicin	Solvent evaporation Spray-drying	Drug release	Smaller particle size (VMD < 3 µm), higher encapsulation efficiency (100%) and faster release (77% at 24 h) for particles obtained by spray-drying compared to those prepared by solvent evaporation	[82]
PLGA	Rifampicin	Spray-drying	Drug release	Pulmonary surfactants do not affect rifampicin release, which is pH dependent. Microspheres deliver rifampicin to macrophages rather than in alveolar lining liquid, given the pH influence	[85]
PLGA	Budesonide	Solvent evaporation	Drug release	Particle size: approximately 1 µm, encapsulation efficiency: 70%, controlled drug release (53%) during 3 weeks	[69]
PLGA	Insulin	Solvent evaporation	Aerosolization with a DPI	Large and porous particles with large diameter: > 5 µm, low density: < 0.1 g/cm3, respirable fraction: 50%	[53]
PLGA-PCL (CS)	Rifampicin	Solvent evaporation	Drug release	VMD: approximately 2 µm, encapsulation efficiency: 30-40%, sustained drug release (40-50%) during 21 days	[70]
EPC	Salbutamol	Spray-drying	Aerosolization with a DPI	Very low density (0.02 g/cm^3), respirable fraction: 20 - 60%	[79]

CS: chitosan; **DPI**: dry powder inhaler; **EPC**: egg phosphatidylcholine; **PCL**: poly-ε-caprolactone; **PLA**: polylactic acid; **PLGA**: polylactic-co-glycolic acid; **THA-INHMS**: tetraheptylammonium-isoniazid methanesulfonate; **VMD**: volume median diameter

Table 5 (continuation). Description of *in vitro* studies performed with microparticulate systems developed for lung drug delivery

Main excipient	Associated molecule	Preparation method	Performed studies	Major findings	Ref.
EPC	Cromolyn sodium, albuterol, formoterol	Spray-drying	Aerosolization with a pMDI	Hollow porous particles with VMD: 2-4 µm, tap density: 0.06-0.12 g/cm^3, respirable fraction: 70%. Particles are stable in HFA propellant	[59]
DPPC-albumin	Insulin Albuterol	Spray-drying	Aerosolization with a DPI	MMAD: 2-5 µm, respirable fraction: 50-92%. Albumin is responsible for sponge-like shape of microparticles	[55-56,78]
CS-gelatin	Betamethasone	Spray-drying	Drug release	Particle size: 1-5 µm, low density: < 0.4 g/cm^3, encapsulation efficiency: up to 95%, sustained release for 12 h	[76,117]
OED	Leuprolide	Spray-drying	Drug release Stability	Controlled release dependent on choice of OED or on combination of several OEDs in different ratios. Microparticles are stable for 3 months in 4-40°C and 60-75% relative humidity	[74]

CS: chitosan; **DPI**: dry powder inhaler; **DPPC**: dipalmitoylphosphatidylcholine; **EPC**: egg phosphatidylcholine; **HFA**: hydrofluoroalkane; **OED**: oligosaccharide ester derivatives; **MMAD**: mass mean aerodynamic diameter; **pMDI**: pressurized metered dose inhaler; **VMD**: volume median diameter

Most of the microspheres prepared with these polymers are intended to target antitubercular drugs, such as isoniazid and rifampicin, to lung macrophages which are mainly found in the alveolar space [66,70-71,82,85], although the administration of proteins, such as insulin [53] or corticosteroids like budesonide and beclomethasone has also been proposed [65,69].

Beclomethasone-loaded PLA microspheres prepared by solvent evaporation, evidenced a respirable fraction of 42% and a controlled release of the drug over 6 days [65]. Studies on the effect of PLA microspheres prepared by emulsion solvent extraction/evaporation and supercritical fluids techniques [66,71] containing a combination of these two drugs (to reduce drug resistance) or a prodrug of isoniazid (tetraheptylammonium isoniazid methanesulfonate) in macrophage cell lines (J774A.1 and NR8383) demonstrated a higher macrophagic concentration of the drugs upon incubation of cells with microspheres in comparison to the unformulated drugs [66,71]. Rifampicin-loaded PLGA microspheres were also proposed for the treatment of tuberculosis and prepared using both spray-drying [83,86] and emulsion solvent evaporation [70,82], rendering particles adequate for pulmonary delivery, with mean diameters between 2 and 5 μm. Encapsulation efficiencies were around 100% and drug release was faster (77% at 24 h) for particles obtained by spray-drying in comparison to those obtained by solvent evaporation, which was attributed to a predominant accumulation of the drug near the microspheres surface when they were obtained by spray-drying, which did not occur when the technique of solvent evaporation was used [82]. Moreover, in the study performed by *Tomoda et al.*, rifampicin release was found to be pH dependent, with microspheres delivering the drug in macrophages rather than in alveolar lining fluid [85]. *Pandit et al.* further proposed the formulation of microspheres containing a mixture of PLGA and poly-ε-caprolactone (PCL) and coated by chitosan to encapsulate rifampicin. The presence of chitosan was found to increase drug encapsulation, which reached 40%, and microspheres exhibited a controlled release profile over 21 days [70]. Budesonide was also encapsulated in PLGA microspheres as a tool to reduce the expression of the vascular endothelial growth factor, which plays a key role in the angiogenesis in tumours, including lung cancer. This drug was successfully encapsulated with 70% efficacy

and microspheres were shown to provide a sustained release (53%) over three weeks [69]. Finally, we should mention the work from *Edwards et al.* who, as it was previously indicated, was the first to introduce the concept of large porous particles [53]. These PLGA particles, produced by solvent evaporation, exhibit a large diameter (> 5 μm) and a low density (0.1 g/cm^3) and, hence, aerodynamic properties optimal for deep lung deposition, resulting in respirable fractions as high as 50%.

In addition to their *in vitro* characterization, several *in vivo* studies have been performed with microspheres based on PLA and PLGA, in which they were administered intratracheally or by inhalation to guinea pigs, rats or mice, which were used as animal models. Except for two cases, in which the encapsulated drug was budesonide [69] or insulin [53], all of the studies assay microspheres containing antitubercular drugs, such as rifampicin and isoniazid [66-68,71]. All these works reported a higher efficiency of drugs encapsulated in microspheres compared with the intratracheal or intravascular administration of the unformulated drug, either as an increased drug concentration in macrophages [66,71] or as a reduction in the number of *Mycobacterium tuberculosis* in the lung [67-68]. Furthermore, nebulization has proven to be more efficient than intratracheal insufflation as a means to deliver the drug to the macrophages and, therefore, it more effectively reduces the number of viable microorganisms [68]. From the above mentioned studies, three of them should be pointed out.

Table 6. Description of *in vivo* studies performed with microparticulate systems developed for lung drug delivery

Main excipient	Associated molecule	Preparation method	Animal	Delivery method	Major findings	Ref.
PLA	THA-INHMS	Supercritical fluids	Rat	Intratracheal instillation	Microspheres induce higher isoniazid macrophage levels compared to free drug and reduced blood levels of potential toxic metabolite	[71]
PLA	Isoniazid + Rifampicin	Solvent extraction and evaporation	Rat	Inhalation	Inhalation gives higher intracellular drug concentrations, compared to oral delivery of free drug	[66]
PLGA	Rifampicin	Spray-drying	Guinea pig	Intratracheal insufflation	Intratracheal administration of rifampicin microspheres significantly reduces number of bacteria in the lung, compared to free drug	[67]
PLGA	Rifampicin	Solvent evaporation	Guinea pig	Intratracheal insufflation or nebulization	Microspheres nebulization is more efficient at reducing the number of viable microorganisms compared to insufflation. Microspheres are more efficient compared to free drug	[68]
PLGA	Budesonide	Solvent evaporation	Mouse	Intratracheal instillation	Intratracheal administration of microspheres provides higher lung drug levels after 1 week relative to intramuscular administration	[69]
PLGA	Insulin	Solvent evaporation	Rat	Intratracheal powder aerosol ventilation	Large porous microspheres induce low glucose levels (30% of initial value) for 96 h. Insulin bioavailability is 88% relative to sc, whereas nonporous particles yield 12% bioavailability	[53]
DPPC-albumin	Insulin	Spray-drying	Rat	Intratracheal powder aerosol ventilation	Microspheres induce sustained insulin plasma levels for 12 h (similar to subcutaneous administration) and bioavailability of 81% relative to subcutaneous administration	[55]
DPPC-albumin	Albuterol	Spray-drying	Guinea pig	Intratracheal powder aerosol ventilation	Large porous microspheres provide an albuterol effect for 15 h, compared to a 5 h effect achieved with small nonporous particles	[54]
DPPC	Parathyroid hormone (1-34)	Spray-drying	Rat	Intratracheal powder aerosol insufflation	Intratracheal administration of parathyroid hormone microspheres gives 34% absolute bioavailability compared to 18% achieved with subcutaneous administration of free drug. Administration with insufflator achieved better results than with ventilator	[84,98]

DPPC: dipalmitoylphosphatidylcholine; **PLA**: polylactic acid; **PLGA**: polylactic-co-glycolic acid; **THA-INHMS**: Tetraheptylammonium-isoniazid methanesulfonate

Table 6 (continuation). Description of *in vivo* studies performed with microparticulate systems developed for lung drug delivery

Main excipient	Associated molecule	Preparation method	Animal	Delivery method	Major findings	Ref.
EPC	IgG	Spray-drying	Rat	Intratracheal instillation	Microspheres instillation resulted in 27% relative bioavailability compared to intravenous administration of free drug and generated high titers of specific IgG antibodies in serum	[57]
HPC	Fluorescein	Spray-drying	Guinea pig	Intratracheal powder aerosol ventilation	Microspheres enhance fluorescein bioavailability 2-fold as compared to fluorescein control solution	[40]
HPC	Beclometasone	Spray-drying	Asthmatic Guinea pig	Intratracheal powder aerosol ventilation	Microspheres induce prolonged drug retention in the lung compared to free drug	[83]
HA	Insulin	Spray-drying	Beagle dog	Intratracheal powder aerosol insufflation	Microspheres extended insulin mean residence time (MRT) and terminal half-life compared to spray dried pure insulin. Zn^{2+} and HPC improved MRT (7-9 fold), AUC/dose (2.5-5 fold) and T_{max} (3 fold)	[75]
OED	Leuprolide	Spray-drying	Rat	Intratracheal powder aerosol insufflation	Leuprolide was detected in plasma up to 25h post-administration, compared to the 150 min. provided by i.v. administration	[74]
Mannitol	Insulin	Spray-drying	Rat	Intratracheal powder aerosol insufflation	Microspheres induced stronger hypoglycemic response (15% decrease of glucose level) compared to intratracheal insulin solution (5% decrease of glucose level).	[120]

AUC: area under the curve; **EPC**: egg phosphatidylcholine; **HA**: hyaluronic acid; **HPC**: hydroxypropylcellulose; **IgG**: Immunoglobulin G; **OED**: oligosaccharide ester derivatives

Among the works performed with polyester-based microspheres containing antitubercular drugs, the study described by *Zhou et al.* using a prodrug of isoniazid (THA-INHMS, tetraheptylammonium-isoniazid) reports the most significant results. In this study, microparticles prepared using the supercritical fluids technology were evaluated for their potential in targeting the ionisable prodrug of isoniazid THA-INHMS. The charged prodrug was ion-paired with two different hydrophobic cations (terapentylammonium and tetraheptylammonium bromide) and loaded separately into PLA microparticles. A high level of isoniazid was detected in a rat alveolar macrophage cell line (NR8383) following exposure of these cells to drug-loaded microparticles. To confirm that microparticles can target alveolar macrophages *in vivo,* the INH levels in lavaged bronchoalveolar macrophages were compared after the rats were administered INHMS in PLA microparticles by intratracheal instillation. Indeed, as shown in Figure 1, delivering a solution of isoniazid intratracheally led to a peak of the drug in the macrophages at 30 minutes, corresponding to approximately 140 ng/mL, after which the drug was no longer detected. On the contrary, when PLA microspheres containing the prodrug were intratracheally administered, the first peak in the macrophages was detected after approximately 1 h and remained above 2800 ng/mL for 48 h [71].

Insulin-loaded porous PLGA microspheres enabled increased systemic absorption of the peptide, inducing low glucose levels (30% of initial value) for as long as 96 h upon intratracheal administration with a ventilator, which was not observed for small nonporous microspheres. Moreover, for large porous particles, insulin bioavailability was 88% relative to subcutaneous injection, whereas small nonporous particles yielded 12% bioavailability [53].

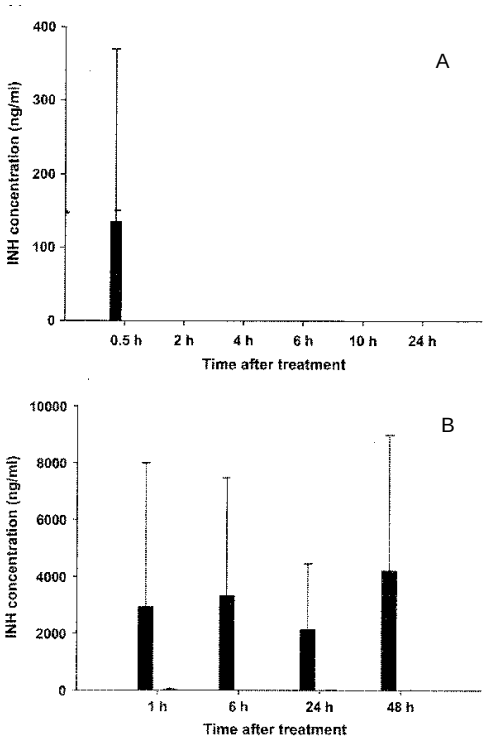

Fig. 1. Concentration of INH in rat plasma and bronchiolavaged AMs after (A) IT instillation of INH solution and (B) IT instillation of THA-INHMS-loaded PLA microparticles. Data are means ± S.D. (n=3, time-dependent concentration of INH in rat plasma in panel A was below the limit of quantification of the LC-MS/MS assay) (Reprinted with permission from Ref. H. Zhou et al., J. Cont. Release, 107, 288, 2005, Copyright Elsevier Science).

The work from *Bandi et al.* should also be mentioned in detail because it is the only report of the application of polyester-based microparticles in the field of lung cancer. The purpose of this study was to determine whether intratracheally instilled polymeric budesonide PLGA microparticles could sustain lung budesonide levels for one week and inhibit early biochemical changes associated with benzo(a)pyrene feeding in a mouse model for lung tumours. Microparticles of budesonide-PLGA, prepared using a solvent evaporation technique, were intratracheally administered to benzo(a)pyrene fed mice, and the results from intratracheal administration were compared to those obtained by intramuscular administration at one week post-administration by comparing drug levels in the lung tissue and bronchoalveolar lavage. Budesonide-PLGA microparticles (1-2 μm,

budesonide loading efficiency of 69-94%) sustained *in vitro* budesonide release for over 21 days and resulted in higher budesonide levels in the bronchoalveolar lavage and lung tissue compared with the intramuscular route. They reduced malondialdehyde accumulation, glutathione depletion, vascular leakage and endothelial growth factor and c-myc expression in benzo(a)pyrene-fed mice, indicating the potential of locally delivered sustained-release particles to inhibit angiogenic factors in lung cancer. In fact, as seen in Table 7, intratracheal administration of microparticles led to much higher budesonide levels in both lung tissue and bronchoalveolar lavage [appr. 225 ng.(mg tissue)$^{-1}$.(mg dose)$^{-1}$ and 61 ng.mL^{-1}, respectively], when comparing to intramuscular administration of microparticles [appr. 16 ng.(mg tissue)$^{-1}$.(mg dose)$^{-1}$, and 23 ng.mL^{-1}, respectively]. A suspension of the drug was further administered by the intramuscular route, resulting in drug levels lower than any of those reported by the microparticles, which is consistent with the capability of the microparticles to sustain drug release, as mentioned before when describing the *in vitro* studies [69].

Table 7. Budesonide levels in the lung tissue and BAL following single dose administration of budesonide-PLGA 50:50 (intrinsic viscosity: 0.17 dL.g^{-1}) microparticles or budesonide suspension to bezo(a)pyrene mice. Drug levels were quantified at the end of one week following drug administration (*Reprinted with permission from Ref. N. Bandi et al., J. Pharm. Pharmacol., 57, 851, 2005, Copyright Ingenta*)

Drug levels	**Intramuscular suspension**	**Intramuscular microparticles**	**Intratracheal microparticles**
Lung tissue ng (mg tissue)$^{-1}$(mg dose)$^{-1}$)	6.14 ± 0.94	15.76 ± 4.30	224.93 ± 21.65*
Bronchoalveolar lavage (ng.mL^{-1})	n.d.	22.91 ± 20.15	60.65 ± 20.85*

Budesonide was administered at a dose of 150, 500, and 500 µg for intratracheal microparticle, intramuscular suspension, and intramuscular microparticle groups, respectively. *$P < 0.05$, significance between intratracheal and intramuscular groups. Data are expressed as mean ± s.d. for n=5 for lung tissue, n=3 for bronchoalveolar lavage with intramuscular suspension, n=4 for bronchoalveolar lavage with intratracheal and intramuscular microparticles. n.d. indicates drug levels were below detection limits in the intramuscular suspension group.

As was previously shown, *Zhou et al.* showed that PLA microparticles were able to target alveolar macrophages *in vivo*. Concerning toxicity, it is known that isoniazid induces liver toxicity, which is caused by acetylhydrazine that is formed by hydrolysis of acetylisoniazid, the major metabolite of isoniazid. In this respect, *Zhou et al.* reported that the pulmonary administration of isoniazid-loaded PLA microspheres bypassed hepatic first-pass metabolism, reducing the blood levels of acetylisoniazid [71].

5.1.2. Lipidic microparticles

The incorporation of lipids in particulate formulations has been gaining popularity since it has been reported that addition of extra lipids enhance airway permeability due to transient alterations to local lipids concentration and/or surfactant organization, although the mechanism of this process is not known so far [98]. Moreover, enhanced drug absorption induced by the lipids was also reported. The mechanism of absorption enhancement was attributed to the presence of surfactant on the alveolar surface and the addition of extra phospholipids hastened the surfactant recycling process, leading to increased uptake of the protein into the systemic circulation [45,99-100]. Furthermore, the presence of lipids was already described to reduce phagocytic uptake upon interaction of microparticles with alveolar macrophages in culture [43], as previously mentioned.

As previously mentioned in this chapter, since aggregation lowers the respirable fraction of an inhalation aerosol, an active goal of the pharmaceutical industry has been the design of dry powders engineered as large and porous particles which have recently been demonstrated to be a promising approach to increase deposition, as well as to obtain sustained release of the carried drug in the alveoli [5,53]. Large (> 5 μm) and porous (< 0.4 g/cm^3) aerosol particles yielding aerodynamic diameters (1-5 μm) suitable for deep lung deposition can be successfully inspired into the lungs. These powders can be prepared using combinations of generally recognized as safe (GRAS) excipients and, particularly, applying soluble excipients approved for inhalation such as lactose, as well as materials that are endogenous to the lungs, like phospholipids, i.e.

dipalmitoylphosphatidylcholine (DPPC). The production of particulates containing these last referred materials, mostly achieving large porous particles, will be addressed. In all cases, the preparation procedure was a previously described spray-drying technique, and efforts were focused on exploring the dependence of the dry powders physical characteristics, i.e. particle size, tap density and morphology, on the formulation and spray-drying parameters [54-56,78-79,84].

Steckel and Brandes proposed the production of low density drug particles using a modified spray-drying technique which consists of spray-drying an oil-in-water emulsion, leading to particles with a network-like morphology and irregular shape. The oil-in-water emulsion consisting of an aqueous phase containing the dissolved model drug (salbutamol sulphate), suitable surfactants such as poloxamer or phosphatidylcholine**,** an optional bulking agent like lactose or cyclodextrin derivative, and a lipid-phase that is essentially a liquefied propellant, was spray-dried from a pressurized canister. The main excipient utilized for the particle formation is hydrated egg phosphatidylcholine which is endogenous to the lung. Through this process, particles of very low density (0.02 g/cm^3) and a drug load of 40% were obtained. These particles exhibited a porous to hollow structure and irregular shape depending on the composition of the aqueous phase [79]. The particles' properties resulted in good powder flowability, making the powders ideally suited for use in carrier-free dry powder inhalers.

Vanbever et al. widely exploited another approach, demonstrating that the powder composition and solution properties greatly affected particle characteristics. In particular, they verified the important role of lipid content in the formation of large and porous particles. They prepared dry powders of water-soluble excipients (e.g. lactose, albumin) combined with water-insoluble material (e.g. lung surfactant) using a standard single-step spray-drying process, and found that by properly choosing excipient concentration and varying the spray-drying parameters, a high degree of control was achieved over the physical properties of the produced microspheres. Mean geometric diameters ranged between 3 and 15 μm and tap densities between 0.04 and 0.6 g/cm^3. It was further observed that the particle size was maximized (8 μm) and density reached the minimum value (0.1 g/cm^3), therefore obtaining ideal particles, when particles

contained 60% DPPC. Particles possessing high porosity and large size, with theoretical estimates of mean aerodynamic diameter between 1-3 μm, exhibited emitted doses as high as 96% and respirable fractions ranging up to 49% or 92% depending on the measurement technique. The incorporation of albumin was also reported, and it seems that it is responsible for the sponge-like shape of the particles, suggesting that the combination of these two excipients in the powder formulation facilitates the formation of porous particles and/or induces long particle life [56]. Moreover, this combination of albumin/DPPC could be an optimal candidate to be part of an inhalation system, as both excipients are present in abundant concentration in the lungs [101], so their use in aerosols should not lead to significant accumulation of these endogenous materials in the lung following chronic daily administration. Additionally, *Bosquillon and co-workers* studied the influence of the powder composition and spray-drying parameters on aerosolization properties, measured in terms of the respirable fraction of the emitted dose. Between all the tested compositions, the albumin/lactose/DPPC (30/10/60) powder demonstrated particularly efficient aerosolization performance, reaching respirable fraction values as high as 50% using a first-generation inhaler device [78]. Following this exhaustive characterization, these dry powders were evaluated to determine their capacity to provide sustained insulin plasma levels. After verifying the integrity of insulin in dried particles *in vitro*, it was demonstrated that inhaled powders provide sustained plasma levels with a similar pharmacokinetic profile and bioavailability to those of the subcutaneous injected form, the bioavailability being 49% relative to subcutaneous (sc) injection of the soluble form of insulin and 81% relative to sc injection of the same formulation used for inhalation [55].

A similar dry powder, except in this case it included albuterol (β_2-specific-adrenergic amine and short-acting bronchodilator agonist) as active drug, demonstrated the ability to produce sustained local protection from carbachol-induced bronchoconstriction for at least 15 hours, whereas inhalation of small nonporous albuterol particles protected against bronchoconstriction for up 5 hours. The change in airway resistance in response to the carbachol challenge was almost identical at the three doses (10, 100 and 200 μg) of inhaled albuterol, corresponding to a significant inhibition (50-60%) of carbachol-induced

bronchoconstriction. These results indicate that a dose as low as 10 μg of albuterol encapsulated in the inhaled large porous particles offered statistically significant protection of animal airways from the carbachol challenge for at least 15 hours. While it was difficult to specify the contribution of the "deep-lung" fraction of deposited particles to bronchodilation (given that β-receptors are widespread in the respiratory tract), it is possible that the long-lasting protection from bronchoconstriction by the inhaled porous albuterol particles is at least partially due to the more slowly cleared deep-lung particles since the large particle size enables escape from phagocytosis. The absence of substantial side effects was verified over a period of 24 hours by evaluating cardio-respiratory parameters as well as pulmonary inflammation. An important finding of this study is that sustained release of a hydrophilic substance (albuterol) can be achieved from large and porous particles, by combining the drug with a high percentage of DPPC, which is an endogenous lung excipient and remains insoluble in water for long periods of time. As a whole, these results pointed out that inhalation of porous albuterol dry powder might be clinically beneficial to patients with chronic asthma and other lung diseases by effectively preventing bronchoconstriction for long periods of time, diminishing the frequency of drug use, and minimizing side effects [54].

Another practical application of these particles, in which DPPC content was shown to be crucial to guarantee the above mentioned characteristics, is their application to systemically deliver parathyroid hormone (PTH, 1-34) (an endogenous polypeptide of 84 amino acids that is synthesized in the chief cells of the parathyroid glands and regulates calcium homeostasis and bone turnover) after intratracheal administration in rats.

Initially, the absolute PTH bioavailability was 21% for the powder form of PTH/albumin/lactose/DPPC and 18% after subcutaneous injection in rats. The powder had an average particle diameter between 3.9 and 5.9 μm, a tap density of 0.06 g/cm^3, an MMAD (mass mean aerodynamic diameter) between 3.9 and 5.9 μm and reached up to 98% emitted dose and up to 61% fine particle fraction in the multi-stage liquid impinger using a Spinhaler® inhaler device. After checking the binding of PTH to albumin (78%), the withdrawl of the latter from the powder

led to increased absolute bioavailability after inhalation from 21 to 34%, compared to 18% of PTH sc injection in the absence of albumin. No acute inflammation appeared in the lung up to 48h after a single inhalation. According to the authors, the main novelty of this study consisted of the demonstration of unexpected physical interactions between the drug and excipients that caused a significant decrease in systemic absorption [85]. Subsequently, the same research group tried to optimize the absorption of PTH in the lung by determining factors favouring its transport from the air spaces into the bloodstream. For this purpose, they simultaneously conducted pharmacokinetic and regional lung deposition studies *in vivo* in rats, following intratracheal administration of PTH in solution or the dry powder form, the powder being administered using a ventilator and an insufflator. Inhalation of the PTH powder using the insufflator resulted in high systemic bioavailability, despite deposition of most of the formulation in the upper airways. In this study, it was demonstrated that the increased absorption was related to the DPPC content, which revealed permeation enhancer properties even though it was abundantly present locally in pulmonary surfactant [98].

Finally, a new formulation technology of engineered lipid-based drug-loaded hollow porous microspheres (PulmoSpheres™) produced by spray-drying should be mentioned since their main excipient was also a phosphatidylcholine derivative. They are prepared in a two-step process. In the first step, an oil-in-water emulsion is prepared using oils, such as perflubron or perfluoroctyl ethane [58], which serve as the "blowing agent" during the spray-drying second step, retarding shrinkage of droplets while simultaneously creating pores in the particle surface. These particles, encapsulating cromolyn sodium, albuterol sulphate and formoterol fumarate, have been shown to stabilize drug suspensions in hydrofluoralkane propellants with improved physical stability and aerosolization efficiency. They are lighter and larger than the typical dry powder particles, displaying a mass density of approximately 0.4 $g.cm^3$ and geometric diameter of > 5 μm, exhibiting hollow and porous characteristics. Accordingly, these particles can be more efficiently aerosolized than smaller nonporous particles, leading to higher respirable fractions of the formulation. The hollow porous morphology of the particle allows the propellant to permeate freely within the particles, creating a novel form of suspension termed a homodispersion™, wherein the dispersed

and continuous phases are identical, and are separated by an insoluble, interfacial layer of drug and excipient. Homodispersion formation improves suspension stability by minimizing the difference in density between the particles and the medium, and by reducing attractive forces between particles; thus leading to improved dose uniformity. Excellent aerosolization efficiencies are also observed with fine particle fractions of about 70%. When IgG-loaded microparticles were intratracheally administered to rats, 27% relative bioavailability of IgG was achieved compared to intravenous administration of free drug and high titers of specific IgG antibodies were detected in serum. In conclusion, the production of particles with such characteristics provide a new formulation technology for stabilizing suspensions of drugs in hydrofluoroalkane propellants with improved content uniformity and aerosolization efficiency [58-59]. Moreover, they serve as a platform to deliver a wide variety of compounds including peptides, proteins, vaccines and, in particular, immunoglobulins to the respiratory mucosa [58,60,102].

Large and porous particles are currently one of the most promising approaches in the field of pulmonary delivery. The possibility of particles endowment with a large geometric size enables avoidance or delay of macrophagic capture, given the knowledge that phagocytosis is maximized for particles with size in the range of 1 - 2 μm [15,103]. On the other side, their low density renders them aerodynamic diameters which are adequate for lung delivery, thus making these particles the objective of many research groups worldwide.

5.2. Microparticles made of natural hydrophilic mucoadhesive materials

5.2.1. Cellulose-based microparticles

Hydroxypropylcellulose (HPC) is a water soluble and mucoadhesive polymer with a long tradition in several pharmaceutical formulations as a mucoadhesive and/or sustained release excipient, for example it has been used in nasal administration to decrease the mucociliary clearance rate in the nasal cavity [104]. The application of such HPC powder systems was extended to inhalation formulations by preparing by spray-drying microspheres, incorporating a poorly soluble drug model drug, fluorescein (acid form, aqueous solubility 13.5 μg/mL),

and a variety of HPC polymers in different fluorescein-HPC ratios. The drug was incorporated in the microspheres in either the crystalline or amorphous form and, therefore, in addition to mucoadhesion, the microspheres potentially provide sustained-release or enhanced-dissolution characteristics.

Respirable-sized HPC microparticles were produced from a variety of HPC grades using a spray-drying technique. These particles, encapsulating either crystalline or amorphous fluorescein or beclometasone, displayed aerodynamic diameters (MMAD) between 1 and 3 μm and, hence, were adequate for pulmonary delivery. They were assayed *in vivo* in guinea pigs by intratracheal administration of powder aerosols. The results indicated that the pulmonary absorption of poorly soluble fluorescein was enhanced when formulating the molecule in HPC microspheres. The spray-drying of ethanol solutions, dissolving both fluorescein and HPC, altered fluorescein´s crystallinity in the amorphous form, which enhanced dissolution when compared to the crystalline counterpart. More importantly, these microspheres were successful in retarding mucociliary clearance when highly viscous HPCs were employed. Consequently, amorphous fluorescein-HPC high viscosity microspheres showed rapid absorption with T_{max} = 0 min and, hence, achieved 88% bioavailability, a value 1.9-fold higher that that obtained for the crystalline compound (control 45.6%). This was only achieved by virtue of both increased dissolution of amorphous fluorescein and the retarded mucociliary clearance in the lung. The formulation may be successful in reducing the therapeutic dose of poorly soluble inhalation drugs such as beclometasone and, thus reducing the risks of undesired side-effects associated with extra-lung and/or systemic absorption of the drug. When the appropriate HPC polymer was selected, microspheres achieved a bioavailability of 88% (relative to intravenous profile) relative to 46% of unformulated fluorescein, an effect that was attributed to the HPC mucoadhesive properties [40]. On the other hand, inhaled HPC microspheres encapsulating beclometasone dipropionate had the potential of prolonging the drug therapeutic effect by prolonging the inhibition of eosinophil infiltration into the airways of asthmatic guinea pigs for up to 24 h, compared to 6 h with the unformulated drug. Furthermore, increasing the drug dose was not necessary for this benefit, thereby reducing the risks of undesired side effects associated with extra-lung and/or systemic absorption of the drug [83].

5.2.2. Polysaccharide microparticles

Chitosan (CS) is a polysaccharide with well-documented favorable biological properties such as biocompatibility, low toxicity and biodegradability [105-106]. Furthermore, it is mucoadhesive [108] (its mucoadhesive properties are mediated by an electrostatic interaction between the positively charged CS amino groups and the negatively charged sialic acid residues of the mucus) and has the capability of promoting macromolecule permeation through well organized epithelia (nasal, intestinal, ocular, buccal, pulmonary) [48,108-113]. Obtained from the deacetylation of chitin, CS is formed from D-glucosamine and N-acetylglucosamine units [114], whose β-(1-4) glycosidic bonds between glucosamine units can be destroyed, namely by pulmonary lysozyme [116]. Based on these excellent properties, our group has been investigating the use of CS to develop mucoadhesive delivery systems specifically adapted for administration of drugs and therapeutic macromolecules by the different mucosal routes. CS has been proposed elsewhere to be a polymeric component of pulmonary drug delivery systems [72,76-77,116]. At present, we are evaluating CS nano- and microparticles as potential protein lung carriers. In this section we will comment on our work on CS microparticles.

Microspheres are produced by spray drying polymer solutions or dispersions of different types (salts, molecular weights, deacetylation degrees) of CS alone or with extra ingredients like the polysaccharide glucomannan (GM). Furthermore, CS microspheres are prepared by a double emulsion/solvent evaporation method, which consists of adding a certain volume of an organic solvent in a CS aqueous solution by sonication to form the first simple emulsion, O_1/W, which was then added to cottonseed oil containing surfactant, obtaining the $O_1/W/O_2$ emulsion. Thereafter, the system was stirred to allow the inner phase solvent to diffuse and evaporate from the CS phase, leading to polymer precipitation. The preparation procedures are being conveniently adapted to obtain particles with different morphological characteristics and adequate aerodynamic properties to reach and deposit in the alveolar region where the protein is intended to be delivered and absorbed. Our hypothesis was that once in the absorption site, CS would improve pulmonary protein absorption by

interacting with the epithelial cells as had been previously reported for CS nanoparticles [110,113]. Results show that the morphology and surface appearance of the CS microspheres (see Figures 2 and 3), as well as their densities and aerodynamic diameters, are highly dependent on their composition (presence of glucomannan), CS deacetylation degree, preparation method and, for microspheres obtained from an emulsion, the type of inner organic solvent (Table 8). Microspheres prepared by spray drying a CS solution were spherical and had a small size of around 2.2 μm.

Table 8. Densities and aerodynamic diameters of chitosan microspheres obtained by spray-drying and double emulsification ($O_1/W/O_2$) / evaporation techniques (n=3)

Preparation method	Polymer	Feret´s diameter (μm)	ρ_r (g/cm^3)	ρ_a (g/cm^3)	D_{aer} (μm)
Spray-drying	CS (DD > 80%)	2.04 ± 0.93	1.48 ± 0.09	0.48 ± 0.01	1.96 ± 1.53
Spray-drying	CS (DD = 23%)	1.79 ± 1.16	1.36 ± 0.04	0.38 ± 0.03	1.46 ± 1.45
Spray-drying	CS:GM (25:75) CS (DD >80%)	2.69 ± 1.1	1.20 ± 0.08	0.30 ± 0.02	1.64 ± 1.46
Spray-drying[1]	CS:GM (25:75) CS (DD >80%)	2.20 ± 1.08	1.42 ± 0.03	0.23 ± 0.02	1.07 ± 1.35
Emulsion ($O_1/W/O_2$) solvent evaporation[2]	CS (DD >80%)	2.64 ± 1.10	1.46 ± 0.03	0.50 ± 0.01	3.52 ± 1.77

ρ_r: real density; **ρ_a**: apparent density; **d_{aer}** mean count (number) aerodynamic diameter determined using an Aerosiser® analyzer and real density values; **Feret´s diameter** was determined by optical microscopy; **CS**: chitosan; **GM**: glucomanann; **DD**=: deacetylation degree

[1] the spray-dried polymer dispersion has a concentration of 0.1% w/w; [2]dicloromethane was used as inner phase organic solvent.

It is very noteworthy that there was an evolution from the spherical shape of CS microspheres prepared using CS with a deacetylation degree (DD) of 83% to the very characteristic convoluted surface corresponding to the most reacetylated CS (DD = 23%) particles and to those containing glucomannan in their composition. Their tap densities were as low as 0.23 ± 0.02 g/cm^3 and their

aerodynamic diameters were less than 5 μm, thus demonstrating the adequacy of these small microspheres to be delivered to the deep lung. Furthermore, the modification of these properties may have a significant impact on the agglomeration properties of the dispersed particles. Microspheres obtained by emulsion solvent evaporation had a geometric particle size of appr. 3 μm, apparent density of 0.5 g/cm^3 and aerodynamic diameter of less than 5 μm, thus being suitable for pulmonary drug delivery.

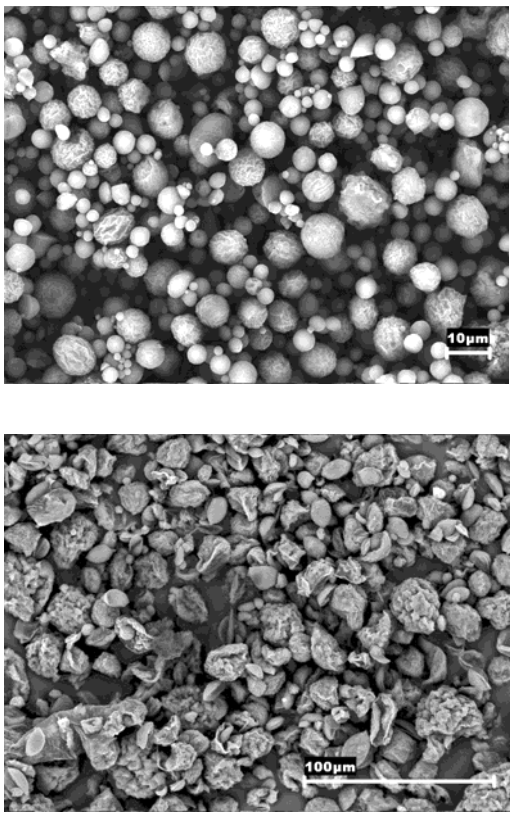

Fig. 2. SEM microphotographs of CS microspheres produced by emulsification/solvent evaporation-method using (a) dichloromethane and (b) ethylene acetate as inner oil phase.

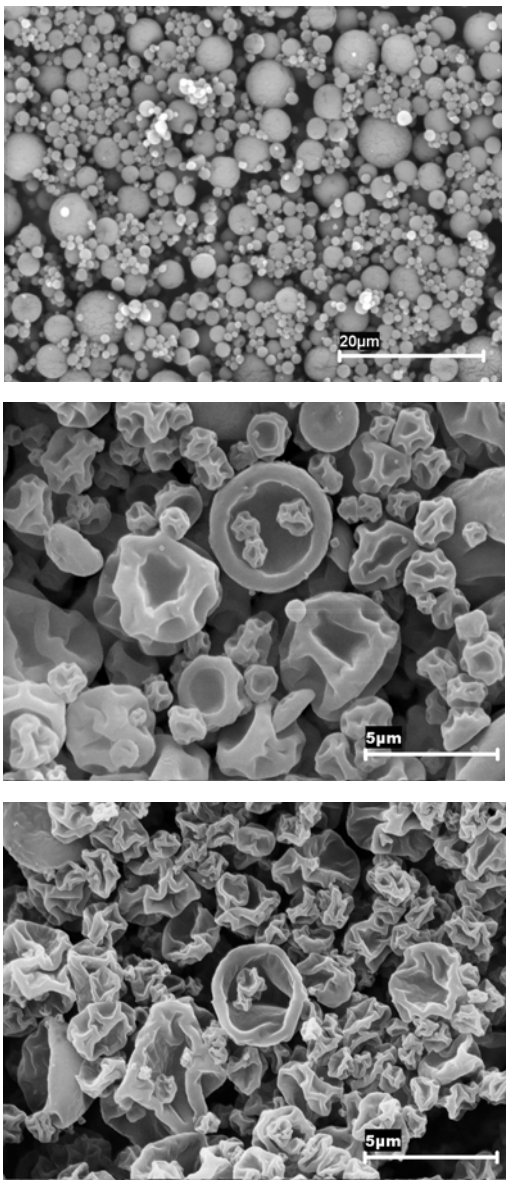

Fig. 3. SEM microphotographs of CS microspheres produced by spray-drying: (a) CS (deacetylation degree > 85%) solution, (b) CS (deacetylation degree 23%) dispersion and (c) CS-glucomannan (25:75) solution.

The application of these microspheres as lung protein carriers was investigated using insulin and fluorescein isothiocyanate-labeled bovine serum albumin (FITC-BSA) as model compounds. High protein association efficiencies up to 90%-100% were obtained with microspheres prepared by both techniques. We are currently evaluating the *in vivo* behavior of the insulin loaded microspheres. More specifically, the extent of hypoglycemic responses following intratracheal administration of powder insulin-loaded formulations to rats is being compared to that corresponding to insulin solution. Preliminary results are very encouraging, demonstrating that microspheres induce a prolonged reduction of glucose levels (time to reach the minimum plasma glucose level increases from 180 to 240 min for emulsion evaporation microspheres, while the minimum % of glucose level reached at this time increases approx. 1.6 times for both types of particles) (data not shown). Interestingly, CS microspheres, whose physicochemical properties were modified through the use of different crosslinking agents, have been shown to be compatible with the hydrofluoralkane propellant P134a and, therefore, are good candidates for lung delivery via pressurized metered dose inhalers (pMDI) [72].

Huang et al. produced betamethasone-loaded CS microspheres by spray-drying with encapsulation efficiency up to 95%, using CS as raw material and type-A gelatin and ethylene oxide-propylene oxide block copolymer (Pluronic F68) as modifiers. Microspheres are spherical and smooth and have a size distribution of 1-5 μm and a density of < 0.4 g/cm^3, all of these properties being compatible with their use for therapy via the lungs [76,117]. Furthermore, by properly choosing excipient type and concentration, a high degree of control was achieved over the physical and release properties of microparticles. Although CS has been described in the literature as biocompatible, biodegradable and non-toxic, few studies have focused on this subject. Therefore, these authors decided to examine biological effects related to inflammation of rat lung upon contact with the produced particles. They demonstrated that CS could induce proinflammatory responses in rat lung tissues in a dose-dependent manner, these responses were probably related to its cationic polyelectrolyte properties (high positive surface charge of + 45 mV), although the effects were mild relative to lipopolysaccharides. The lower doses tested were within the upper range of levels previously used in

some therapeutic applications in which CS was used for pulmonary DNA delivery in mice [118]; but relatively higher doses of CS may be needed for delivery of other non-DNA therapeutic agents. Therefore, the main conclusion of this study was that these effects need to be considered in the context of therapeutic application via pulmonary delivery, especially if relatively high concentrations of CS are used. Furthermore, the type of CS chosen is crucial since the factors referred to greatly influence CS toxicity are the type of salt, the molecular weight and the deacetylation degree. In this respect, a higher degree of deacetylation of CS, which represents a higher positive zeta potential of the particles, was related to a higher *in vitro* cytotoxicity [119]. Accordingly, in this context, the use of less deacetylated CS could be desirable. With this idea in mind, we have recently tested the Calu-3 cells sensitivity to chitosans of different deacetylation degree (> 80%, 47% and 38%) in both proliferating and well-differentiated cells, observing significant differences. As an example, for a chitosan concentration of 1mg/mL, cell viability in proliferating cells remained around 100% respect to buffer control after 4 hours incubation, for both less deacetylated chitosans, whereas it was only 20% for the high deacetylated polymer. However, it must be mentioned that this marked difference was less pronounced in differentiated cells.

Hyaluronic acid (HA) is a naturally occurring hydrogel based on a linear polysaccharide comprised of repeating units of D-glucuronic acid and N-acetyl-D-glucosamine, linked by β-1,4 and β-1,3 glycosidic bonds. It is a hygroscopic, amorphous material that slowly dissolves in water to form highly viscous solutions. Applications using HA for pulmonary controlled drug delivery are reported in literature [75]. Inhalable dry powders (mass mean aerodynamic diameter, MMAD = 1-4 μm), which were produced by co-spray-drying HA and insulin, induced modifications in insulin pharmacokinetics (the mean residence time, MRT and terminal half-life were extended when compared to spray-dried pure insulin) following administration to conscious dogs. Furthermore, addition of Zn^{2+} or hydroxipropylcellulose to the microspheres improved MRT (more than 9 and 7 fold, respectively), AUC/dose (2.5 and 5 fold, respectively) and Tmax (by a factor of 3 in both cases) [75].

5.3. Others

Materials such as mannitol and oligosaccharide ester derivatives (OED) have been also applied to produce microparticles to be delivered through the pulmonary route, using a spray-drying technique [74,120]. OEDs are low molecular weight, lipophilic sugar based compounds and they appeared as intent to address some technical problems (poor physical stability, erosion prior to drug release) presented by other polymers frequently used to obtain microspheres. Mannitol is one of the excipients most used in lung delivery, given its innocuous properties and low hygroscopicity.

Using ester derivatives from lactose and trehalose, *Alcock et al.* produced microspheres encapsulating leuprolide. These microspheres displayed a controlled release of the drug which was dependent on the selected OED or combination of several OEDs, and demonstrated to be stable for 3 months in 4-40ºC and 60-75% humidity. Moreover, upon intratracheal administration of the microspheres to rats, leuprolide was detected in plasma for up to 25 hours, while the drug was detected for only 150 min. after i.v. administration [74]. *Okamoto et al.* produced mannitol-insulin microparticles which induced a stronger hypoglycemic response (glucose level decreased 15%) compared to an insulin solution (glucose diminished 5%), both administered intratracheally [120].

More recently, papers reporting the combination of some of the previously mentioned delivery systems to form a single one have arisen. For example, nanoparticles have been encapsulated inside microspheres in an attempt to integrate their advantages while avoiding their particular limitations, thus leading to more efficient delivery systems [63,121-122]. Delivery systems developed on this basis intended for pulmonary administration of drugs will be addressed in a specific section in this chapter.

6. NANOPARTICULATE LUNG DRUG DELIVERY CARRIERS

Among the previously mentioned novel carrier systems, nanoparticulate-based technologies have reached a position of evidence and their application has been introduced as an exciting alternative for drug administration through several routes [1,42,123-125], mainly because it was demonstrated that particle size

plays a key role in their ability to cross epithelia, with transport being more favorable for nanoparticles (particles in the nanometric range) than for microparticles [1,126-127]. Furthermore, it has been demonstrated that transport is more favorable for some hydrophilic polymers. These colloidal carriers have recently been proposed as vehicles for drug transport to the lung epithelium, as we will overview in this section, using a wide range of materials such as polyesters, polysaccharides and polyacrylates [7,29]. Moreover, they have shown several important advantages, including improvement of drug stability and, in some cases, the ability to control the drug release profile. Furthermore, an experiment with latex nanoparticles revealed that, given their small size, they are able to avoid mucociliary clearance and phagocytic activity [103,128], while nanoparticles made of diverse polymers were efficiently taken-up by alveolar epithelial cells [44,95,129]. There is no consensus concerning the ideal size range to avoid or delay macrophage mediated phagocytosis. However, it has been reported that this phagocytic activity is maximum for particles of 1-2 μm, decreasing for both smaller and larger particles out of this range [15,103,130]; generally, there is an agreement that for particles in the micrometer range, the smaller the particle size, the higher the probability of being captured [15,131].

In general, nanoparticles can be formulated and administered either in aqueous or dry powder form [132-133], the latter representing a possibility to overcome the frequent stability problems. The challenge of developing adequate particulate delivery systems is really succeeding, and an appreciable amount of new carriers are appearing. In fact, the combination of various delivery systems to form a single complex system, like the production of dry powders containing colloidal systems, in order to solve aerodynamic and stability limitations, was recently proposed by several authors [63,132,134-136].

Following in this section, we will present selected research works reporting the design and application of some new nanoparticulate technologies for pulmonary administration. Table 9 shows a summary of the polymers and materials used to produce the referred nanoparticulates. Special mention will be made to the application of nanoparticles in gene therapy. Studies reporting *in vitro* characterization of the systems, as well as those containing studies on pulmonary

cell lines and *in vivo* studies will be described. Furthermore, Tables 10 and 11 summarize, respectively, the most relevant nanoparticulate systems developed for lung delivery as well as the most interesting aspects of the *in vitro* and *in vivo* studies performed with them, indicating polymers, preparation methods, type of studies and major results.

Table 9. Main excipients used to produce nanoparticulate lung drug delivery carriers

Synthetic hydrophobic excipients	
Polyester derivatives	Polylactic-co-glycolic acid (PLGA), polylactic acid (PLA)
Acrylic polymers	Polybutylcyanoacrylate (PBCA), polyhexylcyanoacrylate (PHCA)
Lipids	Lecithin, gliceryl behenate
Natural hydrophilic excipients	
Proteins	Gelatin, albumin
Polysaccharides	Chitosan (CS)

6.1. Nanoparticles made of synthetic hydrophobic materials

6.1.1. Nanoparticles of polyester derivatives

As was previously discussed, biodegradable and biocompatible derivatives of the lactic acid, PLA and PLGA, are excellent materials to prepare particulate lung carriers given their documented safety. The preparation of nanoparticles based on these polyester derivatives has been performed using techniques such as emulsion solvent evaporation [44,137-138] and solvent displacement [95-96,113]. Solvent displacement, also called nanoprecipitation, involves the use of an organic phase which is completely soluble in the external aqueous phase. The organic phase diffuses instantaneously to the external aqueous phase, inducing the immediate precipitation of the polymer. After nanoparticle formation, the solvent is eliminated and the suspension concentrated under reduced pressure [42].

Table 10. Description of *in vitro* studies performed with nanoparticulate systems developed for lung drug delivery

Main excipient	Associated molecule	Preparation method	Performed studies	Major findings	Ref.
PLGA-PVA	Rifampicin Isoniazid Pyrazinamide	Solvent evaporation	Aerosol nebulization behaviour	96% of aerosol particles are in the respirable fraction size range (< 6 µm). Aerosol droplets have MMAD of 1.9 µm. Optimum nebulization is achieved with jet and ultrasonic nebulizers	[137]
PVA-g-PLGA	Coumarin-6	Nanoprecipitation	Aerosol nebulization behaviour	Presence of nanoparticles does not negatively affect aerosol droplets size, which have an MMAD of approximately 4 µm	[96]
DEAPA-PVA-g-PLGA (CMC)	—	Nanoprecipitation	Nebulization Cell culture (A549)	Nanoparticles' zeta potential is controlled by CMC content. Presence of CMC has a positive effect on nanoparticle stabilization and internalization by lung cells	[95]
PLGA-WGA	—	Solvent evaporation	Cell culture (A549) Confocal microscopy of fluorescent nanoparticles	Nanoparticles are taken up and internalized by cells via a specific interaction with WGA-receptors	[44]
PLGA-WGA-IPM	Paclitaxel	Solvent evaporation	Cell culture (A549)	IPM increases nanoparticles' porosity. Higher antiproliferation activity compared to conventional paclitaxel formulation, which is attributed to more efficient cellular uptake via WGA-receptor mediated endocytosis.	[138]
CS-PLGA	Elcatonin	Nanoprecipitation	Aerosol nebulization behaviour	51% of nanoparticle suspension is in the respirable fraction size range. Aerosol droplets have a geometrical diameter of 6.5 µm	[113]
PBCA PHCA	—	Emulsion polymerization	Cell culture (16HBE14o- and primary airway epithelium)	PBCA and PHCA nanoparticles are highly toxic to pulmonary cell lines	[143]

CMC: carboxymethylcellulose; **CS**: chitosan; **DEAPA**: diethylamino-propylamine; **HFA**: hydrofluoroalkane; **IPM**: isopropyl myristate; **MMAD**: mass mean aerodynamic diameter; **PBCA**: polybutylcyanoacrylate; **PHCA**: polyhexylcyanoacrylate; **PLGA**: polylactic-co-glycolic acid; **pMDI**: pressurized metered dose inhaler; **PVA**: polyvinyl alcohol; **PVA-g-PLGA**: polyvinyl alcohol–grafted–polylactic-co-glycolic acid; **TPP**: tripolyphosphate; **WGA**: wheat germ agglutinin

Table 10 (continuation). Description of *in vitro* studies performed with nanoparticulate systems developed for lung drug delivery

Main excipient	Associated molecule	Preparation method	Performed studies	Major findings	Ref.
PBCA	Insulin	Emulsion polymerization	Insulin release	Nanoparticles show a biphasic release profile with initial burst effect (50%) followed by slower release	[144]
Lecithin	Salbutamol	Microemulsion freeze-drying	Aerosolization with a pMDI	Nanoparticles are efficiently dispersed in HFA propellant. 58-65% of particles are in the respirable fraction size range, with a MMAD of 1.2-1.5 μm	[148]
Gelatin Albumin	—	Desolvation	Cell culture (16HBE14o- and primary airway epithelium)	Gelatin and albumin nanoparticles show little or no cytotoxicity	[143]
CS-TPP	Fluorescein isothyocyanate	Ionic gelation	Cell culture (A549)	Higher uptake of nanoparticles by A549 cells, compared to CS solutions. Nanoparticle internalization by the cells occurs predominantly by adsorptive endocytosis initiated by non-specific interaction between nanoparticles and cell membranes and partially mediated by clathrin-mediated processes	[129]

CS: chitosan; **HFA**: hydrofluoroalkane; **MMAD**: mass mean aerodynamic diameter; **PBCA**: polybutylcyanoacrylate; **pMDI**: pressurized metered dose inhaler; **TPP**: tripolyphosphate

PLGA nanoparticles containing 14% (w/w) PVA and encapsulating the antitubercular drugs rifampicin, isoniazid and pyrazinamide, were produced by *Pandey et al.* by a solvent evaporation technique, previously commented on. Nanoparticle sizes varied within 190 and 290 nm and associated the drugs with efficacies between 57 and 68%. Drug-loaded nanoparticle suspensions were shown to be efficiently aerosolized with a nebulizer; 96% of the aerosolized particles were in the respirable fraction and the resultant aerosol droplets presented a mass mean aerodynamic diameter (MMAD) of approximately 1.9 μm. Therefore, the nanoparticle formulation was considered to be suitable for delivering the encapsulated drugs into the deep pulmonary regions [137].

Nanoparticles consisting of polyvinyl alcohol (PVA)-grafted-PLGA were produced using the method of nanoprecipitation (PVA/PLGA ratios = 1:10 and 1:20), encapsulating coumarin-6 as a model drug. The obtained particle size was approximately 100 nm and the encapsulation efficiency was around 37%. Nanoparticle suspensions were nebulized without further processing using three different nebulizers. The aerosol patterns were compared to those of 0.9% NaCl and 5% glucose solution, which were used as controls. When using nebulization as the aerosol generation process, nanoparticles are known to be efficiently incorporated in the respirable fraction of aerosolized droplets (when compared to larger particles), because nanoparticles size perfectly fits the droplet size range (1-5 μm) [139]. Therefore, as expected, the generated aerosols were generally considered to be within this respirable fraction and the presence of nanoparticles did not negatively affect the aerosol droplet size in a clinically relevant manner when compared to the used controls, indicating the suitability of the nanoparticles for pulmonary administration using nebulization. However, the technique of aerosol generation (jet, ultrasonic and piezo-electric nebulizer) was shown to influence the aggregation of nanoparticles during the aerosolization process. Only jet and ultrasonic nebulizers resulted in adequate aerosol droplets for lung delivery [96], which suggests that the adequate nebulization technique should be cautiously selected to maximize the therapeutic effect. Moreover, the same authors proposed the production of nanoparticles containing PVA-grafted-PLGA with a backbone of diethylamino-propylamine (DEAPA-PVA-g-PLGA), with some also comprising carboxymethylcellulose (CMC) in concentrations ranging

from 0 to 400 µg CMC/mg polymer. The main advantage of this system is that the amphiphilic properties of the polymer DEAPA-PVA-g-PLGA made nanoparticles preparation by the solvent displacement method possible without adding the usual surfactant stabilizer that was required for the preparation of the first mentioned system [95]. This is of crucial importance for the pulmonary application, since it is known that the inhalation of high amounts of synthetic surfactants may affect the surface tension of the pulmonary surfactant, thus resulting in inflammation or impaired natural functions [46]. The referred nanoparticles had sizes ranging between 70 and 250 nm and their zeta potential was dependent on the CMC concentration, being strongly positive when no CMC was present and decreasing gradually, reaching accentuated negative values when the formulation comprised 400 µg CMC/mg polymer. 50 µg CMC/mg polymer was the point where zeta potential changed from positive to negative. Although cell association was low, the anionic nanoparticles were the only ones internalized by the A549 cells, an alveolar epithelial cell line, and were the most stable during nebulization; therefore anionic nanoparticles are expected to be the most suitable for aerosol therapy [95]. Unfortunately, an explanation for these particle/cell interaction patterns was not provided.

Mo and Lim prepared PLGA nanoparticles conjugated with wheat germ agglutinin (WGA) by the solvent evaporation method, as already commented on. These nanoparticles, with a size around 250 nm, were efficiently taken-up by the A549 cells in a time-, temperature- and concentration-dependent saturable process. Nanoparticle internalization was confirmed by confocal microscopy and fluorescein isothiocyanate-bovine serum albumin (FITC-BSA)-loaded PLGA nanoparticles were used as control. The conclusion was that the high internalization of the WGA-PLGA nanoparticles was preceded by a specific interaction with WGA-binding receptors in the cells and was mediated by caveolae-dependent endocytic pathways [44]. In a subsequent study, isopropyl myristate was further added to the WGA-PLGA nanoparticles, which encapsulated paclitaxel, a chemotherapeutic drug, with an efficiency of 66%. The addition of isopropyl myristate resulted in the formation of pores and channels in the nanoparticles, therefore facilitating the drug release. The release profile showed an initial burst effect in the first 5 h, followed by a slower release for 5 days,

Table 11. Description of *in vivo* studies performed with nanoparticulate systems developed for lung drug delivery

Main excipient	Associated molecule	Preparation method	Animal	Administration method	Major findings	Ref.
PVA-PLGA	Rifampicin Isoniazid Pyrazinamide	Solvent evaporation	Guinea pigs	Nebulization	Nanoparticles give significantly higher plasmatic levels of drug from 6 h up to 192 h compared to free drug	[137]
CS-PLGA	Elcatonin	Nanoprecipitation	Guinea pigs	Nebulization	CS modified nanoparticles give a prolonged pharmacological action and are eliminated slower than unmodified particles	[113]
PBCA	Insulin	Emulsion polymerization	Rats	Intratracheal instillation	Nanoparticles give more prolonged hypoglycaemia than insulin solutions	[144]
Gliceryl behenate	^{99m}Tc	Melted homogenization	Rats	Nebulization	Solid lipid nanoparticles are significantly taken up by the lymphatics. They are suitable for imaging or lung cancer therapy	[147]

CS: chitosan; **PBCA**: polybutylcyanoacrylate; **PLGA**: polylactic-co-glycolic acid; PVA: polyvinyl alcohol; **^{99m}Tc**: radiolabeled Tecnetium

which resulted in the release of 40% paclitaxel. Furthermore, studies in A549 cells resulted in a 5-fold increase in drug action also at 5 h, compared to the conventional commercial formulation of paclitaxel. The high anti-proliferation activity of these nanoparticles was attributed to more efficient cellular uptake via WGA-receptor-mediated endocytosis. Moreover, once in the cytoplasm, isopropyl myristate facilitated the release of the loaded paclitaxel, thereby contributing to a stronger effect of the drug [138].

Another approach for surface modification was the alteration of PLGA nanospheres with chitosan, a natural polymer (for further characterization of chitosan consult next section *polysaccharides*), which were prepared by the nanoprecipitation method. Produced nanoparticles encapsulated efficiently the peptide elcatonin and had a size of approximately 650 nm. Nanoparticles were successfully aerosolized with a nebulizer, resulting in aerosol droplets with a geometrical diameter of 6.5 μm, which resulted in a respirable fraction of 51% [113].

So far, few *in vivo* studies were performed with polyester-based nanoparticles for pulmonary delivery. *Pandey et al.* evaluated PLGA nanoparticles containing antitubercular drugs, developed as referred to above. These nanoparticles were efficiently aerosolized to guinea pigs, using a nebulizer, and plasmatic drug levels were evaluated using a solution of the free drug administered orally as a control. Following nebulization, drugs could be detected in the plasma from 6 h up to 144 h (rifampicin) and 192 h (isoniazid and pyrazinamide), contrary to what was observed after oral administration in which case the drugs were detected only until 12 h. Figure 4 displays plasma *vs* time profiles of isoniazid, following nebulization of drug loaded nanoparticles and oral administration of the free drug in solution. The PVA content (approximately 15%) was reported to provide stability by forming a barrier to the diffusional release of the drugs, resulting in a sustained release [137].

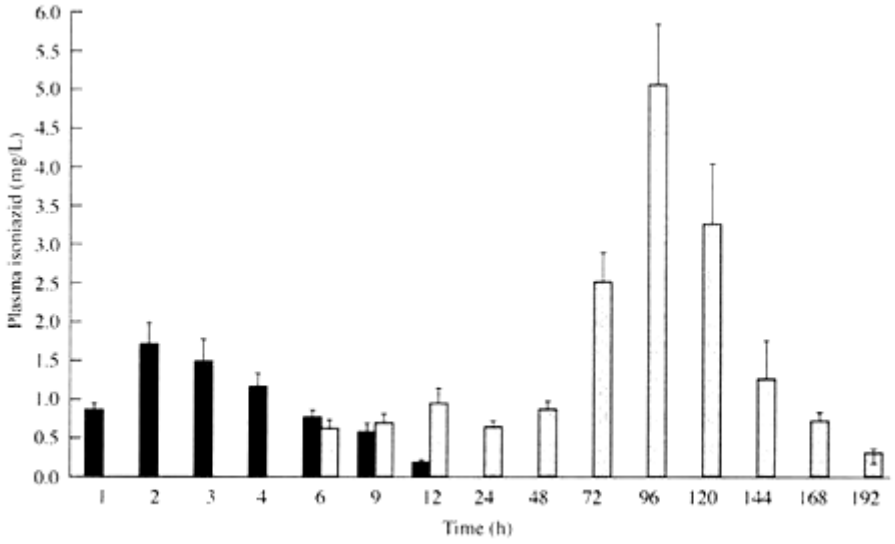

Fig. 4. Plasma profile of isoniazid following the nebulization of drug-loaded PLG-NP, and oral administration of parent drug. Values are mean ± S.D., n = 6-8. Black bars, oral isoniazid; grey bars, nebulized isoniazid-loaded PLG-NP (Reprinted with permission from Ref. [124] R. Pandey et al., J. Antimic. Chemother., 52, 981, 2003, Copyright The British Society for Antimicrobial Therapy @ 2003).

In another *in vivo* study, surface modified PLGA nanospheres with chitosan, which were aerosolized with a nebulizer to guinea pigs, had a slower elimination rate from the lung than the unmodified particles. Moreover, chitosan modification resulted in a prolonged and stronger hypocalcemic effect of elcatonin. Figure 5 shows blood calcium levels *vs* time following pulmonary administration of drug loaded modified and unmodified nanospheres. The observed behaviour of the chitosan-modified nanospheres was attributed to the mucoadhesive properties of chitosan, as well as to its ability to open the intercellular tight junctions [113].

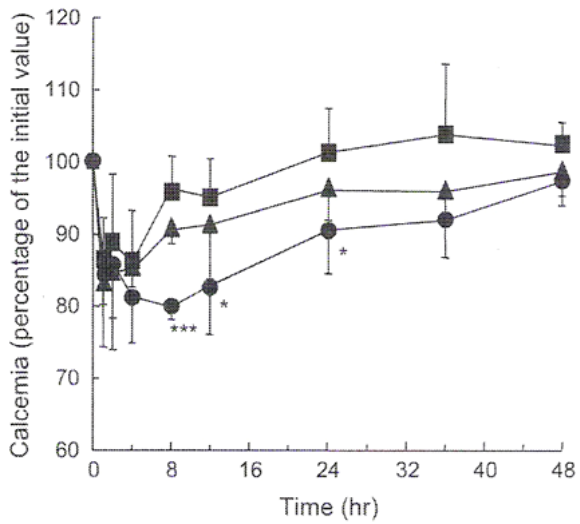

Fig. 5. Profiles of the blood calcium level after pulmonary administration of the elcatonin-loaded nanosphere suspension (100 IU/kg) to male guinea pigs (6 weeks). (■) Elcatonin solution; (▲) noncoated PLGA nanospheres; (●) chitosan-coated PLGA nanospheres. Data are presented as the means ± S.D. (n = 5). ***p<0.001, *p<0.05 compared with elcatonin solution. (Reprinted from Publication J. Control. Release, 102, H. Yamamoto et al., Surface-modified PLGA nanospheres with chitosan improved pulmonary delivery of calcitonin by mucoadhesion and opening of the intercellular tight junctions, 373, Copyright (2003), with permission from Elsevier).

6.1.2. Nanoparticles of acrylic polymers

Regarded as non-toxic and highly biocompatible, acrylate derivatives are currently components of drug delivery systems developed for many routes of administration [140-141]. In fact, the first nanoparticulate systems containing cyanoacrylates were reported in the 70s and in the early 80s. *Couvreur et al.* developed biodegradable poly(alkylcyanoacrylate) (PACA) nanoparticles by a simple polymerization reaction [42]. Since then, these nanoparticles have been the object of intensive research in the area of polymeric colloidal drug carriers and many applications have emerged in the field of drug delivery [141], including delivery via the pulmonary route. The technique of emulsion polymerization is still used and consists of the emulsification of droplets of water-insoluble monomers in an external aqueous and acidic phase that contains a stabilizer, under magnetic stirring. The monomers polymerize relatively fast by an anionic

polymerization mechanism, with a polymerization rate that is dependent on the pH of the medium. At acidic pH, between 2 and 4, the reaction is relatively slow, yielding nanospheres with a narrow-size distribution (frequently 200 nm and in some cases less than 50 nm) [42,142].

Brzoska et al. produced nanoparticles composed of polybutylcyanoacrylate (PBCA) or polyhexylcyanoacrylate (PHCA), using the previously described technique. The nanoparticles had sizes between 110 and 240 nm, however, they were shown to be highly toxic to a primary culture of airway epithelial cells as well as to the 16HBE14o- cell line [143]. This observation pointed out that care should be taken when using these polymers by the pulmonary route. However, to our knowledge, this is a unique study evaluating the toxicity of these polymers in pulmonary cell lines, and further studies are needed to confirm the suggested toxicity. Furthermore, we think it is important to take into account that cell cultures are very susceptible to external factors that are not always easily controlled. The best way to confirm the safety of these polymers should be the performance of *in vivo* studies that allow the accurate evaluation of the lung tissue, evidencing eventual damage caused by the polymers.

Insulin-loaded PBCA nanoparticles were produced by emulsion polymerization, with a mean size around 250 nm. Insulin was associated with an efficiency of 80% and, upon intratracheal administration of the nanoparticle suspension to normal rats, peptide doses of 10 or 20 IU/kg reached a reduction in serum glucose levels comparable to that obtained with a solution with the same insulin amount, however achieving more prolonged effects. The duration of glucose levels below 80% of basal was considered as a criterion to evaluate the formulation's efficacy. As can be observed in Figure 6a, with the dose of 10 IU/kg, the PBCA nanoparticles formulation reached a minimum glucose level of 30% at 4 h, while the solution reached the minimum value of 20% at the same time interval. However, the 80% blood glucose level was reached after 8h for the solution and at 16 h for the nanoparticles. When using 20 IU/kg (Figure 6b), the blood glucose level reached minimum points of 14% at 8 h for the nanoparticles and 4% at 6 h for the respective insulin solution. Again, the recuperation to normal levels was

faster when the solution was administered (80% at 12 h for the solution and at 20 h for the nanoparticles).

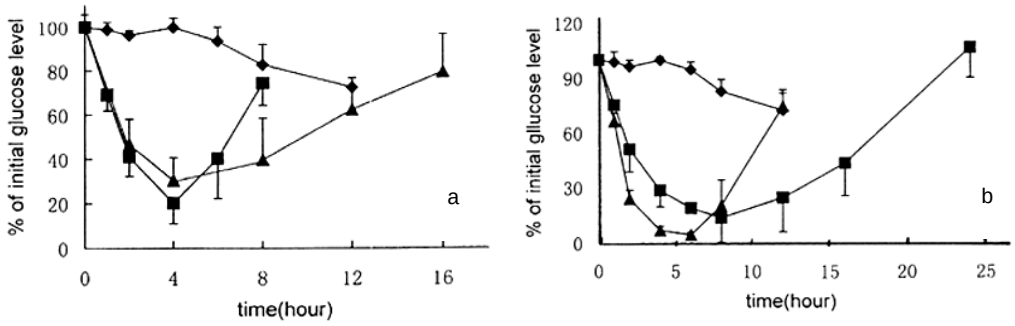

Fig. 6. Hypoglycemic effect of a single intratracheal administration of a) insulin-loaded nanoparticles of 10 IU.kg^{-1} (▲) and insulin solution of 10 IU. kg^{-1} (■); b) insulin-loaded nanoparticles of 20 IU.kg^{-1} (■) and insulin solution of 20 IU. kg^{-1} (▲) to normal rats fasted overnight. The glucose concentration at time zero served as the basis for comparison (%). Results are means for 5 or 6 animals. The control (♦) is phosphate buffer solution (pH 7) (Reprinted from Publication Int. J. Pharm., 218, Q. Zhang et al., Prolonged hypoglycemic effect of insulin-loaded polybutylcyanoacrylate nanoparticles after pulmonary administration to normal rats, 75, Copyright (2001), with permission from Elsevier).

These studies registered the possibility that administering nanoparticles, which may achieve similar, if not better reductions in the glucose levels as with administration of solution with the same insulin amount, results in a more prolonged effect, which pointed out the controlled release of insulin from the nanoparticles [144]. The intratracheal administration of a suspension is not a method that could be used in humans, therefore it is not feasible for clinical trials. The correct method for nanoparticle administration as a suspension would be nebulization. This sort of study is not reported and the authors do not refer to the nanoparticles' stability, an important issue concerning the administration and storage of suspensions.

6.1.3. Lipidic nanoparticles

The excellent potential of using lipids to prepare drug delivery pulmonary carriers has been shown in the previous section. Solid lipid nanoparticles (SLN) were recently proposed as novel drug delivery systems. Firstly reported by Müller's group from Berlin in the 90s for intravenous administration due to their biocompatibility, they have been repeatedly proposed as interesting approaches in drug delivery since they provide low cytotoxicity and controlled drug release due to the solid lipid matrix [145-146]. Recently, they were proposed in the pulmonary field to act as colloidal carriers for cytotoxic drugs intended for lung cancer treatment, as well as radiolabeled agents for lymphoscintigraphy. In this manner, solid lipid nanoparticles composed of glyceryl behenate, containing a radiolabel (^{99m}Tc), were produced by the melted homogenization technique, resulting in a mean size around 200 nm. Upon nebulization to rats, gamma scintigraphic images showed a significant uptake of the radiolabeled SLN into the lymphatics, rendering them suitable as carriers to be applied in either imaging techniques or lung therapy [147].

Dickinson et al. developed a formulation of lecithin-based nanoparticles, using water/lecithin/propanol/iso-octane microemulsions containing 40-45% (w/w) of surfactant (lecithin/propanol). Nanoparticles were frozen and freeze-dried, obtaining a size of less than 100 nm, and salbutamol was used as model drug. These nanoparticles were efficiently dispersed in co-solvent modified HFA-227, a pMDI propellant, due to the presence of the surfactant. Upon aerosolization from this device, the mass mean aerodynamic diameter (MMAD) and fine particle fraction, which were 1 - 1.5 μm and 55 - 65%, respectively, were found to be suitable for systemic pulmonary administration of drugs [148].

6.2. Nanoparticles made of natural hydrophilic materials

6.2.1. Protein-based nanoparticles

Proteins, such as gelatin and albumin, are natural hydrophilic polymers, with evident advantages from a manipulation (avoidance of organic solvents) and drug transport point of view. The major drawbacks of these materials are the easy degradation and the potential antigenicity when administered by the parenteral

route. Nevertheless, information on their antigenicity by pulmonary route is still scarce, therefore further *in vivo* toxicity studies will have to be performed to assess the safety of carriers based on these polymers. Nanoparticles based on albumin and gelatin are usually prepared by a desolvation technique. This method consists of dissolving the protein in water, subsequently desolvating with a solvent such as alcohol or acetone. Finally, cross-linking with glutaraldehyde takes place, leading to the formation of colloidal particles [42]. *Brzoska et al.* produced gelatin and human serum albumin (HSA) based nanoparticles by the above described desolvation technique. Having a size around 240-280 nm, they were assayed using a primary culture of airway epithelial cells and the 16HBE14o- cell line with no observed toxicity. Confocal microscopy analysis showed that gelatin nanoparticles and HSA nanoparticles were incorporated into airway epithelium cells in a concentration- and temperature-dependent manner. At 4°C there was no uptake, in contrast to what happens at 37°C, indicating that nanoparticle penetration is an active endocytic process. Taking these features into account, the referred nanoparticles (HSA and gelatin-based) were considered to be highly suitable drug or gene carriers via the pulmonary route [143].

6.2.2. Nanoparticles of polysaccharides

Our group has developed chitosan/tripolyphosphate (CS/TPP) nanoparticles by an ionic gelation technique [149] which were reported to be efficient carriers of several peptides through distinct routes of administration, including nasal and ocular routes, promoting their absorption as well [110-112]. This technique consists of the interaction between the positively charged chitosan amino group and the negatively charged phosphate groups of pentasodium tripolyphosphate (TPP). Recently, we have evaluated the cytotoxicity of chitosan nanoparticles in bronchial Calu-3 cells. Results showed that chitosan nanoparticles significantly decreased the cytotoxicity of the polymer, increasing the IC_{50} (concentration inhibiting cell viability with 50%) about 10-fold compared to the CS solution.

Using the same technique, *Huang et al.* produced FITC-labelled CS/TPP nanoparticles with a mean size of approximately 200 nm and investigated their

uptake by A549 cells, an alveolar cell line of human origin. Results showed a higher uptake of the chitosan nanoparticles compared to the chitosan solution. Moreover, uptake of the nanoparticles was concentration- and temperature-dependent, increasing with concentration and significantly reduced at 4ºC compared to 37ºC. This led the authors to conclude that internalization of nanoparticles by the cells occurs predominantly by adsorptive endocytosis initiated by non-specific interactions between nanoparticles and cell membranes, and is partially mediated by a clathrin-mediated process [129].

In recent years, there has been a boom of research into non-viral vectors intended for gene delivery, including cationic polymers, cationic lipids/liposomes and, more recently, polymeric nanostructures. These nanostructures are gaining popularity because they are easily produced and scaled-up, there is no size limit on the DNA to be delivered, there are fewer immunological and safety implications, they offer the potential of sustained release of gene/gene products within the transfected cells [150-151] and can be targeted by the attachment of cell-specific ligands [152].

Among the materials used to obtain nanoparticulate carriers, polycationic polymers, and particularly chitosan, have emerged as promising vehicles for non-viral plasmid DNA (pDNA) delivery [153-154] and, very recently, for *in vivo* delivery of small interfering RNA (SiRNA) used as a genetic vaccine against the respiratory syncytial virus infection [155]. Consisting of a simple chitosan-based gene delivery system, it is comprised of ionic complexes, i.e. polyplexes, which are mainly assembled through ionic interactions between the positively charged groups of chitosan and the negatively charged groups of pDNA. Moreover, the ability to form these polyplexes is dependent on chitosan structural parameters, i.e. the degree of deacetylation and the molecular weight [154,156-157]. Although these polyplexes are promising for mucosal pDNA delivery, they still suffer from several limitations, such as undefined physical shapes, dissociation in the presence of anions and a limited capacity to co-associate other functional molecules, like proteins, to the polyplex structure, which could help to overcome the cellular barriers for efficient gene transfer and expression. One strategy proposed to solve these limitations is based on the addition of a desolvating agent, which induces phase separation and,

consequently, the formation of coacervates, generally called nanospheres or nanoparticles [153,158-160], whose transfection efficiency is comparable to that of polyplexes. Another strategy to form defined chitosan nanoscale gene carriers is to hydrophobically modify chitosan, thus enabling it to self-assemble in aqueous solution [161-162].

Finally, in order to overcome the above mentioned limitations with polyplexes, *Koping-Hoggard et al.* have adopted the ionic-gelation technique, previously developed in our group for the encapsulation of peptides and proteins [110,149], to incorporate pDNA and small oligonucleotides into chitosan nanoparticles. In this technique, the DNA molecule to be encapsulated is previously incorporated in the cross-linking TPP solution and, in this case, the nanoparticle formation would not only be determined by electrostatic interactions between chitosan and DNA, but it would also be governed by the cross-linking agent. Just as was expected, nanoparticles formed as a result of this process have a more compact structure, with controlled release properties that are expected to influence the performance of the system both *in vitro* and *in vivo.* A qualitative assessment of the *in vivo* efficiency of this system was obtained by administering nanoparticles loaded with pDNA encoding beta-galactosidase (pLacZ) intratracheally to mice, using naked pLacZ as a control. Nanoparticles made from low molecular weight chitosan resulted in a strong beta-galactosidase gene expression in mouse lungs 72 h after administration, in contrast to the high molecular weight chitosan particles and naked plasmid [163].

7. LUNG DRUG DELIVERY CARRIERS COMBINING NANO- AND MICROPARTICLES

In the recent years, we have been assisting to the appearance of very innovative drug delivery systems, which are in fact the combination of a few other systems. It was in the later 90s when, to our best knowledge, the encapsulation of nanospheres inside microspheres was first reported in an attempt to improve the inhalation efficacy of nanospheres [132]. However, the basic idea of combining systems appeared before, with the encapsulation of particulate matter inside lipid vesicles [164-165]. Encapsulation of vesicles inside a second vesicle has also been

reported [121]. Several research groups followed the idea towards a pulmonary drug delivery application, with the strong challenge of overcoming aerosolization and stability problems. Table 12 summarizes data on combined drug delivery systems developed for pulmonary administration, describing the composition of each of the integrated systems, the preparation methods and the major findings.

Tsapis et al. developed a formulation comprised of nanoparticle-loaded microspheres using polystyrene nanoparticles. These nanoparticles were simply added to a mixture of DPPC, dimyristoylphosphatidylethanolamine (DMPE) and lactose, and spray dried afterwards. The resultant microspheres had adequate properties for pulmonary administration, with aerodynamic diameters ranging between 3-5 μm, and the ability to be readily dissolved into a nanoparticle suspension upon contact with an aqueous medium [63]. *Sham et al.* developed a similar formulation, preparing lactose microspheres containing either gelatin or cyanoacrylate nanoparticles (obtained by desolvation and emulsion polymerization, respectively) by spray drying. The presented microspheres also yielded aerosols with aerodynamic characteristics suitable for efficient pulmonary delivery; their aerodynamic diameter was around 3 μm, which resulted in fine particle fraction of 40%. The nanoparticles were also recovered from the microspheres without significant changes in their size or zeta potential, after being dissolved in an aqueous medium [166]. Another formulation of microspheres encapsulating nanoparticles was proposed by *Cook et al.*, who prepared terbutaline sulphate nanoparticles by emulsification and subsequently spray-dried using hydrogenated palm oil as an excipient in an attempt to achieve a sustained release of the drug. The microspheres were adequate for pulmonary administration since they had an aerodynamic diameter of 3.9 μm and exhibited a fine particle fraction of 47% and mass mean aerodynamic diameter (MMAD) of 3.9 μm. Moreover, a sustained release of the drug was achieved [167].

Table 12. Description of combined microencapsulated nanoparticle systems adequate for pulmonary administration

Nanoparticle composition	Nanoparticle preparation method	Microsphere composition	Microsphere preparation method	Major findings	Ref.
Polystyrene	Commercially supplied	DPPC, DMPE, lactose	Spray-drying	Aerodynamic diameters between 3 and 5 µm	[63]
Gelatin Cyanoacrylate	Desolvation Emulsion polymerization	Lactose	Spray-drying	40% of the particles in the respirable fraction and MMAD around 3 µm	[166]
Terbutaline sulphate	Emulsification	Hydrogenated Palm Oil	Spray-drying	47% of the particles in the respirable fraction and MMAD of 3.9 µm. Sustained release of the drug was achieved	[167]

DMPE: dimiristoylphosphatidylethanolamine; **DPPC**: dipalmitoylphosphatidylcholine; **MMAD**: mass mean aerodynamic diameter

Table 12. Description of combined microencapsulated nanoparticle systems adequate for pulmonary administration

Nanoparticle composition	Nanoparticle preparation method	Microsphere composition	Microsphere preparation method	Major findings	Ref.
Polystyrene	Commercially supplied	DPPC, DMPE, lactose	Spray-drying	Aerodynamic diameters between 3 and 5 µm	[63]
Gelatin Cyanoacrylate	Desolvation Emulsion polymerization	Lactose	Spray-drying	40% of the particles in the respirable fraction and MMAD around 3 µm	[166]
Terbutaline sulphate	Emulsification	Hydrogenated Palm Oil	Spray-drying	47% of the particles in the respirable fraction and MMAD of 3.9 µm. Sustained release of the drug was achieved	[167]

DMPE: dimiristoylphosphatidylethanolamine; **DPPC**: dipalmitoylphosphatidylcholine; **MMAD**: mass mean aerodynamic diameter

8. MAIN REMARKS:

From the above mentioned comments, it is clear that drug administration through the pulmonary route represents an excellent and alternative opportunity for some new molecules, as well as for some others which did not gather good results through other routes. Special mention should be paid to the encouraging results related to the absorption of peptides and proteins. However, many challenges have to be faced from now on and drugs will only be successfully administered through the lung when drug carriers have such properties that enable them to overcome the distinct barriers, such as difficult accessibility, aerodynamic specificities and the mucociliary clearance. In this manner, nanoparticles and microparticles have been proposed as carriers for pulmonary administration, using a wide range of polymers and materials, since they can offer efficient and controlled delivery, as well as protection of the encapsulated molecules.

ACKNOWLEDGMENTS

This work was supported by the Spanish Government (CICYT, SAF2002-03314) (Cofinanced by FEDER Funds). The Predoctoral fellowship to Ana Grenha from Fundação para a Ciência e Tecnologia, Portugal (SFRH/BD/13119/2003) is highly appreciated.

REFERENCE LIST

1. M. J. Alonso, Biomed. Pharmacother. **58**, 168 (2004).
2. P.L. Smith, J. Control. Release. **46**, 99 (1997).
3. J. L. Cleland, A. Daugherty and R. Mrsny, Curr. Opin. Biotech. **12**, 212 (2001).
4. H. Takeuchi, H. Yamamoto and Y. Kawashima, Adv. Drug Deliv. Rev. **47**, 39 (2001).
5. D. A. Edwards, A. Ben-Jebria and R. Langer, J. App. Physiol. **84**, 379 (1998).
6. A. Clark, Drug Del. Systems Sci. 2, **73** (2002).
7. H. M. Courrier, N. Butz and T. F. Vandamme, Crit. Rev. Ther. Drug Carr. Syst. **19**, 425 (2002).
8. J. S. Patton, Adv. Drug. Deliv. Rev. **19**, 3 (1996).

9. G. Taylor and I. Kellaway, in: *Drug delivery and targeting. For pharmacists and pharmaceutical scientists* edited A. Hillery, A. Lloyd and J. Swarbrick, Taylor & Francis, New York (2001), p. 269.

10. B. Fawcett, in *Tratado de histología* edited B. Fawcett and D. W. Fawcett, Interamericana McGraw-Hill, Madrid (1995), p. 765.

11. L. P. Gartner and J. L. Hiatt, *Histología: Texto y Atlas*, Interamericana McGraw-Hill, Madrid (1997).

12. E. E. Schneeberger and R. D. Lynch, in *Fluid and solute transport in the airspaces of the lungs* edited R. M. Effros and H. K. Chang, Marcel Dekker, New York (1994), p. 1.

13. F. Geneser, *Histología: Sobre bases biomoleculares*, Editorial Medica Panamericana, Madrid (2000).

14. X. Yang, K. A. Joseph, C. J. Malanga and Y. Rojanasakul, Int. J. Pharm. **195**, 93 (2000).

15. F. Ahsan, I. P. Rivas, M. A. Khan and A. I. Suárez-Torres, J. Control. Release. **79**, 29 (2002).

16. E. R. Jacobs and T. E. DeCoursey, in Fluid and solute transport in the airspaces of the lungs edited R. M. Effros and H. K. Chang, Marcel Dekker, New York (1994), p. 151.

17. H. G. Burkitt, B. Young and J. W. Heath, *Histología funcional Wheater*, Churchill Livingstone, Madrid (1993).

18. A. Rios, M. E. Gordillo, C. Bocanegra and J. A. Maldonado, in *Administración de medicamentos: Teoria y práctica* edited B. S. Ramos and M. D. Aznar, Diaz de Santos, Madrid (1994), p. 131.

19. P. Gehr, F. H. Y. Green, M. Geiser, V. I. Hof, M. M. Lee and S. Schurch, J. Aerosol Med. **9**, 163 (1996).

20. K. McDonald and G. Martin, Int. J. Pharm. **201**, 89 (2000).

21. I. J. Smith and M. Parry-Billings, Pulmon. Pharmacol. Ther. **16**, 79 (2003).

22. I. J. Smith, Drug Deliv. Syst. Sci. **2**, 63 (2002).

23. H. Okamoto, H. Todo, K. Iida and K. Danjo, Kona. **20**, 71 (2002).

24. H. Schulz, Pharm. Sci. Technol. Today. **1**, 336 (1998).

25. J. Hanes, M. Dawson, Y. Har-el, J. Suh and J. Fiegel, in Pharmaceutical inhalation aerosol technology edited A. J. Hickey, Marcel Dekker, New York (2004), p. 489.

26. J. Heyder, J. Gebhart, G. Rudolf, C. F. Schiller and W. Stahlhofen, J. Aerosol Sci. **17**, 811 (1986).

27. N. R. Labiris and M. B. Dolovich, Br. J. Clin. Pharmacol. **56**, 588 (2003).

28. A. R. Clark, in *Pharmaceutical inhalation aerosol technology* edited A. J. Hickey, Marcel Dekker, New York (2004), p. 571.

29. S. – A. Cryan, AAPS Journal. **7**, E20 (2005).

30. M. Sakagami and P. R. Byron, Clin. Pharmacok. **44**, 263 (2005).

31. J. S. Patton and R. M. Platz, Adv. Drug Deliv. Rev. **8**, 179 (1992).

32. Z. Shen, Q. Zhang, S. Wei and T. Nagai, Int. J. Pharm. **192**, 115 (1999).

33. H. G. Folkesson, M. A. Matthey, B. R. Westrom, K. J. Kim, B. W. Karlsson and R. H. Hastings, J. Appl. Physiol. **80**, 1431 (1996).

34. D. R. Gill, L. A. Davies, I. A. Pringle and S. C. Hyde, Cell. Mol. Life Sci. **61** 355 (2004).

35. L. Garcia-Contreras, T. Morçöl, S. J. D. Bell and A. J. Hickey, AAPS Pharmsci. **5**, 1 (2003).

36. M. A. Myers, D. A., Thomas and L. Stranb, Exp. Lung Res. **19**, 1 (1993).

37. A. Yamamoto, S. Okumura, Y. Fukuda, M. Fukui, K. Takahashi and S. Muranishi, J. Pharm. Sci. **86**, 1144 (1997).

38. L. Heinemann, W. Klappoth, K. Rave, B. Hompesch, R. Linkeschowa and T. Heise, Diabetes Care. **23**, 1343 (2000).

39. H. O. Alpar, S. Somavarapu, K. N. Atuah and V. W. Bramwell, Adv. Drug Deliv. Rev. **57**, 411 (2005).

40. M. Sakagami, K. Sakon, W. Kinoshita and Y. Makino, J. Control. Release. **77**, 117 (2001).

41. K. Yamada, M. Odomi, N. Okada, T. Fujita and A. Yamamoto, J. Pharm. Sci. **94**, 2432 (2005).

42. M. J. Alonso, in *Microparticulate systems for the delivery of proteins and vaccines* edited S. Cohen and H. Bernstein, Marcel Dekker, New York (1996) p. 203.

43. C. Evora, I. Soriano, R. A. Rogers, K.M. Shakesheff, J. Hanes and R. Langer, J. Control. Release. **51**, 143 (1998).

44. Y. Mo and L.-Y. Lim, J. Pharm. Sci. **93**, 20 (2004).

45. A. Hussain, J. J. Arnold, M. A. Khan and F. Ahsan, J. Control. Rel. **94**, 15 (2004).

46. M. Suzuki, M. Machida, K. Adachi, K. Otabe, T. Sugimoto, M. Hayashi and S. Awazu, J. Toxicol. Sci. **25**, 49 (2000).

47. H. Todo, H. Okamoto, K. Iida and K. Danjo, Int. J. Pharm. **220**, 101 (2001).

48. A. Portero, C. Remuñan-Lopez and H. M. Nielsen, Pharm. Res. **19**, 169 (2002).

49. C. Prego, M. Garcia-Fuentes, D. Torres and M. J. Alonso, J. Control. Release. **101**, 151 (2005).

50. D. Teijeiro-Osório, C. Remuñán-López and H. M. Nielsen, Proc. 32 Ann. Meet. Exp. Control. Release Soc. Miami, FL (2005), #378.

51. S. Kobayashi, S. Kondo and K. Juni, Pharm. Res. **11**, 1239 (1994).

52. Y. Tabata and I. Ikada, Biomaterials. **9**, 356 (1998).

53. D. A. Edwards, J. Hanes, G. Caponetti, J. Hrkach, A. Ben-Jebria, M. L. Eskew, J. Mintzes, D. Deaver, N. Lotan and R. Langer, Science. **276**, 1868 (1997).

54. A. Ben-Jebria, D. Chen, M. L. Eskew, R. Vanbever, R. Langer, and D. A. Edwards, Pharm. Res. **16**, 555 (1999).

55. R. Vanbever, A. Ben-Jebria, J. Mintzes, R. Langer and D. A. Edwards, Drug Develop. Res. **48**, 178 (1999).

56. R. Vanbever, J. Mintzes, J. Wang, J. Nice, D. Chen, R. Batycky, R. Langer and D. A. Edwards, Pharm. Res. **16**, 1735 (1999).

57. C. Dunbar, G. Scheuch, K. Sommerer, M. DeLong, A. Verma and R. Batycky, Int. J. Pharm. **245**, 179 (2002).

58. A. I. Bot, T. E. Tarara, D. J. Smith, S. R. Bot, C. M. Woods and J. G. Weers, Pharm. Res. **17**, 275 (2000).

59. L. Dellamary, T. E. Tarara, D. J. Smith, C. H. Woelk, A. Adractas, M. L. Costello, H. Gill and J. G. Weers, Pharm. Res. **17**, 168 (2000).

60. A. I. Bot, D. J. Smith, S. R. Bot, L. Dellamary, T. E. Tarara, S. Harders, W. Phillips, J. G. Weers and C. M. Woods, Pharm. Res. **18**, 971 (2001).

61. S. Steiner, A. Pfützner, B. R. Wilson, O. Harzer, L. Heinemann and K. Rave, Exp. Clin. Endocrinol. Diabetes. **110**, 10 (2002).

62. A. Pfützner, A. E. Mann and S. S. Steiner, Diabetes Tech. Ther. **4**, 589 (2002).

63. N. Tsapis, D. Bennet, B. Jackson, D. A. Weitz and D. A. Edwards, Proc. Nat. Acad. Sci. **99**, 12001 (2002).

64. V. A. Philip, R. C. Mehta, M. K. Mazumder and P. P. DeLuca, Int. J. Pharm. **151**, 165 (1997).

65. M. M. El-Baseir and I. W. Kellaway, Int. J. Pharm. **175**, 135 (1998).

66. R. Sharma, D. Saxena, A. K. Dwivedi and A. Misra, Pharm. Res. **18**, 1405 (2001).

67. S. Suarez, P. O'Hara, M. Kazantseva, C. E. Newcomer, R. Hopfer, D. N. McMurray and A. J. Hickey, J. Antimicrob. Chemother. **48**, 431 (2001).

68. S. Suarez, P. O'Hara, M. Kazantseva, C. E. Newcomer, R. Hopfer, D. N. McMurray and A. J. Hickey, Pharm. Res. **18**, 1315 (2001).

69. N. Bandi, S. P. Ayalasomayajula, D. S. Dhanda, J. Iwakawa, P.-W. Cheng and U. B. Kompella, J. Pharm. Pharmacol. **57**, 851 (2005).

70. S. Pandit, C. Martin and H. O. Alpar, J. Drug Deliv. Sci. Technol. **15**, 281 (2005).

71. H. Zhou, Y. Zhang, D. L. Biggs, M. C. Manning, T. W. Randolph, U. Christians, B. M. Hybertson and K. Ng, J. Control. Release. **107**, 288 (2005).

72. R. O. Williams, M. K. Barron, M. J. Alonso and C. Remuñan-Lopez, Int. J. Pharm. **174**, 209 (1998).

73. K. Morimoto, H. Katsumata, T. Yabuta, K. Iwanaga, M. Kakemi, Y. Tabata and Y. Ikada, J. Pharm. Pharmacol. **52**, 611 (2000).

74. R. Alcock, J. A. Blair, D. J. O'Mahony, A. Raoof and A. V. Quirk, J. Control. Release. **82**, 429 (2002).

75. K. Surendrakumar, G. P. Martin, E. C. M. Hodgers, M. Jansen and J. A. Blair, J. Control. Release. **91**, 385 (2003).

76. Y. C. Huang, M. K. Yeh, S.-N. Cheng and C. H. Chiang, J. Microencap. **20**, 459 (2003).

77. Y. C. Huang, A. Vieira, K. L. Huang, M. K. Yeh and C. H. Chiang, J. Biomed. Mater. Res. **75A**, 283 (2005).

78. C. Bosquillon, C. Lombry, V. Préat and R Vanbever, J. Control. Release. **70**, 329 (2001).

79. H. Steckel and H. G. Brandes, Int. J. Pharm. **278**, 187 (2004).

80. B. G. Jones, P. A. Dickinson, M. Gumbleton and I. W. Kellaway, J. Pharm. Pharmacol. **54**, 1065 (2002).

81. V. Sanna, N. Kirschvink, P. Gustin, E. Gavini, I. Roland, L. Delattre and B. Evrard, AAPS PharmsciTech. **5**, 1 (2003).

82. P. O'Hara and A. J. Hickey, Pharm. Res. **17**, 955 (2000).

83. M. Sakagami, W. Kinoshita, K. Sakon, J. Sato and Y. Makino, J. Control. Release. **80**, 207 (2002).

84. V. Codrons, F. Vanderbist, R. K. Verbeeck, M. Arras, D. Lison, V. Préat and R. Vanbever, J. Pharm. Sci. **92**, 938 (2003).

85. K. Tomoda, S. Kojima, M. Kajimoto, D. Watanabe, T. Nakajima and K. Makino, Coll. Surf. B - Biointerfaces. **45**, 1 (2005).

86. Y. F. Maa, P. A. Nguyen, T. Sweeney, S. J. Shire and C. C. Hsu, Pharm. Res. **16**, 249 (1999).

87. M. Skiba, F. Bounoure, C. Barbot, P. Arnaud and M. Skiba, J. Pharm. Pharm. Sci. **8**, 409 (2005).

88. O. C. Chidavaenzi, G. Buckton, F. Koosha and R. Pathak, Int. J. Pharm. **159**, 67 (1997).

89. Y. F. Maa and S. J. Prestrelski, Current Pharm. Biotechnol. **1**, 283 (2000).

90. K. Koushik and U. B. Kompella, Drug Deliv. Technol. **4**, 40 (2004).

91. C. Elvira, A. Fanovich, M. Fernández, J. Fraile, J. San Román and C. Domingo, J. Control. Release. **99**, 231 (2004).

92. H. Schiavone, S. Palakodaty, A. Clark, P. York and S. T. Tzannis, Int. J. Pharm. **281**, 55 (2004).

93. A. R. C. Duarte, M. S. Costa, A. L. Simplício, M. M. Cardoso and C. M. Duarte, Int. J. Pharm. **308**, 168 (2006).

94. D. E. Perrin and J. P. English, in *Handbook of biodegradable polymers* edited A. J. Domb, J. Kost and D. M. Wiseman, Harwood Academic Publishers, New York (1997), p. 3.

95. L. A. Dailey, E. Kleemann, M. Wittmar, T. Gessler, T., Schmehl, C. Roberts, W. Seeger and T. Kissel, Pharm. Res. **20**, 2011 (2003).

96. L. A. Dailey, T. Schmehl, T., Gessler, M. Wittmar, F. Grimminger, W. Seeger and T. Kissel, J. Control. Release. **86**, 131 (2003).

97. M. Schnabelrauch, S. Vogt, Y. Larcher and I. Wilke, Biomol. Eng. **19**, 295 (2002).

98. V. Codrons, F. Vanderbist, B. Ucakar, V. Préat and R. Vanbever, J. Pharm. Sci. **93**, 1241 (2004).

99. S. M. McAllister, H. O. Alpar, Z. Teitelbaum and D. B. Bennett, Adv. Drug Deliv. Rev. **19**, 89 (1996).

100. R. Mitra, I. Pezron, Y. Li and A. K. Mitra, Int. J. Pharm. **217**, 25 (2001).

101. S. I. Rennard, G. Basset, D. Lecossier, K. M. O'Donnell, P. Pinkston, G. P. Martin and R. G. Crystal, J. Appl. Physiol. **60**, 532 (1986).

102. L. Dellamary, D. J. Smith, A. Bloom, S. R. Bot, G. R. Guo, H. Deshmuk, M. Costello and A. I. Bot, J. Control. Release. **95**, 489 (2004).

103. K. Makino, H. Yamamoto, K. Higuchi, N. Harada, H. Ohshima and H. Terada, Colloid Surf. B - Biointerfaces. **27**, 33 (2003).

104. T. Nagai and Y. Machida, in *Bioadhesive drug delivery systems* edited V. Lenaerts and R. Gurny, CRC Press, Boca Raton (1990), p. 169.

105. S. Hirano, H. Seino, Y. Akiyama and I. Nonaka, Polym. Mat. Sci. Eng. **59**, 897 (1988).

106. M. Dornish, A. Hagen, E. Hansson, C. Peucheur, F. Vedier and O. Skaugrud, in *Advances in chitin science* edited A. Domard, G. A. F. Roberts and K. M. Varum, Jacques Andre publisher, Lyon (1997), p. 664.

107. C. M. Lehr, J. A. Bouwstra, E. H. Schacht and H. E. Junginger, Int. J. Pharm. **78**, 43 (1992).

108. P. Artursson, T. Lindmark, S.S. Davis and L. Illum, Pharm. Res. **11**, 1358 (1994).

109. G. Borchard, H. L. Lußen, G. A. De Boer, J. C. Verhoef, C. M. Lehr and H. E. Junginger, J. Control. Release. **39**, 131 (1996).

110. R. Fernández-Urrusuno, P. Calvo, C. Remuñán-López, J. L. Vila-Jato and M. J. Alonso, Pharm. Res. **16**, 1576 (1999).

111. R. Fernández-Urrusuno, D. Romani, P. Calvo, J. L. Vila-Jato and M. J. Alonso, S. T. P. Pharm. Sci. **9**, 429 (1999).

112. A. de Campos, A. Sanchez and M. J. Alonso, Int. J. Pharm. **224**, 159 (2001).

113. H. Yamamoto, Y. Kuno, S. Sugimoto, H. Takeuchi, and Y. Kawashima, J. Control. Release. **102**, 373 (2005).

114. R. A. A. Muzzarelli, in *The polysaccharides* edited G. O. Aspinall, Academic Press, Orlando (1985), p. 417.

115. R. A. A. Muzzarelli, Cell. Mol. Life Sci. **53**, 131 (1997).

116. H. Okamoto, S. Nishida, H. Todo, Y. Sakakura, K. Iida and K. Danjo, J. Pharm. Sci. **92**, 371 (2003).

117. Y. C. Huang, M. K. Yeh and C. H. Chiang, Int. J. Pharm. **242**, 239 (2002).

118. M. Bivas-Benita, K. E. van Meijgaarden, K. L. Franken, H. E. Junginger, G. Borchard, T. H. Ottenhoff and A. Geluk, Vaccine. **22**, 1609 (2004).

119. M. Huang, E. Khor and L.-Y. Lim, Pharm. Res. **21**, 344 (2004).

120. H. Okamoto, M. Aoki and K. Danjo, J. Pharm. Sci. **89**, 1028 (2000).

121. D. McPhail, L. Tetley, C. Dufes and I. F. Uchegbu, Int. J. Pharm. **200**, 73 (2000).

122. A. R. Pohlmann, V. Weiss, O. Mertins, N. P. Silveira and S. S. Guterres, Eur. J. Pharm. Sci. **16**, 305 (2002).

123. K. A. Janes, P. Calvo and M. J. Alonso, Adv. Drug Deliv. Rev. **47**, 83 (2001).

124. S. A. Agnihotri, N. N. Mallikarjuna and T. M. Aminabhavi, J. Control. Release. **100**, 5 (2004).

125. M. J. Alonso and A. Sanchez, in *Carrier-based drug delivery* edited S. Svenson, American Chemical Society, New York (2004) p. 283.

126. P. Jani, G. W. Halbert, J. Langridge and A. T. Florence, J. Pharm. Pharmacol. **42**, 821 (1990).

127. M. P. Desai, V. Labhasetwar, G. L. Amidon and R. J. Levy, Pharm. Res. **13**, 1838 (1996).

128. S. Schurch, P. Gehr, V. Im Hof, M. Geiser and F. H. Y. Green, Respir. Physiol. **80**, 17 (1990).

129. M. Huang, M. Zengshuan, E. Khor and L.–Y. Lim, Pharm. Res. **19**, 1488 (2002).

130. S. Akhtar and K. J. Lewis, Int. J. Pharm. **151**, 57 (1997).

131. S. Rudt and R. H. Müller, J. Control. Release. **22**, 263 (1992).

132. Y. Kawashima, T. Serigano, T. Hino, H. Yamamoto and H. Takeuchi, Pharm. Res. **15**, 1748 (1998).

133. Y. Kawashima, H. Yamamoto, H. Takeuchi, S. Fujioka and T. Hino, J. Control. Release. **62**, 279 (1999).

134. H. Kikuchi, H. Yamauchi and S. Hirota, Chem. Pharm. Bull. **39**, 1522 (1991).

135. T. R. Desai, R. E. W. Hancock and W. H. Finlay, Eur. J. Pharm. Sci. **20**, 459 (2003).

136. W. F. Wolkers, H. Oldenhof, F. Tablin and J. H. Crowe, Biochim. Biophys. Acta. **1661**, 125 (2004).

137. R. Pandey, A. Sharma, A. Zahoor, S. Sharma, G. K. Khuller and B. Prasad, J. Antimicrob. Chemother. **52**, 981 (2003).

138. Y. Mo and L.- Y. Lim, J. Control. Release. **107**, 30 (2005).

139. O. N. M. McCallion, K. M. G. Taylor, M. Thomas and A. J. Taylor, Int. J. Pharm. **133**, 203 (1996).

140. M. Dittgen, M., Durrani and K. Lehmann, S. T. P. Pharm. Sci. **7**, 403 (1997).

141. E. Fattal, M. T. Peracchia and P. Couvreur, in *Handbook of biodegradable polymers* edited A. J. Domb, J. Kost, D. M. Wiseman, Harwood Academic Publishers, New York (1997), p. 183.

142. B. Seijo, E. Fattal, L. Roblot-Treupel and P. Couvreur, Int. J. Pharm. **62**, 1 (1990).

143. M. Brzoska, K. Langer, C. Coester, S. Loitsch, T. O. F. Wagner and C. V. Mallinckrodt, Biochem. Biophys. Res. Com. **318**, 562 (2004).

144. Q. Zhang, Z. Shen and T. Nagai, Int. J. Pharm. **218**, 75 (2001).

145. C. Schwarz, W. Mehnert, J. S. Lucks and R. H. Müller, J. Control. Release. **30**, 83 (1994).

146. R. H. Müller, K. Mäder and S. Gohla, Eur. J. Pharm. Biopharm. **50**, 161 (2000).

147. M. A. Videira, M. F. Botelho, A. C. Santos, L. F. Gouveia, J. J. P. Lima and A. J. Almeida, J. Drug Target. **10**, 607 (2002).

148. P. A. Dickinson, S. W. Howells and I. W. Kellaway, J. Drug Target. **9**, 295 (2001).

149. P. Calvo, C. Remuñan-Lopez, J. L. Vila-Jato and M. J. Alonso, J. App. Polym. Sci. **63**, 125 (1997).

150. A. Vila, A. Sanchez, C. Perez and M. J. Alonso, Polym. Adv. Technol. **13**, 851 (2002).

151. G. Carlesso, E. Kozlov, A. Prokop, D. Unutmaz and J. M. Davidson, Biomacromolecules. **6**, 1185 (2005).

152. S. P. Vyas, A. Singh and V. Sihorkar, Crit. Rev. Ther. Drug Carr. Syst. **18**, 1 (2001).

153. M. Kumar, A. K. Behera, R. F. Lockey, J. Zhang, G. Bhullar, C. P De la Cruz, L. C. Chen and K. W. Leong, Hum. Gene Ther. **13**, 1415 (2002).

154. M. Koping-Hoggard, K. M. Varum, M. Issa, S. Danielsen, B. E. Christensen, B. T. Stokke and P. Artursson, Gene Ther. **11**, 1441 (2004).

155. W. Zhang, H. Yang, X. Kong, S. Mohapatra, H. San Juan-Vergara, G. Hellermann, S. Behera, R. Singam, R. F. Lockey, S. S. Mohapatra, Nat. Med. **11**, 56 (2005).

156. F. C. MacLaughlin, R. J. Mumper, J. Wang, J. M. Tagliaferri, I. Gill, M. Hinchcliffe and A. P. Rolland, J. Control. Release. **56**, 259 (1998).

157. M. Koping-Hoggard, I. Tubulekas, C. Y. Guan, K. Edwards, M. Nilsson, K. M. Varum and P. Artursson, Gene Ther. **8**, 1108 (2001).

158. K. W. Leong, H. Q. Mao, V. L. Truong-Le, K. Roy, S. M. Walsh and J. T. August, J. Control. Release. **53**, 183 (1998).

159. M. Kumar, X. Kong, A. K. Behera, G. R. Hellermann, R. F. Lockey and S. S. Mohapatra, Genet. Vaccines Ther. **1**, 3 (2003).

160. A. Bozkir and O. M. Saka, Drug Delivery. **11**, 107 (2004).

161. K. Y. Lee, I. C. Kwon, Y. H. Jo and S. Y. Jeong, J. Control. Release. **51**, 213 (1998).

162. H. S. Yoo, J. E. Lee, H. Chung, I. C. Kwon and S. Y. Jeong, J. Control. Release. **103**, 235 (2005).

163. M. Köping-Hóggard, N. Csaba and M. J. Alonso (submitted)

164. S. G. Antimisiaris, P. Jayasekera and G. Gregoriadis, J. Immunol. Methods. **166**, 271 (1993).

165. J. Arrault, C. Grand, W. C. K. Poon and M. E. Cates, Europhys. Lett. **38**, 625 (1997).

166. J. O. Sham, Y. Zhang, W. H. Finlay, W. H. Roa and R. Löbenberg, Int. J. Pharm. **269**, 457 (2004).

167. R. O. Cook, R. K. Pannu and I. W. Kellaway, J. Control. Release. **104**, 79 (2005).

Parte Experimental

Antecedentes, hipótesis y objetivos

ANTECEDENTES

Del trabajo de revisión presentado como introducción de esta memoria, se puede destacar:

1. La administración de medicamentos por vía pulmonar ha sido, en los últimos años, objeto de gran atención, ya que se presenta como una alternativa muy interesante para la administración no invasiva de macromoléculas terapéuticas con fines sistémicos. Ofrece la ventaja de que la absorción se produce con rapidez, dada la elevada irrigación, permeabilidad y superficie de absorción del epitelio alveolar, evitándose además, el efecto de primer paso hepático y la degradación gastrointestinal asociada a la vía oral (Clark, 2002; Courrier y col., 2002). Todo ello se traduce en una mejora de la biodisponibilidad de las macromoléculas administradas por vía pulmonar.

2. La formulación de macromoléculas terapéuticas en forma de polvos con características adecuadas para inhalación, ofrece ventajas desde el punto de vista de su estabilidad, en comparación con las disoluciones de las mismas, así como también de manipulación de la dosis por parte del paciente (Taylor y Kellaway, 2001; Clark, 2002, Smith, 2002).

3. Las microsferas son vehículos particularmente interesantes para la administración pulmonar de principios activos, debido a la posibilidad de modular sus propiedades para adaptarlas al objetivo final que se persigue en este tipo de administración, que no es otro que vencer los mecanismos de defensa del pulmón (recodo orofaríngeo, aclaramiento mucociliar, macrófagos alveolares) y lograr su depósito en las zonas más profundas del mismo. En este sentido, la composición y el método de producción del sistema son factores clave para obtener microsferas morfológica y aerodinámicamente adecuadas, que garanticen que toda la dosis pueda llegar al lugar de acción deseado. De esta manera disminuirá tanto el número de dosis necesarias para obtener el mismo efecto, como también

los efectos secundarios (Edwards y col., 1998; Vanbever y col., 1999). Si el objetivo final de la administración es obtener una absorción sistémica, el diámetro aerodinámico de las microsferas debe situarse entre 1 y 5 μm (Taylor y Kellaway, 2001), lo que permitirá que alcancen y se depositen en los alvéolos.

4. Las nanopartículas poliméricas han sido propuestas como vehículos adecuados para el transporte de macromoléculas terapéuticas hacía el epitelio pulmonar, evitando su eliminación precoz tanto por el aclaramiento mucociliar como por mecanismos fagocíticos (Schurch y col., 1990; Makino y col., 2003). Además, en algunos casos, se ha comprobado su capacidad para ser captadas por células epiteliales bronquiales y alveolares (Dailey y col., 2003; Mo y Lim, 2004).

5. El quitosano es un polisacárido de origen natural que ha sido objeto de una creciente atención, en particular por su capacidad para actuar como vehículo de macromoléculas terapéuticas a través de superficies mucosas. Propiedades como la biocompatibilidad, baja toxicidad y biodegradabilidad (Hirano y col., 1988; Dornish y col., 1997), así como su carácter mucoadhesivo (Lehr y col., 1992) y el efecto promotor de la absorción a través de distintas mucosas, entre las que se incluye la pulmonar (Florea y col., 2005; Yamamoto y col., 2005; Yamada y col., 2005), han convertido a este biopolímero en un excelente candidato para el desarrollo de nuevos sistemas de administración de fármacos a nivel de mucosas. Nuestro grupo de investigación ha desarrollado un método simple y rápido de gelificación iónica para la obtención de nanopartículas de quitosano/tripolifosfato, que se basa en la interacción iónica entre los grupos amino cargados positivamente del quitosano y el contra-ión tripolifosfato. Estas nanopartículas han demostrado poseer una excelente capacidad para asociar proteínas, así como también para incrementar su absorción a través de distintas mucosas como la nasal, intestinal y ocular (Fernández-Urrusuno y col., 1999a, b; De Campos y col., 2001; Vila y col., 2002), resultando significativamente más eficaces que las disoluciones del polímero.

6. La incorporación de lípidos en las formulaciones destinadas a la administración pulmonar, se ha revelado como una alternativa de gran interés, debido a su posible interacción con los fosfolípidos endógenos del pulmón, que presumiblemente promoverá la absorción de las macromoléculas asociadas y reducirá la captación de los vehículos por parte de los macrófagos (McAllister y col., 1996; Evora y col., 1998; Mitra y col., 2001; Jones y col., 2002; Hussain y col., 2004).

7. La combinación de dos o más sistemas de administración (nanopartículas, micropartículas, vesículas lipídicas, etc.), permite integrar en un mismo vehículo las ventajas de cada uno de ellos por separado, eliminando sus potenciales limitaciones (Antimisiaris y col., 1993; Kawashima y col., 1998; McPhail y col., 2000). Así, por ejemplo, se propuso el recubrimiento de nanopartículas de cisplatino con fosfolípidos como una alternativa novedosa para el tratamiento del cáncer al permitir la internalización del sistema en las células por endocitosis; mientras que la encapsulación de nanopartículas de quitosano conteniendo albúmina en vesículas lipídicas, se planteó para la inmunización por vía oral (Chupin y col., 2004; Jain y col., 2006). Asimismo, se investigó la encapsulación de nanopartículas en microsferas como alternativa para mejorar la eficacia de inhalación de las nanopartículas (Tsapis y col., 2002; Sham y col., 2004; Cook y col., 2005). Hasta la fecha, no se ha descrito ningún sistema basado en la producción de microsferas que contengan nanopartículas de quitosano o complejos de lípidos y nanopartículas de quitosano, que resulte adecuado para la administración pulmonar de péptidos y proteínas terapéuticas.

HIPÓTESIS

1. Los biomateriales hidrofílicos - como el polisacárido quitosano - y lipofílicos - como los fosfolípidos endógenos dipalmitoilfosfatidilcolina (DPPC) y dimiristoilfosfatidilglicerol (DMPG) -, dada su biocompatibilidad, baja toxicidad y sus propiedades promotoras de la absorción, son materiales particularmente interesantes para la administración pulmonar de macromoléculas terapéuticas con fines sistémicos.

2. El quitosano y los fosfolípidos permitirán obtener sistemas coloidales de liberación, como nanopartículas de quitosano o complejos de lípidos y nanopartículas de quitosano, con distintas características, recurriendo a técnicas de preparación muy sencillas y suaves y, por lo tanto, adecuadas para la incorporación de macromoléculas terapéuticas.

3. La técnica de atomización permitirá microencapsular nanopartículas de quitosano o sistemas combinados de lípidos y nanopartículas de quitosano, obteniéndose microsferas con propiedades morfológicas y aerodinámicas adecuadas (diámetro aerodinámico comprendido entre 1 y 5 µm) para depositarse en la zona alveolar, tras su administración por vía pulmonar.

4. La selección del manitol como excipiente para la formación de las microsferas por atomización, proporcionará un soporte inerte y altamente soluble en medio acuoso, que previsiblemente permitirá la rápida liberación de los sistemas coloidales microencapsulados y, en consecuencia, de la proteína asociada a los mismos, una vez que se haya producido el contacto de las microsferas con el fluido pulmonar.

OBJETIVOS

Teniendo en cuenta los aspectos anteriormente comentados, así como las hipótesis de partida que se acaban de plantear, el objetivo global de esta Tesis se ha dirigido al desarrollo de sistemas microparticulares conteniendo nanopartículas de quitosano o complejos de nanopartículas de quitosano y lípidos, destinados a la administración sistémica de péptidos y proteínas por vía pulmonar.

Para cumplir este objetivo, el trabajo se ha planteado en una serie de etapas que, a fin de facilitar el seguimiento de esta memoria, se especifican a continuación junto con sus correspondientes objetivos parciales.

Sección I. Preparación y evaluación del comportamiento *in vitro* de microsferas de manitol conteniendo nanopartículas de quitosano

El objetivo de esta etapa ha sido el diseño de microsferas de manitol con propiedades morfológicas y aerodinámicas adecuadas para su administración por vía pulmonar y para su depósito a nivel alveolar, que contienen nanopartículas de quitosano, previamente preparadas por gelificación iónica entre el quitosano y el tripolifosfato pentasódico (TPP). Para conseguir este objetivo, se utilizó la técnica de atomización y se evaluó la influencia de distintas variables (relación manitol/nanopartículas, concentración final de sólidos) sobre las características finales de los sistemas desarrollados. Asimismo, se asociaron dos proteínas modelo a las nanopartículas, la insulina y la albúmina de suero bovino marcada con fluoresceína (FITC-BSA), investigando la influencia del procedimiento de atomización sobre las características físico-químicas de las nanopartículas microencapsuladas y sobre el perfil de liberación. Además, se analizó en detalle la estructura del sistema combinado "*microsferas conteniendo nanopartículas*", recurriendo para ello a técnicas como la microscopía confocal, espectroscopía de fotoelectrones de Rayos X (XPS) y espectrometría de masas de iones secundarios por tiempo de vuelo (TOF-SIMS).

Los resultados del trabajo desarrollado se recogen en el **Artículo 2**: "*Microencapsulated chitosan nanoparticles for lung protein delivery*" (publicado en *European Journal of Pharmaceutical Sciences* 25 (2005) 427-437) y en el **Artículo 3**: "*Chitosan nanoparticle-loaded microspheres: structure and surface characterisation*" (sometido a evaluación por *Macromolecules*).

Sección II. Producción y caracterización del comportamiento *in vitro* de microsferas de manitol conteniendo complejos de lípidos y nanopartículas de quitosano

El objetivo que nos planteamos en esta etapa ha consistido en el desarrollo y optimización de las condiciones de elaboración de sistemas complejos formados por nanopartículas de quitosano y lípidos, y en la producción de microsferas conteniendo los referidos sistemas; buscando igualmente que presenten características morfológicas y aerodinámicas adecuadas para la administración pulmonar. Para ello, se seleccionaron dos fosfolípidos endógenos del pulmón - la dipalmitoilfosfatidilcolina (DPPC) y el dimiristoilfosfatidilglicerol (DMPG) - y se recurrió al método de hidratación del film lipídico, utilizando una suspensión de nanopartículas de quitosano, en lugar de agua, para producir los complejos. Las microsferas fueron preparadas igualmente por un procedimiento de atomización, utilizando el manitol como excipiente portador. Se evaluaron las propiedades morfológicas y aerodinámicas de las microsferas, así como la influencia de la composición lipídica y del proceso de atomización sobre las propiedades físico-químicas de los complejos lípido/nanopartículas y sobre el perfil de liberación del péptido modelo insulina asociado a las nanopartículas de quitosano. Además, la composición superficial de los complejos fue exhaustivamente investigada, utilizando las técnicas de espectroscopía de fotoelectrones de Rayos X (XPS) y espectrometría de masas de iones secundarios por tiempo de vuelo (TOF-SIMS).

Los resultados obtenidos en el trabajo realizado para alcanzar este objetivo se recogen en el **Artículo 4**: "*Microspheres containing lipid/chitosan nanoparticles complexes for pulmonary delivery of therapeutic proteins*" (sometido a evaluación

por *European Journal of Pharmaceutics and Biopharmaceutics*) y en el **Artículo 5**: "*Surface characterisation of lipid/chitosan nanoparticles assemblies, using XPS and TOF-SIMS*" (en preparación para someter a evaluación por *Journal of the American Chemical Society*).

Sección III. Estudio del comportamiento *in vitro* de las microsferas de manitol conteniendo nanopartículas de quitosano en cultivos de células Calu-3 y A549

El objetivo de este estudio ha sido investigar el comportamiento de las microsferas de manitol conteniendo nanopartículas de quitosano, en dos líneas celulares pulmonares de origen humano, una bronquial (Calu-3) y otra alveolar (A549). Para ello, se analizó el efecto de las microsferas sobre la viabilidad celular, así como sobre la integridad de las uniones intercelulares. Finalmente, se investigó la interacción de los sistemas con las células, usando la técnica de microscopia confocal.

Los resultados del trabajo correspondiente a esta etapa se recogen en el **Artículo 6** "*Chitosan nanoparticle-containing microspheres are compatible with respiratory epithelial cells in vitro*" (sometido a evaluación por *Biomaterials*).

Sección IV. Evaluación preliminar *in vivo* de las microsferas de manitol conteniendo nanopartículas de quitosano, en ratas

El objetivo de este estudio ha consistido en investigar la distribución de las microsferas en el pulmón, así como la absorción pulmonar de un péptido modelo encapsulado en las mismas. La distribución de las microsferas en pulmón tras la administración intratraqueal a ratas de microsferas conteniendo nanopartículas cargadas con FITC-BSA, fue investigada cualitativamente, utilizando la técnica de microscopía confocal. La absorción pulmonar fue evaluada utilizando nanopartículas conteniendo insulina microencapsuladas y midiendo la respuesta hipoglucémica a distintos tiempos.

Los resultados obtenidos a partir de estos estudios, se recogen en una sección específica de esta memoria (**Sección IV**).

Referencias bibliográficas

Antimisiaris, S.G., Jayasekera, P., Gregoriadis, G., 1993. Liposomes as vaccine carriers. Incorporation of soluble and particulate antigens in giant vesicles. J. Immunol. Methods. 166, 271-280.

Chupin, V., de Kroon, A.I.P.M., de Kruijff, B., 2004. Molecular architecture of nanocapsules, bilayer-enclosed solid particles of cisplatin. JACS. 126, 13816-13821.

Clark, A., 2002. Formulation of proteins and peptides for inhalation. Drug Deliv. Syst. Sci. 2, 73-77.

Cook, R.O., Pannu, R.K., Kellaway, I.W., 2005. Novel sustained release microspheres for pulmonary drug delivery. J. Control. Release. 104, 79-90.

Courrier, H.M., Butz, N., Vandamme, T.F., 2002. Pulmonary drug delivery systems: recent developments and prospects. Crit. Rev. Ther. Drug Carr. Syst. 19, 425-498.

Dailey, L.A., Schmehl, T., Gessler, T., Wittmar, M., Grimminger, F., Seeger, W., Kissel, T., 2003. Nebulization of biodegradable nanoparticles: impact of nebulizer technology and nanoparticle characteristics on aerosol features. J. Control. Release. 86, 131-144.

De Campos, A., Sanchez, A., Alonso, M.J., 2001. Chitosan nanoparticles: a new vehicle for the improvement of the delivery of drugs to the ocular surface. Application to cyclosporin A. Int. J. Pharm. 224, 159-168.

Dornish, M., Hagen, A., Hansson, E., Peucheur, C., Vedier, F., Skaugrud, O., 1997. Safety of Protasan™: Ultrapure chitosan salts for biomedical and pharmaceutical use. In: Domard, A., Roberts, G. A. F., Varum, K. M. (Eds.), Advances in chitin science. Jacques Andre publisher, Lyon, pp. 664-670.

Edwards, D.A., Ben-Jebria, A., Langer, R., 1998. Recent advances in pulmonary drug delivery using large, porous inhaled particles. J. Appl. Physiol. 84, 379-385.

Evora, C., Soriano, I., Rogers, R.A., Shakesheff, K.M., Hanes, J., Langer, R., 1998. Relating the phagocytosis of microparticles by alveolar macrophages to surface chemistry: the effect of 1,2-dipalmitoylphosphatidylcholine. J. Control. Release. 51, 143-152.

Fernandez-Urrusuno, R., Calvo, P., Remuñan-Lopez, C., Vila-Jato, J. L., Alonso, M. J., 1999a. Enhancement of nasal absorption of insulin using chitosan nanoparticles. Pharm. Res. 16, 1576-1581.

Fernandez-Urrusuno, R., Romani, D., Calvo, P., Vila-Jato, J.L., Alonso, M.J., 1999b. Development of a freeze-dried formulation of insulin-loaded chitosan nanoparticles intended for nasal administration. S. T. P. Pharm. Sci. 9, 429-436.

Florea, B.I., Thanou, M., Junginger, H.E., Borchard, G., 2005. Enhancement of bronchial octreotide absorption by chitosan and *N*-trimethylchitosan shows linear in vitro/in vivo correlation. J. Control. Release. 110, 353-361.

Hirano, S., Seino, H., Akiyama, Y., Nonaka, I., 1988. Biocompatibility of chitosan by oral and intravenous administrations. Polym. Mater. Sci. Eng. 59, 897-901.

Hussain, A., Arnold, J.J., Khan, M.A., Ahsan, F., 2004. Absorption enhancers in pulmonary protein delivery. J. Control. Release. 94, 15-24.

Jain, S., Sharma, R.K., Vyas, S.P., 2006. Chitosan nanoparticles encapsulated vesicular systems for oral immunization: preparation, in-vitro and in-vivo characterization. J. Pharm. Pharmacol. 58, 303-310.

Jones, B.G., Dickinson, P.A., Gumbleton, M., Kellaway, I.W., 2002. Lung surfactant phospholipids inhibit the uptake of respirable microspheres by the alveolar macrophage NR8383. J. Pharm. Pharmacol.. 54, 1065-1072.

Kawashima, Y., Serigano, T., Hino, T., Yamamoto, H., Takeuchi, H., 1998. A new powder design method to improve inhalation efficiency of pranlukast hydrate dry powder aerosols by surface modification with hydroxypropylmethylcellulose phthalate nanospheres. Pharm. Res. 15, 1748-1752.

Lehr, C.M., Bouwstra, J.A., Schacht, E.H., Junginger, H.E., 1992. In vitro evaluation of mucoadhesive properties of chitosan and some other natural polymers. Int. J. Pharm. 78, 43-48.

Makino, K., Yamamoto, H., Higuchi, K., Harada, N., Ohshima, H., Terada, H., 2003. Phagocytic uptake of polystyrene microspheres by alveolar macrophages: effects of the size and surface properties of the microspheres. Colloids Surf. B - Biointerfaces. 27, 33-39.

McAllister, S.M., Alpar, H.O., Teitelbaum, Z., Bennett, D.B., 1996. Do interactions with phospholipids contribute to the prolonged retention of polypeptides within the lung? Adv. Drug Deliv. Rev. 19, 89-110.

McPhail, D., Tetley, L., Dufes, C., Uchegbu, I.F., 2000. Liposomes encapsulating polymeric chitosan based vesicles - a vesicle in vesicle system for drug delivery. Int. J. Pharm. 200, 73-86.

Mitra, R., Pezron, I., Li, Y., Mitra, A.K., 2001. Enhanced pulmonary delivery of insulin by lung lavage fluid and phospholipids. Int. J. Pharm. 217, 25-31.

Mo, Y., Lim, L.-Y., 2004. Mechanistic study of the uptake of wheat germ agglutinin-conjugated PLGA nanoparticles by A549 cells. J. Pharm. Sci. 93, 20-28.

Schurch, S., Gehr, P., Im Hof, V., Geiser, M., Green, F.H.Y., 1990. Surfactant displaces particles toward the epithelium in airways and alveoli. Respir. Physiol. 80, 17-32.

Sham, J.O., Zhang, Y., Finlay, W.H., Roa, W.H., Löbenberg, R., 2004. Formulation and characterization of spray-dried powders containing nanoparticles for aerosol delivery to the lung. Int. J. Pharm. 269, 457-467.

Smith, I.J., 2002. Developments in inhalation technology. Drug Deliv. Syst. Sci. 2, 63-65.

Taylor, G., Kellaway, I., 2001. Pulmonary drug delivery. In: Hillery, A., Lloyd, A., Swarbrick, J. (Eds.), Drug delivery and targeting. For pharmacists and pharmaceutical scientists. Taylor & Francis, New York, pp. 269-300.

Tsapis, N., Bennett, D., Jackson, B., Weitz, D.A., Edwards, D.A., 2002. Trojan particles: large porous carriers of nanoparticles for drug delivery. Proc. Nat. Acad. Sci. 99, 12001-12005.

Vanbever, R., Ben-Jebria, A., Mintzes, J., Langer, R., Edwards, D.A., 1999. Sustained release of insulin from insoluble inhaled particles. Drug Develop. Res. 48, 178-185.

Vila, A., Sánchez, A., Tobío, M., Calvo, P., Alonso, M.J., 2002. Design of biodegradable particles for protein delivery. J. Control. Release. 78, 15-24.

Yamada, K., Odomi, M., Okada, N., Fujita, T., Yamamoto, A., 2005. Chitosan oligomers as potential and safe absorption enhancers for improving the pulmonary absorption of Interferon-a in rats. J. Pharm. Sci. 94, 2432-2440.

Yamamoto, H., Kuno, Y., Sugimoto, S., Takeuchi, H., Kawashima, Y., 2005. Surface-modified PLGA nanosphere with chitosan improved pulmonary delivery of calcitonin by mucoadhesion and opening of the intercellular tight junctions. J. Control. Release. 102, 373-381.

Sección I. Preparación y evaluación del comportamiento *in vitro* de microsferas de manitol conteniendo nanopartículas de quitosano

Artículo 2

MICROENCAPSULATED CHITOSAN NANOPARTICLES FOR LUNG PROTEIN DELIVERY

Ana Grenha, Begoña Seijo, Carmen Remuñán-López*

Dept. of Pharmacy and Pharmaceutical Technology, University of Santiago de Compostela, Faculty of Pharmacy, Campus Sur, 15782 Santiago de Compostela, Spain.

* Corresponding author: Phone: 0034 981 563100 – ext. 15405

Fax: 0034 981 547148

E-mail: ffcarelo@usc.es

Artículo publicado en "European Journal of Pharmaceutical Sciences. 25 (2005) 427-437"

Abstract

It has already been demonstrated that spray-drying is a very valuable technique for producing dry powders adequate for pulmonary delivery of drugs. We have developed chitosan/tripolyphosphate nanoparticles that promote peptide absorption across mucosal surfaces. The aim of this work was to microencapsulate protein-loaded chitosan nanoparticles using typical aerosol excipients such as mannitol and lactose, producing microspheres as carriers of protein loaded nanoparticles to the lung. The results showed that the obtained microspheres are mostly spherical and possess appropriate aerodynamic properties for pulmonary delivery (aerodynamic diameters between 2 and 3 μm, apparent density lower than 0.45 g/cm^3). Moreover, microspheres morphology was strongly affected by the content of chitosan nanoparticles. These nanoparticles have shown a good protein loading capacity (65-80%), providing the release of 75-80% insulin within 15 minutes, and can be easily recovered from microspheres after contact with an aqueous medium, with no significant changes in their size and zeta potential values. Therefore, this work demonstrated that protein-loaded nanoparticles can be successfully incorporated into microspheres with adequate characteristics to reach the deep lung, which after contact with its aqueous environment are expected to be able to release the nanoparticles and, thus, the therapeutic macromolecule.

Keywords: Chitosan nanoparticles, dry powders, ionic gelation, microspheres, pulmonary protein delivery, spray-drying

1. Introduction

Over the last few years, absorption of therapeutic macromolecules administered by pulmonary route has received great attention. The large alveolar surface area suitable for drug absorption, low thickness epithelial barrier, extensive vascularization and relatively low proteolytic activity compared to other administration routes, together with the absence of the first-pass effect, make the pulmonary delivery of peptides and proteins an outstanding target (Patton and Platz, 1992; Clark, 2002; Courrier et al., 2002). The prerequisite for reliable and specific lung protein delivery is the design of adequate carrier systems.

Microspheres have recently been proposed for pulmonary administration, once they can be designed to achieve appropriate morphological and aerodynamic characteristics for that purpose. The success of the inhaled particles depends mostly on their size and density and, hence, aerodynamic diameter (Taylor and Kellaway, 2001). The respirable fraction of these powders, generally the fraction of particles with an aerodynamic diameter ranging from 1 to 5 μm, should be as high as possible to guarantee a maximum deposition in the deep lung (Bosquillon et al., 2001a).

Independently of the method used to produce the aerosol, before reaching the deep lung, inhaled particles must overcome certain obstacles and lung defence mechanisms, essentially the effect of the airways structure and the mucus layer, which protects the epithelium in the tracheobronchial region. Particles targeted to the deep lung should be small enough to pass through the mouth, throat and conducting airways and reach the deep lung, but not so small that they fail to deposit and are breathed out again. Therefore, they should have an aerodynamic diameter between 1 and 5 μm. Even so, a certain number of particles will be transported away from the lung by mucociliary clearance (Rios et al., 1994; Gehr et al., 1996; Clark, 2002; Courrier et al., 2002). Once in the deep lung, particles will have to face at least two other defense mechanisms: the alveolar macrophages and the enzymatic activity. The alveolar surface is covered by a thin layer of fluid with suspended macrophages, which play an important role in lung defence. With the capacity of moving freely in the surface, they are able to engulf “foreign” substances from the airway surface, eliminating potential

damaging agents (Clark, 2002; Courrier et al., 2002). There is no consensus concerning the ideal size range to avoid or delay macrophages phagocythosis. However, it has been reported that the phagocytic activity is maximum for particles of 1-2 μm, decreasing for both smaller and larger particles out of this range (Aktar and Lewis, 1997; Ahsan et al., 2002; Makino et al., 2003); and generally, all authors agree that, for particles in the micrometer range, the smaller the particle size, the higher is the probability of being captured (Rudt and Müller, 1992; Ahsan et al., 2002). Concerning the second defence mechanism (enzymatic activity), it is known that the lung presents a lower enzymatic activity when compared to other mucosal surfaces, such as the gastric (Evora et al., 1998). However, some enzymes have already been identified, as protease inhibitors, isozymes of the cytochrome P-450 family and lysozyme (Patton and Platz, 1992; Duszyk, 2001). This is a 14.5 KD cationic enzyme (Duszyk, 2001), which is synthesized and released by the human surface epithelial cells, as well as pulmonary alveolar macrophages (Konstan et al., 1981). Secreted in large quantities in human airways (10-20 mg/day), lysozyme is able to hydrolyze chitins, which presents β-(1-4) glycosidic bonds between glucosamine (Muzzarelli, 1997).

Nanoparticles (size within the nanometer range) have recently been proposed as valuable vehicles for efficient drug transport to the lung epithelium while avoiding unwanted mucociliary clearance and phagocytic mechanisms (Schurch et al., 1990; Makino et al., 2003). However, nanoparticles utility for pulmonary application is severely hindered because of their low inertia, due to their excessively small dimensions and mass, which causes them to escape from lung deposition and be predominantly exhaled (Heyder et al., 1986; Finlay et al., 1997; Finlay and Gehmlich, 2000; Clark, 2002). Furthermore, their small size leads to particle-particle aggregation, making physical handling of nanoparticles difficult in liquid and dry powder forms. To solve these limitations, the production of spray-dried powders containing nanoparticles which dissolve in the lungs into polymeric nanoparticles whose dimensions are sufficiently small to avoid mucociliary and phagocytic clearance until the particles have delivered their therapeutic payload has been recently reported (Kawashima et al., 1998; Pohlmann et al., 2002; Tsapis et al., 2002; Sham et al., 2004). In this respect,

once reaching the alveolar epithelium, large biotechnology molecules might not be able to cross it. Therefore, an ideal lung carrier protein system should allow the enhancement of protein absorption as well (Heinemann et al., 2000).

Chitosan (CS) is a polysaccharide with well-documented relevant properties as biocompatibility, low toxicity and biodegradability (Hirano et al., 1988; Dornish et al., 1997). Furthermore it is mucoadhesive (Lehr et al., 1992) and has the capacity of promoting macromolecules permeation through well organized epithelia (Artursson et al., 1994; Borchard et al., 1996; De Campos et al., 2001; Portero et al., 2002). Obtained from the deacetylation of chitin, CS is formed of D-glucosamine and N-acetilglucosamine units (Muzzarelli, 1985), whose unions can be destroyed, as previously mentioned, by pulmonary lysozyme (Muzzarelli, 1997). We have recently reported the preparation of chitosan/tripolyphosphate (CS/TPP) nanoparticles via an extremely mild and rapid ionotropic gelation procedure with the counter-ion sodium TPP (Calvo et al., 1997a). These nanoparticles have shown an excellent capacity for protein entrapment and an improvement of peptide absorption by several mucosal routes, such as the nasal and ocular (Fernández-Urrusuno et al., 1999a, b; De Campos et al., 2001). Furthermore, microspheres were obtained by spray-drying these CS/TPP nanoparticles with no additional excipients. They were compatible with the hydrofluoralkane propellant P134a and, therefore, good candidates for lung delivery via pressurized metered dose inhalers (pMDI) (Williams et al., 1998).

In this work, we report the preparation and characterization of dry powders containing protein-loaded CS/TPP nanoparticles using typical aerosol excipients. For these purposes, we chose bovine insulin as model protein to be associated to nanoparticles and used mannitol and lactose as excipients. These carbohydrates are approved by the Food and Drug Administration (FDA) and other regulatory organisms for inhalation purposes (Bosquillon et al., 2001a) due to their non-toxic and readily degradable properties after administration. Microencapsulated protein-loaded CS/TPP nanoparticles were prepared using a spray-drying technique; their aerodynamic properties were characterized and their ability to deliver the nanoparticles and afterwards, the therapeutic macromolecule was evaluated “in vitro”. Based on the previous considerations and acquired

knowledge about the CS/TPP nanoparticles benefits by other administration routes, we hypothesized that these microspheres, with an aerodynamic diameter between 1 and 5 μm, once inhaled are expected to reach and deposit in the deep lung, where the carrier carbohydrate will dissolve, delivering the nanoparticles, which will then promote the absorption of the associated therapeutic macromolecule.

2. Materials and methods

2.1. Chemicals

Chitosan (CS) in the form of hydrocloride salt (Protasan® 213 Cl, deacetylation degree = 86%, viscosity = 95 mPa) was purchased from Pronova Biopolymer, A.S. (Norway). Pentasodium tripolyphosphate (TPP), glycerol, D-mannitol (Ma), bovine insulin (Mw = 5.7 KD), lysozyme from egg white and phosphate buffered saline tablets (PBS) pH 7.4 were supplied by Sigma Chemicals Co. (USA). α-lactose monohydrate (La) was a kind gift from Meggle (Germany). Ultrapure water (MilliQ Plus, Millipore Ibérica, Spain) was used throughout. All other chemicals were reagent grade.

2.2. Preparation of chitosan nanoparticles

Chitosan/tripolyphosphate (CS/TPP) nanoparticles were prepared according to the procedure developed by our group, based on the ionotropic gelation of CS with TPP (Calvo et al, 1997a). Briefly, CS and TPP were dissolved in purified water in order to obtain solutions of 1 mg/ml (w/v) and 0.42 - 0.69 mg/ml (w/v), respectively, to reach final theoretical CS/TPP ratios of 3.6:1 to 6:1 (w/w). The nanoparticles were spontaneously formed upon incorporation of 1.2 ml of TPP solution in 3 ml of the CS solution, under mild magnetic stirring at room temperature. Insulin was dissolved in 0.01M NaOH (0.9 mg insulin/0.6 ml NaOH) and incorporated into the TPP solution afterwards (pH = 11.6), to prepare the protein loaded CS/TPP nanoparticles (insulin theoretical content = 30% (w/w) based on CS). Nanoparticles were concentrated by centrifugation on a 10 μl

glycerol bed (16000×g, 30 min, 15ºC; Beckmann Avanti 30, Beckmann, USA) and resuspended in 100 µl of purified water after discarding the supernatants.

CS/TPP nanoparticles were also prepared on a large scale, by adding 12 ml of the TPP solution to 30 ml of CS, maintaining the stirring conditions. Nanoparticles were centrifuged (8000×g, 30 min, 15ºC) and the resuspension volumes were proportionally adapted.

2.3. Determination of nanoparticles process yield

The nanoparticles production yield was calculated by gravimetry. Fixed volumes of nanoparticle suspensions were centrifuged (16000×g, 30 min, 15ºC) and sediments were freeze-dried over 24 h (24 h at -34ºC and gradual ascent until 20ºC), using a Labconco Freeze Dryer (Labconco, USA) (n = 3).

The process yield was calculated as follows:

$$\text{Process yield (\%)} = \frac{\text{Nanoparticles weight}}{\text{Total solids (CS+TPP + Insulin) weight}} \times 100$$

2.4. Characterization of nanoparticles

The morphological examination of nanoparticles was conducted by transmission electron microscopy (TEM) (CM 12 Philips, Eindhoven, Netherlands). The samples were stained with 2% (w/v) phosphotungstic acid and placed on copper grids with Formvar® films for TEM observation.

Measurements of nanoparticles size and zeta potential were performed on freshly prepared samples by photon correlation spectroscopy and laser doppler anemometry, respectively, using a Zetasizer® 3000 HS (Malvern Instruments, Malvern, UK). For the particle size analysis, each sample was diluted to the appropriate concentration with filtered (0.2 µm filters Millex®-GN, Millipore Iberica, Spain) ultrapure water. Each analysis lasted 180 sec and was performed at 25ºC with a detection angle of 90º. For the determination of the electrophoretic mobility, samples were diluted with KCl 0.1 mM and placed in the electrophoretic

cell, where a potential of ± 150 mV was established. Three batches of each formulation were analyzed in triplicate (n = 3).

2.5. Determination of protein loading capacity of nanoparticles

The nanoparticles association efficiency was determined upon their separation from the aqueous preparation medium containing the non-associated protein by centrifugation (16000×g, 30 min, 15ºC). The amount of free insulin was determined in the supernatant by the MicroBCA protein assay (Pierce, USA), measuring the absorbances by spectrophotometry (Shimadzu UV-Visible Spectrophotometer UV-1603, Japan) at 562 nm. A calibration curve was made using the supernatant of blank nanoparticles. Each sample was assayed in triplicate (n = 3). The nanoparticles protein association efficiency and loading capacity were calculated as follows:

$$\text{Association efficiency (\%)} = \frac{\text{Total insulin amount} - \text{Free insulin amount}}{\text{Total insulin amount}} \times 100$$

$$\text{Loading capacity (\%)} = \frac{\text{Total insulin amount} - \text{Free insulin amount}}{\text{Nanoparticles weight}} \times 100$$

2.6. Preparation of dry powders containing chitosan nanoparticles

Aqueous solutions of the excipients lactose and mannitol were prepared by dissolution in purified water, to obtain concentrations of 7.5 - 10% (w/v). CS/TPP nanoparticle suspensions in the excipients were obtained by resuspending the nanoparticles sediments obtained after centrifugation, with the aqueous solution of the excipients, in order to achieve excipient/nanoparticles ratios of 95/5, 90/10, 80/20 and 50/50 (w/w). The final suspension concentrations ranged from 0.84% to 8.4% (w/v).

Dry powders were obtained by spray-drying aqueous solutions of the excipients and suspensions of CS/TPP nanoparticles in the excipients using a laboratory-scale spray-dryer (Büchi® Mini Spray Dryer, B-290, Switzerland). The spray-drying conditions were: feed rate of 2.5 ml/min, two fluids external mixing 0.7 mm nozzle, inlet temperatures were maintained at 160 ± 2ºC (when mannitol was used as excipient) and 135 ± 2ºC (for lactose), resulting in outlet temperatures of and 108 ± 3ºC and 85 ± 3ºC, respectively. The air flow rate and the aspirator were constant at 400 Nl/h and 80%, respectively. The spray-dried powders were collected and stored in a dessicator, at room temperature, until use.

2.7. Determination of spray-drying process yield

The spray-drying production yield was calculated by gravimetry, comparing the total solids amount with the resultant powder (microspheres) amount after spray-drying, as follows (n = 3):

$$\text{Process yield (\%)} = \frac{\text{Microspheres weight}}{\text{Total solids (CS + TPP + aerosol excipient) weight}} \times 100$$

2.8. Microspheres morphological characterization

Microspheres were viewed using a scanning electron microscope (SEM, Leo 435VP, UK). The dry powders were placed onto metal plates and a 200 nm-thick gold palladium film was sputter coated on the samples (High Resolution Sputter Coater SC7640, Termo VG Scientific, UK) before viewing. The particle size was estimated as the Feret´s diameter (distance between two tangents on opposite sides of the particles) and was directly determined with an optical microscope (Olympus BH-2, Japan) and was estimated as the mean of 300 particles measurement (n = 300).

2.9. Determination of powder density

Real density was determined using a Helium Picnometer (Micropycnometer, Quanta Chrome, model MPY-2, USA) (n = 3). Apparent tap density was obtained by measuring the volume of a known weight of powder in a 10 ml test-tube after mechanical tapping (30 tap/min, Tecnociencia, Spain). After registration of the initial volume, the test-tube was submitted to tapping until constant volume was achieved, according to a previously described method (El-Gibaly, 2002) (n = 3).

2.10. Evaluation of dry powder aerodynamic properties

Aerodynamic diameters were obtained using a TSI Aerosizer® LD equipped with an Aerodisperser® (Amherst Process Instrument, Inc; Amherst, Ma, USA), whose measuring principle is based on the measurement of the particles time of flight in an air stream, according to the following equation (n = 3):

$$C_d \frac{\pi d^2}{4} \rho_a \frac{(V_a - V_p)}{2} = 1/6\, \pi d^3 \rho_p \frac{dV_p}{dt}$$

where C_d: drag coefficient, d: particle diameter, ρ_a: density of air, V_a: velocity of air, V_p: velocity of particle, and ρ_p: density of particle.

2.11. Nanoparticles recovery from dry powders in aqueous medium

To recover the nanoparticles from the microspheres, 50 mg of the spray-dried powders were incubated in 3 ml of PBS pH 7.4 for 90 min, under mild magnetic stirring, at room temperature. The nanoparticles morphology and physicochemical properties (size and zeta potential) were analyzed by TEM, photon correlation spectroscopy and laser doppler anemometry, respectively (n = 3).

2.12. Evaluation of nanoparticles stability in the presence of lysozyme

The stability of fresh and recovered nanoparticles (CS/TPP = 3.6:1) of a representative dry powder (mannitol/nanoparticles ratio of 95/5) was analyzed following their incubation in a solution of lysozyme in PBS pH 7.4 (0.2 and 0.8

mg/ml, final particle concentration: 3.5 mg/ml), at 37ºC, under mild horizontal shaking, for 90 min. At appropriate time intervals (5, 15, 30, 60 and 90 min), the mean particle size was analyzed using the Zetasizer®, as previously described (Calvo et al., 1997b) (n = 3).

2.13. In vitro release studies of insulin from CS/TPP nanoparticles and dry powders

The release of insulin was determined by incubating the nanoparticles (CS/TPP = 6:1) or the nanoparticle-loaded microspheres (mannitol/nanoparticles ratio of 80/20) in 5 ml of pH 7.4 phosphate buffer (0.15 mg nanoparticles/ml, 0.75 mg microspheres/ ml), with horizontal shaking, at 37ºC.

At appropriate time intervals (15, 30, 60 and 90 min) individual samples were filtered (0.22 μm filters Millex®-GV, low protein binding, Millipore Ibérica, Spain) and the amount of protein released evaluated in the supernatants by the MicroBCA protein assay (Pierce, USA) measuring the absorbances by spectrophotometry (Shimadzu UV-Visible Spectrophotometer UV-1603, Japan) at 562 nm (n = 3).

2.14. Statistical analysis

The t-test and the one-way analysis of variance (ANOVA) with the pairwise multiple comparison procedures (Student-Newman-Kleus Method) were performed to compare two or multiple groups, respectively. All analysis were run using the SigmaStat statistical program (Version 1, Jandel Scientific, USA) and differences were considered to be significant at a level of $P < 0.05$.

3. Results and Discussion

As stated in the introduction, in this work, a new hydrophilic dry powder consisting in carbohydrate microspheres containing protein-loaded CS/TPP nanoparticles was prepared using exceptionally mild conditions. Furthermore, the system was aerodynamically characterized “in vitro” and its ability to deliver the nanoparticles and the model therapeutic protein insulin was investigated; thus demonstrating its potential for pulmonary administration of peptides and proteins.

3.1. Preparation and characterization of chitosan nanoparticles

Nanoparticles with CS/TPP ratios of 3.6:1 to 6:1 were obtained. Figure 1a displays the TEM microphotograph of representative fresh CS/TPP nanoparticles, which evidence a compact structure.

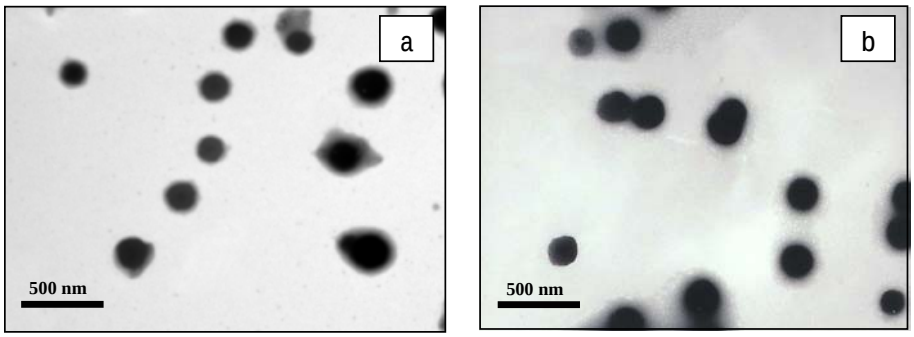

Fig. 1. TEM microphotograph of: (**a**) freshly prepared and (**b**) recovered nanoparticles (CS/TPP = 3.6:1).

As shown in table 1, the incorporation of increasing amounts of TPP with respect to CS, led to a significant increase in the process yield ($P < 0.05$), the maximum yield (approximately 60%) being achieved for the 3.6:1 CS/TPP ratio, which can be explained by the nanoparticles formation mechanism, as previously reported (Fernandez-Urrusuno et al., 1999b). Blank (without associated insulin) CS/TPP nanoparticles displayed a particle size in the range of approximately 300 nm to 390 nm and a positive zeta potential from + 34 mV to + 45 mV, with the lowest size and zeta potential also being obtained for the highest TPP concentration (CS/TPP = 3.6:1) ($P < 0.05$). The results depicted in table 1 correspond to nanoparticles prepared using the low scale conditions (3 and 1.2 ml of CS and TPP, respectively). The large scale process resulted in nanoparticles with similar characteristics (data not shown).

The association of insulin to nanoparticles of ratios 3.6:1 and 4:1 did not succeed, leading to precipitation, which can be due to the competition between TPP and insulin for the same places in CS molecules. Protein entrapment to nanoparticles with CS/TPP ratios of 5:1 and 6:1 ranged between 65% and 80% and the loading of insulin varied within 22% and 30% (table 2), the CS/TPP ratio

of 5:1 (with the highest TPP content) leading to the higher association efficiency of insulin ($P < 0.05$). These nanoparticles are more reticulated than the 6:1 ones, leading to a smaller size and it is very likely that this reticulation allowed them to capture more insulin.

Table 1. Process yields and physicochemical properties of blank (without insulin) nanoparticles prepared with different chitosan/tripolyphosphate (CS/TPP) theoretical ratios (mean ± SD, n = 3)

CS/TPP (w/w)	Process yield (%)	Size (nm)	Zeta potential (mV)
3.6:1	60 ± 4	300 ± 17	+ 34.3 ± 1.5
4:1	40 ± 3	356 ± 06	+ 38.3 ± 2.9
5:1	20 ± 5	377 ± 26	+ 44.1 ± 5.2
6:1	12 ± 4	388 ± 35	+ 45.0 ± 4.7

Process yield (%) = (Nanoparticles weight / Total solids weight) x 100

The comparison of results presented in tables 1 and 2, corresponding to the blank and the insulin loaded nanoparticles, respectively, indicate that the incorporation of insulin in the nanoparticles led to a significantly higher production yield ($P < 0.05$) and to a significant decrease ($P < 0.05$) on zeta potential as reported elsewhere (Fernandez-Urrusuno et al., 1999a), not having a pronounced effect on particle size. Taking into account that insulin is dissolved in NaOH 0.01M, with basic pH, the protein is above its isoelectric point (pI 5.3) resulting in a negative charge. As a consequence, the association of insulin with the positively charged CS/TPP nanoparticles is favoured, decreasing the zeta potential value.

Table 2. Process yields, physicochemical properties and association efficiencies of insulin loaded nanoparticles prepared with different chitosan/tripolyphosphate (CS/TPP) theoretical ratios (mean ± SD, n = 3).

CS/TPP (w/w)	Process yield (%)	Size (nm)	Zeta potential (mV)	Association efficiency (%)	Loading capacity (%)
5:1	54 ± 4	388 ± 61	+ 32.6 ± 0.7	81.0 ± 5.6	29.8 ± 1.4
6:1	60 ± 4	419 ± 27	+ 33.9 ± 0.6	65.6 ± 4.8	22.3 ± 1.6

Process yield (%) = (Nanoparticles weight / Total solids weight) x 100
Association efficiency (%) = [(Total insulin amount –Free insulin)/Total insulin amount] x 100
Loading capacity (%) = [(Total insulin amount–Free insulin)/Nanoparticles weight] x 100

3.2. Microspheres preparation and morphological characterization

Previous to microencapsulation, CS/TPP nanoparticles were incubated in the candidate excipients for spray-drying (lactose and mannitol; 19.9 mg/ml, at room temperature, for 1 h), in order to assess the excipients effect (for example, due to adsorption) on the nanoparticles size and zeta potential. Besides the observed differences on these parameters were statistically significant ($P < 0.05$) for both excipients, nanoparticles size only changed about 50 nm (approx. 15% of the initial size), which was an adequate size range considering the aim of the work. As well, the zeta potential increased around 1 mV, keeping the desired positive charge of the nanoparticles (data not shown). Therefore, it could be concluded that nanoparticles characteristics were not affected by the contact with the referred excipients.

In this work, dry powders were obtained using lactose and mannitol as excipients, with production yields ranging from 52 to 76%. Both these excipients were selected as they are approved by the Food and Drug Administration (FDA) for pulmonary delivery, and so, widely applied in aerosolization (Bosquillon et al., 2001b). We investigated the effects of distinct formulation variables (aerosol excipient/nanoparticles theoretical ratio; concentration of the spray-drying suspension) on the microspheres aerodynamic and morphologic properties.

As can be observed in SEM microphotographs depicted in figure 2, morphology was dependent on powder composition. Microspheres obtained from

mannitol aqueous solutions without nanoparticles had mostly a spherical shape, but appear to be a little aggregated. In contrast (data not shown), microspheres obtained from lactose aqueous solutions were very well defined, non-aggregated spherical particles. Those produced from the mixture of 90% mannitol and 10% lactose also had a spherical shape and were less aggregated than mannitol ones, showing better defined limits. Upon incorporation of CS/TPP nanoparticles, the resulting mannitol microspheres showed more defined limits and spherical shape as the nanoparticles amount increased with respect to mannitol. This suggests that the incorporation of nanoparticles as a solid structure contributes to the enhancement of microspheres morphology, once these can "grow" around a solid body. Hence, the microspheres general aspect improved from those containing mannitol/nanoparticles ratio of 100/0 to those with mannitol/nanoparticles ratio of 80/20.

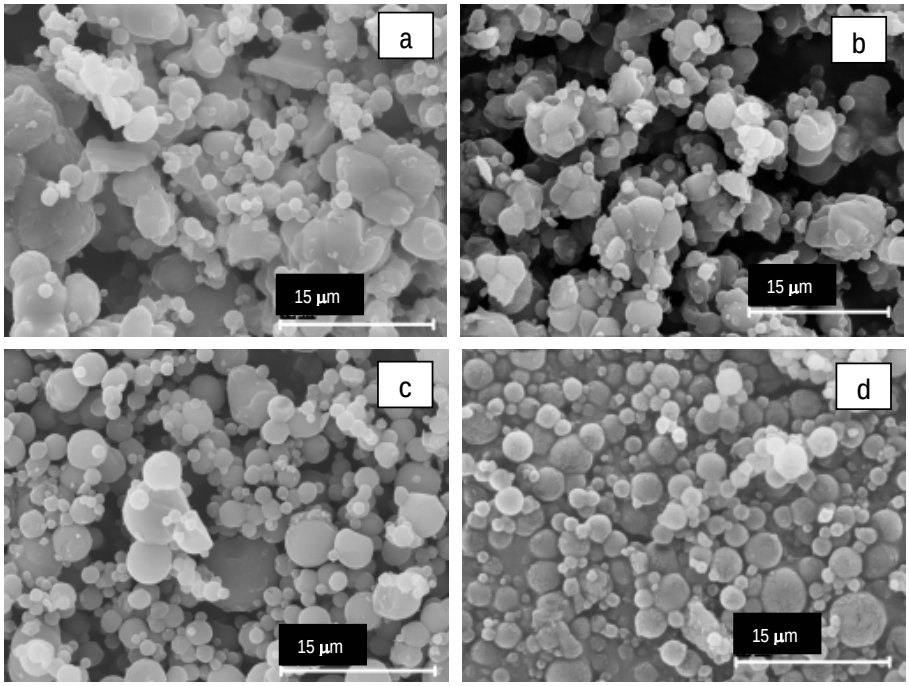

Fig. 2. SEM microphotographs of microspheres prepared with different mannitol/ nanoparticles (Ma/NP) theoretical ratios and solids content (SC), expressed as Ma/NP - SC: (**a**) 100/0 - 10% (control mannitol microspheres); (**b**) 95/5 - 8.4%; (**c**) 80/20 - 2.1%; (**d**) 50/50 - 0.84%.

The morphology of mannitol/nanoparticles 50/50 microspheres was similar to that of mannitol/nanoparticles 80/20, which means that 20% (w/w) of nanoparticles is the minimum amount of nanoparticles needed to obtain non aggregated dry powders with adequate morphology. The solids content were adjusted in each case to obtain suspensions of nanoparticles displaying good flow properties for passing through the spray-dryer needle. In the formulation comprising mannitol with 10% (w/v) lactose, we did not observe an improvement on particles morphology when incorporating nanoparticles (data not shown). Anyhow, no differences were found between microspheres made of mannitol with nanoparticles and both mannitol and lactose with nanoparticles.

Microspheres produced using lactose, although morphologically adequate, were not feasible for our purposes. Due to their high hygroscopic properties, some minutes after recovering the lactose powder (with or without nanoparticles), it became sticky and handling was not easy. This could be due to the production of essentially amorphous material, typical of the spray-drying process (Chidavaenzi et al., 1997, 2001). Therefore, concerning the morphology, the mannitol/nanoparticles 80/20 formulation was considered to be the most adequate.

In our work, SEM microphotographs of several broken microspheres indicate that, at least, some of the obtained microspheres are hollow (figure 3).

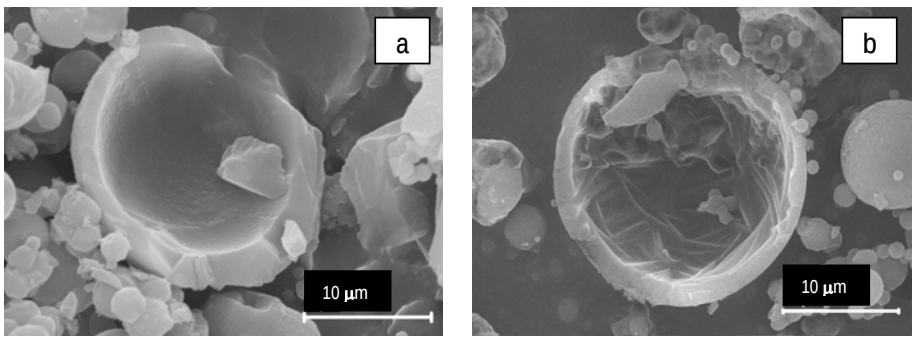

Fig. 3. SEM microphotographs of broken microspheres: (**a**) mannitol/nanoparticles 90/10 - 8.4% solids content; (**b**) solely mannitol – 10% solids content.

However, further studies, i.e. confocal analysis, must be conducted in order to know exactly what the nanoparticles localization in the microspheres is (inside as an independent structure, incorporated in their walls and/or adsorbed in their outer faces).

The production of nanoparticle-loaded microspheres was previously reported (Kawashima et al., 1998; Pohlmann et al., 2002; Tsapis et al., 2002; Sham et al., 2004) using both spray-drying and freeze-drying techniques, and materials of a different nature, such as gelatin, polybutylcyanoacrylate, hydroxypropylmethylcellulose phthalate, poly (ε-caprolactone), polylactic acid, polystyrene and silica. Our spray-dried system has two main advantages compared to those. First, it can act as enhancing agent of macromolecules absorption due to the CS/TPP nanoparticles content. Furthermore, as it was previously commented, it is made of solely hydrophilic polymers and is prepared in an entirely aqueous medium, without requiring any organic solvent, sonication or aggressive conditions (very mild techniques). The high temperature used, inherent to all the spray-drying processes, is known not to compromise the stability of the associated protein (Broadhead et al., 1992).

3.3. Particle size, density and aerodynamic properties

The particle size of a powder formulation intended for inhalation is, together with the particle density, a prominent factor in the success of the formulation, because it strongly influences the dispersion and sedimentation properties of the powder (Taylor and Kellaway, 2001; Courrier et al., 2002). As previously mentioned, the aerodynamic diameter of particles for optimal lung administration should be of approximately 1 to 5 μm (Bosquillon et al., 2001a).

The physical and aerodynamic properties of the produced powders are depicted in table 3. Feret diameters varied between 1.9 and 4.0 μm, real densities were approximately 1.5 g/cm^3 and tap densities were low, ranging from 0.3 to 0.45 g/cm^3, which render aerodynamic diameters of 2-3 μm. Therefore, all the dry powders were theoretically suitable for administration to the deep lungs.

Table 3. Physical and aerodynamic properties of dry powders prepared with different mannitol/nanoparticles (Ma/NP) ratios and solids content (SC) (mean ± SD, n = 3).

Ma/NP (w/w)	SC (%)	Feret diameter (μm)	Real density (g/cm³)	Apparent density (g/cm³)	Aerodynamic diameter (μm)
80/20	2.1	3.1 ± 1.2	1.57 ± 0.14	0.30 ± 0.01	2.71 ± 0.06
80/20 *	2.1	3.2 ± 1.4	1.48 ± 0.18	0.28 ± 0.01	2.17 ± 0.02
90/10	0.84	1.9 ± 1.0	1.47 ± 0.05	0.39 ± 0.01	2.07 ± 0.02
90/10	4.2	2.7 ± 1.2	1.54 ± 0.07	0.34 ± 0.01	2.17 ± 0.06
90/10	8.4	4.0 ± 1.8	1.52 ± 0.03	0.45 ± 0.01	2.97 ± 0.03
95/5	8.4	3.2 ± 1.4	1.52 ± 0.04	0.40 ± 0.01	2.30 ± 0.02

* Microspheres containing lactose (mannitol/lactose ratio = 90/10)

Solids content is the total solids concentration (%) of the spraying suspensions.

Feret diameters (μm) (distances between two tangents on opposite sides of the particle) were determined by optical microscopy. Real and apparent densities (tap densities) (g/cm³) were assayed by helium picnometry and by a tapping procedure, respectively. Aerodynamic diameters were obtained using an Aerosizer®.

The tendency was that the aerodynamic diameter increases with growing concentrations of the spray-drying suspensions, as has been clearly observed for powders constituted of mannitol/nanoparticles of theoretical 90/10 ratio with solids content of 0.84%, 4.2% and 8.4% (w/v) (table 3, figure 4) ($P < 0.05$): the lowest aerodynamic diameter (approximately 2 μm) corresponds to the lowest solids content powder and the highest (approximately 3 μm) to that prepared with 8.4% solids content. This can be easily explained by the basis of the spray-drying process: at a constant feed rate, an increase in the concentration of the spraying solution means an increase in the solids contained in the liquid which is sprayed in a specific moment, giving rise to a larger droplet and dry particle formation (Chidavaenzi et al., 1997). With respect to real densities, no statistically significant differences were found among the different powders containing nanoparticles; in contrast to what it was observed for the tap densities ($P < 0.05$).

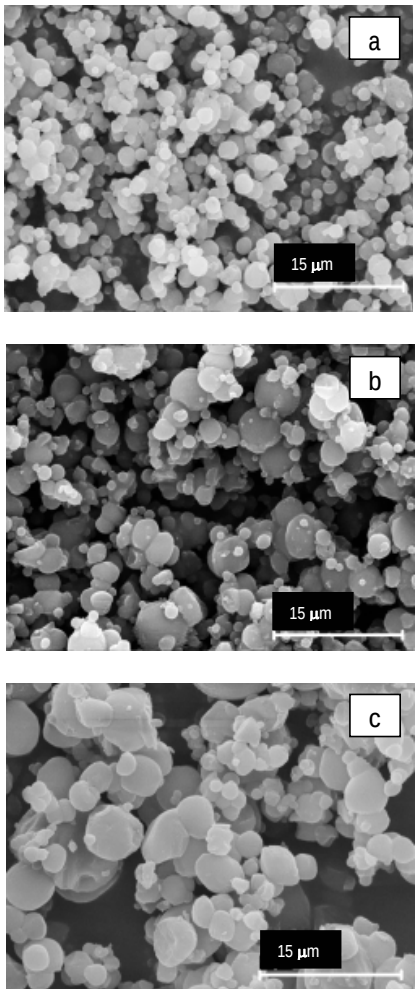

Fig. 4. SEM microphotographs of microspheres prepared with a mannitol/nanoparticles 90/10 theoretical ratio and different solids content: (**a**) 0.84%; (**b**) 4.2%; (**c**) 8.4%.

Concerning aerodynamic characteristics, we also consider that the dry powder consisting on mannitol/nanoparticles (80/20) (solids content = 2.1%), with an aerodynamic diameter of 2.71 µm, is the most suitable to succeed in carrying the nanoparticles to the lung.

3. 4. Recovery of nanoparticles from microspheres in aqueous medium

It is assumed that the airway surface liquid has a pH of approximately 7, close to that of the interstitial fluid and plasma (Kyle et al., 1990; Walters, 2002). Taking this into account, we decided to investigate the dry powders ability to deliver the nanoparticles following incubation in PBS pH 7.4. We observed that after incubating the powders in the aqueous medium under low stirring rate, the aerosol excipient was immediately dissolved, resulting in a nanoparticle suspension. As observed when comparing the TEM microphotographs collected in figure 1, recovered nanoparticles present an aspect similar to that found in freshly prepared formulations. Table 4 represents the quotients of nanoparticles size and zeta potential after recovering with respect to fresh nanoparticles.

Table 4. Nanoparticles size and zeta potential variations after recovering from microspheres prepared with different mannitol/nanoparticles (Ma/NP) theoretical ratios and solids content (SC) (fresh nanoparticles: size = 406 ± 20 nm, Zeta potential = +34.3 ± 0.1 mV; mean ± SD, n = 3).

Ma/NP (w/w)	SC (%)	Δ Size (nm)	Δ Zeta potential (mV)
80/20	2.1	1.21 ± 0.04	1.08 ± 0.03
80/20 *	2.1	1.19 ± 0.04	1.00 ± 0.02
90/10	4.2	1.12 ± 0.14	0.95 ± 0.01
90/10	8.4	1.15 ± 0.02	1.01 ± 0.02
95/5	8.4	1.00 ± 0.14	1.01 ± 0.01

* Microspheres containing lactose (mannitol/lactose ratio = 90/10)

Solids content is the total solids concentration (%) of the spraying suspensions.

Δ Size = Recovered nanoparticles size / Fresh nanoparticles size

Δ Zeta potential = Recovered nanoparticles Zeta potential / Fresh nanoparticles Zeta potential

The mean particle size before spray-drying was about 400 nm and increased significantly ($P < 0.05$) after nanoparticles recovering in the case of some of the formulations [mannitol/nanoparticles 80/20 - 2.1%, mannitol/nanoparticles 90/10 - 8.4% and (mannitol-lactose 90-10)/nanoparticles 80/20 - 2.1%], reaching a maximum value of 490 nm to the former one. Nevertheless, in spite of the slight enlargement and little change in zeta potential presented by some nanoparticles, they are still in the nano-range and the increase is irrelevant for our purposes. Furthermore, they continue to present a high positive surface potential, thus allowing their interaction with the negatively charged mucosa. The enlargement of particles size after spray-drying was also found by Sham *et al.* for powders prepared with lactose and gelatin nanoparticles and was attributed to eventual changes in conformation due to the thermal conditions of the spray-drying process (Sham et al., 2004).

Therefore, from this study we could conclude that after reaching the deep lung, microspheres are expected to quickly dissolve in the lung aqueous covered epithelium, releasing the CS/TPP nanoparticles. The employed excipients are highly soluble in aqueous medium, so we do not foresee any problem concerning the nanoparticles *in vivo* release process.

3.5. Effect of lysozyme on nanoparticles stability

The dry powder formulation containing a mannitol/nanoparticles 95/5 theoretical ratio and a 8.4% solids content, was chosen to perform the stability study of the recovered nanoparticles in the presence of enzymes. The enzyme concentration of 0.2 mg/ml was used taking into account the studies conducted by Konstan *et al.*, who found that this was the maximum lysozyme concentration in human tracheobronchial secretions (Konstan et al., 1981). Furthermore, we chose the 0.8 mg/ml concentration to investigate the nanoparticles behavior in extreme conditions. In this study, lysozyme was dissolved in PBS pH 7.4, resulting in a pH of 6.8-7.0, which is close both to the lung pH and the optimal pH for lysozyme enzymatic activity (pH 6.4) (Calvo et al., 1997b). Preliminary studies showed that the incubation of lysozyme with PBS under the same

conditions used throughout the study did not result in formation of any kind of structures (aggregates or other).

As shown in figure 5, both fresh and recovered nanoparticles were affected by the incubation process in the presence of lysozyme, their size decreasing when increasing the incubation time with the enzyme. Tested formulations showed a decrease in the nanoparticles size immediately after initial contact with the enzyme.

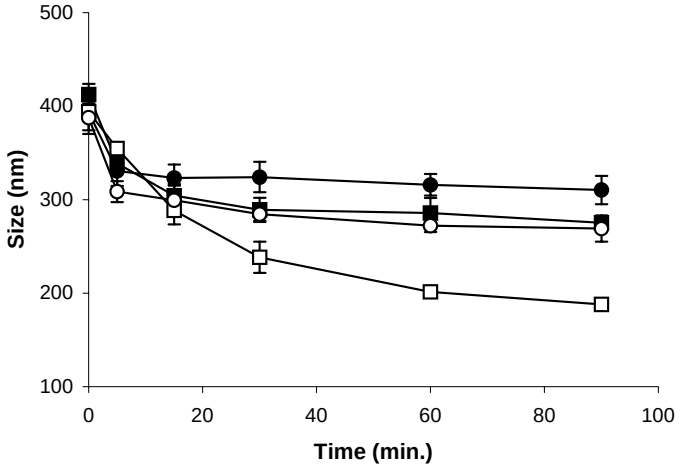

Fig. 5. Evolution of the nanoparticles (CS/TPP = 3.6:1) size following their incubation in a lysozyme solution in PBS pH 7.4, at 37°C for 2 h: (●) fresh nanoparticles, lysozyme 0.2 mg/ml; (■) fresh nanoparticles, lysozyme 0.8 mg/ml; (○) recovered nanoparticles, lysozyme 0.2 mg/ml; (□) recovered nanoparticles, lysozyme 0.8 mg/ml (mean ± SD, n = 3).

The incubation of fresh nanoparticles with 0.2 mg lysozyme/ml, led to a reduction of 80 nm in the particle size within 90 minutes. However, when the enzyme concentration increased to 0.8 mg/ml, the nanoparticles size fell in 140 nm. A similar behavior was found with recovered nanoparticles. After incubation with 0.2 mg lysozyme/ml, nanoparticles size decreased 120 nm, while incubation with 0.8 mg lysozyme/ml led to a total reduction of 200 nm. In fact, only 5 minutes after incubation, every assayed formulations showed significantly different nanoparticles sizes ($P < 0.05$) when compared to the initial values, with diminutions of 60-90 nm. After that, the reduction was gradual and more

accentuated when lysozyme was present at a higher concentration. These results were very predictable, considering the previous knowledge that lysozyme can attack CS, hydrolyzing the glycoside bonds between the acetylglucosamine units (Muzzarelli, 1997). Fresh nanoparticles seem to be less affected than recovered nanoparticles, once their size decreases less. Although, significant differences on the extent of size decrease between fresh and recovered nanoparticles were only found upon incubation with the highest enzyme concentration ($P < 0.05$). The different behavior within fresh and recovered nanoparticles, probably related to the presence of mannitol, needs to be further investigated to reach a conclusive justification for it. Moreover, a lysozyme concentration of 0.8 mg/ml was more damaging than 0.2 mg/ml, leading to significantly greater decreases in particle size ($P < 0.05$), indicating that nanoparticles stability was concentration-dependent. Probably, more enzyme allowed the hydrolysis of more glucosamine units.

3.6. In vitro release studies

Figure 6 depicts the release profiles of insulin from representative fresh nanoparticles (CS/TPP ratio of 6:1) and dry powders containing insulin-loaded nanoparticles (mannitol/nanoparticles ratio = 80/20, solids content = 2.1%) in PBS pH 7.4 at 37ºC. As expected, the results show that insulin release was very rapid (Fernández-Urrusuno et al., 1999a); at 15 minutes, the maximum amount of insulin being released (75-80%) for both fresh nanoparticles and nanoparticle-loaded microspheres.

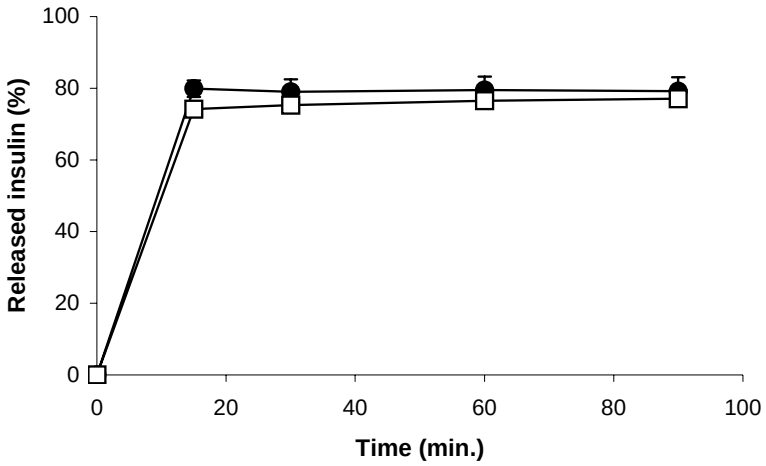

Fig. 6. Release profiles of insulin from (●) nanoparticles (CS/TPP = 6:1) and (□) microspheres (mannitol/nanoparticles = 80/20, solids content = 2.1 %, CS/TPP = 6:1), in PBS pH 7.4 at 37°C (insulin = 30% w/w based on CS; mean ± SD, n = 3).

As concluded in previous works, this *in vitro* release behavior suggests that the interaction between CS and insulin is very weak, allowing the insulin release from the nanoparticles by a dissociation mechanism (Fernández-Urrusuno et al., 1999a). Moreover, it can be observed that the spray-drying excipient (mannitol) does not influence the protein release profile, which is due to its high solubility in the aqueous release medium, allowing the immediate nanoparticles delivery.

4. Conclusions

The present work demonstrates that protein-loaded nanoparticles can be successfully incorporated in microspheres by means of a spray-drying process, resulting in dry powders with suitable properties for lung delivery. The mannitol/nanoparticles ratio significantly affects the microspheres morphology, showing improved spherical shapes with increasing amounts of nanoparticles. Growing concentrations of the spray-drying suspensions led to an increase in the particles aerodynamic diameter. Recovering of nanoparticles from microspheres is efficiently conducted *in vitro* after incubation in an aqueous medium. Therefore,

after contact with the lung aqueous environment, microspheres are expected to release the nanoparticles and, as a consequence, the therapeutic macromolecule. As expected, chitosan nanoparticles are degraded by lysozyme. The microencapsulation process does not affect the insulin release profile, and at 15 minutes the maximum amount of insulin released had already been reached. Therefore, microspheres would act simply as nanoparticles and, consequently, protein carriers to the lungs. This system is proposed for systemic delivery of therapeutic macromolecules, considering the already known properties of chitosan to promote peptide absorption. In addition, it could also be used as a tool in therapy of lung local diseases, such as cystic fibrosis or cancer.

Acknowledgements

This work was supported by the Spanish Government (CICYT, SAF2002-03314). The Predoctoral fellowship to Ana Grenha from Fundação para a Ciência e Tecnologia, Portugal (SFRH/BD/13119/2003) is highly appreciated.

References

Ahsan, F., Rivas, I.P., Khan, M.A., Suárez-Torres, A.I., 2002. Targeting to macrophages: role of physicochemical properties of particulate carriers – liposomes and microspheres – on the phagocytosis by macrophages. J. Control. Release. 79, 29-40.

Akhtar, S., Lewis, K.J., 1997. Antisense oligonucleotide delivery to cultured macrophages is improved by incorporation into sustained-release biodegradable polymer microspheres. Int. J. Pharm. 151, 57-67.

Artursson, P., Lindmark, T., Davisa, S.S., Illum, L., 1994. Effect of chitosan on the permeability of monolayers of intestinal epithelial cells (Caco-2). Pharm. Res. 11, 1358-1361.

Borchard, G., Luβen, H.L., De Boer, G.A., Verhoef, J.C., Lehr, C.M., Junginger, H.E., 1996. The potential of mucoadhesive polymers in enhancing intestinal peptide drug absorption III: Effects of chitosan glutamate and carbomer on epithelial tight junctions in vitro. J. Control. Release. 39, 131-138.

Bosquillon, C., Lombry, C., Préat, V., Vanbever, R., 2001a. Influence of formulation excipients and physical characteristics of inhalation dry powders on their aerosolization performance. J. Control. Release. 70, 329-339.

Bosquillon, C., Lombry, C., Préat, V., Vanbever, R., 2001b. Comparison of particle sizing techniques in the case of inhalation dry powders. J. Pharm. Sci. 90, 2032-2041.

Broadhead, J., Edmond-Rouan, S.K., Rhodes, C.T., 1992. The spray drying of pharmaceuticals. Drug. Develop. Ind. Pharm. 18, 1169-1206.

Calvo, P., Remuñán-López, C., Vila-Jato, J.L., Alonso, M.J., 1997a. Novel hydrophilic Chitosan-Polyethylene Oxide nanoparticles as protein carriers. J. Appl. Polym. Sci. 63, 125-132.

Calvo, P., Vila-Jato, J.L., Alonso, M.J., 1997b. Effect of lysozyme on the stability of polyester nanocapsules and nanoparticles: stabilization approaches. Biomaterials. 18, 1305-1310.

Chidavaenzi, O.C., Buckton, G., Koosha, F., Pathak, R., 1997. The use of thermal techniques to assess the impact of feed concentration on the amorphous content and polymorphic forms present in spray dried lactose. Int. J. Pharm. 159, 67-74.

Chidavaenzi, O.C., Buckton, G., Koosha, F., 2001. The effect of co-spray drying with polyethyleneglycol 4000 on the cristallinity and physical form of lactose. Int. J. Pharm. 216, 43-49.

Clark, A., 2002. Formulation of proteins and peptides for inhalation. Drug Del. Syst. & Sci. 2, 73-77.

Courrier, H.M., Butz, N., Vandamme, T.F., 2002. Pulmonary drug delivery systems: recent developments and prospects. Crit. Rev. Ther. Drug Carr. Syst. 19, 425-498.

De Campos, A., Sánchez, A., Alonso, M.J., 2001. Chitosan nanoparticles : a new vehicle for the improvement of the delivery of drugs to the ocular surface. Application to cylosporin A. Int. J. Pharm. 224, 159-168.

Dornish, M., Hagen, A., Hansson, E., Peucheur, C., Vedier, F., Skaugrud, O., 1997. Safety of Protasan™: Ultrapure chitosan salts for biomedical and pharmaceutical use. In: Domard, A., Roberts, G.A.F., Varum, K.M. (Eds.), Advances in chitin science. Jacques Andre publisher, Lyon, pp. 664-670.

Duszyk, M., 2001. CFTR and lysozyme secretion in human airway epithelial cells. Eur. J. Physiol. 443, S45-S49.

El-Gibaly, I., 2002. Development and in vitro evaluation of novel floating chitosan microcapsules for oral use: comparison with non-floating chitosan microspheres. Int. J. Pharm. 294, 7-21.

Evora, C., Soriano, I., Rogers, R.A., Shakesheff, K.M., Hanes, J. Langer, R., 1998. Relating the phagocytosis of microparticles by alveolar macrophages to surface chemistry: the effect of 1,2-dipalmitoylphosphatidylcholine. J. Control. Release. 51, 143-152.

Fernández-Urrusuno, R., Calvo, P., Remuñán-López, C., Vila-Jato, J.L., Alonso, M.J., 1999a. Enhancement of nasal absorption of insulin using chitosan nanoparticles. Pharm. Res. 16, 1576-1581.

Fernández-Urrusuno, R., Romani, D., Calvo, P., Vila-Jato, J.L., Alonso, M.J., 1999b. Development of a freeze-dried formulation of insulin-loaded chitosan nanoparticles intended for nasal administration. STP Pharm. Sci. 9, 429-436.

Finlay, W.H., Gehmlich, M.G., 2000. Inertial sizing of aerosol inhaled from two dry powder inhalers with realistic breath patterns versus constant flow rates. Int. J. Pharm. 210, 83-95.

Finlay, W.H., Stapleton, K.W., Zuberbuhler, P., 1997. Fine particle fraction as a measure of mass depositing in the lung during inhalation of nearly isotonic nebulized aerosols. J. Aerosol Sci. 28, 1301-1309.

Gehr, P., Green, F.H.Y., Geiser, M., Hof, V.I., Lee, M.M., Schurch, S., 1996. Airway surfactant, a primary defence barrier: mechanical and immunological aspects. J. Aerosol Med. 9, 163-181.

Heinemann, L., Klappoth, W., Rave, K., Hompesch, B., Linkeschowa, R., Heise, T., 2000. Intra-individual variability of the metabolic effect of inhaled insulin together with an absorption enhancer. Diabetes Care. 23, 1343-1347.

Heyder, J., Gebhart, J., Rudolf, G., Schiller, C.F., Stahlhofen, W., 1986. Deposition of particles in the human respiratory tract in the size range 0.005 – 15 μm. J. Aerosol Sci. 17, 811-825.

Hirano, S., Seino, H., Akiyama, Y., Nonaka, I., 1988. Biocompatibility of chitosan by oral and intravenous administrations. Polym. Mat. Sci. Eng. 59, 897-901.

Kawashima, Y., Serigano, T., Hino, T., Yamamoto, H., Takeuchi, H., 1998. A new powder design method to improve inhalation efficiency of pranlukast hydrate dry powder aerosols by surface modification with hydroxypropylmethylcellulose phthalate nanospheres. Pharm. Res. 15, 1748-1752.

Konstan, M.W., Chen, P.W., Sherman, J.M., Thomassen, M.J., Woodm, R.E., Boat, T.F., 1981. Human lung lysozyme: sources and properties. Am. Rev. Resp. Dis. 123, 120-124.

Kyle, H., Ward, J.P., Widdicombe, J.G., 1990. Control of pH of airway surface liquid of the ferret trachea in vitro. J. Appl. Physiol. 68, 135-140.

Lehr, C.M., Bouwstra, J.A., Schacht, E.H., Junginger, H.E., 1992. In vitro evaluation of mucoadhesive properties of chitosan and some other natural polymers. Int. J. Pharm. 78, 43-48.

Makino, K., Yamamoto, N., Higuchi, K., Harada, N., Ohshima, H., Terada, H., 2003. Phagocytic uptake of polystyrene microspheres by alveolar macrophages: effects of the size and surface properties of the microspheres. Colloid. Surf. B-Biointerfaces. 27, 33-39.

Muzzarelli, R.A.A., 1985. Chitin. In: Aspinall, G.O. (Ed.), The polysaccharides (Vol.3). Academic Press, Orlando, pp. 417-450.

Muzzarelli, R.A.A., 1997. Human enzymatic activities related to the therapeutic administration of chitin derivatives. Cell. Mol. Life Sci. 53, 131-140.

Patton, J.S., Platz, R.M., 1992. Pulmonary delivery of peptides and proteins for systemic action. Adv. Drug Deliv. Rev. 8, 179-196.

Pohlmann, A.R., Weiss, V., Mertins, O., Silveira, N.P., Guterres, S.S., 2002. Spray-dried indomethacin-loaded polyester nanocapsules and nanospheres: development, stability evaluation and nanostructure models. Eur. J. Pharm. Sci. 16, 305-312.

Portero, A., Remuñán-López, C., Nielsen, H.M., 2002. The potencial of chitosan in enhancing peptide and protein absorption across the TR146 cell culture model – an in vitro model of the bucal epithelium. Pharm. Res. 19, 169-174.

Rios, A., Gordillo, M.E., Bocanegra, C., Maldonado, J.A., 1994. Administración nasal e inhalatoria. In: Ramos, B.S., Aznar, M.D. (Eds.), Administración de medicamentos: Teoria y práctica. Diaz de Santos, Madrid, pp. 131-149.

Rudt, S., Müller, R.H., 1992. In vitro phagocytosis of nano- and microparticles by chemiluminescence. I. Effect of analytical parameters, particle size and particle concentration. J. Control. Release. 22, 263-272.

Schurch, S., Gehr, P., Im Hof, V., Geiser, M., Green, F., 1990. Surfactant displaces particles toward the epithelium in airways and alveoli. Resp. Physiol. 80, 17-32.

Sham, J.O., Zhang, Y., Finlay, W.H., Roa, W.H., Löbenberg, R., 2004. Formulation and characterization of spray-dried powders containing nanoparticles for aerosol delivery to the lung. Int. J. Pharm. 269, 457-467.

Taylor, G., Kellaway, I., 2001. Pulmonary drug delivery. In: Hillery, A., Lloyd, A., Swarbrick, J. (Eds.), Drug delivery and targeting. Taylor & Francis, New York, pp. 269-300.

Tsapis, N., Bennett, D., Jackson, B., Weitz, D.A., Edwards, D.A., 2002. Trojan particles: large porous carriers of nanoparticles for drug delivery. Proc. Nat. Acad. Sci. 99, 12001-12005.

Walters, D.V., 2002. Lung lining liquid – The hidden depths. Biol. Neonate. 81, S2-S5.

Williams, R.O., Barron, M.K., Alonso, M.J., Remuñán-López, C., 1998. Investigation of a pMDI system containing chitosan microspheres and P134a. Int. J. Pharm. 174, 209-222.

Artículo 3

CHITOSAN NANOPARTICLE-LOADED MICROSPHERES: STRUCTURE AND SURFACE CHARACTERISATION

Ana Grenha[1], Begoña Seijo[1], Carmen Serra[2] and Carmen Remuñán-López[1]*

[1]Dept. of Pharmacy and Pharmaceutical Technology, University of Santiago de Compostela, Faculty of Pharmacy, Campus Sur, 15782 Santiago de Compostela, Spain. [2]C.A.C.T.I., University of Vigo, E-36310, Vigo,Spain.

* Corresponding author: Phone: 0034 981 563100 – ext. 15405

Fax: 0034 981 547148

E-mail: ffcarelo@usc.es

Artículo sometido a evaluación por "Macromolecules"

Abstract

In this work, we aimed to characterise the surface and the internal structure of mannitol microspheres containing chitosan/tripolyphosphate nanoparticles, which were prepared by spray-drying. These microspheres were recently proposed as valuable candidates to transport therapeutic protein-loaded nanoparticles to the lungs owing to their favourable aerodynamic properties. To observe the distribution of chitosan nanoparticles and mannitol in the microspheres, specific characterisation techniques such as confocal laser scanning microscopy, X-ray photoelectron spectroscopy and time-of-flight secondary ion mass spectrometry were used. Results showed that mannitol is distributed in the whole particle and nanoparticles are homogeneously mixed with mannitol. Moreover, both components were detected in the microspheres surface, mannitol being present to a higher extent, which is in agreement with the theoretical mannitol/nanoparticles ratio of microspheres (80/20). Therefore, this work confirmed that chitosan nanoparticles were successfully encapsulated in mannitol microspheres, providing a homogeneous distribution of the nanoparticles and, hence, of the nanoencapsulated therapeutic macromolecule.

1. Introduction

Pulmonary administration of therapeutic macromolecules is receiving increased attention nowadays. The requisite for a reliable and specific delivery to the lungs is the use of powder carrier systems which possess adequate aerodynamic properties to reach the desired area. In this sense, microspheres have been extensively investigated, since they can be tailored to appropriate morphological and aerodynamic properties.[1] Nanoparticles have also been proposed as delivery systems for proteins and peptides to the lung epithelium.[2-6] However, they present some limitations for this purpose, considering their reduced dimensions and mass, which make lung deposition a difficult issue, potentially exposing them to exhalation.[7-10] Furthermore, stability concerns due to the nanoparticles formulation as aqueous suspensions should also be taken into account. Our group has developed a new ionotropic gelation nanotechnology which is extremely mild and rapid, and allows the production of chitosan/tripolyphosphate (CS/TPP) based nanoparticles.[11] These nanoparticles have shown to possess an excellent capacity for protein entrapment and for improvement of mucosal peptide absorption through several epithelia such as the nasal,[12] ocular[13] and intestinal.[14,15] Taking into account the above mentioned limitations presented by the colloidal carriers in the field of pulmonary administration, we proposed in a previous work the microencapsulation of protein-loaded nanoparticles using the carbohydrate mannitol, as an attempt to improve their aerosolisation to the lungs and to ensure their intact delivery at the drug absorption site, so that these restrictions could be solved.[6]

The obtained microspheres presented adequate aerodynamic properties for pulmonary delivery. Furthermore, the physicochemical properties of the microencapsulated nanoparticles and the release profile of insulin were shown to not be negatively affected by the spray-drying process. Moreover, nanoparticles could be easily recovered upon incubation of the microspheres in an aqueous medium.[6] However, in that work we did not address the question of the microspheres structure and, more specifically, the nanoparticles distribution within the microspheres.

It is of great interest to analyse and visualise the spatial distribution of the involved structures, in order to confirm whether or not nanoparticles are homogeneously encapsulated in the microspheres and, hence, whether or not the nanoentrapped therapeutic protein is homogeneously distributed within the aerosolized powder. This will obviously influence the aerosol powder reproducibility and efficacy. In this manner, techniques such as confocal laser scanning microscopy (CLSM), X-ray photoelectron spectroscopy (XPS) and static time of flight secondary ion mass spectrometry (TOF-SIMS) should, altogether, provide information on the accurate characterisation of the microspheres internal and external structure. CLSM works on the basis of the fluorescent signals emitted by the different structures composing the material under evaluation, allowing a non-destructive and high-resolution image of samples. Its main advantage is the ability to provide visualisation of images parallel to the sample surface both at internal and external levels, at multiple depths, without any mechanical sectioning. Moreover, using different fluorescent labels for each independent structure to be analysed, marked compounds can be identified unambiguously.[19-21] Concerning the characterisation of drug delivery systems, this technique has already been applied to determine the localisation of nanoparticles incorporated in microspheres.[5,22] Nevertheless, the technique itself is not very precise in providing information on the most superficial composition of the microspheres. The surface region of a biomaterial, a region only a few atomic layers deep, is the interface between the biomaterial and the biological environment, which triggers the sequence of biological events occurring when a biomaterial or biomedical device enters the organism. Furthermore, the determination of the microspheres surface properties could be of great importance, given the knowledge that the chemical composition of particles surface governs interparticulate forces that influence dispersion of powder aerosols during inhalation.[16] Therefore, for a better understanding of the relation between surface properties and biological performance, it is necessary to characterise the biomaterial surface in detail. This entails determining the composition, structure and distribution of all components present on the surface. Accurate surface characterisation can be achieved using XPS and TOF-SIMS.

XPS is probably the most commonly used of the surface analysis techniques due to its non-destructive character. Upon exposition of the sample to an X-ray beam, the binding energies of characteristically emitted photoelectrons are measured, providing information on the elements from which they originate, as well as the chemical bonding of the elements.[23] XPS has been extensively used in the field of biomedical research with different aims such as characterisation of polyurethane membranes for cardiovascular application,[24] confirmation of chitosan and gelatin coating on polylactide-co-glycolide acid (PLGA) surfaces[25] and determination of surface composition of microspheres and nanoparticles.[16,26,27] In contrast to electron spectroscopy techniques like XPS, TOF-SIMS not only provides information on the elements present, but also offers detailed molecular information with high sensitivity, which is often called the surface "fingerprint". In this technique, the sample surface is impinged by ions of some energy, which causes the emission of intact molecules that are specific of the uppermost monolayer of the surface, usually varying within 2 and 5 nm. The ejected fractions which present surface charge, which are specific for each electron configuration, allow the detection of specific chemical elements.[28,29] This technique is much more recent than XPS, so its application in drug delivery is less extended. Nevertheless, TOF-SIMS has been used a few times to characterise surfaces of particles or powders, such as polystyrene or cellulose beads.[30,31]

In the present study we aimed to investigate the distribution of chitosan nanoparticles in mannitol microspheres. For this purpose, the inner structure of microspheres was characterized upon fluorescent labelling of the different constituents, mannitol and nanoparticles, using confocal laser scanning microscopy. Moreover, surface sensitive analyses of the microspheres using XPS and static TOF-SIMS was performed in order to accurately characterise the microspheres surface composition, determining whether or not nanoparticles are present.

Experimental section

Materials. Chitosan (CS) in the form of hydrochloride salt (Protasan® 213 Cl, deacetylation degree: 86%, viscosity: 95 mPa) was purchased from Pronova Biopolymer, A.S. (Norway). Pentasodium tripolyphosphate (TPP), glycerol, D-mannitol, phosphate buffered saline tablets (PBS) pH 7.4 and fluorescein isothiocyanate albumin (FITC-BSA) were supplied by Sigma Chemicals (USA). Bodipy® 630/650-X, SE was obtained from Molecular Probes (Netherlands). Ultrapure water (MilliQ Plus, Millipore Iberica, Spain) was used throughout.

Preparation of chitosan nanoparticles. CS/TPP nanoparticles were prepared according to the procedure developed by our group, based on the ionotropic gelation of CS with TPP anions, in which the positively charged amino groups of CS interact with the negatively charged TPP.[26] Briefly, CS and TPP were dissolved in purified water in order to obtain solutions of 1 mg/ml (w/v) and 0.69 mg/ml (w/v), respectively, to reach a final CS/TPP ratio of 3.6:1 (w/w). The spontaneous formation of nanoparticles occurs upon incorporation of 12 ml of the TPP solution in 30 ml of the CS solution, under gentle magnetic stirring at room temperature.

The FITC-BSA loaded CS/TPP nanoparticles were obtained following the protein dissolution in purified water (0.9 mg FITC-BSA/0.6 mL H_2O) and incorporation in the TPP solution (pH = 9.2) prior to the nanoparticles formation. The protein concentration in the TPP solution was calculated in order to obtain nanoparticles with a theoretical content of 30% (w/w) FITC-BSA with respect to CS.

Nanoparticles were concentrated by centrifugation at 16000×g on a 10 µl glycerol bed for 30 min at 15ºC (Beckman Avanti 30, Beckman, USA). The supernatants were discarded and nanoparticles were resuspended in 100 µl of purified water.

The nanoparticles production yield was calculated by gravimetry. Fixed volumes of nanoparticle suspensions were centrifuged (16000×g, 30 min, 15ºC) and sediments were freeze-dried over 24 h at -34ºC, followed by a gradual

increase of temperature until 20ºC, using a Labconco Freeze Dryer (Labconco, USA) (n = 3).

The process yield was calculated as follows:

$$\text{Process yield (\%)} = \frac{\text{Nanoparticles weight}}{\text{Total solids (CS + TPP + FITC-BSA) weight}} \times 100$$

Physicochemical characterisation of nanoparticles. The morphological examination of CS/TPP nanoparticles was conducted by transmission electron microscopy (TEM) (CM 12 Philips, Eindhoven, Netherlands). The samples were stained with 2% (w/v) phosphotungstic acid and placed on copper grids with Formvar® films for TEM observation.

Measurements of nanoparticles size and zeta potential were performed on fresh prepared samples by photon correlation spectroscopy and laser doppler anemometry, respectively, using a Zetasizer® 3000 HS (Malvern Instruments, Malvern, UK). For the particle size analysis, each sample was diluted to the appropriate concentration with filtered (0.2 μm filters Millex®-GN, Millipore Iberica, Spain) ultrapure water. Each analysis lasted 180 sec and was performed at 25ºC with a detection angle of 90º. For the determination of the electrophoretic mobility, samples were diluted with KCl 0.1 mM and placed in the electrophoretic cell, where a potential of ± 150 mV was established. Three batches of each formulation were analyzed in triplicate (n = 3).

Determination of FITC-BSA loading capacity. The nanoparticles association efficiency was determined upon separation of nanoparticles from the aqueous preparation medium containing the nonassociated protein by centrifugation (16000×g, 30 min, 15ºC). The amount of free FITC-BSA was determined in the supernatant measuring directly the absorbance by spectrophotometry (Shimadzu UV-Visible Spectrophotometer UV-1603, Japan) at 494 nm. A calibration curve was made using the supernatant of unloaded nanoparticles. Each sample was assayed in triplicate (n = 3). The nanoparticles protein loading capacity and association efficiency were calculated as follows:

$$\text{Loading capacity (\%)} = \frac{\text{Total FITC-BSA weight} - \text{Free FITC-BSA weight}}{\text{Nanoparticles weight}} \times 100$$

$$\text{Association efficiency (\%)} = \frac{\text{Total FITC-BSA weight} - \text{Free FITC-BSA weight}}{\text{Total FITC-BSA weight}} \times 100$$

Preparation of dry powders containing chitosan nanoparticles. Dry powders containing unloaded or FITC-BSA loaded CS/TPP nanoparticles were obtained by spray-drying a suspension of CS/TPP nanoparticles in mannitol, as previously reported.[6] The nanoparticle suspension in mannitol was obtained by resuspending the nanoparticle sediments obtained after centrifugation, with an aqueous solution of mannitol, to achieve a theoretical mannitol/nanoparticle ratio of 80/20 (w/w) and a final solids content of 2.1% (w/v). This carbohydrate/nanoparticle ratio was chosen as it leads to the production of microparticles with adequate morphologic and aerodynamic characteristics for pulmonary administration.[6] When necessary, mannitol was previously stained with a fluorescent label to allow its visualization with confocal microscopy. The fluorophore Bodipy® was added to the mannitol solution (167 µl of a 1 mg/mL solution of Bodipy®; 0.32 µg Bodipy®/mg mannitol) before nanoparticle resuspension, prior to spray drying. The spray-drying process was performed using a laboratory-scale spray-dryer (Büchi® Mini Spray Dryer, B-290, Switzerland), under the following conditions: two fluids external mixing 0.7 mm nozzle, feed rate of 2.5 mL/min, inlet and outlet temperatures of 160 ± 2°C and 108 ± 3°C, respectively. The air flow rate and the aspirator were kept constant at 400 Nl/h and 80%, respectively. Dry powders were collected and stored in a dessicator at room temperature until use.

The spray-drying process yield was calculated by gravimetry, comparing the total solids weight with the resultant weight of microspheres after spray-drying, as follows (n = 3):

$$\text{Process yield (\%)} = \frac{\text{Microspheres weight}}{\text{Total solids (CS+TPP+mannitol) weight}} \times 100$$

Microspheres surface and aerodynamic characterisation

Morphological analysis of microspheres. Microspheres were viewed using a scanning electron microscope (SEM, Leo 435VP, UK). Dry powders were placed onto metal plates and a 200 nm-thick gold palladium film was sputter-coated on the samples (High Resolution Sputter Coater SC7640, Termo VG Scientific, UK) before viewing. Furthermore, the Feret's diameter (distance between two tangents on opposite sides of the particle) was directly determined with an optical microscope (Olympus BH-2, Japan), this being estimated as the mean of 300 particles size (n = 300).

Determination of microspheres density. Real density was determined using an Helium Pycnometer (Micropycnometer, Quanta Chrome, model MPY-2, USA) (n = 3). The apparent tap density was obtained by measuring the volume of a known weight of powder in a 10 ml test-tube after mechanical tapping (30 tap/min, Tecnociencia, Spain). After registration of the initial volume, the test-tube was submitted to tapping until constant volume was achieved, according to a previously described method[32] (n = 3).

Evaluation of aerodynamic diameter. Aerodynamic diameters were obtained using a TSI Aerosizer® LD equipped with an Aerodisperser® (Amherst Process Instrument, Inc; Amherst, Ma, USA), whose measuring principle is based on the measurement of the particles time of flight (n = 3), according to the following equation:

$$C_d \frac{\pi d^2}{4} \rho_a \frac{(V_a - V_p)}{2} = 1/6\, \pi d^3 \rho_p \frac{dV_p}{dt}$$

where C_d: drag coefficient, d: particle diameter, ρ_a: density of air, V_a: velocity of air, V_p: velocity of particle, and ρ_p: density of particle.

***In vitro* release studies of FITC-BSA from nanoparticles and dry powders.** The release of FITC-BSA was determined by incubating the nanoparticles (CS/TPP 3.6:1) and the nanoparticle-loaded microspheres (mannitol/nanoparticles = 80/20, nanoparticles CS/TPP = 3.6:1) in 5 ml of pH 7.4 phosphate buffer (0.15 mg nanoparticles/ml, 0.75 mg microspheres/ml), with horizontal mechanical shaker (Heidolph Promax 1020, Germany), at 37ºC.

At appropriate time intervals (1, 2, 4, 6 and 8 days), individual samples were filtered (0.22 μm filters Millex®-GV, low protein binding, Millipore Iberica, Spain) and the amount of protein released was evaluated in the supernatants, by directly measuring the absorbance by spectrophotometry (Shimadzu UV-Visible Spectrophotometer UV-1603, Japan) at 494 nm (n = 3).

Structural characterisation of nanoparticle-loaded microspheres using confocal laser scanning microscopy (CLSM). The internal structure of the nanoparticle-loaded microspheres was observed by CLSM, using a TCS-SP2 vertical microscope (Leica GmbH, Germany), which collects images using different detectors for fluorescent signals, which in this case were obtained by two laser lines: Argon 488 nm and Helium-Neon 633 nm.

Small aliquots of the dry powder comprised of nanoparticle-loaded microspheres (nanoparticles loaded with FITC-BSA, mannitol labelled with Bodipy®) were placed on a glass slide and a drop of immersion oil was added to avoid particle displacement during viewing. Laser excitation wavelengths of 488 and 633 nm were used to scan the powder, and fluorescent emissions from FITC-BSA (emission λ = 500-570 nm) and Bodipy® (emission λ = 650-660 nm) were collected using separate channels. Images were acquired with a magnification of 100 x, using an oil immersion lens (HCX PL Fluotar). The greyscale images obtained from each scan were pseudo-coloured green (FITC-BSA) and red (Bodipy®) and overlapped afterwards (LCS Lite, Leica Confocal Software, Leica GmbH, Germany) to obtain a multicoloured image.

Microspheres surface analysis using X-ray photoelectron spectroscopy (XPS) and static time of flight secondary ion mass spectrometry (TOF-SIMS). Blank (without encapsulated protein) nanoparticle-loaded mannitol microspheres and microspheres comprised only of mannitol, were gently compacted into small stainless-steel troughs, and unloaded CS/TPP nanoparticles were directly placed on a polish monocristaline silicon wafer used as sample holder. The surface of these three samples was afterwards analysed using X-ray photoelectron spectroscopy (XPS, VG Escalab 250 iXL ESCA, VG Scientific, UK) and static time-of-flight secondary ion mass spectrometry (TOF-SIMS, TOF-SIMS IV, Ion-Tof GmbH, Germany). Mannitol microspheres and CS/TPP nanoparticles were used separately as controls. The XPS measurements were carried out using monochromatic Al-Kα radiation (hν=1486.92 eV) and photoelectrons were collected from a take off angle of 90º relative to the sample surface. Measurements were performed in a Constant Analyser Energy mode (CAE) with a 100 eV pass energy for survey spectra and 20eV pass energy for high resolution spectra. Charge referencing was done by setting the lower binding energy C1s photopeak at 285.0 eV C1s hydrocarbon peak. The high resolution spectra fitting is based on "Chi-squared" algoritm used to determine the soundness of a peak fit. The experimental conditions (X-ray source, power and analysis area), were the kept constant for each analysis.

For TOF-SIMS analyses, samples were bombarded with a pulsed Gallium primary ion beam ($69Ga^+$) generated with a liquid metal ion gun operated at 15 kV and 45º incidence with respect to the sample surface. The secondary ions generated were extracted with a 10 KV voltage and their time of flight from the sample to the detector was measured in a reflectron mass spectrometer. Electron flood gun charge compensation was necessary during measurements. A raster size of 500 µm × 500 µm was used and at least three different spots were analyzed under the "static" condition with ion doses of about $\approx 10^{12}$ ions/cm^2. The calibration of the mass spectra in the positive mode was based on hydrocarbon peaks such as CH_2^+, CH_3^+, $C_2H_2^+$, and $C_3H_5^+$.The experimental conditions (ion type, beam voltage and primary ion dose), were maintained constant for each experiment.

Statistical analysis. The t-test was used to perform the statistical analysis. All analysis were run using the SigmaStat statistical program (Version 3, Systat Software, USA) and differences were considered to be significant at a level of $P < 0.05$.

Results and Discussion

As stated in the introduction, in this work we have performed a detailed characterisation of a previously developed drug delivery system intended for pulmonary delivery, which consists in CS/TPP nanoparticles encapsulated in mannitol microspheres by a spray-drying technique. Figure 1 displays the chemical structure of the three constituents of the system, CS, TPP and mannitol.

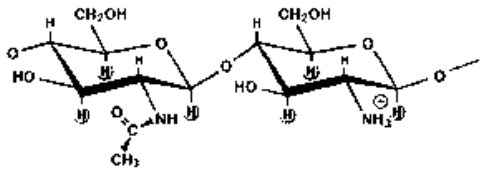

Chitosan (CS)

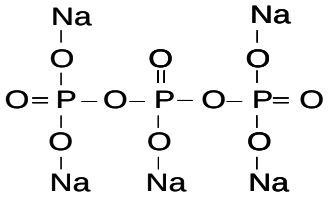

Tripolyphosphate (TPP)

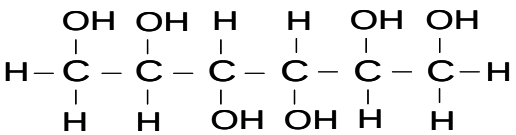

Mannitol

Fig. 1. Chemical structures of chitosan (CS), tripolyphosphate (TPP) and mannitol.

Extremely sensitive and accurate techniques of surface analysis such as XPS and TOF-SIMS were used to determine the microspheres surface composition. Moreover, confocal microscopy was applied in order to evaluate the nanoparticles distribution in the system; thus demonstrating the ability of the spray-drying technique to provide an adequate entrapment of the CS/TPP nanoparticles in inert carrier microspheres.

Preparation and characterisation of the systems. CS/TPP nanoparticles were produced using CS and TPP solutions, by a very mild ionic gelation method, as described in the methodology section. Figure 2 displays the TEM microphotograph of representative CS/TPP nanoparticles, showing that these are spherical, compact and non- aggregated structures.

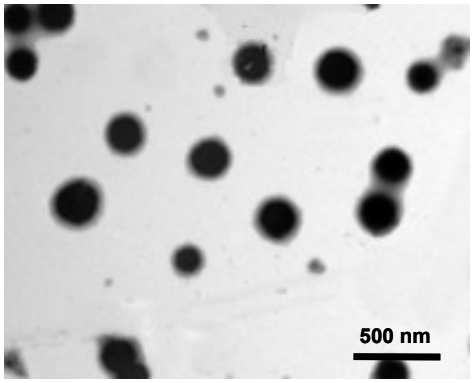

Fig. 2. TEM microphotograph of unloaded chitosan nanoparticles.

Table 1 depicts the physicochemical characteristics of unloaded (without encapsulated protein) and FITC-BSA loaded CS/TPP nanoparticles, FITC-BSA being selected as a model and labelling protein. The CS/TPP nanoparticles, produced with a process yield of 55 - 60%, present a size between 300 and 380 nm and a positive zeta potential of approximately + 34 mV.

Table 1. Process yields and physicochemical properties of unloaded (without protein) and FITC-BSA loaded nanoparticles (mean ± SD, n = 3).

Formulation	Process yield (%)	Size (nm)	Zeta potential (mV)	Association efficiency (%)	Loading capacity (%)
Unloaded	60 ± 4	300 ± 17	+ 34.3 ± 1.5	—	—
FITC-BSA loaded	55 ± 8	382 ± 16	+ 33.5 ± 3.3	89 ± 4	31 ± 1

Process yield (%) = [Nanoparticles weight / Total solids weight] x 100
Association efficiency (%) = [(Total FITC-BSA amount –Free FITC-BSA)/Total FITC-BSA amount] x 100
Loading capacity (%) = [(Total FITC-BSA amount–Free FITC-BSA)/Nanoparticles weight] x 100

As expected, FITC-BSA was successfully encapsulated in CS/TPP nanoparticles with association efficiency of approximately 90% and loading capacity as high as 31%. Protein incorporation did not lead to changes in the production yield or zeta potential. However, nanoparticles size showed a slight, although significant ($P < 0.05$), increase with the protein incorporation which, however, did not compromise our objectives.

Aerodynamic characteristics are the limiting parameters to the success in pulmonary delivery of powders, despite morphology representing an important factor, essentially considering particle aggregation, which may interfere in the flowing properties. The production of CS/TPP nanoparticle-loaded mannitol microspheres was previously described as an outstanding drug delivery system of proteins by the pulmonary route, given the adequate morphological and aerodynamic properties presented by these powders and their ability to release nanoparticles, and consequently the encapsulated peptide insulin, upon contact with an aqueous medium.[6] As can be observed in the SEM microphotograph depicted in Figure 3, microspheres obtained by spray-drying are spherical, not being aggregated, and they further present a smooth surface.

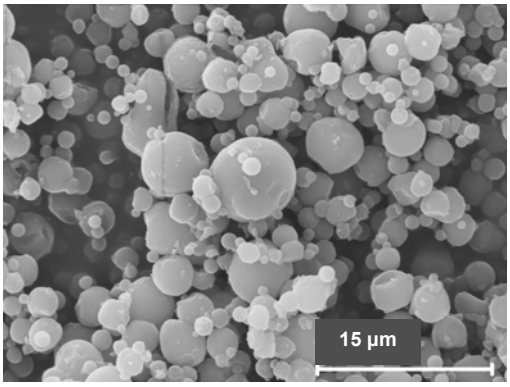

Fig. 3. SEM microphotograph of microspheres prepared with a mannitol/ nanoparticles (Ma/NP) theoretical ratio of 80/20 and a solids content of 2.1%.

The aerodynamic diameter, which is a combination of the particle size and density, influences the dispersion and sedimentation patterns, and should vary within 1 and 5 µm to allow an optimal lung deposition.[1,33] Microspheres produced in this work presented a Feret diameter of 3.1 µm, real density of approximately 1.5 g/cm^3 and a tap density as low as 0.3 g/cm^3, which rendered an aerodynamic diameter of 2.7 µm, adequate for lung delivery.

FITC-BSA was not released from the nanoparticles or nanoparticle-loaded microspheres within 8 days, the resultant absorbance being under the limit of detection of the equipment. The lower or absent release of FITC from chitosan nanoparticles was also reported by *Huang et al.*, who registered a maximum release of 1% in 24 hours, at pH 7.4.[34] The aqueous diffusion coefficient of a molecule is inversely related to its molecular weight[35] and it is likely that the high molecular weight of FITC-BSA (67 KDa) is responsible for the hindrance of its diffusion through the chitosan nanoparticles. Chitosan nanoparticles present a hydrogel structure and the existent mesh space in the hydrogel, which enables molecules diffusion, is the responsible for the size exclusion process for the associated molecules which release by this mechanism. The mesh can change from the collapsed to the swollen state, depending on the pH.[36] As the swelling of chitosan is greatly reduced at pH 7.4, selected to perform the *in vitro* release studies, it is possible that the mesh sizes available for the diffusion of FITC-BSA, which presents a size of 7.2 nm, were too small, thus preventing the release of the

protein. Therefore, taking into account this absence of release, it was confirmed the satisfactory selection of FITC-BSA as labelling protein to perform the subsequent studies of nanoparticle-loaded microspheres structural characterisation by confocal microscopy.

Structural characterisation of nanoparticle-loaded microspheres. From the observation of the SEM microphotograph collected in Figure 3, we could see that the produced dry powders have a spherical shape, as mentioned above. However, the SEM technique was not able to provide evidence on the nanoparticles localisation in the microspheres. In contrast, the application of a technique such as confocal microscopy permitted more clear information on the microspheres structure. Figure 4A shows three microphotographs corresponding to a cross-section of a microsphere, where from left to right it is shown the red channel (A1), which detects the signal of mannitol labelled with Bodipy®; the green channel (A2), which detects the signal emitted by the FITC-BSA labelled nanoparticles and, finally, the overlapping of both channels (A3). Figure 4B depicts three different sections of a series, obtained by varying values in the z axis, each section being separated from the subsequent one by 0.8 μm. From B1 to B3, the detector is moving from the middle of the microsphere to one of the tops. From the observation of these images (A and B), we could deduce that mannitol is distributed within the whole particle, forming a kind of continuous matrix, where the nanoparticles are homogeneously dispersed.

Similar results were obtained by *Sham et al.*, when preparing dry powders comprised of lactose and polycyanoacrylate nanoparticles. In their study, the nanoparticles were distributed within the whole microsphere, as occurs in our case, but the main difference is that our nanoparticles are evenly dispersed while theirs tend to accumulate in clusters, an effect that they explained as result of the adhesive nature and the surface energy of the nanoparticles.[5]

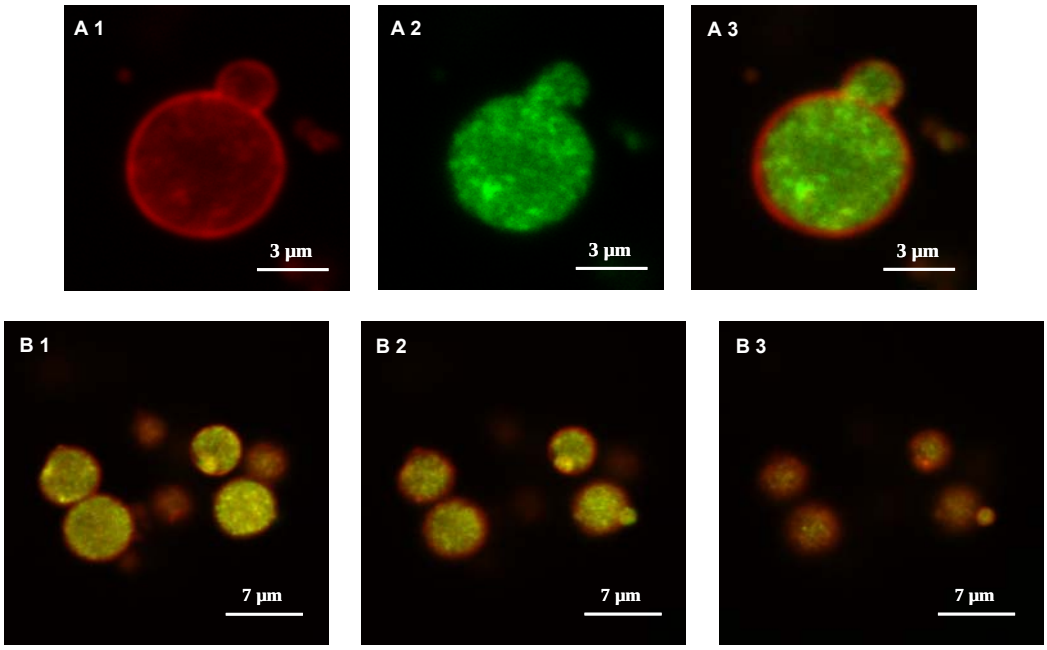

Fig. 4. Confocal imaging of microspheres, prepared with mannitol stained with Bodipy® (red) and nanoparticles labelled with FITC-BSA (green). A1: red channel, A2: green channel, A3: overlapping of both channels. B1, B2 and B3 correspond to the overlapping of both channels in different sections of the same series, separated in the z axis by 0.8 µm.

In the present work, CLSM images suggested that nanoparticles are efficiently encapsulated in the microsphere, being completely coated by a mannitol layer, which apparently forms a structure similar to a wall. Using this technique, the presence of nanoparticles in the outer side of the microspheres was not detected, since the most external signal detected is the red one, corresponding to mannitol. This wall effect was previously found by *Cook et al.* when encapsulating, using spray-drying, terbutaline nanoparticles in hydrophobic microspheres comprised of hydrogenated palm oil and dipalmitoylphosphatidylcholine. Also using CLSM as technique, they determined the absence of nanoparticles in the first 400 nm of the microspheres as well as a complete external layer of the hydrophobic components.[22]

In this work, most of the observed particles evidenced the presence of mannitol and CS/TPP nanoparticles within the whole particle, albeit during the confocal scanning of the powders a few hollow microspheres could be visualised

(Figure 5). It is important to notice that this occurred punctually and mostly for particles much larger than the mean size, which generally evidenced some kind of a hole or breach. In fact, we believe that the produced dry powder is mainly constituted of solid microspheres, which was also suggested by the high value obtained for real density (1.57 g/cm^3), as proposed elsewhere.[37]

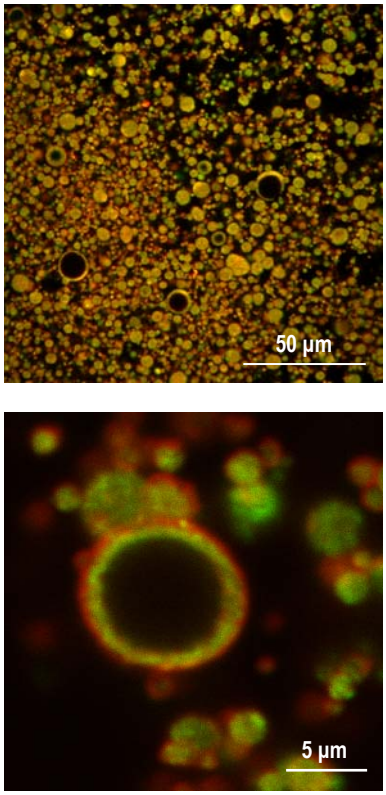

Fig. 5. Confocal images of hollow microspheres, showing overlapping of green and red channels.

Similarly, in a study performed with Eudragit® nanoparticles obtained using an air jet atomizer, it was found that the few hollow particles obtained, derived from their own collapse.[38] Spray-drying involves atomisation of a liquid into fine droplets and subsequent evaporation of the solvent as the material passes through the drying chamber.[39] During this step, a polymer film is formed on the surface of the droplet. If the vapour pressure of the solvent is too high, the

remaining solvent in the interior breaks through the film, resulting in collapsed and possibly hollow particles.[40] Therefore, we believe that in our study the hollow microspheres are particles that collapsed due to the high temperatures. This observation also corroborates the results presented in our previous paper, in which SEM microphotographs of some broken microspheres was shown. At that time, we inferred that at least some of the microspheres were hollow,[6] but we also referred to the necessity of further characterisation to achieve precise information on this subject.

Microspheres surface analysis. As commented above, CLSM images suggested that mannitol completely involved the nanoparticles, being present as an external shell of the microspheres. Although high resolution images could be obtained with this microscopy technique, it did not allow an accurate analysis of the surface composition of the microspheres, which would be determinant to know the localisation of nanoparticles and mannitol. As it has been previously commented, the determination of these surface properties could be of major importance from the point of view of the behaviour of powder aerosols during inhalation as well as of their biological performance. In this manner, specific techniques of surface analysis, such as XPS or TOF-SIMS, which deal with the determination of the chemical elements present in the most superficial layer of the samples and in this case of the microspheres, should provide us with unquestionable information on the surface composition.

Table 2 displays the results of surface composition obtained from the individual surface analysis of control nanoparticles, control mannitol and microspheres containing both nanoparticles and mannitol; the percentage of each chemical element present in the sample being determined. The XPS survey of control CS/TPP nanoparticles detected the expected elements, such as C, N, P and O, albeit traces of Si were also found, which could be a result of the Si-based sample holder substrate or a consequence of the processing of the exoskeleton components from the original material, as reported elsewhere.[41] The XPS assay detected in the nanoparticles approximately 54% of C and 34% of O. Moreover, 5% N and 3% P were detected, which, according to the chemical structures

depicted in Figure 1, corresponds to the presence of, respectively, CS and the crosslinking agent TPP.

Table 2. Surface composition (atomic percentage), determined by XPS, of CS/TPP nanoparticles, mannitol and microspheres (mannitol/nanoparticles = 80/20).

Element	CS/TPP nanoparticles (%)	Mannitol (%)	Microspheres (%)
C	53.8	56.2	54.9
O	33.8	43.8	43.3
N	4.5	0	0.6
P	2.7	0	0
Si	5.2	0	1.2
Ratio N/C	0.084	0	0.011
Ratio C/O	1.592	1.283	1.268

The obtained atomic percentages were comparable to those previously reported by *Matienzo and Winnacker* when analysing chitosan films (61% C, 31% O and 6% N), although slight differences could be explained by the use of chitosans with different deacetylation degrees (86% in our case *vs* 70% in theirs), as well as by the fact that we analysed chitosan nanoparticles containing TPP, while they assayed pure chitosan films.[41] Furthermore, in our work, a C/O ratio of approximately 1.6 was obtained, which is similar to the 1.4 that was found by *Calvo et al.* in a study with CS nanoparticles (CS/TPP = 4.4:1). In addition, we found a C/N ratio of 11.9, which is slightly higher than that obtained by *Calvo et al.* (10.9) and which reflects the lower amount of chitosan we used (CS/TPP = 3.6:1 *vs* 4.4:1 used in the referred study).[26]

As expected, the analysis of the control mannitol only detected signal of C (56%) and O (44%), typical elements of this substance (see Figure 1), the C/O ratio being 1.283. When analysing the surface of microspheres containing mannitol and CS/TPP nanoparticles, high amount**s** of C and O were detected, but

also small amounts of N, an element exclusive of the CS/TPP nanoparticles, were found. However, it should be noted that the amount of N detected in the control nanoparticles was 4.5%, while in the microspheres only 0.6% was identified, indicating the presence of less nanoparticles in the latter. Moreover, Si signal was also identified, which as previously said could be attributed to the processing of chitin shells and, therefore, to the presence of chitosan. Despite this indicates the presence of nanoparticles in the microspheres surface, it is important to notice that the C/O ratio found in the microspheres is very similar to that of control mannitol (1.283 and 1.268, respectively). This indicates that the microspheres surface is mostly composed of mannitol, but nanoparticles are also detected, though to a lower extent, which is consistent with the mannitol/nanoparticles ratio (mannitol/nanoparticles = 80/20) composing microspheres.

Figure 6 displays the positive mass spectra between 180 and 290 amu, obtained by TOF-SIMS for each of the analysed samples. The obtained results corroborated those previously observed by XPS, indicating that there is a high resemblance between the elemental composition of the control mannitol and microspheres containing mannitol and nanoparticles. In fact, we could observe masses (M) which have been reported as specific and typical of mannitol, such as the M183 (molecular ion + H^+) in both mannitol and microspheres containing nanoparticles.[42] On the other side, comparing the spectra of microspheres with that of control nanoparticles, similar masses which correspond to positive ions characteristic of the nanoparticles can be identified in both samples. Given the absence of bibliographic support on the typical masses of this mixture CS/TPP, we assume that characteristic ions from nanoparticles are those identified in their spectra, which should appear in the microspheres spectrum in the case that nanoparticles are detected in the microspheres surface. These characteristic ions, such as M193 ($CH_{19}P_2N_6O$), M249 ($C_{10}H_{18}PO_5$) and M281 ($C_4H_{21}N_{14}O$), among others, result from the starting material (CS and TPP) and can arise from the fragmentation of both compounds, from the fragmentation of the phosphated polymer if there is any chemical reaction between CS and TPP, or even from the association of fragments of both. Moreover, M221.2 was further detected in the microspheres possibly being due to the N-acetyl-D-glucosamine molecular ion ($C_8H_{15}NO_6$), which is the basic unit of chitosan molecules.[42]

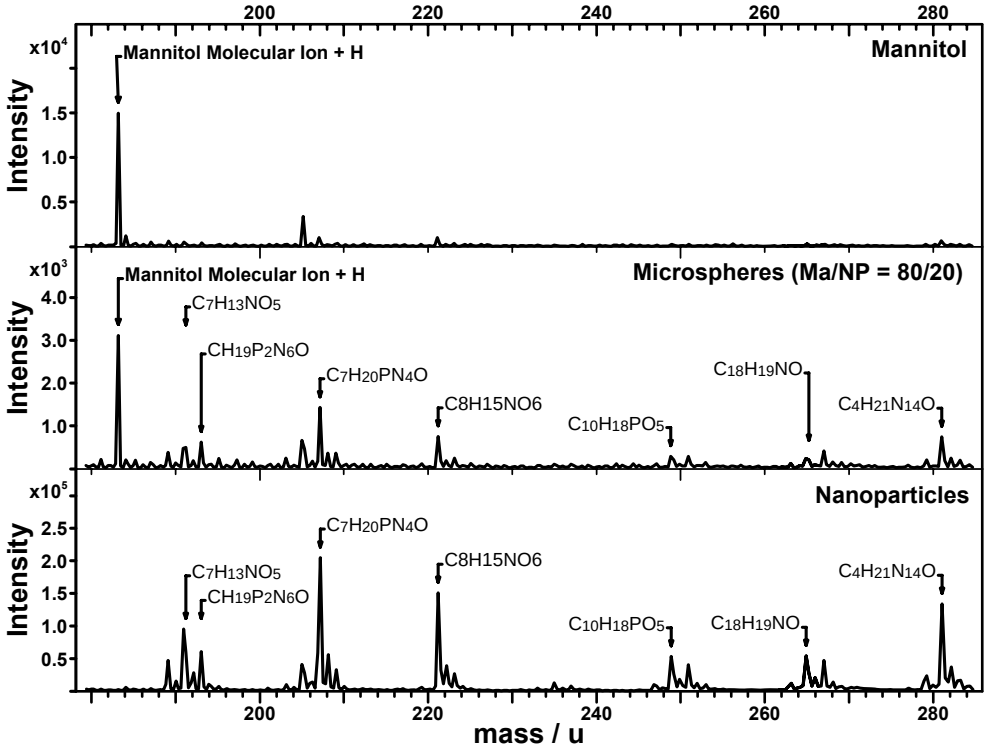

Fig. 6. Mass spectra obtained by TOF-SIMS of control mannitol, nanoparticle-loaded microspheres (mannitol/nanoparticles (Ma/NP) = 80/20) and control CS/TPP nanoparticles.

Considering the intensities of the referred peaks and comparing them in the spectra of each sample, it was demonstrated that although much of the surface is covered by mannitol, nanoparticles could also be detected. Given the novelty of this technique, no references were found reporting results of the application of TOF-SIMS on this material and, thus, the establishment of comparisons with previous developed works was not possible.

A global analysis of the results obtained by XPS and TOF-SIMS indicated that mannitol constitutes the most part of the microspheres surface and that nanoparticles were detected to a lower extent. Moreover, these results are in

agreement with a homogeneous distribution of the nanoparticles in the microspheres, as suggested by the CLSM technique.

Conclusions. The present work demonstrates that microspheres containing chitosan/ tripolyphosphate (CS/TPP) nanoparticles dispersed in mannitol, previously proposed for pulmonary delivery of macromolecules, can be structurally characterised using innovative techniques such as confocal laser scanning microscopy (CLSM), X-ray photoelectron spectroscopy (XPS) and time-of-flight secondary ion mass spectrometry (TOF-SIMS). The examination by CLSM indicated that the nanoparticles were efficiently encapsulated in the microspheres, being homogenously distributed within the whole particle. Moreover, the specific and accurate analysis of the microspheres surface using extremely surface sensitive techniques such as XPS and TOF-SIMS, demonstrated the presence of mannitol and nanoparticles on the microspheres surface. However, a higher proportion of mannitol was detected, in agreement with the mannitol/nanoparticles ratio of the microspheres. Therefore, given the successful microencapsulation of the CS/TPP nanoparticles, it was confirmed that this drug delivery system is a promising carrier of protein-loaded nanoparticles and, hence, of therapeutic proteins to the lung.

Acknowledgements. This work was supported by the Spanish Government (CICYT, SAF2002-03314, Feder cofinanced). The Predoctoral fellowship to Ana Grenha from Fundação para a Ciência e Tecnologia, Portugal (SFRH/BD/13119/2003) is highly appreciated.

References

(1) Taylor, G.; Kellaway, I. In *Drug delivery and targeting. For pharmacists and pharmaceutical scientists*, Hillery, A., Lloyd, A., Swarbrick, J., Eds.; Taylor & Francis: New York, 2001; p 269.

(2) Zhang, Q.; Shen, Z.; Nagai, T. *Int. J. Pharm.* **2001**, 218, 75-80.

(3) Tsapis, N.; Bennet, D.; Jackson, B.; Weitz, D. A.; Edwards, D. A. *Proc. Nat. Acad. Sci.* **2002**, 99, 12001-12005.

(4) Dailey, L. A.; Schmehl, T.; Gessler, T.; Wittmar, M.; Grimminger, F.; Seeger, W.; Kissel, T. *J. Control. Release.* **2003**, 86, 131-144.

(5) Sham, J. O.; Zhang, Y.; Finlay, W. H.; Roa, W. H.; Löbenberg, R. *Int. J. Pharm.* **2004**, 269, 457-467.

(6) Grenha, A.; Seijo, B.; Remuñan-Lopez, C. *Eur. J. Pharm. Sci.* **2005**, 25, 427-437.

(7) Heyder, J.; Gebhart, J.; Rudolf, G.; Schiller, C. F.; Stahlhofen, W. *J. Aerosol Sci.* **1986**, 17, 811-825.

(8) Finlay, W. H.; Stapleton, K. W.; Zuberbuhler, P. *J. Aerosol Sci.* **1997**, 28, 1301-1309.

(9) Finlay, W. H.; Gehmlich, M. G. *Int. J. Pharm.* **2000**, 210, 83-95.

(10) Clark, A. *Drug Deliv. Syst. Sci.* **2002**, 2, 73-77.

(11) Calvo, P.; Remuñan-Lopez, C.; Vila-Jato, J. L.; Alonso, M. J. *Pharm. Res.* **1997**, 14, 1431-1436.

(12) Fernandez-Urrusuno, R.; Calvo, P.; Remuñan-Lopez, C.; Vila-Jato, J. L.; Alonso, M. J. *Pharm. Res.* **1999**, 16, 1576-1581.

(13) De Campos, A.; Sanchez, A.; Alonso, M. J. *Int. J. Pharm.* **2001**, 224, 159 168.

(14) Alonso-Sande, M.; Cuña, M.; Remuñán-López, C.; Teijeiro-Osorio, D.; Alonso-Lebrero, J. L.; Alonso, M. J. *Macromolecules* **2006**, 39, 4152-4158.

(15) Cuña, M.; Alonso-Sande, M.; Remuñan-Lopez, C.; Pivel, J. P.; Alonso-Lebrero, J. L.; Alonso, M. J. *J. Nanosci. Nanotechnol.* **2006**, 6, 2887-2895.

(16) Bosquillon, C. ; Rouxhet, P. G.; Ahimou, F. ; Simon, D. ; Culot, C.; Préat, V. Vanbever, R. *J. Control. Release.* **2004**, 99, 357-367.

(17) Steckel, H.; Brandes, H. G. *Int. J. Pharm.* **2004**, 278, 187-195.

(18) Todo, H.; Okamoto, H.; Iida, K.; Danjo, K. *Int. J. Pharm.* **2004**, 271, 41-52.

(19) Lamprecht, A.; Schäfer, U. F.; Lehr, C. M. *Int. J. Pharm.* **2000**, 196, 223-226.

(20) Alvarez-Román, R.; Naik, A.; Kalia, Y. N.; Fessi, H.; Guy, R. H. *Eur. J. Pharm. Biopharm.* **2004**, 58, 301-316.

(21) White, N. S.; Errington, R. J. *Adv. Drug Deliv. Rev.* **2004**, 57, 17-42.

(22) Cook, R. O.; Pannu, R. K.; Kellaway, I. W. *J. Control. Release.* **2005**, 104, 79-90.

(23) Turner, N. H.; Schreifels, J. A. *Anal. Chem.* **1998**, 70, 229R-250R.

(24) Lin, W.-C.; Tseng, C.-H.; Yang, M.-C. *Macromol. Biosci.* **2005**, 5, 1013-1021.

(25) Zhu, A. P.; Fang, N.; Chan-Park, M. B.; Chan, V. *Biomaterials* **2006**, 27, 2566-2576.

(26) Calvo, P.; Remuñan-Lopez, C.; Vila-Jato, J. L.; Alonso, M. J. *J. Appl. Polym. Sci.* **1997**, 63, 125-132.

(27) Dong, Y.; Feng, S. *Biomaterials* **2004**, 25, 2843-2849.

(28) Hagenhoff, B. *Mikrochimica Acta* **2000**, 132, 259-271.

(29) Belu, A. M.; Graham, D. J.; Castner, D. G. *Biomaterials* **2003**, 24, 3635-3653.

(30) Davies, M. C.; Brown, A.; Newton, J. M.; Chapman, S. R. *Surf. Interface Anal.* **1988**, 11, 591-595.

(31) John, C. M.; Odom, R. W.; Salvati, L.; Annapragada, Ananth V.; Lu, M. Y. F. *Anal. Chem.* **1995**, 67, 3871-3878.

(32) El-Gibaly, I. *Int. J. Pharm.* **2002**, 294, 7-21.

(33) Courrier, H. M.; Butz, N.; Vandamme, T. F. *Crit. Rev. Ther. Drug Carr. Syst.* **2002**, 19, 425-498.

(34) Huang, M.; Zengshuan, M.; Khor, E.; Lim, L.-Y. *Pharm. Res.* **2002**, 19, 1488-1494.

(35) Polson, A. *J. Phys. Colloid. Chem.* **1950**, 54, 169-174.

(36) Peppas, N. A. *Colloid. Interface Sci.* **1997**, 2, 531-537.

(37) Gilani, K.; Najafabadi, A. R.; Barghi, M.; Rafiee-Tehrani, M. *Eur. J. Pharm. Biopharm.* **2004**, 58, 595-606.

(38) Eerikäinen, H.; Kauppinen, E. I. *Int. J. Pharm.* **2003**, 263, 69-83.

(39) Roos, Y. H. *Lait* **2002**, 82, 475-484.

(40) Raula, J.; Eerikäinen, H.; Kauppinen, E. I. *Int. J. Pharm.* **2004**, 284, 13-21.

(41) Matienzo, L. J.; Winnacker, S. K. *Macromol. Mat. Eng.* **2002**, 287, 871-880.

(42) Linstrom, P. J., Mallard, W.G., Eds.; *NIST Chemistry WebBook, NIST Standard Reference Database*; National Institute of Standards and Technology: Gaithersburg, MD, 2005 (http://webbook.nist.gov).

Sección II. Producción y caracterización del comportamiento *in vitro* de microsferas de manitol conteniendo complejos de lípidos y nanopartículas de quitosano

Artículo 4

MICROSPHERES CONTAINING LIPID/CHITOSAN NANOPARTICLES COMPLEXES FOR PULMONARY DELIVERY OF THERAPEUTIC PROTEINS

Ana Grenha, Carmen Remuñán-López, Edison L. S. Carvalho, Begoña Seijo*

Dept. of Pharmacy and Pharmaceutical Technology, University of Santiago de Compostela, Faculty of Pharmacy, Campus Sur, 15782 Santiago de Compostela, Spain.

* Corresponding author: Phone: 0034 981 563100 – ext. 14881
Fax: 0034 981 547148
E-mail: ffseijo@usc.es

Artículo sometido a evaluación por "European Journal of Pharmaceutics and Biopharmaceutics"

Abstract

Chitosan/tripolyphosphate nanoparticles have already demonstrated to promote peptide absorption through several mucosal surfaces. We have recently developed a new drug delivery system consisting of complexes formed between preformed chitosan/tripolyphosphate nanoparticles and phospholipids, named as lipid/chitosan nanoparticles (L/CS-NP) complexes. The aim of this work was to microencapsulate these protein-loaded L/CS-NP complexes by spray-drying, using mannitol as excipient and obtaining microspheres with adequate properties for pulmonary delivery. Results show that the obtained microspheres are spherical and present appropriate aerodynamic characteristics for lung delivery (aerodynamic diameters around 2 – 3 μm and low apparent tap density of 0.4 - 0.5 g/cm^3). The physicochemical properties of the L/CS-NP complexes are affected by the phospholipids composition, which provide a controlled release of the encapsulated protein (insulin), which was successfully associated to the system (68%). The complexes can be easily recovered from the mannitol microspheres upon incubation in aqueous medium, maintaining their morphology and physicochemical characteristics. Therefore, this work demonstrates that protein-loaded L/CS-NP complexes can be efficiently microencapsulated, resulting in microspheres with adequate properties to provide a deep inhalation pattern. Furthermore, they are expected to release their payload (the complexes and, consequently, the encapsulated macromolecule) after contacting with the lung aqueous environment.

Keywords: chitosan nanoparticles, dry powders, microspheres, phospholipids, pulmonary delivery, spray-drying

1. Introduction

The pulmonary administration of therapeutic macromolecules is currently receiving increased attention, and the design of adequate carriers appears as the limiting factor to success in this process. In this respect, microspheres have been proposed, since they can be tailored to exhibit appropriate aerodynamic properties [1] and they should possess a very narrow range of aerodynamic diameter, usually accepted to vary between 1 and 5 μm [1,2].

The application of colloidal systems such as liposomes, which consist of an aqueous core encapsulated within one or more phospholipid bilayer membranes [3,4], as an interesting alternative for the administration of biomolecules through several mucosal surfaces [3,5] has been encouraged, since they are versatile and tend to be relatively innocuous (they are composed of natural and biodegradable compounds), whilst providing protection to the encapsulated material [4,6-8]. Their organised structure permits the association of drugs to both the aqueous and lipid phase, depending on their solubility characteristics, and drug release can usually be controlled, depending on the bilayers number and composition [4,8,9]. In order to achieve an improved controlled release, the incorporation of a drug-loaded vesicle inside a second vesicle, the encapsulation of particulate matter inside lipid vesicles, or even the adsorption of lipid bilayers onto polyelectrolyte-coated capsules have been reported [10-14]. Moreover, in our laboratory, a new drug delivery system consisting of lipid/chitosan nanoparticles (L/CS-NP) complexes, intended for gastric delivery as a first approach was recently developed and permitted the protection of chitosan nanoparticles from the acidic gastric environment [15]. Similar structures proved to be useful for oral immunisation, leading to higher titers of serum IgG when compared to unmodified nanoparticles [16]. Nanoassemblies composed of spherical polystyrene cores surrounded by lipid layers have been further reported as promising carriers in biotechnology, as drug, antigen or gene delivery systems [17-20] and some of these assemblies also proved to be efficiently applied in cancer therapy [21-23].

Liposomes intended for pulmonary administration have been introduced in the form of dry powders, as an approach to overcome the known stability problems of liposome suspensions [24-26]. Their use has also been suggested for

sustained lung release of several drugs and their interaction with the endogenous phospholipids was proposed as a contribution to the prolonged retention of peptides within the lung. Furthermore, enhanced drug absorption provided by phospholipids similar to those composing the pulmonary surfactant was also reported, although the mechanism of absorption enhancement is still unknown [27-30]. One of the major problems concerning the pulmonary administration of particulate systems is the rapid capture by the alveolar macrophages on reaching the alveolar region [8,31], which is known to be affected by several factors such as particle size, surface properties, composition and local concentration [32-36]. In this respect, the macrophagic capture of PLGA microparticles upon interaction of microparticles with alveolar macrophages in culture, was reported to be reduced by the inclusion of phosphatidylcholine, -serine and -ethanolamine in the formulation [37].

Nanoparticles have also been recently proposed as delivery systems for peptides and proteins along the pulmonary route [38-42], their production being possible with a wide variety of polymers and nanotechnologies [43,44]. In this respect, chitosan is a very attractive polysaccharide due to its low toxicity, biodegradability and mucoadhesivity [45-47]. Our group has reported the preparation of chitosan/tripolyphosphate (CS/TPP) nanoparticles by an extremely mild and rapid ionotropic gelation procedure between chitosan and its counterion TPP [48], which show an excellent protein association capacity, as well as an improvement of peptide absorption through several epithelia, such as the nasal, ocular and intestinal [49-52]. Furthermore, we recently reported the production of microspheres as carriers for protein-loaded chitosan nanoparticles to the lung, with the aim of improving their aerosolisation patterns. These microspheres were obtained by spray-drying a suspension of nanoparticles in mannitol, and thus exhibited adequate aerodynamic properties for lung delivery. Moreover, nanoparticles could easily be recovered from microspheres upon incubation with an aqueous medium, without significant changes in their morphology and physicochemical properties [42].

The spray-drying technique allows the encapsulation of sensitive peptide drugs in microspheres [53] and it has been reported to produce microspheres with

adequate aerodynamic properties for lung delivery [42,54-56]. The spray-drying of liposomes without compromising their stability has been reported [57]. Furthermore, in a work reporting the spray-drying of solid lipid nanoparticles, the presence of carbohydrates like mannitol, lactose and trehalose provided an increased stability to the spray-dried product, because the sugar layer around the particles prevented the lipids coalescence [58].

In this work, the production of microspheres containing lipid/chitosan nanoparticles complexes, intended for the pulmonary administration of macromolecules, using a spray-drying technique is reported. For this purpose, mannitol, which is known for its non-toxic and degradable properties [2], was chosen as microencapsulation excipient and insulin as the model protein. Microspheres aerodynamic properties were characterised, as well as their ability to deliver *in vitro* the lipid/nanoparticle complexes. Moreover, the effect of different lipid compositions on the complexes physicochemical characteristics and on the nanoparticles release profile was investigated. Considering the previous acquired knowledge about nanoparticles, liposomes and microspheres, we realized that this combinatorial technology, using these three systems, would be a valuable approach to integrating their respective advantages, while avoiding their particular disadvantages and, thus, leading to an efficacious drug delivery system.

2. Materials and methods

2.1. Chemicals

Chitosan (CS) in the form of hydrochloride salt (Protasan® 213 Cl, deacetylation degree: 86%, viscosity: 95 mPa) was purchased from FMC Biopolymer AS (Norway). Dipalmitoylphosphatidylcholine (DPPC) and dimyristoylphosphatidyl glycerol (DMPG) were supplied by Lipoid (Germany). Pentasodium tripolyphosphate (TPP), glycerol, D-mannitol (Ma), phosphate buffered saline tablets (PBS) pH 7.4 and bovine insulin were supplied by Sigma Chemicals (USA). Ultrapure water (MilliQ Plus, Millipore Iberica, Spain) was used throughout. All other chemicals were reagent grade.

2.2. Preparation of chitosan nanoparticles (CS-NP)

CS-NP were prepared according to the procedure developed by our group, based on the ionotropic gelation of CS with TPP, in which the positively charged amino groups of CS interact with the negatively charged TPP [48]. Briefly, CS and TPP were dissolved in purified water in order to obtain solutions of 1 mg/mL and 0.42 mg/mL, respectively. The spontaneous formation of nanoparticles occurred upon incorporation of 1.2 mL of the TPP solution in 3 mL of the CS solution (final CS/TPP ratio of 6:1 (w/w)), under mild magnetic stirring (Plate A-13 Serie D, SBS, USA) at room temperature.

The insulin loaded CS-NP were obtained following the protein dissolution in NaOH 0.01 M (0.9 mg insulin/0.6 mL NaOH) and it's consequent incorporation in the TPP solution (pH = 11.6; 0.6 mL TPP solution + 0.6 mL insulin solution). The insulin concentration in the TPP solution was calculated in order to obtain CS-NP with a theoretical content of 30% (w/w) insulin respective to CS.

CS-NP were concentrated by centrifugation at 16000×g on a 10 µl glycerol bed for 30 min at 15ºC (Beckman Avanti 30, Beckman, USA). The supernatants were discarded and nanoparticles were re-suspended in 100 µl of purified water.

CS-NP were also prepared in a large scale, adding 12 mL of the TPP solution to 30 mL of the CS solution and maintaining the stirring conditions. They were centrifuged at 10000×g and the re-suspension conditions were proportionally adapted. CS-NP produced in large scale were used to prepare all the formulations of lipid/nanoparticles (L/CS-NP) complexes, with the low scale being used only to characterise nanoparticles.

2.3. Determination of CS-NP production yield

The CS-NP production yield was calculated by gravimetry. Fixed volumes of nanoparticle suspensions were centrifuged (16000×g, 30 min, 15ºC) and sediments were freeze-dried for 24 h at -34ºC, followed by a gradual ascent until 20ºC, using a Labconco Freeze Dryer (Labconco, USA) (n = 3).

The process yield (P.Y.) was calculated as follows:

$$\text{P. Y. (\%)} = \frac{\text{CS-NP weight}}{\text{Total solids (CS + TPP + insulin) weight}} \times 100$$

Eq. (1)

2.4. Characterisation of CS-NP

Measurements of CS-NP size and zeta potential were performed by photon correlation spectroscopy and laser doppler anemometry, respectively, using a Zetasizer® 3000 HS (Malvern Instruments, Malvern, UK). For the particle size analysis, each sample was diluted to the appropriate concentration with filtered (0.2 µm filters Millex®-GN, Millipore Iberica, Spain) ultrapure water. Each analysis lasted 180 sec and was performed at 25ºC with a detection angle of 90º. For the determination of the electrophoretic mobility, samples were diluted with KCl 0.1 mM and placed in the electrophoretic cell, where a potential of ± 150 mV was established. Three batches of each formulation were analysed in triplicate (n = 3).

2.5. Determination of insulin loading capacity

The CS-NP association efficiency was determined upon separation of nanoparticles from the aqueous preparation medium containing the non-associated protein by centrifugation (16000×g, 30 min, 15ºC). The amount of free insulin was determined in the supernatant by the MicroBCA protein assay (Pierce, USA), measuring the absorbances by spectrophotometry (Shimadzu UV-Visible Spectrophotometer UV-1603, Japan) at 562 nm. A calibration curve was made using the supernatant of unloaded CS-NP. Each sample was assayed in triplicate (n = 3). The CS-NP protein loading capacity (L.C.) and association efficiency (A.E.) were calculated as follows:

$$\text{L. C. (\%)} = \frac{\text{Total insulin amount} - \text{Free insulin amount}}{\text{CS-NP weight}} \times 100$$

Eq. (2)

$$\text{A. E. (\%)} = \frac{\text{Total insulin amount} - \text{Free insulin amount}}{\text{Total insulin amount}} \times 100$$

Eq. (3)

2.6. Preparation of lipid/chitosan nanoparticle (L/CS-NP) complexes

The L/CS-NP complexes were prepared by adding a suspension of previously prepared CS-NP to a dry lipid film, following a procedure previously developed by our group [15]. Briefly, DPPC or a mixture of DPPC and DMPG (10:1 molar ratio) were dissolved in 20 mL of chloroform, obtaining a 0.3 mM lipid concentration, and 50 mg of glass beads were added to increase the surface area available to form the film. The organic solvent was then removed by evaporation under reduced pressure on a rotary evaporator (Buchi® R-114, Buchi, Switzerland) at approximately 55ºC, for 3 h on a nitrogen atmosphere, leading to the formation of a thin film of dry lipid [24,59,60]. This film was then hydrated for 30 min with a suspension of the CS-NP (unloaded or insulin loaded), forming L/CS-NP systems of ratio 3:1 (w/w). Immediately afterwards, the complexes were filtered under vacuum to allow for their separation from the glass beads. Control vesicles were produced under the same conditions, using water as the hydrating phase.

2.7. Characterisation of the L/CS-NP complexes

The morphological examination of the complexes was conducted by optical (Olympus BH-2, Japan) and transmission electron microscopy (TEM) (CM 12 Philips, Netherlands). For TEM observation, samples were stained with 2% (w/v) phosphotungstic acid and placed on copper grids, previously covered with Formvar® films.

The size of the control vesicles and L/CS-NP complexes was determined by the Coulter counter method (Coulter® Multisizer II, Coulter Electronics, England), equipped with a tube with an orifice aperture of 50 µm. To perform the measurements, 20 µl of the previously obtained suspension of complexes were dispersed in 100 mL of the electrolyte Isoton II (filtered, phosphate-buffered saline solution PBS). The instrument was previously calibrated using Isoton II and monodisperse latex microspheres of 13 µm, both supplied by Coulter (n = 3). Zeta potential measurements were performed by laser doppler anemometry, using the Zetasizer®. Samples were diluted with KCl 0.1 mM and placed in the electrophoretic cell, where a potential of ± 150 mV was established. Three batches of each formulation were analysed in triplicate (n = 3).

2.8. Preparation of dry powders containing L/CS-NP complexes

Dry powders containing the L/CS-NP complexes were obtained by a spray-drying technique, as previously described for the microencapsulation of nanoparticles [42]. Briefly, an aqueous solution of mannitol was added to the previously obtained suspension of L/CS-NP complexes, in order to achieve a theoretical mannitol/complexes ratio of 80/20 (w/w), and a final solids content of 2.1% (w/v). The chosen carbohydrate/complexes ratio was the optimum used to prepare microspheres containing mannitol and nanoparticles, as reported before, the resultant microspheres presenting adequate aerodynamic properties for pulmonary delivery [42]. The spray drying process was performed using a laboratory-scale spray-dryer (Büchi® Mini Spray Dryer, B-290, Buchi, Switzerland), with the following conditions: a two fluids external mixing 0.7 mm nozzle was used, feed rate was 2.5 mL/min, inlet and outlet temperatures were 120 ± 2ºC and 85 ± 2ºC, respectively. The air flow rate and the aspirator were constant at 400 Nl/h and 80%, respectively. Microspheres were collected and stored in a dessicator at room temperature until use.

2.9. Determination of spray-drying process yield

The spray-drying process yield (P.Y.) was calculated by gravimetry, comparing the total solids weight of the spray suspension with the resultant powder weight after spray-drying, as follows (n = 3):

$$\text{P.Y. (\%)} = \frac{\text{Microspheres weight}}{\text{Spray suspension total solids (L/CS-NP + mannitol) weight}} \times 100$$

Eq. (4)

2.10. Morphological analysis of microspheres

Microspheres were visualised using a scanning electron microscope (SEM, Leo 435VP, UK). Dry powders were placed onto metal plates and a 200 nm-thick gold palladium film was sputter coated on the samples (High Resolution Sputter Coater SC7640, Termo VG Scientific, UK) before viewing. The particle size was determined as the Feret's diameter (distance between two tangents on opposite sides of the particles) and was directly determined with an optical microscope (Olympus BH-2, Japan), where a 300 particles measurement (n = 300) is estimated as the mean.

2.11. Determination of microspheres density

Real density was determined using a Helium Pycnometer (Micropycnometer, Quanta Chrome, model MPY-2, USA) (n = 3). Apparent tap density was obtained by measuring the volume of a known weight of powder in a 10 mL test-tube after mechanical tapping (30 tap/min, Tecnociencia, Spain). After registration of the initial volume, the test-tube was submitted to tapping until constant volume was achieved, according to a previously described method [61] (n = 3).

2.12. Evaluation of aerodynamic properties

Aerodynamic diameters were obtained using a TSI Aerosizer® LD equipped with an Aerodisperser® (Amherst Process Instrument, Inc; Amherst, Ma, USA), where the measuring principle is based on the measurement of the particles time of flight in an air stream (n=3), according to the following equation:

$$C_d \frac{\pi d^2}{4} \rho_a \frac{(V_a - V_p)}{2} = 1/6\, \pi d^3 \rho_p \frac{dV_p}{dt}$$

Eq. (5)

where C_d: drag coefficient, d: particle diameter, ρ_a: density of air, V_a: velocity of air, V_p: velocity of particle, and ρ_p: density of particle.

2.13. Recovery of L/CS-NP complexes from dry powder (complexes loaded-microspheres) in aqueous medium

In order to recover the initial L/CS-NP complexes from the dry powders, approximately 50 mg of the microspheres were incubated in 3 mL of PBS pH 7.4 for 90 min, under mild magnetic stirring (Plate A-13 Serie D, SBS, USA), at room temperature. Thereafter, the recovered complexes morphology, size and zeta potential were analyzed by TEM (CM 12 Philips, Eindhoven, Netherlands), Coulter counter method (Coulter® Multisizer II, Coulter Electronics, England) and laser doppler anemometry (Zetasizer® 3000 HS, Malvern Instruments, Malvern, UK), respectively (n = 3).

2.14. *In vitro* release studies of insulin from CS-NP, L/CS-NP complexes and dry powders (complexes loaded-microspheres)

The release of insulin was determined by incubating the different formulations (CS-NP, L/CS-NP complexes and complexes-loaded microspheres) in 5 mL of pH 7.4 phosphate buffer (0.21 mg CS-NP/mL, 0.83 mg complexes/mL,

4.18 mg microspheres/mL), with mild horizontal shaking (Promax 1020, Heidolph, Germany) at 37ºC. A further release study using a physical mixture of insulin and unloaded L/CS-NP complexes was performed. This was used as a control in order to evaluate the occurrence of adsorption phenomena.

At appropriate time intervals (15, 30, 60 and 90 min) individual samples were filtered (0.22 μm filters Millex®-GV, low protein binding, Millipore Ibérica, Spain) and the amount of protein released, evaluated in the supernatants by the MicroBCA protein assay (Pierce, USA) measuring the absorbances by spectrophotometry (Shimadzu UV-Visible Spectrophotometer UV-1603, Japan) at 562 nm (n = 3).

2.15. Statistical analysis

The t-test and the one-way analysis of variance (ANOVA) with the pairwise multiple comparison procedures (Student-Newman-Keuls method) were performed to compare two or multiple groups, respectively. All analysis were carried out using the SigmaStat statistical program (Version 3, Systat Software, USA) and differences were considered to be significant at a level of $P < 0.05$.

3. Results and Discussion

In this work, a dry powder integrating a combination of three systems was prepared, comprised of microspheres containing protein-loaded lipid/chitosan nanoparticle (L/CS-NP) complexes intended for pulmonary administration. Furthermore, the system was aerodynamically characterised *in vitro* and its ability to deliver insulin, used as the model therapeutic protein, was investigated.

3.1. Preparation and characterisation of chitosan nanoparticles (CS-NP)

CS-NP were obtained with CS and TPP (CS/TPP = 6:1, w/w), using the ionotropic gelation method described in the methodology section. As shown in Table 1, unloaded (without associated insulin) CS-NP present a size around 430 nm and a positive zeta potential of approximately + 44 mV. Insulin was associated

to the nanosystem with an efficiency of 68%, achieving a particle loading of 36%. As can be observed in the referred Table, the production yield significantly increased ($P < 0.05$) from 22% to 39% with the incorporation of insulin in the CS-NP, which can be easily explained by the nanoparticles formation mechanism, as previously reported [50]. Not only TPP, but also insulin interacts with the CS amino groups, leading to the production of more nanoparticles. The incorporation of insulin in the CS-NP did not have a pronounced effect on particle size, but led to a significant decrease ($P < 0.05$) on the zeta potential, reaching a value around + 34 mV. Taking into account that insulin is dissolved in NaOH 0.01M, with basic pH (aprox. 11), the protein is above its isoelectric point (pI 5.3) resulting in a negative charge. As a consequence, the association of insulin with the positively charged CS-NP is favored, decreasing the zeta potential value.

Table 1. Process yields and physicochemical properties of unloaded and insulin-loaded chitosan/tripolyphosphate nanoparticles (CS-NP) (mean ± SD, n = 3)

Nanoparticles formulation	Process yield (%)	Size (nm)	Zeta potential (mV)	Association efficiency (%)	Loading capacity (%)
Unloaded	22 ± 0	427 ± 22	+ 43.7 ± 2.5	—	—
Insulin-loaded	39 ± 1	443 ± 30	+ 34.6± 0.6	68 ± 4	36 ± 2

Process yield (%) = [Nanoparticles weight / Total solids weight] x 100
Association efficiency (%) = [(Total insulin amount –Free insulin)/Total insulin amount] x 100
Loading capacity (%) = [(Total insulin amount–Free insulin)/Nanoparticles weight] x 100

Data depicted in Table 1 correspond to CS-NP prepared using the low scale conditions (3 and 1.2 mL of CS and TPP, respectively). The scaling-up of their production, using 30 mL of CS and 12 mL of TPP, resulted in CS-NP with similar characteristics, providing another advantage of the ionic gelation as a method of preparing these structures. Unloaded CS-NP obtained in the large scale presented a size of 461 ± 17 nm and a zeta potential of + 43.6 ± 0.3 mV.

3.2. Preparation and characterisation of the L/CS-NP complexes

The L/CS-NP complexes were prepared using two phospholipids (DPPC and DMPG), which are endogenous to the lung, being principal constituents of the pulmonary surfactant [28]. Our systems were produced using only DPPC or a combination of DPPC and DMPG (DPPC-DMPG = 10:1), in an attempt to approximately respect the proportions of phospholipids existing in the alveolar surfactant. It is well known that phospholipids compose 80% - 90% of the surfactant, of which approximately 80% is phosphatidylcholine and 5-10% phosphatidylglycerol [28,62]. Moreover, it has been reported that an ideal mixture of phospholipids occurs when combining those whose hydrocarbon chains differ by only two carbon atoms [63], as happens with DPPC and DMPG, which have 16 and 14 carbon atoms, respectively.

Figure 1 displays the TEM microphotographs of representative fresh L/CS-NP complexes. As expected, the displayed images seem to indicate that, for both assayed formulations, and therefore independent to the lipid constitution, there are not only CS-NP entrapped in the phospholipid vesicles, which can be seen as dense black zones, but also isolated CS-NP (signaled with arrows in the figure) and empty phospholipid vesicles. Similar images were previously observed by *Jain et al.*, who produced chitosan nanoparticles encapsulated in soya lecithin vesicles intended for oral immunisation, in order to overcome the stability problem of unmodified particles in the acidic pH of the stomach [16].

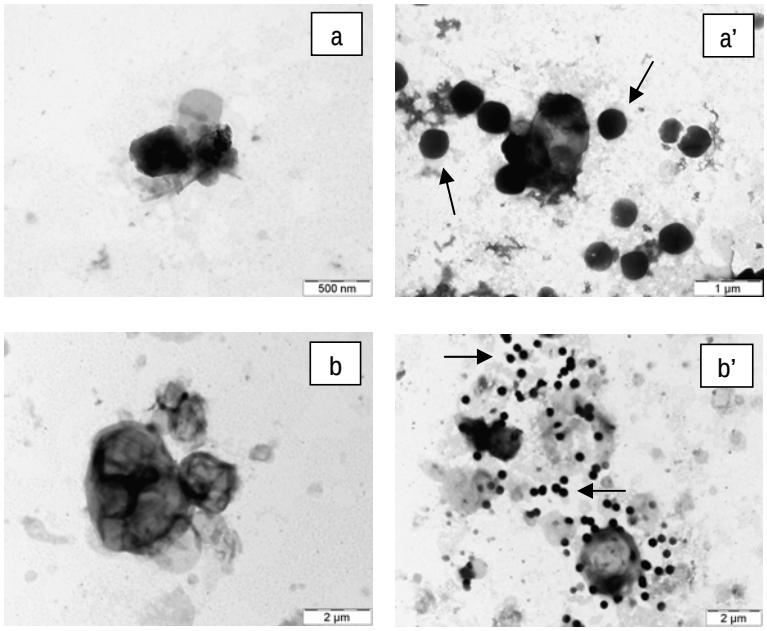

Fig. 1. TEM microphotographs of freshly prepared lipid/nanoparticles (L/CS-NP) complexes (lipid/nanoparticles = 3:1, nanoparticles CS/TPP = 6:1), lipidic fraction composed of: (a, a') – DPPC; (b, b') – DPPC-DMPG = (10:1). Arrows signal isolated nanoparticles.

Figure 2 schematically shows the possible alternatives that we consider for the formation of the complexes by the method used in this study. As can be seen, our hypothesis is that CS-NP can be either completely coated by the phospholipids; or a part of the CS-NP is surrounded by a phospholipid layer, whereas the rest is located at the complexes surface, and thus not being coated by the lipid film.

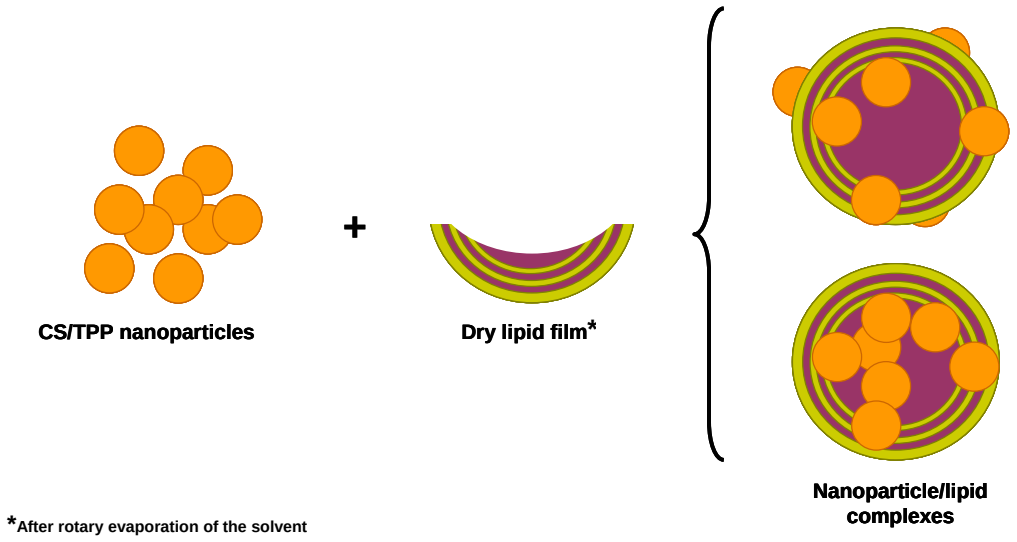

Fig. 2. Schematic representation of the formation mechanism of lipid/nanoparticles (L/CS-NP) complexes.

As shown in Table 2, the two formulations of control vesicles (prepared using water as hydrating solution) display a similar size around 2 μm, sizes being adjusted to a lognormal distribution. Both types of vesicles present a negative zeta potential, but in the case of those composed of DPPC, the value is close to neutrality (- 7 mV), while vesicles containing DMPG display a significantly stronger negative surface ($P < 0.05$), with a potential around - 54 mV. These results were to be expected since DPPC is a neutral phospholipid and DMPG presents a negative charge [64]. In fact, the slight negative zeta potential of DPPC vesicles was previously mentioned as a consequence of the position of the phospholipid polar head, which may vary with the ionic strength and temperature [65].

In regard to L/CS-NP complexes, the hydration of the dried lipid film with the CS-NP suspension did not lead to a significant size alteration for both formulations, when compared to the respective control vesicles. However, a slight increase could be detected in the complexes containing both lipids, which present a final size of approximately 2.5 μm, which could be indicative of a more complete

phospholipidic coating. Obviously, when comparing the size of both complexes to that of the CS-NP, there is a significant difference ($P < 0.05$) evidencing the lipids coating over the CS-NP.

Table 2. Physicochemical properties of control vesicles and lipid/nanoparticles (L/CS-NP) complexes (mean ± SD, n = 3).

System	Size (µm)	Zeta potential (mV)
Control DPPC vesicles	2.2 ± 1.8	- 7.1 ± 4.6
DPPC/CS-NP (unloaded) complexes	1.8 ± 1.8	0.2 ± 1.9
Control DPPC-DMPG vesicles	1.8 ± 1.7	- 54.0 ± 4.2
DPPC-DMPG/CS-NP (unloaded) complexes	2.5 ± 1.6	- 36.2 ± 1.6

CS: chitosan; DPPC: dipalmitoylphosphatidylcholine; DMPG: dimiristoylphosphatidylglycerol; NP: nanoparticles

Despite the fact that size measurements did not allow for a strong differentiation between the two formulations of complexes, zeta potential evaluation did provide further information on their composition and structure. When only DPPC was present in the lipid film composition, the incorporation of the positively charged CS-NP led to a slight, but not significant, modification in the zeta potential values, which varied from -7 mV in control vesicles to 0 mV in L/CS-NP complexes. However, both values are significantly lower ($P < 0.05$) in comparison to that of the CS-NP (+ 44 mV). On the other hand, when the lipid composition included also DMPG, the interaction seemed to be stronger and the zeta potential varied significantly ($P < 0.05$) from - 54 mV in control vesicles to -36 mV in L/CS-NP complexes. On comparing the zeta potential evidenced by the CS-NP, a complete inversion pattern is observed ($P < 0.05$), suggesting the production of a more effective phospholipid coating on the nanoparticles. The results found in our work could be understood as a reflex of the strong negative charge presented by the lipid film containing DPPC and DMPG, which enables a more intense interaction with the positive CS-NP, when comparing to the film composed of DPPC. However, further characterisation of the complexes surface

should be conducted in order to confirm this hypothesis. Furthermore, the lipidic coating will probably take place as a bilayer, because the interaction between solid cores and phospholipids has been reported to exert a strong ordering effect on the phospholipid molecules, as was demonstrated using NMR techniques that were sensitive to lipid organisation [22].

Similar results were also found by *Carvalho et al.*, when coating CS-NP with a phospholipids mixture to enable protection against the stomach acidic pH [15]. This interaction pattern was reported as well by *Moya et al.*, upon adsorption of lipid bilayers onto polyelectrolyte-coated capsules, the strong positive zeta potential of the polyallylamine capsules (+ 40 mV) changing to – 40 mV upon coating with dipalmitoyldiphosphatidic acid (negatively charged phospholipid). According to these authors, the zeta potential changes evidenced the lipid adsorption [13]. It was also reported that the successful coating of polystyrene amidine microspheres with a cationic lipid (dioctadecyldimethilammonium) was confirmed by several studies, including the zeta potential determination, which revealed an inversion from – 40 mV to + 20 mV [18].

3.3. Microspheres morphological and aerodynamic characterisation

The production of CS-NP loaded-mannitol microspheres was previously described. From all the assayed formulations, we found that the one comprising of mannitol/nanoparticles = 80/20 and solids content = 2.1%, was the most suitable for the purpose of carrying CS-NP to the lung, because of its morphological, physical and aerodynamic characteristics [42]. Moreover, the characterisation of the internal structure of these microspheres using confocal microscopy, allowed us to demonstrate that CS-NP were homogeneously dispersed through the whole microparticle [66]. Taking into account these considerations, we hypothesised that the microencapsulation of L/CS-NP complexes in mannitol microspheres by spray-drying, using the same mannitol/encapsulated system ratio, would result in the production of microspheres with adequate properties for pulmonary delivery as well.

Concerns about spray-drying phospholipids were not a problem, considering the knowledge that their stability is not committed after this procedure, due to the short exposure to the heat [53,57]. The spray-drying of insulin was not a concern either, since studies exist reporting that its spray-drying at an inlet temperature of 160ºC, with resultant outlet temperature of 100ºC, caused insignificant degradation of the protein around 0.5% [53,67].

As can be observed in the SEM microphotographs depicted in Figure 3, the spray-drying technique (production yields around 50%) led to the production of well defined microspheres with a spherical shape, not being aggregated.

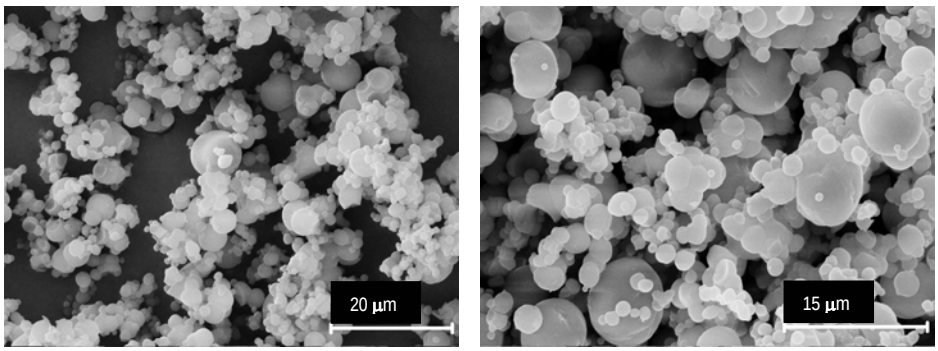

Fig. 3. SEM microphotograph of representative microspheres prepared with mannitol/DPPC-DMPG complexes (theoretical mannitol/complexes ratio = 80/20, solids content = 2.1%, w/v).

Besides the fact that morphology represents an important factor, essentially considering particle aggregation, which may interfere in the flowing properties, aerodynamic characteristics are the limiting parameters to succeed in pulmonary delivery. The aerodynamic diameter, which is a combination of the particle size and density, influences the dispersion and sedimentation patterns [8,68] and, as has been previously commented, should vary between 1 and 5 µm to allow an optimal lung administration, some authors even narrowing this range to an ideal 2-3 µm [2,8]. Physical and aerodynamic properties of the produced microspheres are depicted in Table 3.

Table 3. Physical and aerodynamic properties of microspheres (mannitol/ complexes = 80/20, solids content = 2.1%) (mean ± SD, n = 3).

Complexes formulation	Feret diameter (μm)	Real density (g/cm³)	Apparent density (g/cm³)	Aerodynamic diameter (μm)
DPPC	2.6 ± 1.1	1.44 ± 0.06	0.41 ± 0.04	2.11 ± 0.04
DPPC-DMPG	3.2 ± 1.3	1.42 ± 0.02	0.50 ± 0.01	2.67 ± 0.08

Feret diameters (μm) (distances between two tangents on opposite sides of the particle) were determined by optical microscopy. Real and apparent densities (tap densities) (g/cm³) were assayed by helium picnometry and by a tapping procedure, respectively. Aerodynamic diameters were obtained using an Aerosizer®.

The Feret diameters were approximately 3 μm, apparent tap densities were low and significantly different ($P < 0.05$) for both formulations (containing DPPC and DPPC-DMPG), varying between 0.4 and 0.5 g/cm³ and real densities were around 1.4 g/cm³. These properties rendered aerodynamic diameters (assessed with an Aerosizer®) between 2.1 and 2.7 μm, which are theoretically adequate for pulmonary administration; results being similar to those previously found [42], possibly due to the production of microspheres using the same ratio between mannitol and the microencapsulated system (CS-NP in the previous work and L/CS-NP complexes in the present work), with the same solids content.

3.4. Recovery of L/CS-NP complexes from microspheres in aqueous medium

In the current study, we investigated the ability of the obtained complexes-loaded microspheres to deliver the L/CS-NP complexes following incubation in PBS pH 7.4. This pH was chosen in an attempt to perform the assay in a pH close to that of the airway surface liquid, which is approximately 7 [69,70]. We could observe that after the microspheres incubation in aqueous medium under low stirring, mannitol dissolved, resulting in a suspension of the complexes. Therefore, as it has been previously reported for nanoparticle-loaded microspheres [42], L/CS-NP complexes could be easily recovered from microspheres. Figure 4 depicts microphotographs of recovered complexes of the formulation comprising DPPC-DMPG, which we consider to be representative.

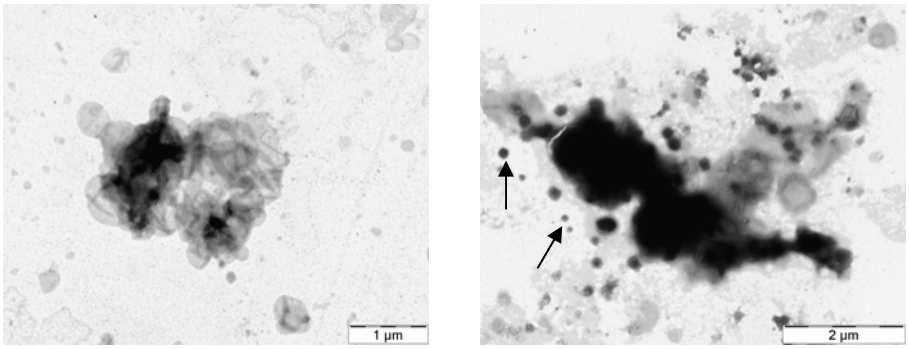

Fig. 4. TEM microphotographs of representative recovered lipid/nanoparticles (L/CS-NP) complexes (lipid/nanoparticles = 3:1, DPPC-DMPG = 10:1, CS/TPP = 6:1). Arrows signal isolated nanoparticles.

When comparing these microphotographs with those collected in Figure 1, the presence of nanoparticles entrapped in the phospholipid vesicles and isolated nanoparticles can still be observed, indicating that complexes morphology have not changed. Therefore, we can confirm that the spray-drying process does not have a negative effect on the complexes morphology. As shown in Table 4, the complexes size remained similar after the spray-drying process and zeta potential only changed significantly ($P < 0.05$) after the recovery process in the formulation containing both lipids, decreasing in about 4 mV. Even though, the observed change was minimum, not compromising the fundamental objectives of this work.

Table 4. Zeta potential values of lipid/nanoparticles (L/CS-NP) complexes, fresh and after recovery from microspheres (mannitol/complexes theoretical ratio = 80/20, solids content of 2.1%; mean ± SD, n = 3).

L/CS-NP complexes formulation	Size (µm)	Zeta potential (mV)
DPPC, freshly prepared	1.8 ± 1.8	0.2 ± 1.9
DPPC, after recovery	1.4 ± 1.9	- 0.6 ± 1.2
DPPC-DMPG, freshly prepared	2.5 ± 1.6	- 36.2 ± 1.6
DPPC-DMPG, after recovery	2.2 ± 1.1	- 40.7 ± 1.5

Therefore, from the results of this study we could hypothesize that after reaching the deep lung, mannitol will dissolve in the lung aqueous covered epithelium, releasing the L/CS-NP complexes previously encapsulated in the microspheres.

3.5. *In vitro* release studies

Figure 5 depicts the release profiles of insulin from CS-NP, fresh L/CS-NP complexes containing either DPPC-DMPG or only DPPC, and microspheres containing L/CS-NP complexes composed of DPPC and DMPG in PBS pH 7.4 at 37ºC. The microspheres formulation containing L/CS-NP complexes with both lipids (DPPC and DMPG) was selected to perform the insulin release studies from the microspheres, since it is considered to be representative of both formulations. As expected, the insulin release from CS-NP was very rapid, exhibiting the typical initial burst effect, and at 15 min the maximum amount of insulin was already delivered (80%). As concluded in previous works, this *in vitro* release behaviour suggests that the interaction between CS and insulin is very weak, allowing the insulin release from the CS-NP by a dissociation mechanism [49]. The insulin release profile displayed by the two L/CS-NP formulations assayed is significantly different ($P < 0.05$) to that of CS-NP. Moreover, there is also a significant difference ($P < 0.05$) between the release profiles of both formulations. Actually, they present a slight initial burst effect, followed by a very slight increase on the protein release until 90 min; the formulation containing only DPPC releasing 43% of the insulin content at 15 min, while the one containing both lipids delivers 30% in the same period of time.

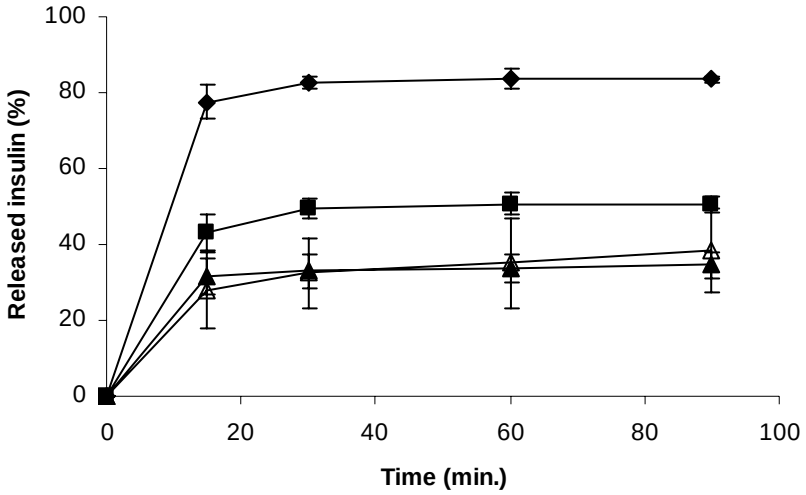

Fig. 5. Release profiles of insulin from (♦) CS/TPP nanoparticles (CS/TPP = 6:1), (■) DPPC/nanoparticles complexes (lipid/nanoparticles = 3:1, CS/TPP = 6:1), (▲) DPPC-DMPG/nanoparticles complexes (DPPC/DMPG = 10:1, lipid/nanoparticles = 3:1, CS/TPP = 6:1) and (Δ) microspheres containing DPPC-DMPG/nanoparticles complexes (mannitol/complexes = 80/20, lipid/nanoparticles = 3:1, DPPC/DMPG = 10:1, CS/TPP = 6:1), in PBS pH 7.4 at 37ºC (insulin = 30% w/w based on CS; mean ± SD, n = 3).

The difference found in the release profile presented by both L/CS-NP complexes formulations is undoubtedly a result of the different interaction between the CS-NP and the phospholipids found for each formulation of complexes. In fact, the formulation we hypothesised to present a stronger interaction between CS-NP and phospholipids (the one containing the phospholipid with the negative charge – DMPG), explained by the attraction between the opposite surface charges, gives rise to a much slower and controlled release of the protein, compared to the formulation comprised of solely DPPC. Taking into account the immediate release from the CS-NP, the difference found in the insulin release profile of the complexes compared to the CS-NP, is certainly a result of the presence of the phospholipid bilayers, which have to be crossed by the protein. Moreover, in the formulation with DMPG, the protein takes more time to be released, possibly due to the formation of a more homogeneous lipid coating. Therefore, these results not only corroborate our predictions about the differences between both formulations, but also reinforce the theory of a more effective lipidic

coating by the formulation containing DMPG, providing a higher control of the therapeutic molecule release. Similar results were previously found in other works [12,15]. In fact, studies with L/CS-NP complexes provided a slow insulin release when a negatively charged phospholipid was included in the system composition [15]. Furthermore, *McPhail et al.* compared the release behaviour of carboxyfluorescein from polymeric vesicles and from polymeric vesicles in phospholipid vesicles (vesicle-in-vesicle system formed with a chitosan derivative enclosed in phospholipid vesicles) in PBS pH 7.4, finding that the release from the encapsulated vesicles was much more controlled [12]. The incubation of unloaded complexes with an insulin solution (data not shown), enabled the detection of released insulin between 92 and 100%. Therefore, we consider that the controlled release showed by the L/CS-NP complexes formulations can not be attributed to adsorption phenomena.

Finally, concerning the L/CS-NP complexes-loaded microspheres, it can be confirmed that, as expected, mannitol does not influence the protein release profile, allowing the immediate delivery of the complexes, as previously reported [42]. Therefore, mannitol would act only as an inert carrier of the L/CS-NP complexes.

4. Conclusions

The present work demonstrates that the proposed technologies are appropriate to obtain complexes between phospholipids and preformed nanoparticles, as well as to produce microspheres containing the referred complexes, which exhibit suitable properties for pulmonary delivery. The phospholipids composition strongly affects the complexes physicochemical characteristics, suggesting that a stronger lipid/nanoparticles interaction occurs when a negatively charged phospholipid is incorporated in the lipid film, consequently resulting in a more efficient lipidic coating of the chitosan nanoparticles. The complexes were efficiently recovered from the microspheres following their incubation in aqueous medium, without significant changes in their properties. The presence of phospholipids is determinant in controlling the release of the encapsulated insulin, particularly when both lipids, DPPC and

DMPG, are present. Moreover, the microencapsulation process does not have any effect on the insulin release profile. As a general conclusion, and taking all these results into account, we believe that the developed system has a great potential for systemic delivery of therapeutic macromolecules by the pulmonary route.

Acknowledgements

This work was supported by the Spanish Government (CICYT, SAF2002-03314, Feder cofinanced). The Predoctoral fellowship to Ana Grenha from Fundação para a Ciência e Tecnologia, Portugal (SFRH/BD/13119/2003) is highly appreciated.

References

[1] D.A. Edwards, A. Ben-Jebria, R. Langer, Recent advances in pulmonary drug delivery using large, porous inhaled particles. J. Appl. Physiol. 84 (1998) 379-385.

[2] C. Bosquillon, C. Lombry, V. Préat, R. Vanbever, Influence of formulation excipients and physical characteristics of inhalation dry powders on their aerosolization performance. J. Control. Release. 70 (2001) 329-339.

[3] A. Sharma, U.S. Sharma, Liposomes in drug delivery: progress and limitations. Int. J. Pharm. 154 (1997) 123-140.

[4] C.J. Kirby, G. Gregoriadis, Liposomes, in: E. Mathiowitz (Eds.), Encyclopedia of Controlled Drug Delivery, John Wiley & Sons, New York, 1999, pp. 461-492.

[5] S.A. Agnihotri, N.N. Mallikarjuna, T.M. Aminabhavi, Recent advances in chitosan-based micro-and nanoparticles in drug delivery, J. Control. Release. 100 (2004) 5-28.

[6] M. Mezei, Liposomes in the topical application of drugs: a review, in: G. Gregoriadis (Ed.), Liposomes as drug carriers: recent trends and progress, John Wiley & Sons, Chichester, 1988, pp. 663-677.

[7] P.J. Mihalko, H. Schreier, R.M. Abra, Liposomes: a pulmonary perspective, in: G. Gregoriadis (Ed.), Liposomes as drug carriers: recent trends and progress, John Wiley & Sons, Chichester, 1988, pp. 679-694.

[8] H.M. Courrier, N. Butz, T.F. Vandamme, Pulmonary drug delivery systems: recent developments and prospects. Crit. Rev. Ther. Drug Carr. Syst. 19 (2002) 425-498.

[9] R.H. Müller, K. Mäder, S. Gohla, Solid lipid nanoparticles (SLN) for controlled drug delivery - a review of the state of the art. Eur. J. Pharm. Biopharm. 50 (2000) 161-177.

[10] S.G. Antimisiaris, P. Jayasekera, G. Gregoriadis, Liposomes as vaccine carriers. Incorporation of soluble and particulate antigens in giant vesicles. J. Immunol. Methods. 166 (1993) 271-280.

[11] J. Arrault, C. Grand, W.C.K. Poon, M.E. Cates, Stuffed onions: Particles in multilamellar vesicles. Europhys. Letters. 38 (1997) 625-630.

[12] D. McPhail, L. Tetley, C. Dufes, I.F. Uchegbu, Liposomes encapsulating polymeric chitosan based vesicles - a vesicle in vesicle system for drug delivery. Int. J. Pharm. 200 (2000) 73-86.

[13] S. Moya, E. Donath, G.B. Sukhorukov, M. Auch, H. Bäumler, H. Lichtenfeld, H. Möhwald, Lipid coating on polyelectrolyte surface modified colloidal particles and polyelectrolyte capsules. Macromolecules. 33 (2000) 4538-4544.

[14] A. Campbell, P. Taylor, O.J. Cayre, V.N. Paunov, Preparation of aqueous gel beads coated by lipid bilayers. Chem. Commun. 21 (2004) 2378-2379.

[15] E.L.S. Carvalho, B. Seijo, M.J. Alonso, Lipid-chitosan nanoparicle complexes (L/CS-Np) for oral insulin delivery : preparation, characterization and in vivo evaluation. Int. J. Pharm. (submitted).

[16] S. Jain, R.K. Sharma, S.P. Vyas, Chitosan nanoparticles encapsulated vesicular systems for oral immunization: preparation, in-vitro and in-vivo characterization. J. Pharm. Pharmacol. 58 (2006) 303-310.

[17] A. Fery, S. Moya, P.-H. Puech, F. Brochard-Wyart, H. Mohwald, Interaction of polyelectrolyte coated beads with phospholipid vesicles. C. R. Phys. 4 (2003) 259-264.

[18] F.M. Correia, D.F.S. Petri, A. M. Carmona-Ribeiro, Colloid stability of lipid/polyelectrolyte decorated latex. Langmuir. 20 (2004) 9535-9540.

[19] A.-L. Troutier, T. Delair, C. Pichot, C. Ladavière, Physicochemical and interfacial investigation of lipid/polymer particle assemblies. Langmuir. 21 (2005), 1305-1313.

[20] A.-L. Troutier, L. Véron, T. Delair, C. Pichot, C. Ladavière, New insights into self-organization of a model lipid mixture and quantification of its adsorption on spherical polymer particles. Langmuir. 21 (2005) 9901-9910.

[21] K.N.J. Burger, R.W.H.M. Staffhorst, H.C. Vijlder, M.J. Velinova, P.H. Bomans, P.M. Frederik, B. Kruijff, Nanocapsules: lipid-coated aggregates of cisplatin with high cytotoxicity. Nat. Med. 8 (2002) 81-84.

[22] V. Chupin, A.I.P.M. de Kroon, B. de Kruijff, Molecular architecture of nanocapsules, bilayer-enclosed solid particles of cisplatin. JACS. 126 (2004) 13816-13821.

[23] M.J. Velinova, R.W.H.M. Staffhorst, W.J.M. Mulder, A.S. Dries, B.A.J. Jansen, B. Kruijff, A.I.P.M. Kroon, Preparation and stability of lipid-coated nanocapsules of cisplatin: anionic phospholipid specificity. Biochim. Biophys. Acta. 1663 (2004) 135-142.

[24] C. Beaulac, S. Sachetelli, J. Lagacé, Aerosolization of low phase transition temperature liposomal tobramycin as dry powder in an animal model of chronic pulmonary infection caused by *Pseudomonas aeruginosa*. J. Drug Target. 7 (1999) 33-41.

[25] Y. Darwis, I.W. Kellaway, The lyophilization and aerosolisation of liposomes for pulmonary drug administration. S.T.P. Pharma Sci. 12 (2002) 91-96.

[26] T.R. Desai, R.E.W. Hancock, W.H. Finlay, Delivery of liposomes in dry poowder form: aerodynamic dispersion properties. Eur. J. Pharm. Sci. 20 (2003) 459-467.

[27] F. Liu, Z. Shao, D.O. Kildsig, A.K. Mitra, Pulmonary delivery of free and liposomal insulin. Pharm. Res. 10 (1993) 228-232.

[28] S.M. McAllister, H.O. Alpar, Z. Teitelbaum, D.B. Bennett, Do interactions with phospholipids contribute to the prolonged retention of polypeptides within the lung? Adv. Drug Deliv. Rev. 19 (1996) 89-110.

[29] R. Mitra, I. Pezron, Y. Li, A.K. Mitra, Enhanced pulmonary delivery of insulin by lung lavage fluid and phospholipids. Int. J. Pharm. 217 (2001) 25-31.

[30] A. Hussain, J.J. Arnold, M.A. Khan, F. Ahsan, Absorption enhancers in pulmonary protein delivery. J. Control. Release. 94 (2004) 15-24.

[31] A. Clark, Formulation of proteins and peptides for inhalation. Drug Deliv. Syst. Sci. 2 (2002) 73-77.

[32] Y. Kubota, S. Takahashi, O. Matsuoka, Dependence on particle size in the phagocytosis of latex particles by rabbit alveolar macrophages cultured in vitro. J. Toxicol. Sci. 8 (1983) 189-195.

[33] S. Rudt, R.H. Müller, In vitro phagocytosis of nano- and microparticles by chemiluminescence. I. Effect of analytical parameters, particle size and particle concentration. J. Control. Release. 22 (1992) 263-272.

[34] S. Aktar, K.J. Lewis, Antisense oligonucleotide delivery to cultured macrophages is improved by incorporation into sustained-release biodegradable polymer microspheres. Int. J. Pharm. 151 (1997) 57-67.

[35] F. Ahsan, I.P. Rivas, M.A. Khan, A.I. Suárez-Torres, Targeting to macrophages: role of physicochemical properties of particulate carriers - liposomes and microspheres - on the phagocytosis by macrophages. J. Control. Release. 79 (2002) 29-40.

[36] K. Makino, H. Yamamoto, K. Higuchi, N. Harada, H. Ohshima, H. Terada, Phagocytic uptake of polystyrene microspheres by alveolar macrophages: effects of the size and surface properties of the microspheres. Colloid. Surf. B - Biointerfaces. 27 (2003) 33-39.

[37] C. Evora, I. Soriano, R.A. Rogers, K.M. Shakesheff, J. Hanes, R. Langer, Relating the phagocytosis of microparticles by alveolar macrophages to surface chemistry: the effect of 1,2-dipalmitoylphosphatidylcholine. J. Control. Release. 51 (1998) 143-152.

[38] Q. Zhang, Z. Shen, T. Nagai, Prolonged hypoglycemic effect of insulin-loaded polybutylcyanoacrylate nanoparticles after pulmonary administartion to normal rats. Int. J. Pharm. 218 (2001) 75-80.

[39] N. Tsapis, D. Bennet, B. Jackson, D.A. Weitz, D.A. Edwards, Trojan particles: large porous carriers of nanoparticles for drug delivery. Proc. Nat. Acad. Sci. 99 (2002), 12001-12005.

[40] L. A. Dailey, E. Kleemann, M. Wittmar, T. Gessler, T. Schmehl, C. Roberts, W. Seeger, T. Kissel, Surfactant-free, biodegradable nanoparticles for aerosol therapy based on the branched polyesters, DEAPA-PVAL-g-PLGA. Pharm. Res. 20 (2003) 2011-2020.

[41] J.O. Sham, Y. Zhang, W.H. Finlay, W.H. Roa, R. Löbenberg, Formulation and characterization of spray-dried powders containing nanoparticles for aerosol delivery to the lung. Int. J. Pharm. 269 (2004) 457-467.

[42] A. Grenha, B. Seijo, C. Remuñan-Lopez, Microencapsulated chitosan nanoparticles for lung protein delivery. Eur. J. Pharm. Sci. 25 (2005) 427-437.

[43] J. Kreuter, Liposomes and nanoparticles as vehicles for antibiotics. Infection. 19 (1991) S224-S228.

[44] M.J. Alonso, Nanoparticulate drug carrier technology. in: S. Cohen, H. Bernstein (Eds.), Microparticulate systems for the delivery of proteins and vaccines, Marcel Dekker, New York, 1996, pp. 203-242.

[45] S. Hirano, H. Seino, Y. Akiyama, I. Nonaka, Biocompatibility of chitosan by oral and intravenous administrations. Polym. Mater. Sci. Eng. 59 (1988), 897-901.

[46] C. M. Lehr, J.A. Bouwstra, E.H. Schacht, H.E. Junginger, In vitro evaluation of mucoadhesive properties of chitosan and some other natural polymers. Int. J. Pharm. 78 (1992) 43-48.

[47] M. Dornish, A. Hagen, E. Hansson, C. Peucheur, F. Vedier, O. Skaugrud, Safety of Protasan™: Ultrapure chitosan salts for biomedical and pharmaceutical use, in: A. Domard, G.A.F. Roberts, K.M. Varum (Eds.), Advances in chitin science, Jacques Andre publisher, Lyon, 1997, pp. 664-670.

[48] P. Calvo, C. Remuñan-Lopez, J.L. Vila-Jato, M.J. Alonso, Novel hydrophilic Chitosan-Polyethylene Oxide nanoparticles as protein carriers. J. Appl. Polym. Sci. 63 (1997) 125-132.

[49] R. Fernandez-Urrusuno, P. Calvo, C. Remuñan-Lopez, J.L. Vila-Jato, M.J. Alonso, Enhancement of nasal absorption of insulin using chitosan nanoparticles. Pharm. Res. 16 (1999) 1576-1581.

[50] R. Fernandez-Urrusuno, D. Romani, P. Calvo, J.L. Vila-Jato, M.J. Alonso, Development of a freeze-dried formulation of insulin-loaded chitosan nanoparticles intended for nasal administration. S.T.P. Pharma Sci. 9 (1999) 429-436.

[51] A. De Campos, A. Sanchez, M.J. Alonso, Chitosan nanoparticles: a new vehicle for the improvement of the delivery of drugs to the ocular surface. Application to cyclosporin A. Int. J. Pharm. 224 (2001) 159-168.

[52] I. Behrens, A.I. Vila-Pena, M.J. Alonso, T. Kissel, Comparative uptake studies of bioadhesive and non-bioadhesive nanoparticles in human intestinal cell lines and rats: the effect of mucus on particle adsorption and transport. Pharm. Res. 19 (2002) 1185-1193.

[53] J. Broadhead, S.K. Edmond-Rouan, C.T. Rhodes, The spray drying of pharmaceuticals. Drug Dev. Ind. Pharm. 18 (1992) 1169-1206.

[54] C. Bosquillon, P.G. Rouxhet, F. Ahimou, D. Simon, C. Culot, V. Préat, R. Vanbever, Aerosolization properties, surface composition and physical state of spray-dried protein powders. J. Control. Release. 99 (2004) 357-367.

[55] H. Steckel, H.G. Brandes, A novel spray-drying technique to produce low density particles for pulmonary delivery. Int. J. Pharm. 278 (2004) 187-195.

[56] H. Todo, H. Okamoto, K. Iida, K. Danjo, Improvement of stability and absorbability of dry insulin powder for inhalation by powder-combination technique. Int. J. Pharm. 271 (2004) 41-52.

[57] P. Goldbach, H. Brochart, A. Stamm, Spray-drying of liposomes for a pulmonary administration. I. Chemical stability of phospholipids. Drug Dev. Ind. Pharm. 19 (1993) 2611-2622.

[58] C. Freitas, R.H. Müller, Spray-drying of solid lipid nanoparticles (SLN™). Eur. J. Pharm. Biopharm. 46 (1998) 145-151.

[59] A.L. Weiner, Liposomes as carriers for polypeptides. Adv. Drug Deliv. Rev. 3 (1989) 307-341.

[60] J.-F. Marier, J. Lavigne, M.P. Ducharme, Pharmacokinetics and efficacies of liposomal and conventional formulations of tobramycin after intratracheal administration in rats with pulmonary *Burkholderia cepacia* infection. Antimicrob. Agents Chemother. 46 (2002) 3776-3781.

[61] I. El-Gibaly, Development and in vitro evaluation of novel floating chitosan microcapsules for oral use: comparison with non-floating chitosan microspheres. Int. J. Pharm. 294 (2002), 7-21.

[62] J.R. Wright, J.A. Clements, Metabolism and turnover of lung surfactant. Am. Rev. Respir. Disease. 135 (1987) 426-444.

[63] K.M.G. Taylor, D.Q.M. Craig, Physical methods of study: differential scanning calorimetry, in: V.P. Torchilin, V. Weissig (Eds.), Liposomes, Oxford University Press, Oxford, 2003, pp. 70-103.

[64] E. Fattal, P. Couvreur, F. Puisieux, Méthodes de préparation des liposomes, in: J. Delattre, P. Couvreur, F. Puisieux, J.R. Philippot, F. Schuber (Eds.), Les liposomes: aspects technologiques, biologiques et pharmacologiques, Editions Inserm, Paris, 1993, pp. 43-52.

[65] K. Makino, T. Yamada, M. Kimura, T. Oka, H. Oshima, T. Kondo, Temperature and ionic strenght induced conformational changes in the lipid head group region of liposomes as suggested by zeta potential data. Biophys. Chem. 41 (1991) 175-183.

[66] A. Grenha, B. Seijo, C. Serra, C. Remuñán-López, Chitosan nanoparticle-loaded microspheres: structure and surface characterisation. Macromolecules (submitted).

[67] H. Okamoto, H. Todo, K. Iida, K. Danjo, Dry powders for pulmonary delivery of peptides and proteins. Kona. 20 (2002) 71-83.

[68] G. Taylor, I. Kellaway, Pulmonary drug delivery, in: A. Hillery, A. Lloyd, J. Swarbrick (Eds.), Drug delivery and targeting. For pharmacists and pharmaceutical scientists, Taylor & Francis, New York, 2001, pp. 269-300.

[69] H. Kyle, J.P. Ward, J.G. Widdicombe, Control of pH of airway surface liquid of the ferret trachea in vitro. J. Appl. Physiol. 68 (1990) 135-140.

[70] D.V. Walters, Lung lining liquid - The hidden depths. Biol. Neonate. 81 (2002), 2-5.

Artículo 5

SURFACE CHARACTERISATION OF LIPID/CHITOSAN NANOPARTICLES ASSEMBLIES, USING XPS AND TOF-SIMS

Ana Grenha[1], Begoña Seijo[1], Carmen Serra[2] and Carmen Remuñán-López[1]*

[1]Dept. of Pharmacy and Pharmaceutical Technology, University of Santiago de Compostela, Faculty of Pharmacy, Campus Sur, 15782 Santiago de Compostela, Spain. [2]C.A.C.T.I., University of Vigo, E-36310, Vigo,Spain.

* Corresponding author: Phone: 0034 981 563100 – ext. 15405

Fax: 0034 981 547148

E-mail: ffcarelo@usc.es

Artículo en preparación para someter a evaluación por "Journal of the American Chemical Society"

Abstract

Chitosan/tripolyphosphate nanoparticles are promising drug delivery systems, which show excellent capacity for protein entrapment and improvement of mucosal peptide absorption. We have recently developed a new drug delivery system consisting of assemblies formed between preformed chitosan nanoparticles and phospholipids (dipalmitoylphosphatidylcholine -DPPC and dimiristoyl phosphatidylglycerol - DMPG) which are endogenous to the lung. These assemblies are prepared by lipid film hydration with a nanoparticles suspension, and were named as L/CS-NP. The aim of this work was to elucidate the architecture of these structures using sensitive surface analysis techniques such as X- ray photoelectron spectroscopy (XPS) and static time-of-flight secondary ion mass spectrometry (TOF-SIMS), as well as to determine their physicochemical characteristics. The combination of zeta potential measurements with the results obtained by XPS and TOF-SIMS, demonstrated that a complete lipid coating of the nanoparticles can be achieved using a lipid film formed by both DPPC and DMPG, this way conferring to the lipid film a strong negative charge, which favors the interaction with the positively charged nanoparticles. Therefore, the major role of electrostatic interactions as driving forces to control the organisation of the lipid/nanoparticles assemblies was clearly evident. The implications of these findings for the structural organisation of the assemblies, for their in vitro behaviour, as well as for their mechanism of formation are discussed.

1. Introduction

Liposomes and nanoparticles have been gaining popularity as alternatives for the administration of biomolecules through several mucosal surfaces,[1,2] given their versatility and relative innocuousness, enabled by the use of natural and biodegradable lipids and polymers in their preparation.[3-6]

The materials composing these systems play an important role in the release of the associated drugs, and the presence of lipids has been reported to enhance macromolecules absorption[7-9] and to reduce alveolar phagocytosis[10]. Furthermore, chitosan nanoparticles (CS-NP), whose production by a very mild process of ionic gelation technique was proposed by our group,[11] display very attractive properties (excellent capacity for protein association and absorption enhancement properties).[12,13] We recently developed a new drug delivery system, consisting in a combination of the preformed CS-NP with phospholipids, forming lipid/nanoparticles (L/CS-NP) asemblies, which was already proposed for oral and pulmonary delivery of therapeutic macromolecules.[14,15] For the latest purpose, L/CS-NP assemblies were microencapsulated in mannitol microspheres. Previous results showed that the physicochemical properties of these assemblies were affected by the phospholipids composition. In addition, phospholipids provided a controlled release of the encapsulated protein, compared to isolated CS-NP, which was in turn dependent on the used lipids.[15] However, so far we did not deal with the real distribution of the nanoparticles in the assemblies, an important issue to verify whether or not they are completely entrapped in the phospholipid film. In fact, results of this characterisation should provide us with essential information in order to interpret the *in vitro* behaviour of the assemblies, such as the release profiles, or inclusive their *in vivo* performance. Such a determination could be performed using sensitive techniques of surface analysis like X-ray photoelectron spectroscopy (XPS) and static time of flight secondary ion mass spectrometry (TOF-SIMS). The interest on the application of these techniques is based on their accuracy and highly sensitiveness, since they offer precise molecular information on the chemical elements present in the most superficial layers of the analysed surfaces.[16-18] The XPS technique has been previously used in the field of drug delivery to determine the surface composition of nanoparticles and microspheres

[19,20] and its application is widespread in biomedical research.[21,22] In contrast, TOF-SIMS is much more recent than XPS, so its application in drug delivery is less extended. Nevertheless, it was used a few times to characterise surfaces of particles or powders, such as polystyrene or cellulose beads.[23,24]

In this work, we report the exhaustive surface characterisation of L/CS-NP assemblies, produced by the hydration of a lipid film with a suspension of CS-NP, which allowed the coating of nanoparticles by a lipid layer. For these purposes, we used advanced techniques such as XPS and TOF-SIMS, which are specific and accurate for surface analysis. Given that we used two different lipid mixtures (DPPC and DPPC-DMPG) to form the assemblies, which evidence different surface charges (respectively neutral and negative), we hypothesised that CS-NP, which are positively charged, would interact more efficiently with the lipid layer when this has a negative charge, as happens when DMPG is present in the formulation.

2. Materials and methods

2.1. Chemicals

Chitosan (CS) in the form of hydrochloride salt (Protasan® 213 Cl, deacetylation degree: 86%, viscosity: 95 mPa) was purchased from FMC Biopolymer AS (Norway). Dipalmitoylphosphatidylcholine (DPPC) and dimyristoylphosphatidylglycerol (DMPG) were supplied by Lipoid (Germany). Pentasodium tripolyphosphate (TPP) and glycerol were supplied by Sigma Chemicals (USA). Chloroform was provided by Merck (Spain). Ultrapure water (MilliQ Plus, Millipore Iberica, Spain) was used throughout. All other chemicals were reagent grade.

2.2. Preparation of CS-NP

CS-NP were prepared according to the procedure developed by our group, based on the ionotropic gelation of CS with TPP anions, in which the positively charged amino groups of CS interact with the negatively charged TPP.[11] Briefly, CS and TPP were dissolved in purified water in order to obtain solutions of 1

mg/mL and 0.42 mg/mL, respectively. The spontaneous formation of nanoparticles occurs upon incorporation of 12 mL of the TPP solution in 30 mL of the CS solution (final CS/TPP ratio of 6:1, w/w), under mild magnetic stirring (Plate A-13 Serie D, SBS, USA) at room temperature.

CS-NP were concentrated by centrifugation at 10000×g on a 100 µl glycerol bed for 40 min at 15ºC (Beckman Avanti 30, Beckman, USA). The supernatants were discarded and nanoparticles were resuspended in 300 µl of purified water. Production yield was calculated by gravimetry. For that purpose, fixed volumes of nanoparticle suspensions were centrifuged and sediments were freeze-dried over 24 h at -34ºC, followed by a gradual ascent until 20ºC, using a Labconco Freeze Dryer (Labconco, USA) (n = 3).

The process yield was calculated as follows:

$$\text{Process Yield (\%)} = \frac{\text{CS-NP weight}}{\text{Total solids (CS + TPP) weight}} \times 100$$

2.3. Characterisation of CS-NP

The morphological examination of CS-NP was conducted by transmission electron microscopy (TEM) (CM 12 Philips, Eindhoven, Netherlands). The samples were stained with 2% (w/v) phosphotungstic acid and placed on copper grids with Formvar® films for TEM observation.

Measurements of CS-NP size and zeta potential were performed by photon correlation spectroscopy and laser doppler anemometry, respectively, using a Zetasizer® 3000 HS (Malvern Instruments, Malvern, UK). For the particle size analysis, each sample was diluted to the appropriate concentration with filtered (0.2 µm filters Millex®-GN, Millipore Iberica, Spain) ultrapure water. Each analysis lasted 180 sec and was performed at 25ºC with a detection angle of 90º. For the determination of the electrophoretic mobility, samples were diluted with KCl 0.1 mM and placed in the electrophoretic cell, where a potential of ± 150 mV was established. Three batches of each formulation were analyzed in triplicate (n = 3).

2.4. Preparation of L/CS-NP assemblies

The assemblies containing phospholipids and CS-NP were prepared by hydration of a dried phospholipid film, following a procedure previously developed in our group.[14,15] Briefly, DPPC or a mixture of DPPC and DMPG (10:1 molar ratio) were dissolved in 20 mL of chloroform, obtaining a 0.3 mM concentration, and 50 mg of glass beads were added to increase the available surface area to form the film. The organic solvent was then removed by evaporation under reduced pressure on a rotary evaporator (Buchi® R-114, Buchi, Switzerland) at approximately 55ºC, during 3 h on a nitrogen atmosphere, leading to the formation of a thin film of dry lipid.[25-27] This film was then hydrated for 30 min with a suspension of the previously prepared CS-NP, forming L/CS-NP assemblies (ratio 3:1, w/w). Immediately, the assemblies were filtered under vacuum to allow their separation from the glass beads. Control vesicles were produced under the same conditions, using water as hydrating phase.

2.5. Characterisation of the L/CS-NP assemblies

2.5.1. Morphological analysis

The morphological examination of the assemblies was conducted by optical (Olympus BH-2, Japan) and transmission electron microscopy (TEM) (CM 12 Philips, Netherlands). For TEM observation, samples were stained with 2% (w/v) phosphotungstic acid and placed on copper grids, previously covered with Formvar® films.

2.5.2. Physicochemical analysis

The size of the control vesicles (hydrated with water) and L/CS-NP assemblies was determined by the Coulter counter method (Coulter® Multisizer II, Coulter Electronics, England), equipped with an orifice tube of 50 µm aperture. To perform the measurements, 20 µl of the previously obtained suspension of assemblies were dispersed in 100 mL of the electrolyte Isoton II (a filtered, phosphate-buffered saline solution PBS) (n = 3). The instrument was previously

calibrated using Isoton II and monodisperse latex microspheres of 13 µm, both supplied by Coulter. Zeta potential measurements were performed by laser doppler anemometry, using the Zetasizer® 3000 HS (Malvern Instruments, Malvern, UK). Samples were diluted with KCl 0.1 mM and placed in the electrophoretic cell, where a potential of ± 150 mV was established. Three batches of each formulation were analyzed in triplicate (n = 3).

2.5.3. Surface analysis

CS-NP, DPPC and DPPC-DMPG control vesicles, and L/CS-NP assemblies (DPPC/CS-NP and DPPC-DMPG/CS-NP) were placed on polish monocristaline silicon wafer, which were used as sample holders. The samples surface was afterwards analysed using X-ray photoelectron spectroscopy (XPS, VG Escalab 250 iXL ESCA, VG Scientific, UK) and static time-of-flight secondary ion mass spectrometry (TOF-SIMS, TOF-SIMS IV, Ion-Tof GmbH, Germany). XPS measurements were carried out using non monochromatic Al-Kα radiation (hν = 1486.62 eV) and photoelectrons were collected from a take off angle of 90º relative to the sample surface. Measurements were performed in a Constant Analyser Energy mode (CAE) with a 100 eV pass energy for survey spectra and 20eV pass energy for high resolution spectra. Charge referencing was done by setting the lower binding energy C1s photopeak at 285.0 eV C1s hydrocarbon peak. The high resolution spectra fitting is based on "Chi-squared" algoritm used to determine the goodness of a peak fit. The chemical functional groups identity was obtained from the high-resolution peak analysis of carbon-1s (C_{1s}), oxygen-1s (O_{1s}) and nitroge-1s (N_{1s}) envelopes. The experimental conditions (X-ray source, power and analysis area), were the kept constant for each analysis.

For TOF-SIMS analyses, a pulsed Gallium primary ion beam ($69Ga^+$) generated with a liquid metal ion gun generated at 15 kV, was used to bombard the samples with 45º incidence respect to the sample surface. The secondary ions generated were extracted with a 10 KV voltage and their time of flight from the sample to the detector was measured in a reflectron mass spectrometer. Electron flood gun charge compensation was necessary during measurements. A raster size of 500 µm × 500 µm was used and at least three different spots were analyzed

under the "static" condition with ion doses of about ≈10^{12} ions/cm^2. The calibration of the mass spectra in the positive mode was based on hydrocarbon peaks such as CH_2^+, CH_3^+, $C_2H_2^+$, and C3H5+.The experimental conditions (ion type, beam voltage and primary ion dose), were maintained constant for each experiment and for compared spectra in the results section.

2.6. Statistical analysis

The t-test and the one-way analysis of variance (ANOVA) with the pairwise multiple comparison procedures (Student-Newman-Keuls method) were performed to compare two or multiple groups, respectively. All analysis were run using the SigmaStat statistical program (Version 3, Systat Software, USA) and differences were considered to be significant at a level of $P < 0.05$.

3. Results and Discussion

In this work, the coating of CS-NP by lipid films was proposed, forming L/CS-NP assemblies, as a strategy to achieve a controlled release of the encapsulated drug and to prevent macrophagic capture in the lungs. L/CS-NP assemblies were formed using two different mixtures, DPPC and DPPC-DMPG, and were characterised for their physicochemical properties. Moreover, the surface composition of the two formulations of assemblies was accurately characterised using sensitive surface analysis techniques such as XPS and TOF-SIMS, providing information on the extent of the interaction between nanoparticles and lipids.

3.1. Preparation and characterisation of CS-NP

CS-NP were produced using CS and TPP, by an ionic gelation technique previously developed in our group, as described in the methodology section.[11] **Figure 1** displays a TEM microphotograph of CS-NP, which evidence a spherical and compact structure. As shown in **Table 1**, CS-NP displayed a size around 400 nm and a positive zeta potential of approximately + 44 mV.

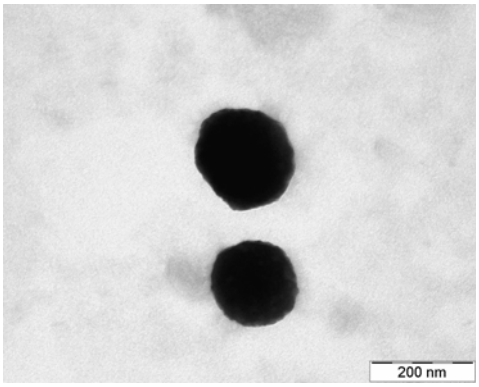

Fig. 1. TEM microphotograph of chitosan nanoparticles (CS-NP).

The L/CS-NP assemblies were prepared by the method described in the methodology section, using DPPC or a mixture of DPPC-DMPG in a molar ratio of 10:1, the DMPG confering a negative charge to the lipid film.

Table 1. Physicochemical properties of control chitosan nanoparticles (CS-NP), control lipid vesicles and lipid/nanoparticles (L/CS-NP) assemblies (mean ± SD, n = 3).

System	Size (µm)	Zeta potential (mV)
Control CS-NP	0.4 ± 0.02	+ 43.7 ± 2.5
Control DPPC vesicles	2.2 ± 1.8	- 7.1 ± 4.6
DPPC/CS-NP assemblies	1.8 ± 1.8	+ 0.2 ± 1.9
Control DPPC-DMPG vesicles	1.8 ± 1.7	- 54.0 ± 4.2
DPPC-DMPG/CS-NP assemblies	2.5 ± 1.6	- 36.2 ± 1.6

CS: chitosan; DMPG: dimiristoylphosphatidylglycerol; DPPC: dipalmotoylphosphatidylcholine; NP: nanoparticles

Figure 2 displays a TEM microphotograph of representative L/CS-NP assemblies. As can be observed in the image, it is suggested that there are nanoparticles surrounded by a phospholipid film, but isolated nanoparticles (signaled with arrows in the figure) and zones of isolated phospholipid vesicles could also be identified. The displayed microphotograph is considered to be representative of both formulations of assemblies (DPPC/CS-NP and DPPC-DMPG/CS-NP), given that no remarkable differences were identified during microscopical viewing of the structures with different lipid composition.

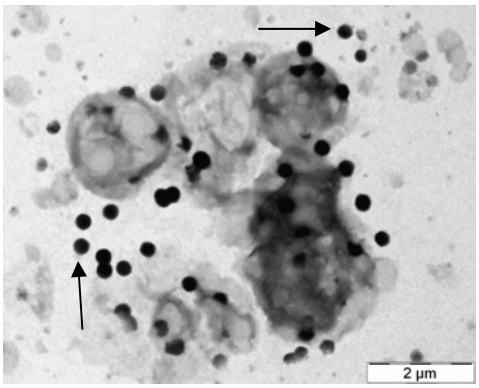

Fig. 2. TEM microphotograph of representative lipid/nanoparticles (DPPC-DMPG/CS-NP) assemblies. Arrows signal isolated nanoparticles.

Sizes of control vesicles and L/CS-NP assemblies were adjusted to a lognormal distribution. As shown in **Table 1**, the control vesicles of DPPC and DPPC-DMPG, which were prepared using water as hydrating solution, both displayed a size around 2 µm. As expected, for control vesicles containing DMPG, a strongly negative surface (- 54 mV) was observed, in comparison to the almost neutral charge (- 7 mV) presented by the DPPC vesicles ($P < 0.05$), as found in other works.[28,29] The formation of the assemblies, as a result of the hydration of the dried lipid film with the CS-NP suspension, did not induce a significant modification of size, comparing to the respective control lipid vesicles; albeit a slight increase could be detected in the assemblies containing the combination of DPPC-DMPG, which present a final size of approximately 2.5 µm. On the contrary, if compared to CS-NP size, a significant difference was found for both assemblies

($P < 0.05$), evidencing the lipids surrounding over the nanoparticles. Zeta potential determinations were, in turn, much more indicative of lipid/nanoparticles interactions than size measurements. When the lipid film is formed only of DPPC, the assemblies display a zeta potential of approximately 0 mV, which is much lower and significantly different ($P < 0.05$) comparing to that evidenced by the CS-NP (+ 44 mV). However, comparing to the control DPPC vesicles, which presented a zeta potential of - 7 mV, no significant differences were found. On the other hand, when assemblies comprised DMPG, the interaction between lipids and nanoparticles seemed to be stronger. Indeed, a complete and significant inversion of the zeta potential was observed ($P < 0.05$), changing from + 44 mV in the nanoparticles to - 36 mV in the assemblies. When comparing to control DPPC-DMPG vesicles, a significant difference was also found ($P < 0.05$), the zeta potential varying from - 54 mV (control vesicles) to - 36 mV (assemblies). Although conscious that these results are not enough to predict the definitive structure of the assemblies, it was suggested that a more effective interaction between the lipid film and the nanoparticles occurred when both DPPC and DMPG were present, certainly as a reflex of the negative charge presented by the lipid film with this composition, which favoured the interaction with the positively charged nanoparticles. Therefore, electrostatic interactions are likely to play a major role on the formation mechanism of these structures. Zeta potential determinations have been often applied to ascertain the formation of assemblies resultant from the combination of different materials, similar to those described in this work.[14,29-31] As a matter of fact, an interaction pattern similar to that found in our work was previously described by *Moya et al.*, upon adsorption of lipid bilayers onto polyallylamine capsules, the strong positive zeta potential of the capsules (+ 40 mV) changing to – 40 mV upon coating with dipalmitoyldiphosphatidic acid, a negatively charged phospholipid.[31] In another work, the effective coating of polystyrene amidine microspheres with the cationic lipid dioctadecyldimethylammonium was confirmed by the zeta potential inversion from – 40 mV to + 20mV.[30] In both studies, the authors concluded that the zeta potential changes evidenced the lipid adsorption, this conclusion being based as well on the coincident results of other assays.[30,31]

3.2. Surface characterisation of L/CS-NP

As commented above, the concomitant analysis of data obtained for size and zeta potential measurements, suggested that adsorption of phospholipids occurs onto the nanoparticles surface and that it is more effective when the lipid film contains both phospholipids, given the presence of a strong negative charge due to the DMPG. However, the evaluation of the assemblies physicochemical characteristics did not allow itself for accurate information of their surface composition, which would provide indubitable data on the localisation of nanoparticles in the formed assemblies. In this manner, specific techniques of surface analysis, such as XPS and TOF-SIMS, which deal with the determination of the chemical elements present in the uppermost layer of the observed surfaces, should offer unquestionable information on the assemblies surface composition. The simultaneous application of zeta potential measurement and surface analysis techniques have been previously described as very valuable to determine the composition and distribution of different materials in complex systems such as the one developed in this work.[29,32]

Table 2 displays the results obtained from the individual XPS analysis of control CS-NP, control phospholipid vesicles constituted of DPPC and DPPC-DMPG and, finally, DPPC/CS-NP and DPPC-DMPG/CS-NP assemblies; the percentage of each chemical element present in the sample being determined.

The XPS survey of control CS-NP nanoparticles detected the expected elements, such as C, O, N and P, albeit traces of Si were also found, which could be a result of the Si-based sample holder substrate or a consequence of the processing of the exoskeleton components from the original material, as reported elsewhere.[33] This assay detected in the nanoparticles 54% C, 34% O and 5% N. Moreover, 3% P were detected, in accordance to the presence of the cross linking agent TPP.

Table 2. Surface composition (atomic percentage) of chitosan nanoparticles (CS-NP), control DPPC vesicles, control DPPC-DMPG vesicles, DPPC/CS-NP assemblies and DPPC-DMPG/CS-NP assemblies, determined by XPS

Element	CS- NP (%)	DPPC vesicles (%)	DPPC/CS-NP assemblies (%)	DPPC - DMPG vesicles (%)	DPPC-DMPG/CS-NP assemblies (%)
C	53.8	81.7	80.2	78.1	78.8
O	33.8	14.0	15.4	16.9	16.3
N	4.5	2.0	1.8	1.8	1.8
P	2.7	2.3	2.0	2.2	2.2
Si	5.2	0	0.6	1.0	0.9
Ratio N/C	0.084	0.025	0.022	0.023	0.023
Ratio C/O	1.592	5.836	5.208	4.618	4.834

These atomic percentages were comparable to those previously observed by *Matienzo and Winnacker* for chitosan films (61% C, 31% O and 6% N), although slight differences can be explained by the use of chitosans with different deacetylation degrees (86% in our case against 70% in theirs) as well as by the fact that we are analysing chitosan nanoparticles containing TPP while they assay pure chitosan films.[33] In addition, a C/O ratio of approximately 1.6 was obtained in this work, which is similar to the 1.4 previously found by *Calvo et al.* in a study with CS-NP.[20]

The analysis of the control phospholipid vesicles detected as well signals of C, O, N and P. For DPPC and DPPC-DMPG, respectively, 82% and 79% C and 14% and 17% O were found, 2% N and 2% P showing to be similar for both lipid compositions. In the N_{1s} spectra from pure DPPC vesicles, N is observed at about 402 eV (data not shown), which is typical of the protonated amine group and coincident with results from other works.[34,35] Additionally, in the C_{1s} region, a

peak is observed at a binding energy of 285 eV, being similar to that found by *Evora et al.* and attributed to the methylene groups of aliphatic chains of DPPC.[10] When observing signals obtained from the assemblies, it is noticeable that they are much more similar to those of the corresponding control lipid vesicles than to nanoparticles. In fact, while CS-NP display 54% C, DPPC/CS-NP assemblies show 80% C and DPPC-DMPG/CS-NP assemblies 79% C, comparable to the 82% and 78% found for the respective control vesicles. The same is observed for O, the CS-NP exhibiting 34%, against 15% and 16% for DPPC/CS-NP and DPPC-DMPG/CS-NP assemblies, respectively, and 14% and 17%, respectively for control vesicles. The N/C ratio obtained for control DPPC and DPPC-DMPG vesicles, respectively, was 0.025 and 0.023. The value of 0.025 determined for pure DPPC is coincident with that deduced from the stoichiometric composition of the molecule ($C_{40}O_6N_1P_1H_{80}$).[34] These values of 0.025 and 0.023 were in fact strongly similar to those obtained for the respective assemblies (0.022 and 0.023, respectively), actually being exactly the same when DPPC and DMPG are composing the lipid film, being in turn very different from those observed for nanoparticles, 0.084. Moreover, the same observation was taken for the C/O ratio, which demonstrated to be 1.6 for nanoparticles, 5.8 and 4.6 for control DPPC and control DPPC-DMPG vesicles, respectively, and 5.2 and 4.8 for the respective assemblies. Considering all these results of XPS, it was found that data obtained for both assemblies are very similar to those observed for the respective control vesicles, thus indicating that the assemblies surface chemistry is dominated by the lipids. Moreover, it was confirmed that the lipid coating is more effective when the lipid film is composed by both lipids DPPC-DMPG, which could be attributed to the negative charge of the lipid film, definitely playing an important role in the interaction between the lipids and the positively charged nanoparticles, as previously suggested by the zeta potential measurements. For the assemblies comprising only DPPC, the surface has a minor but detectable contribution from the nanoparticles and therefore, lipids are dominating the surface chemistry but do not entirely mask the nanoparticles.

The results provided by the TOF-SIMS analysis corroborated those observed by XPS. **Figure 3** displays the mass spectra (160 – 240 amu) obtained by TOF-SIMS of (A) control CS-NP, (B) control DPPC vesicles and (C) DPPC/CS-NP

assemblies; the parts C1 and C2 representing different zones of the DPPC/CS-NP sample.

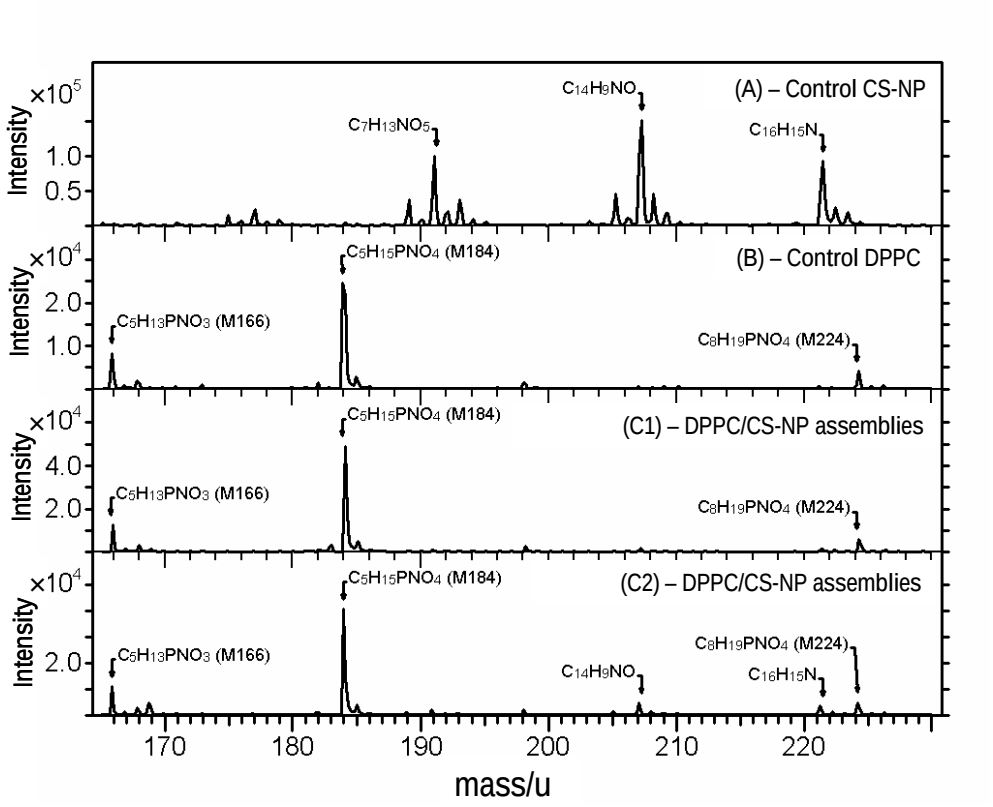

Fig. 3. Mass spectra obtained by TOF-SIMS analysis of (A) control CS-NP; (B) control DPPC vesicles; and (C1,C2) DPPC/CS-NP assemblies.

The spectrum obtained for DPPC/CS-NP assemblies is not identical to that of control DPPC vesicles. However, in some specific zones of the DPPC/CS-NP sample (see C1), there is a perfect resemblance with spectrum of control DPPC (B), indicating that occasionally nanoparticles are completely coated by DPPC. In both spectra B and C, signals which are reported to be typical of DPPC could be identified, such as M166, representing the phosphate region,[36-39] M184 from the entire head group of DPPC (phosphatidylcholine),[37,40-44] and M224 resulting from the cleavage of palmitoyl residues.[37,45,46] Observing spectra C2, besides the identification of the previously referred typical signals from DPPC, signals resultant from the CS-NP, identified in spectrum A, are also recognised, such as

M207 ($C_{14}H_9NO$) and M221 ($C_{16}H_{15}N$). Given the absence of bibliographic support on the typical masses of this mixture of CS and TPP, which form the CS-NP, we assumed ions identified in the control nanoparticles spectra as characteristic. Therefore, if they appear in the assemblies spectra, this confirms the existence of zones where nanoparticles are on the surface of the assemblies, not being coated by the lipid film.

Figure 4 displays the mass spectra (140-240 amu) obtained by TOF-SIMS of (A) control CS-NP, (B) control DPPC-DMPG vesicles and (C) DPPC-DMPG/CS-NP assemblies. In spectrum A, the typical signals of CS-NP referred above were also identified (M191, M207 and M221). On the contrary of what was observed when only DPPC was present in the lipid film, the spectrum obtained for DPPC-DMPG/CS-NP assemblies is similar to that of control DPPC-DMPG vesicles, indicating that the lipid film absolutely dominates the assemblies surface, completely coating the CS-NP. Therefore, the typical signals of DPPC were identified in both spectra, such as M166, M184 and M224.

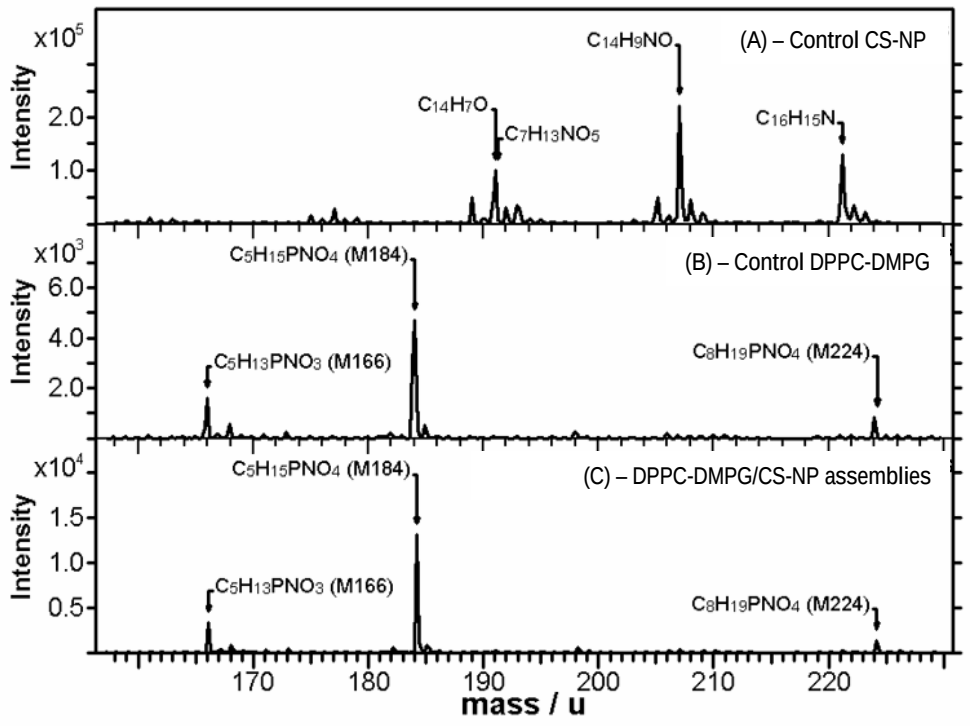

Fig. 4. Mass spectra obtained by TOF-SIMS analysis of (A) control CS-NP; (B) control DPPC-DMPG vesicles; and (C) DPPC-DMPG/CS-NP assemblies.

A global analysis of the results obtained with XPS and TOF-SIMS indicated that the lipid coating of chitosan nanoparticles was more effective when the lipid film was constituted of DPPC and DMPG, having a strongly negative charge, hence indicating that electrostatic forces governed interaction mechanism between both components forming the assemblies. Actually, these results are in agreement with the different release profile of insulin reported for both assemblies formulations, according to which insulin was released more slowly from DPPC-DMPG/CS-NP assemblies.[15] The presence of a lipid coating which completely dominates the assemblies surface in this formulation is in fact coincident with a more sustained release of insulin comparing to the DPPC assemblies, given the need of the peptide to cross a compact lipid layer after being released from the nanoparticles.

3.3 Discussion on the efficacy of L/CS-NP assemblies as protein carriers to the lungs

The composition of drug delivery systems is known to play an important role in the fate of the associated drugs and, in this context, the presence of lipids in formulations intended for pulmonary administration has been demonstrating particular interest. In fact, considering the existence of phospholipids in the lung as the major components of the alveolar surfactant, the addition of extra phospholipids was previously reported to enhance macromolecules absorption.[7-9,47] The macrophagic capture of inhaled particulates has been reported as one of the major issues of pulmonary administration [4,48] and several studies have been conducted in order to overcome this physiological barrier. So far, a few different factors such as particle size, surface properties, composition and local concentration, have been demonstrated to affect phagocytic activity,[49-53] and alveolar macrophagic uptake of PLGA microparticles was demonstrated to decrease by inclusion of various phospholipids, such as phosphatidylcholine, -serine and -ethanolamine in the formulations.[10,47] On the other hand, particles in the nanometer size range demonstrated to be less captured than microparticles.[49-51]

Chitosan is a very attractive polysaccharide due to its low toxicity, biodegradability and mucoadhesivity[54-56] and chitosan nanoparticles have shown an excellent capacity for protein association as well as an improvement of peptide absorption through several epithelia, such as the nasal, ocular and pulmonary.[12,57,58] The L/CS-NP assemblies reported in this work, were prepared using two phospholipids which are endogenous of the lung (DPPC and DMPG), since they are the principal constituents of the lipid part of the pulmonary surfactant.[8] We produced assemblies using DPPC or a combination of DPPC and DMPG in a molar ratio of 10:1, respectively, this combination representing an attempt to approximately respect the lipid proportions of the alveolar surfactant. Moreover, previous studies demonstrated the ability of these L/CS-NP to provide a controlled release of the encapsulated protein as well as their successful encapsulation in mannitol microspheres, which evidenced adequate properties for administration via the pulmonary route.[15]

Taking into account all these considerations, we believe that the delivery system characterised in this study has the potential to succeed as carrier of therapeutic macromolecules to the lung.

4. Conclusions

The present work demonstrated that the proposed methodology of lipid film hydration with a nanoparticles suspension is appropriate to produce an effective coating of the preformed nanoparticles by the phospholipids, forming the lipid/nanoparticles assemblies. The success of this coating depends on the composition of the lipid film chosen to form the structures. The combination of superficial charge measurements and determination of the chemical composition of the surface, elucidated the molecular architecture of the assemblies, demonstrating that the envisioned system really corresponds to polymer particles surrounded by lipids. In fact, the influence of the phospholipids composition on the assemblies formation, primarily suggested by the zeta potential analysis, was likewise confirmed by the accurate surface analysis of the assemblies by XPS and TOF-SIMS. When the lipid film is composed of DPPC, it was observed that the lipid constitutes the most part of the assemblies surface, but the specific presence of nanoparticles was also detected, although to a much lower extent. On the contrary, when DMPG is added to the lipid film, conferring a negative charge, the lipid layer dominated the assemblies surface and a complete coat of the nanoparticles was produced. Therefore, the major role of electrostatic interactions as driving forces to control the organisation between negatively charged lipids and oppositely charged chitosan nanoparticles was clearly evident.

Acknowledgements

This work was supported by the Spanish Government (CICYT, SAF2002-03314, Feder cofinanced). The Predoctoral fellowship to Ana Grenha from Fundação para a Ciência e Tecnologia, Portugal (SFRH/BD/13119/2003) is highly appreciated.

References

(1) Agnihotri, S. A.; Mallikarjuna, N. N.; Aminabhavi, T. M. *J. Control. Release.* **2004**, *100*, 5-28.

(2) Sharma, A., Sharma, U. S. *Int. J. Pharm.* **1997**, *154*, 123-140.

(3) Alonso, M. J.; Sanchez, A. In *Carrier-based drug delivery*; Svenson, S., Ed.; American Chemical Society: New York, 2004; pp. 283-295.

(4) Courrier, H. M.; Butz, N.; Vandamme, T. F. *Crit. Rev. Ther. Drug Carr. Syst.* **2002**, *19*, 425-498.

(5) Kirby, C. J.; Gregoriadis, G. In *Encyclopedia of Controlled Drug Delivery*; Mathiowitz, E., Ed.; John Wiley & Sons: New York, 1999, pp. 461-492.

(6) Mezei, M. In *Liposomes as drug carriers: recent trends and progress*; Gregoriadis, G., Ed.; John Wiley & Sons: Chichester, 1988, pp. 663-677.

(7) Hussain, A.; Arnold, J. J.; Khan, M. A.; Ahsan, F. *J. Control. Release.* **2004**, *94*, 15-24.

(8) McAllister, S. M.; Alpar, H. O.; Teitelbaum, Z.; Bennett, D. B. *Adv. Drug Deliv. Rev.* **1996**,*19*, 89-110.

(9) Mitra, R.; Pezron, I.; Li, Y.; Mitra, A. K. *Int. J. Pharm.* **2001**, *217*, 25-31.

(10) Evora, C.; Soriano, I.; Rogers, R. A.; Shakesheff, K. M.; Hanes, J.; Langer, R. *J. Control. Release.* **1998**, *51*, 143-152.

(11) Calvo, P.; Remuñan-Lopez, C.; Vila-Jato, J. L.; Alonso, M. J. *J. Appl. Polym. Sci.* **1997**, *63*, 125-132.

(12) Fernández-Urrusuno, R.; Calvo, P.; Remuñan-Lopez, C.; Vila-Jato, J. L.; Alonso, M. J. *Pharm. Res.* **1999**, *16*, 1576-1581.

(13) Fernández- Urrusuno, R.; Romani, D.; Calvo, P.; Vila-Jato, J. L.; Alonso, M. J. *S. T. P. Pharma Sci.* **1999**, *9*, 429-436.

(14) Carvalho, E. L. S.; Seijo, B.; Alonso, M. J. Int. J. Pharm. (submitted) .

(15) Grenha, A.; Remuñan-Lopez, C.; Carvalho, E. L. S.; Seijo, B. *Eur. J. Pharm. Biopharm.* (submitted).

(16) Belu, A. M.; Graham, D. J.; Castner, D. G. *Biomaterials.* **2003**, *24*, 3635-3653.

(17) Hagenhoff, B. *Mikrochimica Acta.* **2000**, *132*, 259-271.

(18) Turner, N. H.; Schreifels, J. A. *Anal. Chem.* **1998**, *70*, 229R-250R.

(19) Bosquillon, C.; Rouxhet, P. G.; Ahimou, F.; Simon, D.; Culot, C.; Préat, V.; Vanbever, R. *J. Control. Release.* **2004**, *99*, 357-367.

(20) Calvo, P.; Remuñan-Lopez, C.; Vila-Jato, J. L.; Alonso, M. J. *Pharm. Res.* **1997a**, *14*, 1431-1436.

(21) Lin, W.-C.; Tseng, C.-H.; Yang, M.-C. *Macromol. Biosci.* **2005**, *5*, 1013-1021.

(22) Zhu, A. P.; Fang, N.; Chan-Park, M. B.; Chan, V. *Biomaterials.* **2006**, *27*, 2566-2576.

(23) Davies, M. C.; Brown, A.; Newton, J. M.; Chapman, S. R. *Surf. Interf. Anal.* **1988**, *11*, 591-595.

(24) John, C. M.; Odom, R. W.; Salvati, L.; Annapragada, A. V.; Lu, M. Y. F. *Anal. Chem.* **1995**, *67*, 3871-3878.

(25) Beaulac, C.; Sachetelli, S.; Lagacé, J. *J. Drug Target.* **1999**, *7*, 33-41.

(26) Marier, J.-F.; Lavigne, J.; Ducharme, M. P. *Antimicrob. Agents Chemother.* **2002**, *46*, 3776-3781.

(27) Weiner, A. L. *Adv. Drug Deliv. Rev.* **1989**, *3*, 307-341.

(28) Fattal, E.; Couvreur, P. ; Puisieux, F. In *Les liposomes: aspects technologiques, biologiques et pharmacologiques*; Delattre, J.; Couvreur, P.; Puisieux, F.; Philippot, J. R.; Schuber, F., Eds.; Editions Inserm: Paris, 1993; pp. 43-52.

(29) Troutier, A.-L. ; Delair, T.; Pichot, C.; Ladavière, C. *Langmuir.* **2005**, *21*, 1305-1313.

(30) Correia, F. M.; Petri, D. F. S.; Carmona-Ribeiro, A. M. *Langmuir.* **2004**, *20*, 9535-9540.

(31) Moya, S.; Donath, E.; Sukhorukov, G. B.; Auch, M.; Bäumler, H.; Lichtenfeld, H.; Möhwald, H. *Macromolecules.* **2002**, *33*, 4538-4544.

(32) Feng, S.; Huang, G. *J. Control. Release.* **2001**, *71*, 53-69.

(33) Matienzo, L. J.; Winnacker, S. K. *Macromol. Mater. Eng.* **2002**, *287*, 871-880.

(34) Deleu, M.; Paquot, M.; Jacques, P.; Thonart, P.; Adriaensen, Y.; Dufrêne, Y. F. *Biophys. J.* **1999**, *77*, 2304-2310.

(35) Gerin, P. A.; Dengis, P. B.; Rouxhet, P. G. *J. Chim. Phys.* **1995**, *92*, 1043-1065.

(36) Biesinger, M. C.; Paepegaey, P.-Y.; McIntyre, N. S.; Harbottle, R. R.; Petersen, N. O. *Anal. Chem.* **2002**, *74*, 5711-5716.

(37) Bourdos, N.; Kollmer, F.; Benninghoven, A.; Ross, M.; Sieber, M.; Galla, H.-J. *Biophys. J.* **2000**, *79*, 357-369.

(38) Roddy, T. P.; Cannon, D. M.; Ostrowski, S. G.; Ewing, A. G.; Winograd, N. *Anal. Chem.* **2003**, *75*, 4087-4094.

(39) Ross, M.; Steinem, C.; Galla, H.-J.; Janshoff, A. *Langmuir.* **2000**, *17*, 2437-2445.

(40) Bourdos, N.; Kollmer, F.; Benninghoven, A.; Sieber, M.; Galla, H.-J. *Langmuir.* **2000b**, *16*, 1481-1484.

(41) Cannon, D. M.; Pacholski, M. L.; Winograd, N.; Ewing, A. G. *J. Am. Chem. Soc.* **2000**, *122*, 603-610.

(42) Cliff, B.; Lockyer, N. P.; Corlett, C.; Vickerman, J. C. *Appl. Surf. Sci.* **2003**, *203-204*, 730-733.

(43) McMahon, J. M.; Short, R. T.; McCandlish, C. A. *Rapid Commun. Mass Spectrom.* **1996**, *10*, 335-340.

(44) Nygren, H.; Börner, K.; Hagenhoff, B.; Malmberg, P.; Månsson, J.-E. *Biochim. Biophys. Acta.* **2005**, *1737*, 102-110.

(45) Ostrowski, S. G.; Szakal, C.; Kozole, J.; Roddy, T. P.; Xu, J.; Ewing, A. G.; Winograd, N. *Anal. Chem.* **2005**, *77*, 6190-6196.

(46) Sostarecz, A. G.; Cannon, D. M.; McQuaw, C. M.; Sun, S.; Ewing, A. G.; Winograd, N. *Langmuir.* **2004**, *20*, 4926-4932.

(47) Jones, B. G.; Dickinson, P. A.; Gumbleton, M.; Kellaway, I. W. *J. Pharm. Pharmacol.* **2002**, *54*, 1065-1072.

(48) Clark, A. *Drug Deliv. Syst. Sci.* **2002**, *2*, 73-77.

(49) Ahsan, F.; Rivas, I. P.; Khan, M. A.; Suárez-Torres, A. I. *J. Control. Release.* **2002**, *79*, 29-40.

(50) Aktar, S.; Lewis, K. J. *Int. J. Pharm.* **1997**, *151*, 57-67.

(51) Makino, K.; Yamamoto, H.; Higuchi, K.; Harada, N.; Ohshima, H.; Terada, H. *Colloid. Surf. B - Biointerfaces.* **2003**, *27*, 33-39.

(52) Kubota, Y.; Takahashi, S.; Matsuoka, O. *J. Toxicol. Sci.* **1983**, *8*, 189-195.

(53) Rudt, S.; Müller, R. H. *J. Control. Release.* **1992**, *22*, 263-272.

(54) Dornish, M.; Hagen, A.; Hansson, E.; Peucheur, C.; Vedier, F.; Skaugrud, O. In *Advances in chitin science*; Domard, A.; Roberts, G. A. F.; Varum, K. M., Eds.; Jacques Andre publisher: Lyon, 1997; pp. 664-670.

(55) Hirano, S.; Seino, H.; Akiyama, Y.; Nonaka, I. *Polym. Mater. Sci. Eng.* **1988**, *59*, 897-901.

(56) Lehr, C. M.; Bouwstra, J. A.; Schacht, E. H.; Junginger, H. E. *Int. J. Pharm.* **1992**, *78*, 43-48.

(57) De Campos, A.; Sanchez, A.; Alonso, M. J. *Int. J. Pharm.* **2001**, *224*, 159-168.

(58) Yamamoto, H.; Kuno, Y.; Sugimoto, S.; Takeuchi, H.; Kawashima, Y. *J. Control. Release.* **2005**, 102, 373-381.

Sección III. Estudio del comportamiento *in vitro* de las microsferas de manitol conteniendo nanopartículas de quitosano en cultivos de células Calu-3 y A549

Artículo 6

CHITOSAN NANOPARTICLE-CONTAINING MICROSPHERES ARE COMPATIBLE WITH RESPIRATORY EPITHELIAL CELLS *IN VITRO*

Ana Grenha[1,2], Chris Grainger[2], Lea Ann Dailey[2], Begoña Seijo[1], Gary Martin[2], Carmen Remuñán-López[1], Ben Forbes[2*]

[1] *University of Santiago de Compostela, Dept. of Pharmacy and Pharmaceutical Technology, Faculty of Pharmacy, 15782 Santiago de Compostela, Spain*

[2] *King's College London, Pharmaceutical Science Research Division, London SE1 9NH, UK*

* Corresponding author: Phone: 0044 20 7848 4823

E-mail: ben.forbes@kcl.ac.uk

Artículo sometido a evaluación por "Biomaterials"

Abstract

The aim of this work was to evaluate the biocompatibility of novel respirable powder formulations of nanoparticles (NP) entrapped in mannitol microspheres using human respiratory epithelial cell lines. Microspheres formulated at NP:mannitol ratios of 10:90, 20:80 and 40:60 were evaluated using the Calu-3 and A549 cell lines. The MTT cell viability assay revealed an absence of overt toxicity to Calu-3 or A549 cells following exposure to the formulations containing <1.3 mg/mL NP (0.87 mg/cm^2 cells) for up to 48 h. Transepithelial electrical resistance (TER) and solute permeability in Calu-3 cell layers were determined following exposure of the cells to the NP:mannitol 20:80 formulation. After administration of the formulation dissolved in serum-free cell culture medium (1.3 mg/mL NP suspension) to the cells, neither TER or permeability were altered compared to untreated cell layers. Confocal microscopy did not reveal any NP internalisation under the conditions used in this study, although evidence of mucoadhesion was observed. All the data presented are encouraging with respect to the development of chitosan NP-containing microspheres for the pulmonary administration of therapeutic macromolecules. Not only do the formulations possess suitable aerodynamic characteristics and the capacity to encapsulate proteins as shown previously; they have now been shown to exhibit *in vitro* biocompatibility.

Keywords: A549 cells, Calu-3 cells, inhalation toxicology, respiratory drug delivery, aerosol formulation.

1. Introduction

The pulmonary administration of therapeutic macromolecules for systemic delivery is receiving a great deal of attention on account of the promising anatomical features of the lung; particularly its large absorptive epithelial surface area. The development of adequate delivery systems has become an important issue, with the fundamental requirement that inhaled particles must possess appropriate aerodynamic properties to reach the deep lung [1-3]. A novel hydrophilic system consisting of chitosan nanoparticles (NP) encapsulated in mannitol microspheres has been developed recently for the delivery of proteins by inhalation [4]. These microspheres have aerodynamic diameters suitable for pulmonary administration and, upon contact with an aqueous environment such as lung lining fluid, they dissolve to yield a NP suspension from which their therapeutic payload is released.

Chitosan is generally recognised as a biocompatible and biodegradable polysaccharide, which exhibits low toxicity [5,6]. Furthermore, it is mucoadhesive and can promote macromolecule permeation through well organised epithelia [7]. The chitosan NP used in this study have many advantages, such as mild preparation conditions and an excellent capacity for protein entrapment [8]. Moreover, chitosan NP have proven to be efficient vehicles for the transport of insulin through the nasal mucosa and, consequently, we hypothesise that they may be effective for pulmonary delivery [9]. Yet, before chitosan NP-based systems may be considered suitable for pulmonary administration, it is important to ensure the absence of any adverse effects of the particles towards the respiratory epithelium.

The Calu-3 and A549 respiratory epithelial cell lines have previously been used for *in vitro* evaluation of the safety and efficacy of particulate drug delivery systems [10-13] and to study environmental particle toxicology [14-17]. Calu-3 cell layers form tight junctions *in vitro* [18] and, under suitable culture conditions, exhibit *in vivo*-like barrier properties [19]. Intercellular structures are crucial for epithelial development and function. Tight junctions are the most restrictive intercellular junction, forming a continuous band which completely circumvents the periphery of cells at their mucosal surface [20]. In contrast to Calu-3 cells,

A549 cells do not form functional tight junctions in culture [10,18,21]. As a result, this cell line cannot be used to study the permeability of the epithelial barrier, although this does not prevent the use of A549 cells for particle uptake and cytotoxicity studies.

The safety of inhaled formulations is best evaluated *in vitro* by using a variety of toxicological tests to provide complementary information. Cell viability assays are widely used to evaluate the safety of inhaled materials [12-14,22,23]. Following exposure of respiratory cells to NP *in vitro*, the 3-(4,5-dimethylthiazol-2-yl)-2,5-diphenyltetrazolium bromide (MTT) assay allows quantification of the metabolic activity of a population of cells by means of formation of soluble dark blue crystals that can be quantified by spectrophotometry. Another indicator of adverse effects of particles on epithelial cell layers is any reduction in transepithelial electrical resistance (TER) [22-25]. If a reduction in TER suggests a change in the epithelial layer barrier function, this can be confirmed by measuring the permeability of a fluid phase marker. The use of imaging techniques provides valuable information on particle adhesion to, uptake into, or translocation (transport) across the epithelial cell layer [10,11,15,16,26] and can reveal the extent of interaction between particles and the epithelial cell layers.

The principal aim of this work was to determine the compatibility of the NP-containing inhalation delivery system described previously [4] with the Calu-3 and A549 respiratory cell lines in terms of cytotoxicity and cell layer permeability. A secondary objective was to examine the fate of the particles following application to Calu-3 cell layers using confocal microscopy.

2. Methods and Materials

2.1. Chemicals

Chitosan (CS) in the form of a hydrochloride salt (Protasan® 213 Cl, deacetylation degree 86%, viscosity 95 mPa) was purchased from Pronova Biopolymer, A.S. (Drammen, Norway). Pentasodium tripolyphosphate (TPP), fluorescein isothiocyanate albumin (FITC-BSA), glycerol, D-mannitol (Ma), Dulbecco's modified Eagle's medium nutrient mixture F-12 Ham, Minimum

Essential Medium Eagle (MEM), non-essential amino acids (100%), L-glutamine 200 mM, foetal bovine serum (FBS), gentamicin solution, trypsin-EDTA solution (2.5 g/L trypsin, 0.5 g/L EDTA), trypan blue solution (0.4%), thiazolyl blue tetrazolium bromide (MTT), sodium dodecyl sulphate (SDS), N-N dimethylformamyde (DMF), paraformaldehyde, Hanks' balanced salt solution (HBSS), 4',6-diamidino-2-phenylindole (DAPI) and sodium fluorescein were supplied by Sigma Chemical Company (Madrid, Spain and Poole, UK). Wheat germ agglutinin (WGA) – Texas Red® was provided by Molecular Probes (Paisley, UK). Tissue culture flasks (75 and 162 cm^2 with ventilated caps), 96-well plates and Transwell inserts (0.33 cm^2 polyester 0.4 μm pore size) were from Costar (High Wycombe, UK). Phosphate buffered saline (PBS) tablets were purchased from Oxoid (Basingstoke, UK). Ultrapure water (Elga Option 3 water purifier, High Wycombe, UK) was used throughout. All other chemicals were reagent grade.

2.2. Cell lines

The Calu-3 and A549 cell lines were obtained from the ATCC (Rockville, USA) and used between passages 22–30 and 100–110, respectively. Cell cultures were grown using 75 or 162 cm^2 flasks in a humidified 5% CO_2/95% atmospheric air incubator at 37ºC. For Calu-3 cells, cell culture medium (CCM) was 500 mL Dulbecco's Modified Eagle's Medium/Nutrient Mixture F-12 Ham (1:1), 50 mL foetal bovine serum, 5 mL non-essential amino acid solution, 5 mL L-glutamine solution (200 mM) and 0.5 mL gentamicin (50 mg/mL). For the A549 cells, 500 mL Minimum Essential Medium Eagle, 50 mL foetal bovine serum, 5 mL L-glutamine solution (200 mM) and 0.5 mL gentamicin (50 mg/mL) were used. Medium was exchanged every 2-3 days and cells were subcultured weekly.

2.3. Culture of A549 and Calu-3 cell layers

For the MTT assay, Calu-3 and A549 cells were seeded at a density of 1×10^4 cells/well in 96-well plates in 100 μl of the same medium used for culture in cell culture flasks. The cells were grown at 37°C in a 5% CO_2 atmosphere for 24 h before use in cell viability assays.

For studies of epithelial barrier permeability and confocal microscopy experiments, Calu-3 cells were cultured at an air interface according to the methods of Grainger and co-workers [19]. Briefly, 100 mL of Calu-3 cell suspension was seeded at a density of 5×10^5 cells/cm^2 in Transwell inserts (0.33 cm^2), with 0.5 mL medium in the basolateral chamber. The cells were incubated at 37ºC, 5% CO_2 for 2 d. After this time, medium was aspirated from the apical and basolateral chambers and replaced only in the basolateral chamber, the apical chamber being exposed to the incubator atmosphere. Medium was replaced every 2 days thereafter.

2.4 Preparation of test formulations

Chitosan/tripolyphosphate (CS/TPP) NP were prepared by the ionotropic gelation of CS with a counter-anion TPP, in which the positively charged amino groups of CS interact with the negatively charged TPP [8]. NP were formed spontaneously upon mixing 1.2 mL TPP solution (0.69 mg/mL w/v in purified water) with 3 mL CS solution (1.2 mg/mL w/v in purified water) and stirring at room temperature as described previously [4]. The final CS/TPP ratio was 3.6:1 (w/w). To produce NP loaded with fluorescent protein, FITC-BSA (0.9 mg FITC-BSA/0.6 mL water; pH = 9.2) was incorporated in the TPP solution. The protein concentration in the TPP solution was calculated in order to obtain NP with a theoretical content of 30% (w/w) FITC-BSA respective to CS. NP were concentrated by centrifugation at 10,000 g on a 10 µl glycerol bed, for 30 min at 15ºC (Beckmann Avanti 30, Beckmann, Fullerton, USA). The supernatant was discarded and NP were resuspended in 100 µl of purified water.

Microspheres were produced by spray-drying an aqueous suspension of CS/TPP NP in mannitol solution (final solids concentration of 20 - 40 mg/mL) using a laboratory-scale spray-dryer (Büchi® Mini Spray Dryer, B-290, Switzerland) in order to achieve NP:mannitol ratios of 10:90, 20:80 and 40:60 (w/w). Control (NP-free) mannitol microspheres were also prepared by spray-drying 50 mg/mL mannitol solution. Spray-drying was conducted using a feed rate of 2.5 mL/min, two fluids external mixing 0.7 mm nozzle, inlet and outlet temperatures of 160 ± 2ºC and 108 ± 3ºC, respectively. The air flow rate and the

aspirator were maintained at a constant 400 Nl/h and 80%, respectively. The spray-dried powders were collected and stored in a dessicator at room temperature until use.

2.5. Characterisation of test formulations

Morphological examination of NP was conducted by transmission electron microscopy (TEM) (CM 12 Philips, Eindhoven, Netherlands). The samples were stained with 2% (w/v) phosphotungstic acid and placed on copper grids with Formvar® films for TEM observation.

NP size and zeta potential were determined in freshly prepared samples by photon correlation spectroscopy and laser Doppler anemometry, respectively, using a Zetasizer® 3000 HS (Malvern Instruments, Malvern, UK). For the particle size analysis, each sample was diluted to the appropriate concentration with filtered (0.2 μm filters Millex®-GN, Millipore Iberica, Spain) ultrapure water. Each analysis lasted 180 s and was performed at 25ºC with a detection angle of 90º. For the determination of the electrophoretic mobility, samples were diluted with 0.1 mM KCl and placed in the electrophoretic cell, where a potential of ± 150 mV was established. Three batches of each formulation were analysed for size and zeta potential in triplicate.

The NP production yield was calculated by gravimetry. Fixed volumes of NP suspensions were centrifuged (16,000 g, 30 min, 15ºC) and sediments were lyophilised (24 h at -34ºC and gradual ascent until 20ºC), using a Labconco Freeze Dryer (Labconco, Kansas City, USA) (n = 3). The process yield was calculated as follows:

$$\text{Process yield (\%)} = \frac{\text{Nanoparticle weight}}{\text{Total initial solids weight}} \times 100$$

The NP association efficiency of FITC-BSA was determined upon separation of NP from the aqueous preparation medium containing the non-associated protein

by centrifugation (16,000 g, 30 min, 15ºC). The amount of free FITC-BSA in the supernatant was determined by UV spectrophotometry (Shimadzu UV-Visible Spectrophotometer UV-1603, Japan) at 494 nm. A calibration curve was constructed using the supernatant of blank NP. Each sample was assayed in triplicate (n = 3). The NP protein loading capacity and association efficiency were calculated as follows:

$$\text{Loading capacity (\%)} = \frac{\text{(Total FITC-BSA amount)} - \text{(Free FITC-BSA amount)}}{\text{Nanoparticle weight}} \times 100$$

$$\text{Association efficiency (\%)} = \frac{\text{(Total FITC-BSA amount)} - \text{(Free FITC-BSA amount)}}{\text{Total FITC-BSA amount}} \times 100$$

The release of FITC-BSA was determined by incubating the NP or the NP-loaded microspheres (NP:mannitol = 20:80) in 5 mL of phosphate buffer (PBS) pH 7.4, with horizontal shaking, at 37ºC. At appropriate time intervals (1, 2, 4, 6 and 8 d) individual samples were filtered (0.22 µm filters Millex®-GV, low protein binding, Millipore Iberica, Spain) and the amount of protein released in the filtrate was evaluated by UV spectrophotometry (Shimadzu UV-Visible Spectrophotometer UV-1603, Kyoto, Japan) at 494 nm (n=3).

Microsphere morphology was characterised by scanning electron microscopy (SEM, Leo 435VP, UK). The dry powders were placed onto metal plates and a 200 nm-thick gold palladium film was sputter coated onto the samples (High Resolution Sputter Coater SC7640, Termo VG Scientific, Cambridge, UK) before viewing. Real density was determined using a Helium Pycnometer (Micropycnometer, Quanta Chrome, model MPY-2, Florida, USA) (n = 3). Apparent tap density was obtained by measuring the volume of a known

weight of powder (approximately 2 g) in a 10 mL test-tube after mechanical tapping at 30 tap/min (Tecnociencia, Santiago de Compostela, Spain). After registration of the initial volume, the test-tube was subjected to tapping according to a previously described method until a constant volume was achieved [27] (n = 3). Aerodynamic diameter was obtained by measurement of particle time of flight using a TSI Aerosizer® LD equipped with an Aerodisperser® (Amherst Process Instrument, Inc; Amherst, Ma, USA), (n = 3).

2.6. MTT toxicity assay

The NP-containing mannitol microsphere formulations with three different NP:mannitol ratios (10:90, 20:80 and 40:60) were assayed for cytotoxicity over 24 and 48 h in two cell lines, Calu-3 and A549. NP-free mannitol microspheres and a NP suspension were evaluated separately for any cytotoxicity and sodium dodecyl sulphate (SDS, 2%) was used as a positive control. All formulations and controls were prepared as solution/suspensions in pre-warmed CCM with 2% FBS immediately before application to the cells.

To initiate the assay, culture medium of A549 and Calu-3 cells at 24 h in culture was replaced by 100 µl of fresh medium containing the test solutions or controls at a range of predetermined concentrations (Table 1).

After 24 or 48 h of cell incubation with the formulations, 50 µl of the MTT solution (0.5 mg/mL in PBS, pH 7.3) was added to each well. After 4 h, medium was removed and any formazan crystals generated were solubilised with 100 µl of a surfactant solution comprising 10% SDS in DMF:water (1:1). Upon complete solubilisation of the crystals, the absorbance of each well was measured by spectrophotometry (SpectraMax 190®, Molecular Devices, USA) at 570 nm and corrected for background absorbance using a wavelength of 650 nm.

Table 1. Test solutions/suspensions of mannitol, nanoparticles, or respirable nanoparticle-containing mannitol microspheres in cell culture medium.

Test dilution	Nanoparticle suspension (mg/mL)	Mannitol solution (mg/mL)	Nanoparticle:mannitol concentration (mg/mL)		
			Formulation ratio 10:90	Formulation ratio 20:80	Formulation ratio 40:60
1	1.29	15.00	1.29:11.70	1.29:5.20	1.29:2.17
2	0.43	3.75	0.43:3.87	0.43:1.73	0.43:0.723
3	0.14	0.94	0.14:1.29	0.14:0.58	0.14:0.24
4	0.048	0.23	0.048:0.43	0.048:0.19	0.048:0.080
5	0.016	0.059	0.016:0.14	0.016:0.064	0.016:0.027
6	0.005	0.015	0.005:0.048	0.005:0.021	0.005:0.0089
7	0.0018	0.0037	0.0018:0.016	0.0018:0.0072	0.0018:0.0029

The relative cell viability (%) was calculated as follows:

$$\text{Viability (\%)} = \frac{A - S}{CM - S} \times 100$$

where A is the absorbance obtained for each of the concentrations of the test substance, S is the absorbance obtained for the 2% SDS and CM is the absorbance obtained for untreated cells (incubated with CCM). The latter reading was assumed to correspond to 100% cell viability. The assay was performed on three occasions with six replicates at each concentration of test substance in each instance.

2.7. Transepithelial electrical resistance

The 20:80 NP:mannitol formulation, NP suspension and mannitol solution were tested for any effect on Calu-3 cell layer permeability. The microsphere formulation was dispersed in FBS-free CCM before administration to the cell layers (100 µl), at 0.005 and 1.3 mg/ml NP. The control NP suspensions and

mannitol solutions contained the same concentrations of NP/mL or an equivalent concentration of mannitol in FBS-free CCM as those produced by dissolution of the microparticle formulations, i.e. 0.005 to 1.3 mg/mL NP and 0.02 to 5.2 mg mannitol/mL. TER was measured using chopstick electrodes and an EVOM® volt meter (STX-2, and Evom G, World Precision Instruments, UK). TER measurements were taken at 0.5, 1, 2, 4, 6, 24 and 48 h after administration. TER values were calculated by subtracting the resistance of the cell-free culture inserts and correcting for the surface area of the Transwell insert. Cell layers incubated with CCM were used as the reference (control) from which to calculate changes from control TER. All experiments were performed in triplicate on three occasions.

2.8. Cell layer permeability to sodium fluorescein

Calu-3 cell layers (TER 726 ± 131 Ω cm^2) were used for experiments after 7-8 d of culture. The NP:mannitol 20:80 formulation was dissolved in FBS-free cell CCM at a NP concentration of 1.3 mg/mL and untreated cells (incubated with FBS-free CCM alone) were used as a control. At t = -30 min, 0.1 mL FBS-free CCM was applied to the apical chamber. Cell layers were incubated for 30 min at 37ºC to equilibrate and TER was measured. Culture solutions were aspirated from both Transwell chambers and 100 µl of the test suspension or FBS-free CCM was added to the apical chamber, while 600 µl of 10% FBS-containing CCM was added to the basolateral chamber. The test suspensions were incubated with the cell layers for 2, 24 or 48 h, after which TER was measured and cell layer permeability to sodium fluorescein was assayed.

Sodium fluorescein permeability was measured by replacing the test suspension in the apical chamber with 200 µl of a fluorescein solution 0.2 mg/mL in FBS-free CCM. A sample of this solution (100 µl) was immediately removed for determination of the initial starting concentration. The cell layers were incubated at 37ºC and samples of the basolateral chamber medium were taken at 0.5, 1, 2 and 4 h. The sample volume (100 µl) was replaced with fresh warmed CCM. The TER value was measured on completion of the permeability assay and after a 24 h recovery period.

All samples were transferred to black 96-well plates and diluted with 100 µl of 1 mM NaOH solution. Fluorescence was measured using a fluorometer (Cytofluor® Multi-Well Plate Reader Series 4000, PerSeptive Biosystems, USA) setting the excitation and emission wavelengths at 485 and 530 nm, respectively. Apparent permeability coefficients (P_{app}) were calculated using the following equation:

$$P_{app}\ (cm/s) = (dq/dt) \times (1/A.C_o)$$

where dq/dt is the transport rate, A is the surface area of the Transwell culture support (0.33 cm^2), and C_o is the initial concentration of sodium fluorescein in apical chamber. This procedure was performed in triplicate on three occasions.

2.9. Cell association

Calu-3 or A549 cells were used after 7-8 d of culture in Transwells. The test formulation selected for study was the NP:mannitol 20:80 microspheres with the NP containing FITC-BSA (90% loading efficiency). The FITC-BSA nanoparticles were stable with no release of the protein over 8 days, making it possible to localise NP via the fluorescent signal of the encapsulated BSA (data not shown).

The formulation was administered both as a powder using a Twin Stage Impinger (TSI) as described previously [28] and as a suspension in FBS-free CCM. Cells were incubated with the samples for 2 h at 37ºC. After that period, each well was washed three times with HBSS, and the cells were fixed by incubation with 100 µl of paraformaldehyde 3.7% (v/v) for 10 min at 37ºC. The cells were washed three times with HBSS and, in the case of the Calu-3 cells, were incubated overnight at 37ºC with 100 µl HBSS to allow the mucus layer to be removed from cell surface. After further washing with HBSS, the cells were exposed for 30 min to the cell membrane stain WGA-Texas Red® (100 µl, 30 µg/mL PBS). Afterwards, the cells were washed and the nuclei were stained for

10 min using 4',6-diamidino-2-phenylindole (DAPI) (100 µl, 1 µg/mL water). After a final washing step with HBSS, the Transwell support was excised from the plastic holder, mounted on a glass slide, the cells were immersed in 10% (v/v) glycerol and sealed.

The cell layer was viewed with a confocal microscope (Leica DMIR E2, Leica Microsystems, UK), using laser excitation wavelengths of 205, 488 and 543 nm. Fluorescent emissions from DAPI (emission λ = 430-480 nm), FITC-BSA (emission λ = 510-570 nm) and WGA-Texas Red® (emission λ = 600-630 nm) were collected using separate channels and images were acquired with a magnification of 63x using oil immersion. A gallery of optical slices was collected and xz, yz composites were processed using the Leica Confocal Software (LCS Lite, Leica GmbH, Wetzlar, Germany). The greyscale images obtained from each scan were pseudo-coloured blue (DAPI), green (FITC-BSA) and red (WGA-Texas Red®) and overlapped afterwards to obtain a multicoloured image.

2.10. Statistical analysis

A Student t-test and one way ANOVA were used to perform the statistical analysis. All analyses were performed using the SigmaStat statistical program (Version 3, Systat Software, USA) and differences were considered to be significant at a level of $P < 0.05$.

3. Results

Respirable chitosan NP:mannitol 10:90, 20:80 and 40:60 microspheres were evaluated for their cytotoxicity in two human pulmonary cell lines, Calu-3 (a bronchial epithelial cell line) and A549 (an alveolar epithelial cell line). Images of the three principal experimental components (i.e., NP, microspheres and Calu-3 cells) provide an indication of the morphology of the formulation and epithelial cell layer (Figure 1).

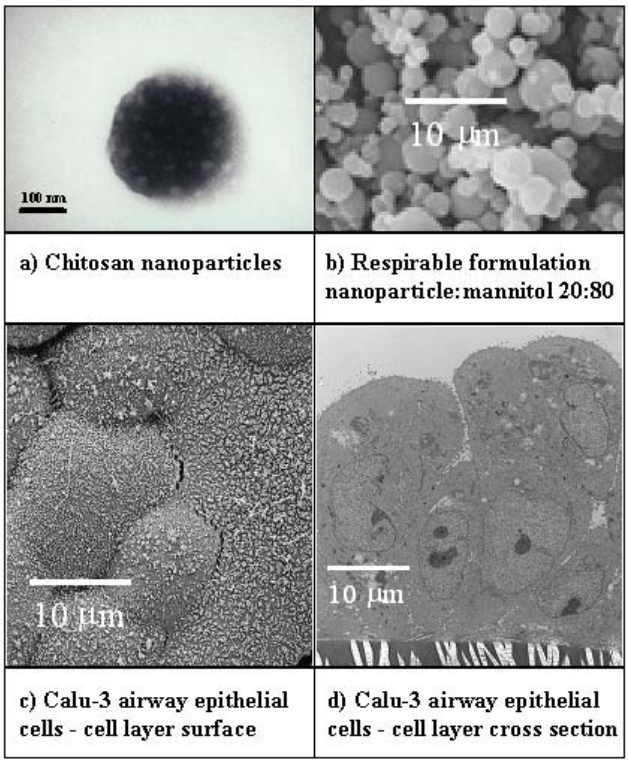

Fig. 1. Electron micrographs of the test material and epithelial cells. (a) Transmission electron micrograph of chitosan nanoparticles, (b) Scanning electron micrograph of the the respirable dry powder formulation (nanoparticle:mannitol 20:80), (c) Scanning electron micrograph of the Calu-3 cell layer, (d) Transmission electron micrograph of the Calu-3 cell layer.

3.1. Characterisation of respirable formulations

The physicochemical characteristics of the NP are provided in Table 2. A yield of 55 - 60% was obtained. Mean NP sizes ranged from 300 to 380 nm with a positive zeta potential, +34 mV. The encapsulation efficiency of FITC-BSA in CS/TPP NP was approximately 90%. The microspheres exhibited real densities of approximately 1.5 g/cm^3 and low apparent tap densities (0.3 - 0.4 g/cm^3), resulting in aerodynamic diameters between 2 and 3 µm.

Table 2. Process yields, physicochemical properties and association efficiencies of chitosan/tripolyphosphate (CS/TPP) nanoparticles (CS/TPP = 3.6:1, mean ± SD, n = 3).

Formulation	Process yield (%)	Size (nm)	Zeta potential (mV)	Association efficiency (%)	Loading capacity (%)
Unloaded (blank) nanoparticles	60 ± 4	300 ± 17	+ 34.3 ± 1.5	—	—
FITC-BSA loaded nanoparticles	55 ± 8	382 ± 16	+ 33.5 ± 3.3	89 ± 4	31 ± 1

- Process yield (%) = [Nanoparticle weight / Total initial solids weight] x 100
- Association efficiency (%) = [(Total FITC-BSA amount –Free FITC-BSA)/Total FITC-BSA amount] x 100
- Loading capacity (%) = [(Total FITC-BSA amount–Free FITC-BSA)/Nanoparticles weight] x 100

3.2. MTT assay

Nanoparticle and mannitol controls. When assayed independently, neither of the formulation components (NP or mannitol controls) reduced the viability of Calu-3 or A549 cells to the extent of a 50% inhibitory concentration (IC_{50}). The lowest cell viability (compared to the untreated control) was ~65% for mannitol solution and ~80% for the NP suspension (Figures 2a and 3a). No difference was found between 24 or 48 h exposure to the formulation controls.

NP-containing formulations. The three respirable formulations, which differ in the NP:mannitol ratio, had similar effects on cell viability to those obtained when the NP suspension was assayed alone (Figures 2 and 3). The only instances in which cell viability was reduced by >50% were: (i) the application of the highest concentration (1.3 mg/mL) of the NP:mannitol 20:80 formulation to Calu-3 cells for 24 or 48 h or A549 cells for 48 h, and (ii) the application of NP:mannitol 40:60 formulation to A549 cells at a concentration of 0.048 mg/mL NP for 48 h.

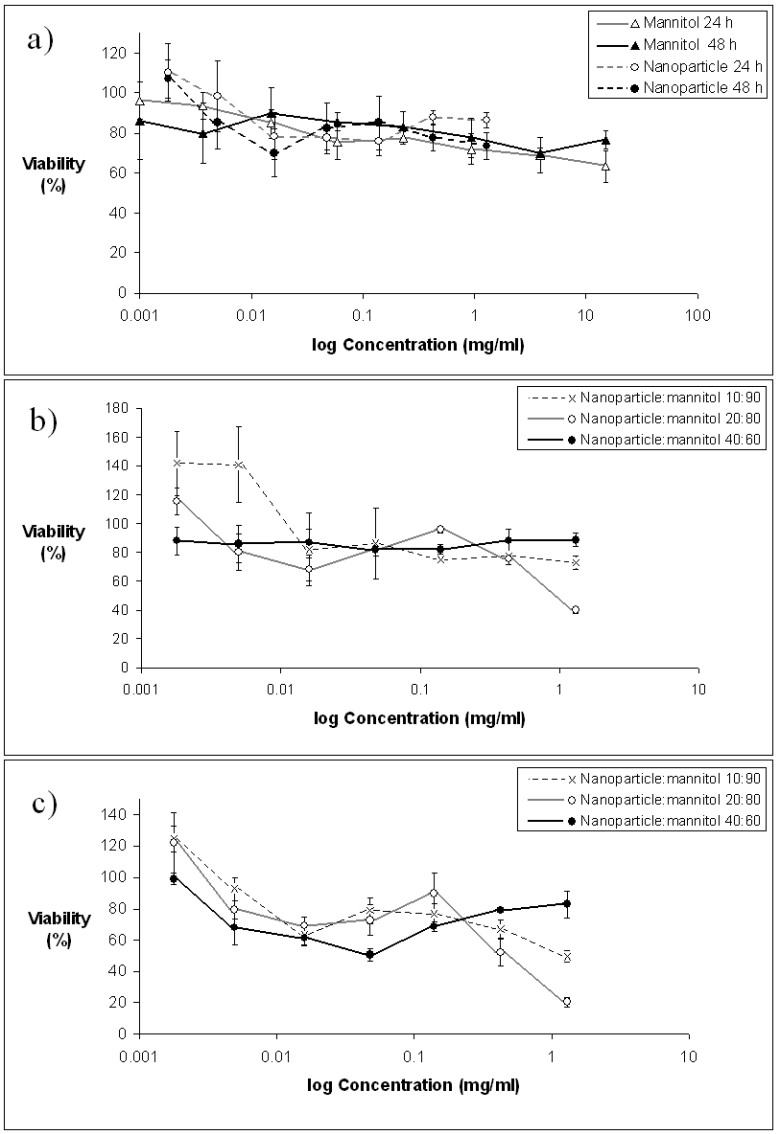

Fig. 2. Calu-3 cell viability measured by MTT cytotoxicity assay after (a) 24 and 48 h exposure to increasing concentrations of the nanoparticle suspension and mannitol solution, (b) 24 h exposure to increasing concentrations of the respirable formulations in cell culture medium, (c) 48 h exposure to increasing concentrations of the respirable formulations in cell culture medium. Data represent mean ± SEM (n=3 experiments, 6 replicates per experiment at each test concentration).

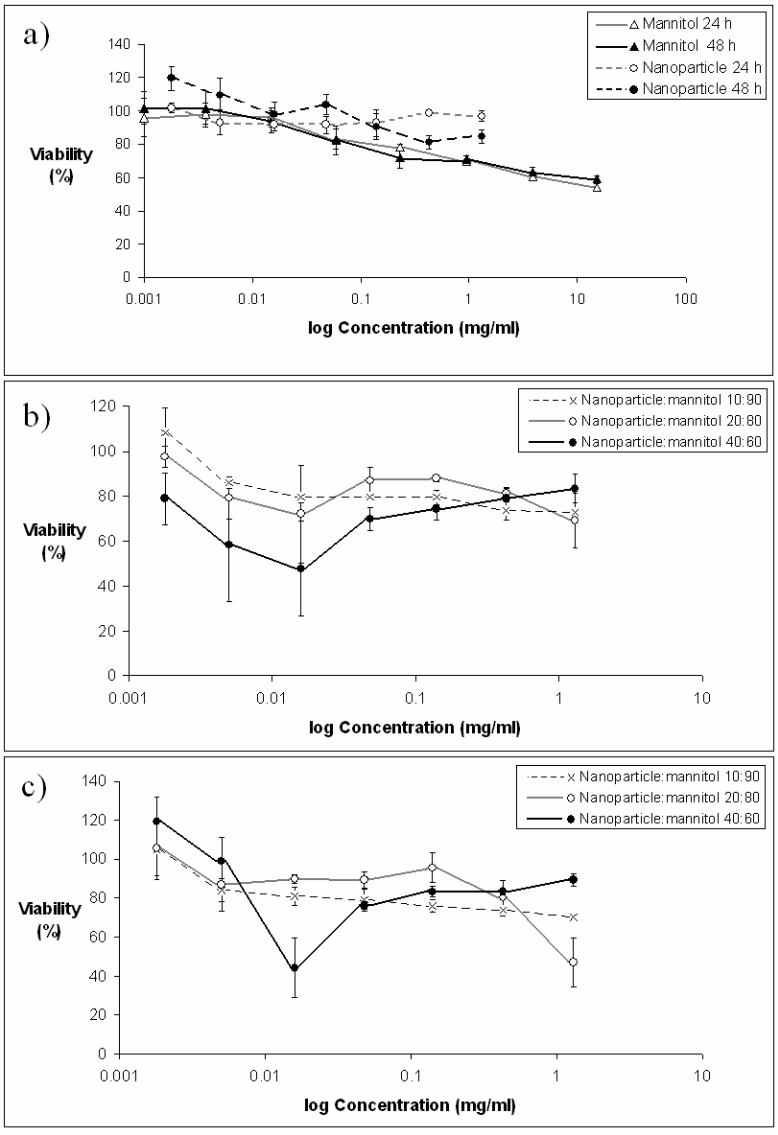

Fig. 3. A549 cell viability measured by MTT cytotoxicity assay after (a) 24 and 48 h exposure to increasing concentrations of the nanoparticle suspension and mannitol solution, (b) 24 h exposure to increasing concentrations of the respirable formulations in cell culture medium, (c) 48 h exposure to increasing concentrations of the respirable formulations in cell culture medium. Data represent mean ± SEM (n=3 experiments, 6 replicates per experiment at each test concentration).

At the 1.3 mg/mL NP dose, the effect of the formulations on Calu-3 cell viability ranked NP:mannitol 20:80>10:90>40:60 after 24 and 48 h. In A549 cells, this discriminatory effect at the highest formulation concentration was not observed at 24 h but was apparent after 48 h. The reduced A549 cell viability (from ~80% at 24 h to ~50% at 48 h; $P < 0.05$) at 0.048 mg/mL NP (NP:mannitol 40:60 formulation) was not consistent with the trend obtained using the rest of the data.

3.3. Calu-3 transepithelial electrical resistance

The NP:mannitol 20:80 formulation was selected for the evaluation of formulation effects on cell layer permeability since this formulation exhibited the most favourable morphological and aerodynamic characteristics, and has previously been tested *in vivo* [29]. Calu-3 cell layers were utilised since the cells form tight junctions and can be used to model the *in vivo* epithelial layer [19].

No effect on the cell layer TER was observed after treatment with mannitol, NP or NP:mannitol 20:80 formulation over a period of 48 h at the maximum concentrations assayed (Figure 4).

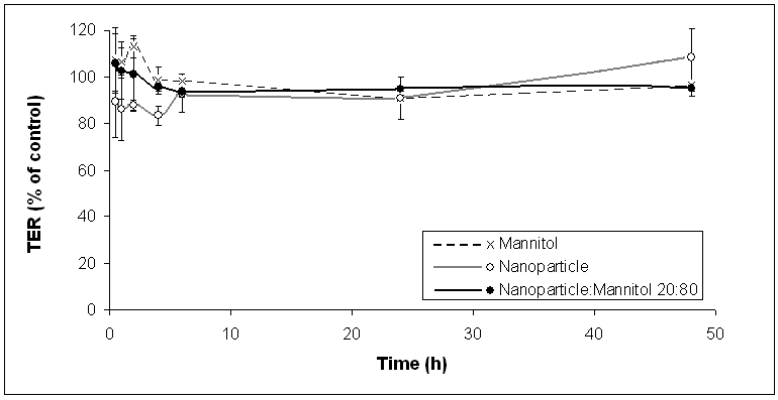

Fig. 4. Transepithelial electrical resistance (TER) of Calu-3 cell layers upon incubation with mannitol solution (5.2 mg/mL), nanoparticle suspension (1.3 mg/mL) and the test formulation dry powder nanoparticle:mannitol 20:80 (1.3 mg/mL NP). Data represent mean ± SEM of three experiments (n=3 per experiment).

The same results were observed for the lower concentrations tested (data not shown). Some TER fluctuation was observed at early time points, but the TER values overall did not differ by > 15% from the control baseline (cells with CCM).

3.4. Calu-3 cell layer permeability

The permeability coefficient (P_{app}) of sodium fluorescein across Calu-3 cell layers after exposure to the NP:mannitol 20:80 formulation (1.3 mg/ml NP in CCM) ranged between P_{app} = 0.76 x 10^{-7} and 1.08 x 10^{-7} cm/s (n = 3 experiments) when measured at 2, 24 and 48 h. These P_{app} were not significantly different ($p > 0.05$) to those measured in FBS-free CCM control at the same time points (P_{app} = 0.69-1.21 x 10^{-7} cm/s).

3.5. Cell association

The microsphere system is designed such that the mannitol from the microparticle dissolves upon contact with the aqueous lung fluid *in vivo*. Similarly, under *in vitro* conditions mannitol will dissolve in the epithelial lining fluid, releasing the chitosan NP in the presence of cultured cells, thereby permitting characterisation of any NP-cell interactions. For these studies, the chitosan NP were loaded with a fluorescent protein (FITC-BSA) to enable tracking of the NP movements. CLSM images were obtained after application of the aerosolised dry powder or the dissolved microspheres (i.e., NP suspension) to either Calu-3 or A549 cells for 2 h (Figure 5). No NP uptake by the cells was observed in either cell line after administration as an aerosol or a suspension. However, rigorous washing of the cell layer failed to remove the NP from the surface of both cell lines indicating particle adhesion to the cell membrane. In Calu-3 cells, this was also an indication that the NP penetrated the mucus layer covering the cell surface.

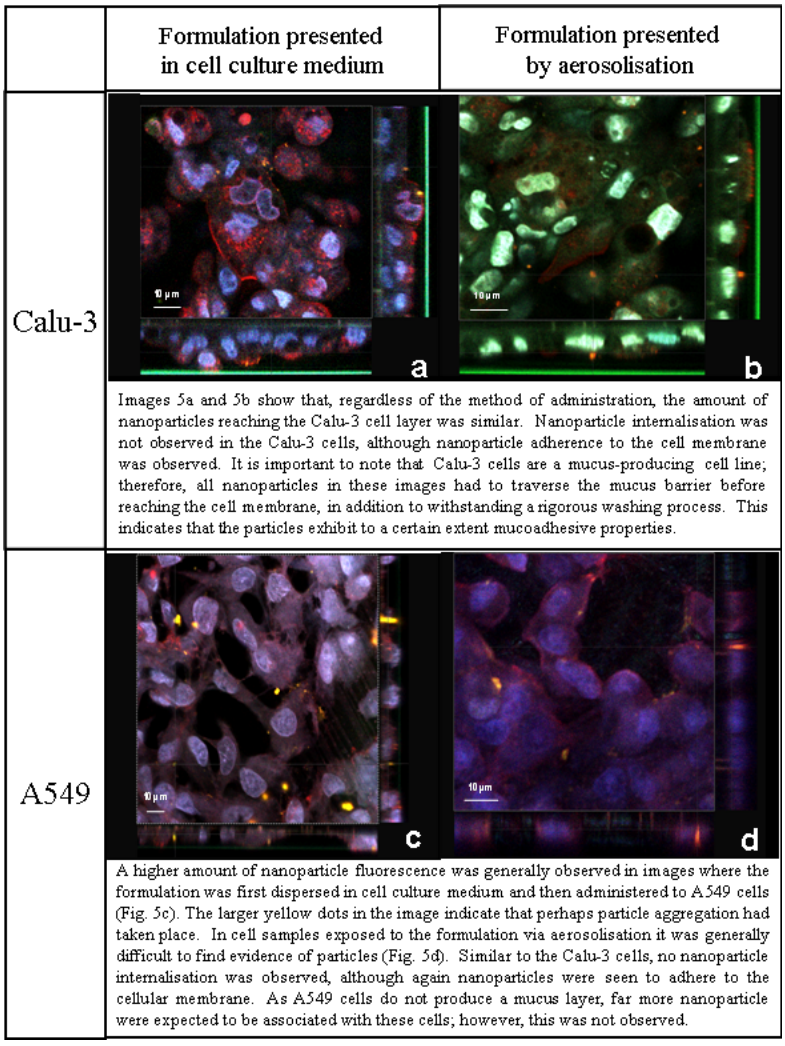

Fig. 5. Scanning electron confocal microscopy (CLSM) micrographs of the association of particles with cells after 2 h incubation with the nanoparticle:mannitol 20:80 administered by aerosolisation (b,d) or presented in cell culture medium (a,c). Each image provides a planar 'slice' through the cell surface, and the cross sectional view of the same section of the cell layer in the x-y and y-z orientation. The images were pseudo-coloured blue (DAPI – nucleus), green (FITC-BSA - nanoparticles) and red (WGA-Texas Red® - membrane). A yellow colour indicates colocalisation of the nanoparticles and the membrane. a) Calu-3 cells, dissolved dry powder, b) Calu-3 cells, aerosolised dry powder, c) A549 cells, dissolved dry powder, d) A549 cells, aerosolised dry powder.

4. Discussion

The formulation of NP as a respirable dry powder for drug delivery to the lung is a novel system designed for pulmonary protein administration [4]. Although NP formulations have great potential for drug delivery, the safety of inhaling NP is a concern. This study demonstrated that the CS/TPP NP-loaded mannitol microsphere formulation did not induce any overt toxicity in the airway or alveolar cell lines used. Under the conditions employed in the cell viability assays, only the highest NP dose of one of the respirable formulations reduced cell viability below 50% (Figures 2 and 3). No effect of the formulations on epithelial cell layer TER was observed. Such results provide the best *in vitro* evidence for an absence of irritancy of the formulations towards the respiratory epithelium.

Experiment dosimetry. The doses used in this study can be compared to concentrations likely to be obtained in the lung lining fluid (mg/mL) or dose per unit area of respiratory epithelial surface (mg/cm^2). The highest concentration in this study (1.3 mg/mL NP) approximates to the concentration that would result from a third of a 10 mg dose-to-the-lung depositing evenly in the small airways (generations 12-16) or a 15 mg dose-to-the-lung depositing evenly across the respiratory region of the lung (generations 17-23). The highest dose per unit area of epithelial surface used in the study (0.87 mg/cm^2), however, is up to 1000 times higher than that which would result in an even distribution of the NP across these lung regions *in vivo*. It can be argued that hotspots of formulation deposition and the release of the entire NP-payload of individual microspheres to juxtapositioned cell surfaces on dissolution could result in localised concentrations similar to those used in this study.

Influence of mannitol on cell viability. A greater reduction in cell viability (compared to untreated control) was produced by the highest mannitol concentration than that measured at the highest NP suspension concentration. Although mannitol is generally considered inert, mannitol inhalation has been investigated clinically as a means of producing pulmonary hyperosmolarity to

enhance respiratory clearance and as a challenge for asthmatics. *In vitro*, mannitol induced hyperosmolarity has been reported to increase respiratory cell layer permeability [23,30], which may have sensitised the cells to NP at the highest formulation concentrations in the current study. Interestingly, mannitol is also sometimes used as an antioxidant *in vitro* and has been observed to exhibit a protective effect against ultrafine particle toxicity [14]. At the highest NP concentration used in this study, there was a tendency for greater reduction in cell viability after incubation with the microsphere formulations than with the NP suspension or mannitol controls. Opposing effects of mannitol in producing osmotic stress but also counteracting NP-induced oxidant stress may account for the differences measured in cell viability at the highest formulation dose since mannitol concentration varies according to the level of NP loading in each formulation.

Influence of chitosan on cell viability. The safety of chitosan in pulmonary drug delivery systems has been investigated previously. Huang and co-workers reported that chitosan delivered as microparticles induced proinflammatory responses in rat lungs [31], indicating the need for a stringent characterisation of the toxicity profile of this polymer. Chitosan in solution, however, has been reported to exhibit low toxicity in respiratory cell lines [32-38]. Direct comparisons between these studies are difficult because of the different assay conditions employed, in particular different degrees of deacetylation, molecular weight and salt form of chitosan. The sensitivity of cells is also likely to vary between different cell lines and under different culture and assay conditions. It is not clear at present whether there is a molecular explanation for the contradictory findings regarding the irritancy of chitosan to the lung cells.

Chitosan solution at a concentration of 15 mg/mL reduced Calu-3 cells viability to approximately 70% [34]. The chitosan used was similar to the chitosan used in the present study (93% deacetylation degree), although its viscosity was lower (40 mPa compared to 95 mPa) and the molecular weight was polydisperse, 100 and 500 kDa. In another study, chitosan produced no adverse effects on 16HBE14o$^-$ cells compared with untreated cells [32]. The cytotoxicity of

chitosans with different molecular weights and extents of deacetylation has been assayed after presentation in solution and as NP using A549 cells. NP containing a similar chitosan to the one used in the present study (213 KDa and 88% deacetylation), which were prepared by the same ionic gelation method, were reported to induce a reduction in cell viability of approximately 70% at a concentration of ~1 mg/mL [33]. This compares with much less effect obtained in our study in which the control NP induced < 50% reduction in Calu-3 or A549 cell viability.

Cell layer permeability. The TER of the Calu-3 cells was not altered in cell layers exposed to the NP:mannitol 20:80 formulation 1.3 mg/mL NP for 48 h (the same period of time used in the MTT test). Although TER provides an indication of cell layer permeability based on ionic flux, such electrical monitoring should be confirmed by direct measurement of solute transport. Equivalent sodium fluorescein transport was measured in treated and untreated Calu-3 cells and confirmed the absence of any change in epithelial cell layer permeability. Chitosan has been shown to decrease TER and act as an absorption enhancer in cell lines representative of mucosae such as buccal TR146, bronchial Calu-3 and 16HBE14o$^-$ and intestinal Caco-2 [32,34,35,37,39]. However, in most studies evaluating the effect of chitosan on the TER value and solute transport, chitosan was applied to the cells as a solution.

Chitosan particles (microparticles or NP) have been evaluated in cell cultures on a limited number of occasions. BSA-loaded chitosan microparticles (200 µg) were administered to a layer of Calu-3 cells and transport of BSA was shown to increase by 12% compared to the control (absence of chitosan) [40]. The total amount of microparticles applied corresponded to 134 µg of chitosan, since the BSA content was reported to be 33%. The highest NP concentration administered to cells in our study contained 1.3 mg/mL NP in 150 µl suspension, which is equal to 150 µg chitosan, and no change in the permeability of the Calu-3 cell layers was detected. In a further study, a decrease in TER of 50-60% was reported in 16HBE14o$^-$ cells upon incubation with chitosan solution (10 mg/mL) and microparticles (2-3 mg), indicating that both formulations were potent

absorption enhancers under the study conditions [32]. These results were obtained using chitosan of the same molecular weight as that used in this study, but a different salt form (glutamate) and the concentration of the chitosan administered to the cells was approximately ten times greater in the earlier study [32]. Another study using chitosan NP showed results similar to those reported here. In this case, incubation of Caco-2 cells with chitosan NP did not cause significant changes in the tight junction permeability (TER) [36].

Particle interaction with cells. The confocal images of the Calu-3 and A549 cells provide no evidence of NP uptake; however, BSA-loaded NP were observed to be in close contact with the cell membrane, suggesting the occurrence of cell adhesion (Figure 5). NP were visible at the cell surface membrane even after the rinsing procedures were employed and, in the case of the Calu-3 cells, after mucus removal, indicating that the mucoadhesive interactions between the NP and cell membrane were strong. The bioadhesive property of chitosan has been reported previously [7,40-42], and appears to operate in the NP formulation. If this is representative of effects *in vivo* after pulmonary deposition of the microspheres, release of a therapeutic payload from the NP within the lung might be attainable.

5. Conclusions

The formulations exhibited a low cytotoxicity in cell lines of human origin from airway and alveolar regions of the pulmonary tract. *In vitro* cell-based assays are generally more sensitive to toxicological insult than *in vivo* experiments. In this context, the absence of overt toxicity of these formulations *in vitro* is an encouraging indicator of the safety of these dry powders as lung delivery systems.

Acknowledgements

This work was financed by the Drug Delivery Research Group, King's College London and the Spanish Government (CICYT, SAF2002-03314, Feder

Cofinanced). The Predoctoral fellowship to Ana Grenha from Fundação para a Ciência e Tecnologia, Portugal (SFRH/BD/13119/2003) is highly appreciated.

References

1. Edwards DA, Ben-Jebria A, Langer R. Recent advances in pulmonary drug delivery using large, porous inhaled particles. J Appl Physiol 1998;84:379-385.

2. Taylor G, Kellaway I. Pulmonary drug delivery. In: Hillery A, Lloyd A, Swarbrick J, editors. Drug delivery and targeting. For pharmacists and pharmaceutical scientists. New York: Taylor & Francis, 2001. p. 269-300.

3. Courrier HM, Butz N, Vandamme TF. Pulmonary drug delivery systems: recent developments and prospects. Crit Rev Ther Drug Carr Syst 2002;19:425-498.

4. Grenha A, Seijo B, Remuñan-Lopez C. Microencapsulated chitosan nanoparticles for lung protein delivery. Eur J Pharm Sci 2005;25:427-437.

5. Hirano S, Seino H, Akiyama Y, Nonaka I. Biocompatibility of chitosan by oral and intravenous administrations. Polym Mater Sci Eng 1988;59:897-901.

6. Dornish M, Hagen A, Hansson E, Peucheur E, Vedier F, Skaugrud O. Safety of Protasan™: Ultrapure chitosan salts for biomedical and pharmaceutical use. In: Domard A, Roberts GAF, Varum KM, editors. Advances in chitin science. Lyon: Jacques Andre publisher, 1997. p. 664-670.

7. Lehr CM, Bouwstra JA, Schacht EH, Junginger HE. In vitro evaluation of mucoadhesive properties of chitosan and some other natural polymers. Int J Pharm 1992;78:43-48.

8. Calvo P, Remuñan-Lopez C, Vila-Jato JL, Alonso MJ. Novel hydrophilic Chitosan-Polyethylene Oxide nanoparticles as protein carriers. J App Polym Sci 1997;63:125-132.

9. Fernández-Urrusuno R, Calvo P, Remuñan-Lopez C, Vila-Jato JL, Alonso MJ. Enhancement of nasal absorption of insulin using chitosan nanoparticles. Pharm Res 1999;16:1576-1581.

10. Foster KA, Yazdanian M, Audus KL. Microparticulate uptake mechanisms of in vitro cell culture models of the respiratory epithelium. J Pharm Pharmacol 2001;53:57-66.

11. Mo Y, Lim L-Y. Mechanistic study of the uptake of wheat germ aglutinin-conjugated PLGA nanoparticles by A549 cells. J Pharm Sci 2004;93:20-28.

12. Bivas-Benita M, Romrijn S, Junginger HE, Borchard G. PLGA-PEI nanoparticles for gene delivery to pulmonary epithelium. Eur J Pharm Biopharm 2004;28:1-6.

13. Amidi M, Romeijn SG, Borchard G, Junginger HE, Hennink WE, Jiskoot W. Preparation and characterisation of protein loaded N-trimethyl chitosan nanoparticles as nasal delivery system. J Control Rel 2006;111:107-116.

14. Stone V, Shaw J, Brown DM, MacNee W, Faux SP, Donaldson K. The role of oxidative stress in the prolonged inhibitory effect of ultrafine carbon black on epithelial cell function. Toxicol In Vitro 1998;12:649-659.

15. Geys J, Coenegrachts L, Vercammen J, Engelborghs Y, Nemmar A, Nemery B, Hoet PHM. In vitro study of the pulmonary translocation of nanoparticles. A preliminary study. Toxicol Lett 2006;160:218-226.

16. Stearns RC, Paulauskis JD, Godaleski JJ. Endocytosis of ultrafines by A549 cells. Am J Respir Cell Mol Biol 2001;24:108-115.

17. Seagrave J, Nikula KJ. Multiple modes of responses to air pollution particulate materials in A549 alveolar type II cells. Inhal Toxicol 2000;12:247-260.

18. Winton HL, Wan H, Cannell MB, Gruenert DC, Thompson PJ, Garrod DR, Stewart GA, Robinson C. Cell lines of pulmonary and non-pulmonary origin as tools to study the effects of house dust mite proteinases on the regulation of epithelial permeability. Clin Exp Allergy 1998;28:1273-1285.

19. Grainger CI, Greenwell LL, Lockley DJ, Martin GP, Forbes B. Culture of Calu-3 cells at the air-liquid interface provides a representative model of the airway epithelial barrier. Pharm Res 2006;23:1482-1490.

20. Matter K, Balda MS. Functional analysis of tight junctions. Methods 2003;30:228-234.

21. Forbes B, Ehrhardt C. Human respiratory epithelial cell culture for drug delivery applications. Eur J Pharm Sci 2005;60:193-205.

22. Westmoreland C, Walker T, Matthews J, Murdock J. Preliminary investigations into the use of a human bronchial cell line (16HBE14o-) to screen for respiratory toxins in vitro. Toxicol In Vitro 1999;13:761-764.

23. Forbes B, Martin GP, Lansley AB. Formulation of inhaled medicines: effect of delivery vehicle on 16HBE14o- bronchial epithelial cells. J Aerosol Med 2000;13:281-288.

24. Fiegel J, Ehrhardt C, Schaefer UF, Lehr C-M, Hanes J. Large porous particle impingement on lung epithelial cell monolayers – toward improved particle characterisation in the lung. Pharm Res 2003;20:788-796.

25. Cooney D, Kazantseva M, Hickey AJ. Development of a size-dependent aerosol deposition model utilising human airway epithelial cells for evaluating aerosol drug delivery. ATLA Altern Lab Anim 2004;32:581-590.

26. Brzoska M, Langer K, Coester C, Loitsch S, Wagner TOF, Mallinckrodt C. Incorporation of biodegradable nanoparticles into human airway epithelium cells - in vitro study of the suitability as a vehicle for drug or gene delivery in pulmonary diseases. Biochem Biophys Res Commun 2004;318:562-570.

27. El-Gibaly I. Development and *in vitro* evaluation of novel floating chitosan microcapsules for oral use: comparison with non-floating chitosan microspheres. Int J Pharm 2002;294:7-21.

28. Tee SK, Forbes B, Larhrib H, Marriott C, Martin GP. Development of an in vitro dissolution-absorption model to evaluate the delivery of aerosolised drug from dry powder inhaler formulations. Drug Deliv Lung 2001;12:115-118.

29. Grenha A, Carrión-Recio D, Seijo B, Vila-Jato JL, Remuñán-López C. Microencapsulated chitosan nanoparticles for insulin lung delivery. Proc 32nd Ann Meeting Control Rel Soc 2005;59.

30. Forbes B, Montoro-Garcia AM, Lansley AB. [14C]-mannitol fluxes across human bronchial epithelial cells following apical exposure to EDTA, lactose, altered pH and anisotonicity. Pharm Res 1997;14:S138.

31. Huang YC, Vieira A, Huang KL, Yeh MK, Chiang CH. Pulmonary inflammation caused by chitosan microparticles. J Biomed Mater Res 2005;75A:283-287.

32. Lim ST, Forbes B, Martin GP, Brown MB. In vivo and in vitro characterization of novel microparticulates based on hyaluronan and chitosan hydroglutamate. AAPS PharmsciTech 2001;2:1-14.

33. Huang M, Khor E, Lim L-Y. Uptake and cytotoxicity of chitosan molecules and nanoparticles: effects of molecular weight and degree of deacetylation. Pharm Res 2004;21:344-353.

34. Florea BI, Thanou M, Junginger HE, Borchard G. Enhancement of bronchial octreotide absorption by chitosan and *N*-trimethylchitosan shows linear in vitro/in vivo correlation. J Control Rel 2005;110:353-361.

35. Portero A, Remuñan-Lopez C, Nielsen HM. The potential of chitosan in enhancing peptide and protein absorption across the TR146 cell culture model - an *in vitro* model of the buccal epithelium. Pharm Res 2002;19:169-174.

36. Behrens I, Vila-Pena AI, Alonso MJ, Kissel T. Comparative uptake studies of bioadhesive and non-bioadhesive nanoparticles in human intestinal cell lines and rats: the effect of mucus on particle adsorption and transport. Pharm Res 2002;19:1185-1193.

37. Smith J, Wood E, Dornish M. Effect of chitosan on epithelial cell tight junctions. Pharm Res 2004;21:43-49.

38. de Campos AM, Diebold Y, Carvalho ELS, Sánchez A, Alonso MJ. Chitosan nanoparticles as new ocular drug delivery systems: *in vitro* stability, *in vivo* fate, and cellular toxicity. Pharm Res 2004;21:803-810.

39. Ranaldi G, Marigliano I, Vespignani I, Perozzi G, Sambuy Y. The effect of chitosan and other polycations on tight junction permeability in the human intestinal Caco-2 cell line. J Nutr Biochem 2002;13:157-167.

40. Witschi C, Mrsny R. *In vitro* evaluation of microparticles and polymer gels for use as nasal platforms for protein delivery. Pharm Res 1999;16:382-390.

41. Takeuchi H, Yamamoto H, Kawashima Y. Mucoadhesive nanoparticulate systems for peptide drug delivery. Adv Drug Deliv Rev 2001;47:39-54.

42. Yamamoto H, Kuno Y, Sugimoto S, Takeuchi H, Kawashima Y. Surface-modified PLGA nanosphere with chitosan improved pulmonary delivery of calcitonin by mucoadhesion and opening of the intercellular tight junctions. J Control Rel 2005;102:373-381.

Sección IV. Evaluación preliminar *in vivo* de las microsferas de manitol conteniendo nanopartículas de quitosano en ratas

En esta sección se describen los estudios *in vivo* preliminares realizados con las microsferas de manitol conteniendo nanopartículas de quitosano cargadas con insulina e isotiocianato de fluoresceína (FITC-BSA), que fueron administradas por vía intratraqueal a ratas previamente anestesiadas. De la revisión bibliográfica realizada previamente relativa a la administración pulmonar de polvos secos a animales, se deduce que la administración intratraqueal es el procedimiento más adecuado, por minimizar las pérdidas de dosis. En consecuencia, nosotros hemos seleccionado esta técnica de administración tanto para la investigación de la distribución *in vivo* de las microsferas conteniendo FITC-BSA asociada a las nanopartículas, como para la evaluación del efecto hipoglucémico tras la administración de las microsferas conteniendo nanopartículas cargadas con insulina. Para observar la distribución en el pulmón de las microsferas conteniendo nanopartículas marcadas con FITC-BSA, se ha seleccionado la técnica de microscopía láser confocal. El tejido pulmonar se ha marcado siguiendo una técnica previamente descrita en la literatura por *Lombry y col.*, utilizando una sal sódica de sulforodamina B, que es un marcador fluorescente anfótero relativamente lipofílico que no tiene carga a pH fisiológico. Esta molécula tiene un coeficiente de reparto elevado (octanol/buffer = 276) y, por lo tanto, es esperable que se distribuya en las regiones más lipofílicas del tejido (los cuerpos lamelares de los pneumocitos tipo II y las capas lipídicas de las membranas celulares) (Pohl y col., 1998; Lombry y col., 2002).

En el caso de la evaluación del efecto hipoglucémico, la disminución de los niveles de glucosa se consideró un indicador adecuado de la eficacia de las formulaciones. Estudios previos realizados por nuestro grupo de investigación, en los que se administraron microsferas a ratas, nos permitieron concluir que la evaluación del efecto hipoglucémico de las formulaciones ensayadas en animales que no tenían libre acceso a la comida durante la realización del estudio, era más precisa si los animales no estaban sometidos también a ayuno la noche anterior al ensayo.

Si bien se conoce su efecto hipoglucémico, la anestesia fue necesaria para realizar la administración intratraqueal. En cualquier caso, al realizar tanto la administración de las microsferas como de la solución control en las mismas

condiciones, las eventuales interferencias que se puedan atribuir a la anestesia quedan equilibradas.

OBJETIVO

El objetivo de este estudio fue investigar *in vivo* el potencial de las microsferas de manitol conteniendo nanopartículas de quitosano como vehículos para la administración pulmonar de macromoléculas terapéuticas con fines sistémicos. Para ello, se determinó cualitativamente la distribución de las microsferas conteniendo nanopartículas cargadas con FITC-BSA en el pulmón, y se evaluó el efecto hipoglucémico inducido por las microsferas de manitol conteniendo nanopartículas de quitosano cargadas con insulina, tras su administración intratraqueal a ratas normales anestesiadas.

En ambos estudios se utilizó como control una disolución de la macromolécula encapsulada (FITC-BSA y insulina). Además, en el ensayo de distribución se utilizaron microsferas de manitol conteniendo la proteína fluorescente, FITC-BSA.

PARTE EXPERIMENTAL

Administración intratraqueal de las microsferas y de las disoluciones control

Como animales de experimentación se utilizaron ratas normales *Sprague-Dawley* macho, con 10-11 semanas de edad y con pesos comprendidos entre 250 y 300 g. Los animales tuvieron libre acceso a agua y comida hasta el inicio del experimento y únicamente al agua durante la realización del mismo. Las ratas fueron anestesiadas mediante una inyección intraperitoneal de pentobarbital (53 mg/kg) y fueron colocadas en una tabla quirúrgica con la parte ventral hacia arriba. A continuación, se realizó una incisión longitudinal en la parte ventral del cuello, dejando expuesta la tráquea (**Figura 1**). Disoluciones control de PBS pH 7.4 (90 µl), de insulina en PBS (90 µl, 17.9 U/kg; estudio del efecto hipoglucémico) y de FITC-BSA en PBS (90 µl; 450 µg/kg; estudio de distribución), fueron instiladas con una jeringa a través de una cánula metálica i.v. [*Johnson &*

Johnson MEDICAL, España] previamente insertada entre dos anillos cartilaginosos de la traquea (**Figura 1**).

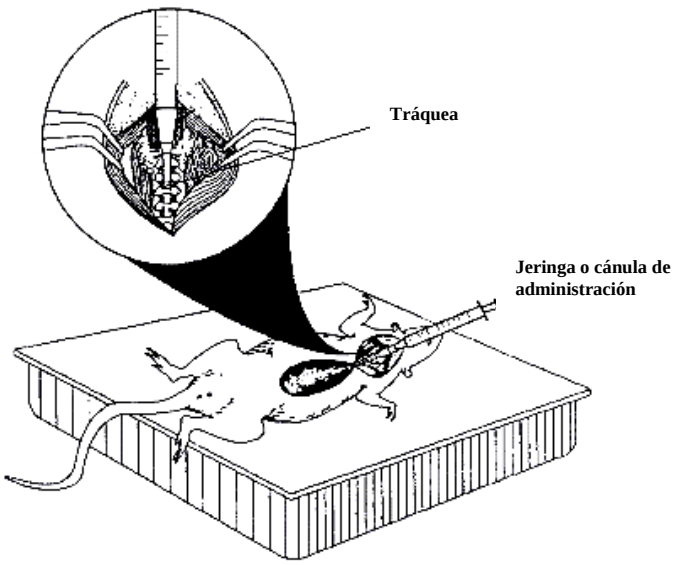

Figura 1. Esquema del método de administración intratraqueal a ratas, de las disoluciones control y microsferas.

La administración de las microsferas (diámetro aerodinámico = 2.7 µm) para el estudio de distribución (microsferas control: manitol/FITC-BSA, FITC-BSA = 450 µg/kg; microsferas conteniendo nanopartículas cargadas con FITC-BSA: manitol/nanopartículas = 80/20, FITC-BSA = 450 µg/kg) y para la determinación del efecto hipoglucémico (microsferas conteniendo nanopartículas cargadas con insulina: manitol/nanopartículas = 80/20; insulina = 16.7 U/kg), fue realizada a través de una cánula traqueal [adaptador en Y, apertura de 1.3 mm, *Harvard Apparatus*] (**Figura 2**).

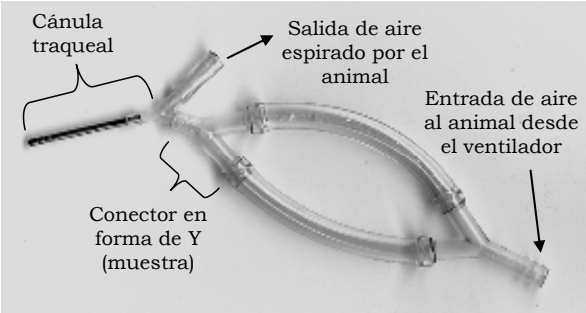

Figura 2. Esquema del dispositivo utilizado para la administración intratraqueal a ratas de las microsferas (los sitios de entrada y salida de aire en el dispositivo se conectaron al ventilador utilizando tubos de Tygon®).

Para ello, se utilizó la punta de una aguja para perforar ligeramente la traquea, lo que facilitó la inserción de la cánula. Esta fue, posteriormente, conectada a un ventilador Harvard® [*Inspira ASV 55-7058, USA, 80 respiraciones/minuto, volumen de respiración = 1.53 cm³, Harvard Apparatus*] (**Figura 3**); equipo que simula el modo fisiológico de respiración del animal.

Figura 3. Ventilador Harvard Apparatus® Inspira ASV, utilizado para la administración intratraqueal a ratas de las microsferas.

Tras la administración de las formulaciones (disoluciones o microsferas), la cánula fue retirada y la tráquea y el cuello de las ratas fue suturado con una sutura quirúrgica [*Johnson & Johnson MEDICAL*, España]. Finalmente, las ratas se recuperan de la anestesia en 1 o 2 horas. Estos estudios fueron realizados de acuerdo con los *Principios de Cuidado de Animales de Laboratorio* (Comisión de Bioética de la Universidad de Santiago de Compostela).

Evaluación de la distribución de las microsferas de manitol conteniendo nanopartículas cargadas con FITC-BSA

A intervalos de tiempo predeterminados (1 hora y 2 horas) tras la administración intratraqueal de las microsferas y de las disoluciones, las ratas fueron sacrificadas por administración de una dosis letal de pentobarbital y sus cavidades torácicas expuestas. A continuación, se introdujo un microperfusor por la parte superior del músculo cardiaco, hasta el interior del tronco inicial de la arteria pulmonar. Entonces, se perfundió una disolución de sulforodamina (100 mL de solución 0.1% de sulforodamina en PBS pH 7.4) utilizando una bomba peristáltica [*Spetec GmbH, Perimax 12, Alemania*] a una velocidad de 20 mL/min. La aurícula derecha fue seccionada para permitir la circulación de la disolución a través del sistema vascular. Inmediatamente después, se fijó el tejido pulmonar utilizando una disolución fijadora (50 mL de 0.6% formaldeído/0.9% glutaraldeído en tampón cacodilato pH 7.4 conteniendo 0.1% sulforodamina) a una velocidad de flujo de 15 mL/min. Los pulmones fueron extraídos, realizándose cortes de aproximadamente 2 mm en el lóbulo superior del pulmón derecho para su observación por microscopía láser confocal [*Leica TCS-SP2, Alemania*], siendo esta zona del pulmón aquella en la que se verifica mayor depósito de las formulaciones, de acuerdo con los resultados de un estudio realizado anteriormente. Los cortes fueron colocados sobre los porta-sustancias escavados y, a continuación, recubiertos con cubre-sustancias. Las longitudes de onda de excitación utilizadas para analizar el tejido pulmonar fueron 488 y 568 nm, para la FITC-BSA y la sulforodamina, respectivamente, recogiéndose las emisiones fluorescentes de la FITC-BSA (λ de emisión = 515 - 545 nm) y de la sulforodamina (λ de emisión =

564 – 648 nm) a través de canales diferentes. Las imágenes en escala de gris fueron obtenidas con lentes de inmersión en aceite de 63× y 100×, y fueron pseudo-coloreadas de verde para la FITC-BSA y de rojo para la sulforodamina, siendo posteriormente sobrepuestas para formar una imagen multicolor.

Evaluación del efecto hipoglucémico de las microsferas conteniendo nanopartículas de quitosano cargadas con insulina

Para la evaluación de los niveles séricos de glucosa tras la administración de las microsferas a ensayar y las disoluciones utilizadas como control, se recogieron muestras de sangre (150-200 µl) de la vena de la cola de las diferentes ratas a tiempos 0, 30, 60, 90, 120, 180, 240, 300, 360 y 480 minutos. A continuación, las muestras fueron centrifugadas a 3500 rpm durante 5 minutos y los niveles séricos de glucosa cuantificados por el método enzimático-colorimétrico de la Glucosa-Oxidasa [*GOD-PAP, SPINREACT*] ($n \geq 3$).

RESULTADOS Y DISCUSIÓN

Con el objetivo de observar cualitativamente la distribución de las microsferas en el pulmón, se administraron a ratas microsferas de manitol conteniendo nanopartículas cargadas con FITC-BSA, que fueron preparadas como se indica en la sección de metodología del **Art. 3**. Tal y como referido en ese artículo, la FITC-BSA no se libera de las nanopartículas al menos durante 8 días, posiblemente debido a su elevado tamaño, que no le permite difundirse a través de la matriz de quitosano de las nanopartículas.

Al cabo de una o dos horas, los animales fueron sacrificados y muestras de sus pulmones observados por microscopia confocal, siguiendo el protocolo que se ha descrito anteriormente en esta sección. Como controles se utilizaron microsferas de manitol con FITC-BSA y una disolución acuosa de FITC-BSA. Observando las imágenes de la **Figura 4**, que corresponden a cortes del pulmón, se puede detectar la presencia de señal fluorescente en los alvéolos, tanto en el caso de los controles citados anteriormente, como en el caso de las microsferas

conteniendo nanopartículas cargadas con FITC-BSA. Por lo tanto, podemos confirmar que las nanopartículas de quitosano cuando se administran microencapsuladas en microsferas de manitol mediante aerosolización son capaces de alcanzar la región alveolar, donde se sabe que tiene lugar la mayor absorción de fármacos.

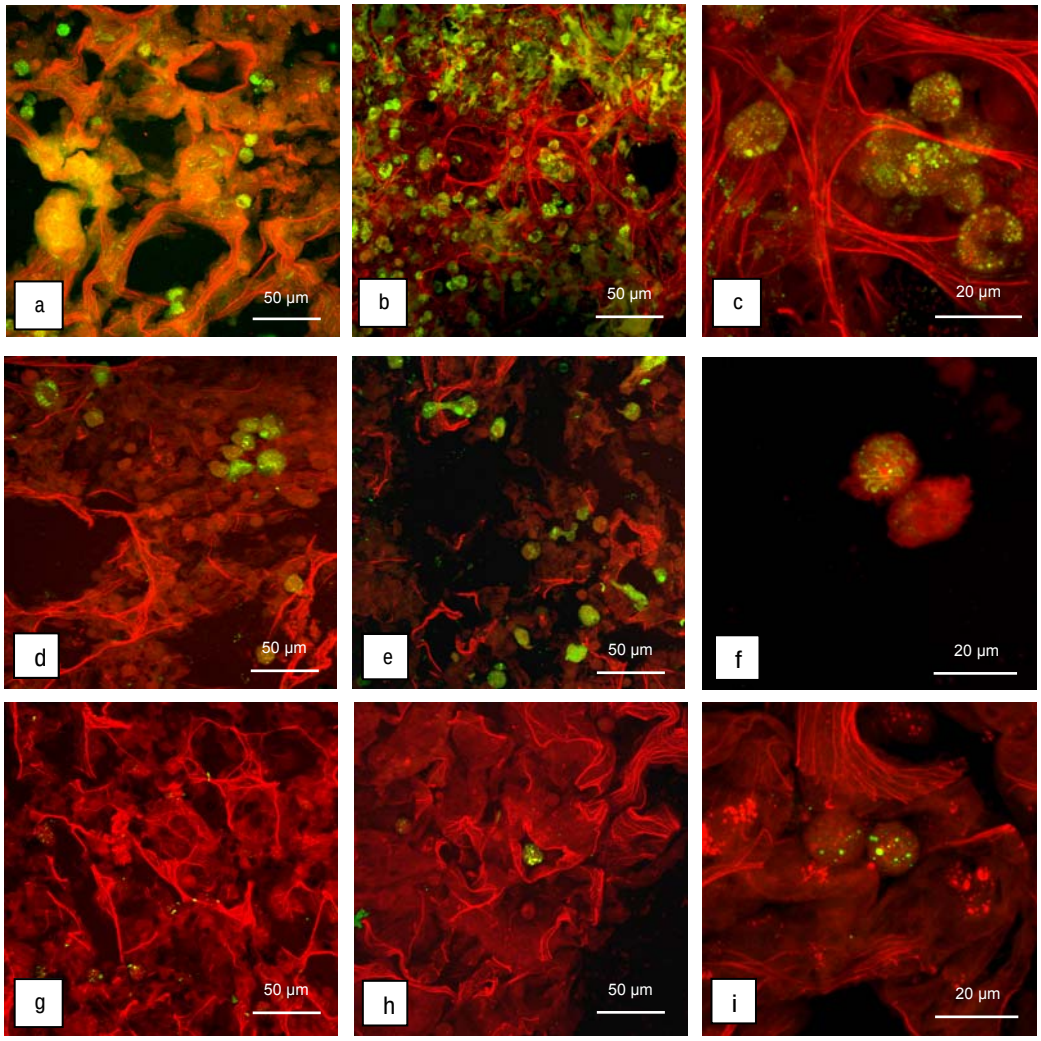

Figura 4. Imágenes de microscopía confocal de los alvéolos (**a**) 1h y (**b, c**) 2h tras instilación intratraqueal de una disolución de FITC-BSA (90 µl; 450 µg/kg); (**d, e, f**) 1h tras administración intratraqueal de microsferas de manitol/FITC-BSA; (**g**) 1h y (**h, i**) 2h tras administración intratraqueal de microsferas de manitol conteniendo nanopartículas de quitosano cargadas con FITC-BSA (450 µg/kg).

En las imágenes correspondientes a la administración de la disolución de FITC-BSA, se puede apreciar que al cabo de una y dos horas, la proteína se ha acumulado en parte de forma homogénea sobre el epitelio, mientras que otra porción ha sido capturada por los macrófagos (Fig. 5a-c). Estos resultados son coincidentes con los encontrados por *Lombry y col.* tras la instilación intratraqueal de una disolución de FITC-BSA (Lombry y col., 2002). La presencia de FITC-BSA en el epitelio incluso al cabo de dos horas se puede justificar por el elevado tamaño de esta proteína (aproximadamente 7 nm) (Patton, 1996). En este sentido, un estudio realizado por *Berg y col.* ha demostrado que el epitelio alveolar de las ratas presenta dos poblaciones de poros: unos de 0.5 nm, que ocupan más del 98% de la superficie de poros, y otros de 3.4 nm, que ocupan aproximadamente el 2% de la superficie total (Berg y col., 1989), lo que justificaría la dificultad con la que se encuentra la proteína para difundir a través del epitelio hacía la circulación sistémica.

Las microsferas de manitol/FITC-BSA control (Fig. 5d-f) dan lugar a la visualización de depósitos fluorescentes en la zona alveolar, presentando una tendencia a acumularse en el interior de los macrófagos. Finalmente, la administración de microsferas de manitol conteniendo nanopartículas cargadas de FITC-BSA, según el protocolo anteriormente descrito, hizo posible que las partículas alcanzaran los alvéolos, una meta esencial para el cumplimiento de los objetivos previstos. Aparentemente, las partículas presentan una tendencia a acumularse en el interior de los macrófagos (Fig. 5g-i). Es sabido que son varias las características físico-químicas de las partículas (tamaño, carga superficial, concentración, carácter hidrofílico, composición) que influyen en la captura macrofágica (Kubota y col., 1983; Tabata y Ikada, 1988; Ahsan y col., 2002; Makino y col., 2003). En el primero trabajo que recoge resultados de la investigación realizada en esta tesis doctoral (**Art. 2**), se ha demostrado que las nanopartículas podrían recuperarse a partir de las microsferas tras su incubación en un medio acuoso, sin que se produzcan alteraciones significativas en su tamaño y potencial zeta (Grenha y col., 2005). No obstante, cabe esperar que la liberación de las nanopartículas a partir de las microsferas sea más lenta en las condiciones encontradas *in vivo*, debido al reducido volumen de fluido existente en los alvéolos. Basándonos en ello, se podría admitir la captura macrofágica de algunas

microsferas durante el tiempo que permanecieran inalteradas en la superficie alveolar, antes de que ocurra una disolución completa del manitol y, a consecuencia, la liberación total de las nanopartículas. Por otro lado, teniendo en cuenta que al disolverse el manitol, se liberan las nanopartículas, y considerando que la FITC-BSA no se libera a partir de estas al menos durante 8 días, tal y como se ha comentado en otro apartado de esta memoria (página 131), las nanopartículas son muy posiblemente las estructuras que se visualizan en el interior de los macrófagos tras la administración.

La eficacia de las microsferas conteniendo nanopartículas cargadas con insulina, que fueron preparadas siguiendo el procedimiento descrito en el Artículo 2, fue evaluada por cuantificación de las concentraciones plasmáticas de glucosa a distintos tiempos tras su administración intratraqueal a ratas normales anestesiadas y comparando los perfiles de glucosa plasmática obtenidos a partir de las mismas, con los correspondientes a la administración de una disolución control de insulina en PBS pH 7.4 y de una disolución de PBS pH 7.4.

La dosis de fármaco que alcanza el trato respiratorio puede verse muy reducida por la retención producida en el equipo empleado para su administración. Para cuantificar dicha retención, y así evitar diferencias en la dosis administrada, con anterioridad a la realización del estudio *in vivo*, se determinó el porcentaje de retención pesando directamente el polvo en el conector en forma de "Y" con la cánula unida, que después se conecta al ventilador para la administración. La diferencia de peso del conector "Y" y de la cánula antes y después de una insuflación (sin conexión al animal) nos permitió calcular el porcentaje de retención (n = 6), lo cual se tuvo en consideración para ajustar la dosis.

La curva de niveles de glucosa obtenida tras la administración de las disoluciones control y de las microsferas conteniendo nanopartículas de quitosano (n ≥ 3) se muestra en la **Figura 5**. Como se puede deducir a partir de estos resultados, a pesar de que la disolución control de insulina se ha administrado en una dosis un poco superior (17.9 U/kg) a la de las microsferas

(16.7 U/kg), éstas últimas dieron lugar a un efecto hipoglucémico significativamente más acentuado durante la primera hora ($P < 0.05$) que la disolución. De hecho, ésta produjo un descenso de los niveles de glucosa de aproximadamente 60% a los 60 minutos, mientras las microsferas conllevaron a una disminución de aproximadamente 90% en el mismo período de tiempo.

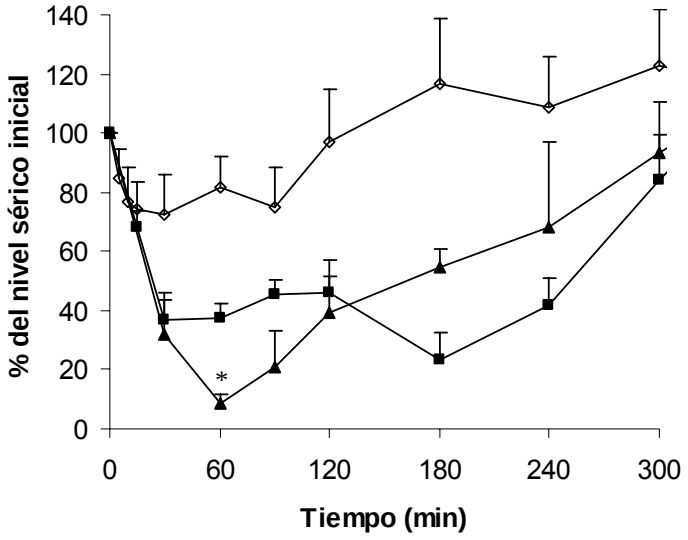

Figura 5. Efecto hipoglucémico tras administración intratraqueal de (◊) una disolución de PBS pH 7.4; (■) una disolución control de insulina (dosis = 17.9 U/kg) en PBS pH 7.4; y (▲) microsferas conteniendo insulina (manitol/nanopartículas=80/20; dosis = 16.7 U/kg) (n≥3). * Diferencias significativas ($P < 0.05$).

A pesar de que estos estudios fueron realizados utilizando un numero reducido de animales, por lo que deben ser tomados con precaución, creemos que son indicativos del potencial de las microsferas de manitol como transportadores eficaces de las nanopartículas de quitosano y, en definitiva, de la proteína encapsulada, hacía la región alveolar, donde la proteína será liberada y absorbida de manera eficaz. El mayor efecto hipoglucémico proporcionado por las microsferas puede ser el reflejo de un efecto promotor de la absorción debido a las nanopartículas de quitosano, como se ha demostrado previamente tras la administración nasal y ocular de una suspensión de nanopartículas similares (Fernández-Urrusuno y col., 1999; De Campos y col., 2001).

Tras alcanzar la concentración mínima de glucosa, se produce una recuperación más rápida de los niveles de glucosa tras administración de las microsferas, que tras la administración de la disolución de insulina. A pesar de que hemos comprobado en ensayos *in vitro* que las nanopartículas se recuperan rápidamente a partir de las microsferas tras su contacto con un medio acuoso, hay que tener en cuenta que el volumen de fluido existente en el pulmón es relativamente reducido, por lo que parece improbable que se produzca una inmersión total e inmediata de las microsferas (Ehrhardt y col., 2002). En otras palabras, la disolución del manitol que forma la estructura de las microsferas podría verse retardada *in vivo*, no permitiendo una liberación inmediata de las nanopartículas y de la insulina, condición esencial para mantener bajos los niveles de glucosa. Además, al disolverse lentamente el manitol, las microsferas podrían mantenerse inalteradas en la superficie alveolar durante algún tiempo, lo que podría permitir su captura por los macrófagos alveolares. Como ya se ha comentado anteriormente, según estudios realizados por otros autores, la fagocitosis depende de algunos parámetros como el tamaño, potencial zeta, propiedades superficiales, concentración de partículas y tiempo de incubación, entre otros (Kubota y col., 1983; Tabata y Ikada, 1988; Rudt y Müller, 1992; Makino y col., 2003). Si consideramos el factor tamaño, la actividad fagocítica es mayor para partículas con tamaño entre 1 e 2 µm, disminuyendo para aquellas con tamaño fuera de ese rango. Así, considerando que las partículas que hemos administrado tienen un tamaño de aproximadamente 3 µm, muy próximo al intervalo considerado de máxima probabilidad de captura, se puede pensar que la recuperación de los valores de glucosa puede además deberse a la captura por los macrófagos, que reduce de esta forma la liberación y absorción de insulina después de la primera hora. La insulina en forma de soluto (cuando se administra en disolución), no puede ser fácilmente captada por los macrófagos, pero también se absorberá menos ya que no se cuenta, en este caso, con la presencia del quitosano, que puede ejercer un efecto promotor de la absorción por abertura de las uniones íntimas que forma el epitelio pulmonar, como ya se ha comentado previamente.

CONCLUSIONES

Los resultados de estos estudios nos permiten considerar que las microsferas de manitol preparadas por la técnica de atomización, son vehículos adecuados para administración pulmonar de nanopartículas de quitosano que actúan como transportadores de péptidos y proteínas.

Referencias bibliográficas

Ahsan, F., Rivas, I.P., Khan, M.A., Suárez-Torres, A.I., 2002. Targeting to macrophages: role of physicochemical properties of particulate carriers - liposomes and microspheres - on the phagocytosis by macrophages. J. Control. Release. 79, 29-40.

Berg, M.M., Kim, K.J., Lubman, R.L., Crandall, E.D., 1989. Hydrophilic solute transport across rat alveolar epitehlium. J. Appl. Physiol. 66, 2320-2327.

Ehrhardt, C., Fiegel, J., Fuchs, S., Abu-Dahab, R., Schaefer, U.F., Hanes, J., Lehr, C.M., 2002. Drug absorption by the respiratory mucosa: cell culture models and particulate drug carriers. J. Aerosol Med. 15, 131-139.

Fernandez-Urrusuno, R., Calvo, P., Remuñan-Lopez, C., Vila-Jato, J.L., Alonso, M.J., 1999. Enhancement of nasal absorption of insulin using chitosan nanoparticles. Pharm. Res. 16, 1576-1581.

Grenha, A., Seijo, B., Remuñan-Lopez, C., 2005. Microencapsulated chitosan nanoparticles for lung protein delivery. Eur. J. Pharm. Sci. 25, 427-437.

Kubota, Y., Takahashi, S., Matsuoka, O., 1983. Dependence on particle size in the phagocytosis of latex particles by rabbit alveolar macrophages cultured in vitro. J. Toxicol. Sci. 8, 189-195.

Lombry, C., Bosquillon, C., Préat, V., Vanbever, R., 2002. Confocal imaging of rat lungs following intratracheal delivery of dry powders or solution of fluorescent probes. J. Control. Release. 83, 331-341.

Makino, K., Yamamoto, H., Higuchi, K., Harada, N., Ohshima, H., Terada, H., 2003. Phagocytic uptake of polystyrene microspheres by alveolar macrophages: effects of the size and surface properties of the microspheres. Colloids Surf. B - Biointerfaces. 27, 33-39.

Patton, J.S., 1996. Mechanisms of macromolecule absorption by the lungs. Adv. Drug Deliv. Rev. 19, 3-36.

Pohl, R., Kramer, P.A., Thrall, R.S., 1998. Confocal laser scanning fluorescence microscopy of intact unfixed rat lungs. Int. J. Pharm. 168, 69-77.

Rudt, S., Müller, R.H., 1992. In vitro phagocytosis of nano- and microparticles by chemiluminescence. I. Effect of analytical parameters, particle size and particle concentration. J. Control. Release. 22, 263-272.

Tabata, Y., Ikada, I., 1988. Effect of the size and surface charge of polymer microspheres on their phagocytosis by macrophage. Biomaterials. 9, 356-362.

Discusión general

DISCUSIÓN GENERAL

Con el objetivo de obtener microsferas con propiedades adecuadas para actuar como transportadores de nanopartículas de quitosano conteniendo péptidos y proteínas al pulmón, se desarrollaron y evaluaron sistemas de diferente naturaleza y composición, cuyo denominador común es la presencia en su estructura de nanopartículas de quitosano. Según se ha indicado en las secciones correspondientes, se han preparado microsferas de manitol conteniendo nanopartículas de quitosano, y microsferas de manitol conteniendo sistemas complejos formados por lípidos y nanopartículas de quitosano. Para ello, se ha puesto a punto un procedimiento de microencapsulación por atomización (***Art. 2*** *y* ***Art. 4***) y se ha investigado el efecto de distintas variables de formulación, sobre las propiedades físico-químicas, estructurales, morfológicas y aerodinámicas de las microsferas y de los sistemas incorporados en ellas (***Art. 2***, ***Art. 3***, ***Art. 4*** *y* ***Art. 5***). Asimismo, hemos evaluado la capacidad de las nanopartículas de quitosano y de los complejos lípido/nanopartículas de quitosano, para asociar macromoléculas terapéuticas, utilizando como péptido y proteína modelo la insulina y la albúmina marcada con isotiocianato de fluoresceína (FITC-BSA), respectivamente (***Art. 2*** *y* ***Art. 4***). Además, se ha determinado la compatibilidad de las microsferas conteniendo nanopartículas, utilizando dos líneas celulares respiratorias de origen humano, la línea Calu-3 y la A549, que son representativas respectivamente de los epitelios bronquial y alveolar (***Art. 6***). Finalmente, se ha llevado a cabo una evaluación preliminar del comportamiento *in vivo* de este sistema microparticular, estudiando su capacidad para alcanzar la región alveolar y para provocar un descenso en los niveles de glucosa, tras la administración intratraqueal a ratas de microsferas conteniendo nanopartículas cargadas con insulina (***Sección IV***).

I. Preparación y caracterización de las microsferas conteniendo nanopartículas de quitosano

La primera parte del trabajo realizado en esta tesis doctoral consistió en la obtención de microsferas de manitol conteniendo nanopartículas de quitosano, utilizando para ello la técnica de atomización. El sistema de partida, es decir las nanopartículas, ha sido caracterizado en cuanto a sus propiedades morfológicas y físico-químicas (***Art. 2***). Las condiciones seleccionadas para su preparación (***Art. 2, Materiales y métodos***) han permitido obtener rendimientos de producción de hasta un 60%, presentando las nanopartículas un tamaño de 300-400 nm y un potencial zeta positivo que varió entre + 34 y + 45 mV, dependiendo de la relación quitosano/tripolifosfato (CS/TPP) utilizada (***Art. 2, Tabla 1***).

Se investigó además, la capacidad de las nanopartículas para actuar como vehículos de macromoléculas terapéuticas (insulina, peso molecular = 5.7 KDa, punto isoeléctrico = 5.3; y FITC-BSA, peso molecular = 67 KDa, punto isoeléctrico = 4.6). Ambas macromoléculas han sido asociadas a las nanopartículas con elevada eficacia, alcanzándose valores de asociación comprendidos entre 81% y 89%, y valores de carga real entre 30% y 31%, para la insulina y la FITC-BSA, respectivamente (***Art. 2, Tabla 2; Art. 3, Tabla 1***). Estos porcentajes tan elevados se pueden explicar por la existencia de fuertes interacciones electrostáticas entre el quitosano y las proteínas. Antes de formar las nanopartículas, la insulina se disuelve en NaOH y la FITC-BSA en agua, para luego mezclarse con la disolución acuosa de tripolisfosfato (TPP). Esta mezcla final (proteína + TPP) presenta, en ambos casos, un pH superior al punto isoeléctrico de las proteínas, lo que hace que éstas estén cargadas negativamente, favoreciendo su interacción con el quitosano que, en disolución acuosa, presenta carga positiva.

La obtención del sistema final, que como se ha comentado está constituido por microsferas conteniendo nanopartículas de quitosano, ha sido posible aplicando un procedimiento de atomización, en el que se ha utilizado el manitol y, puntualmente, la lactosa, dos excipientes típicamente empleados en la formulación de aerosoles. Las microsferas obtenidas fueron caracterizadas en cuanto a sus propiedades aerodinámicas y morfológicas (***Art. 2, Fig. 2*** *y* ***Tabla 3***).

La utilización de la lactosa como excipiente de atomización, aunque permitía obtener microsferas morfológicamente adecuadas, éstas no presentaban propiedades adaptadas a los objetivos fijados, debido sin duda a su elevada higroscopicidad. Por este motivo, después de esta etapa inicial, hemos elegido el manitol para continuar nuestros estudios. La optimización de las condiciones del proceso de atomización por el que se obtienen las microsferas (***Art. 2, Materiales y métodos***), ha hecho posible que se alcancen valores del rendimiento de producción entorno al 76%. Se ha constatado asimismo que la morfología de las partículas depende en gran medida de su composición, es decir, de la relación manitol/nanopartículas (Ma/NP) utilizada; observándose que un aumento en la cantidad de nanopartículas conduce a la obtención de partículas más esféricas y con menor tendencia a la agregación (***Art. 2, Fig. 2***). Comparando las formulaciones obtenidas con las distintas relaciones manitol/nanopartículas (Ma/NP), se ha llegado a la conclusión que un 20% de nanopartículas (Ma/NP = 80/20) (**Figura 1b**) es el contenido mínimo necesario para que se puedan obtener microsferas individualizadas y con una morfología adecuada, es decir, sin la presencia de agregados.

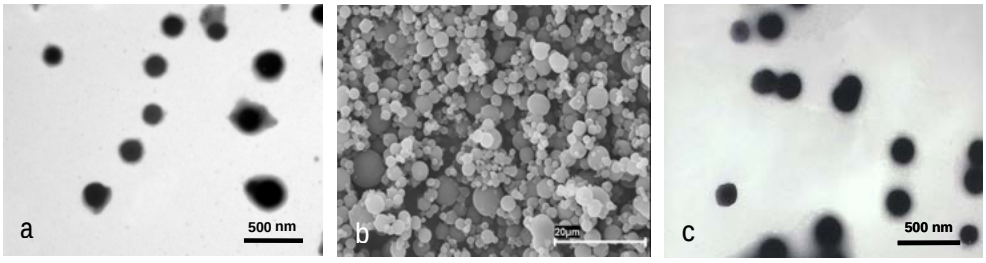

Figura 1. Microfotografías de nanopartículas de quitosano y de microsferas de manitol conteniendo nanopartículas de quitosano, obtenidas por TEM y SEM, respectivamente: a) nanopartículas de quitosano recién-preparadas; b) microsferas conteniendo nanopartículas de quitosano (relación manitol/nanopartículas = 80/20); y c) nanopartículas de quitosano recuperadas a partir de las microsferas.

El diámetro aerodinámico de las microsferas obtenidas se sitúa entre 2 y 3 µm (calculado utilizando el Aerosizer®), presentando una densidad aparente reducida, que varía entre 0.28 y 0.45 g/cm^3 (***Art. 2, Tabla 3***). Teniendo en

cuenta que, para obtener un depósito máximo en la región alveolar, las partículas que se inhalan deben presentar un tamaño situado entre 1 y 5 µm (Heyder y col., 1986; Courrier et al., 2002), las microsferas desarrolladas en este trabajo poseen las características adecuadas para ser consideradas, "a priori", como candidatas para conseguir este propósito. En particular, la formulación Ma/NP = 80/20, ha sido seleccionada para proseguir los estudios, a la vista de que sus características morfológicas y aerodinámicas son las más adecuadas para lograr los objetivos propuestos.

La caracterización morfológica y aerodinámica del sistema desarrollado, puso de manifiesto que la incorporación de las nanopartículas de quitosano en un sistema microparticular de manitol, que actuara como transportador inerte y que presentara propiedades adecuadas para hacerlas llegar a su diana en el árbol respiratorio (los alvéolos), era posible utilizando la técnica de atomización. Sin embargo, la cuestión que se planteaba a continuación es que le sucederá a las microsferas transportadoras y, en consecuencia, a las nanopartículas, una vez alcanzada dicha diana. Uno de los planteamientos iniciales de este trabajo es que, tras entrar en contacto con el fluido alveolar, el manitol que forma la estructura de las microsferas se disuelve, dejando libres las nanopartículas y posibilitando que éstas liberen, en el espacio alveolar, la macromolécula terapéutica que lleven encapsulada, o sean captadas por los macrófagos alveolares. El hecho de que el proceso de atomización pudiera modificar de alguna manera las características de las nanopartículas, podría entre otras cosas, comprometer la liberación de la macromolécula encapsulada. Por esta razón, para averiguar en que condiciones se produce la liberación de las nanopartículas a partir de las microsferas, se ha planteado un estudio de recuperación de las mismas, incubando las microsferas en un medio acuoso que simula el medio fisiológico del pulmón. Para ello, hemos elegido el PBS pH 7.4, ya que se sabe que el liquido superficial pulmonar tiene un pH de aproximadamente 7 (Kyle y col., 1990; Walters, 2002). Tal y como cabe esperar, se observa que, tras incubar las microsferas en un medio acuoso, el manitol se disuelve, dando lugar a una suspensión de nanopartículas en el medio. Tras analizar esta suspensión de nanopartículas recuperadas, se ha podido comprobar en primer lugar que su morfología no sufre alteraciones sustanciales cuando se compara con la que correspondía a las nanopartículas recién elaboradas (**Figura**

1a,c). En cuanto al tamaño y potencial zeta de las nanopartículas recuperadas, en algunas formulaciones se han observado alteraciones que, si bien resultan estadísticamente significativas, no han superado en ningún caso los 100 nm y los 2 mV (***Art. 2, Tabla 4***). Además, estas modificaciones no comprometen en modo alguno los objetivos fijados al inicio del trabajo, ya que las partículas siguen teniendo un tamaño nanométrico y una carga superficial marcadamente positiva.

Considerando en conjunto todos los resultados anteriores, parece lógico pensar que, si el procedimiento de atomización no produce ningún efecto negativo sobre las características morfológicas y fisico-químicas de las nanopartículas, tampoco debiera producirlo sobre el perfil de liberación de la insulina a partir de las nanopartículas microencapsuladas. Para comprobar esta premisa, se realizó un estudio de liberación de la insulina a partir de las microsferas en PBS pH 7.4 a 37ºC, comparándo el perfil obtenido con el correspondiente a las nanopartículas recién preparadas, en las mismas condiciones. Como se observa en las curvas recogidas en la **Figura 2**, la liberación de la insulina a partir de las nanopartículas fue muy rápida, tanto en el caso de las nanopartículas recién elaboradas, como en el caso de las nanopartículas microencapsuladas, detectándose la cantidad máxima de insulina liberada (75 – 80%) a los 15 minutos de comenzar el estudio. Al igual que se ha concluido en trabajos anteriores realizados en nuestro grupo de investigación, este perfil de liberación es indicativo de que la interacción entre la insulina y el quitosano es de carácter débil y, por lo tanto, permite la liberación de la insulina, por un proceso de disociación (Fernández-Urrusuno y col., 1999). Además, no se han observado diferencias significativas en los perfiles de liberación que presentan ambas formulaciones. Por lo tanto, se confirma que el procedimiento de atomización no produce ningún efecto negativo sobre las nanopartículas, lo cual no resulta en absoluto sorprendente, tal y como se ha comentado inicialmente al plantear el trabajo, considerando que el manitol es una sustancia neutra y, por consiguiente, no es esperable que se produzca ninguna interacción entre el manitol y las nanopartículas. Por otro lado, importa referir que otros autores han demostrado que la elevada temperatura del proceso de atomización no compromete la estabilidad de las proteínas asociadas, indicando una vez más la adecuación de esta técnica (Broadhead y col., 1992).

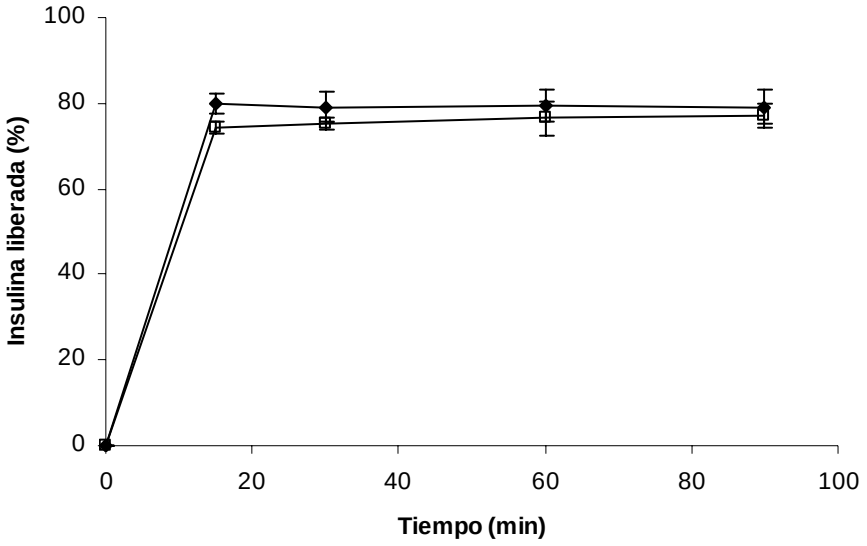

Figura 2. Perfil de liberación de la insulina a partir de (♦) nanopartículas (CS/TPP = 6:1) y (□) microsferas (Ma/NP = 80/20, CS/TPP = 6:1) en PBS pH 7.4 a 37ºC (30% de insulina p/p con relación al CS; media ± D.E., n = 3).

A continuación, y teniendo en cuenta que el quitosano se degrada por acción de la lisozima, que es un enzima que está presente en todas las superficies mucosas, incluida la pulmonar, que tiene la capacidad de hidrolizar las uniones glucosídicas situadas entre las unidades de glucosamina del quitosano, hemos querido evaluar el efecto del enzima sobre la integridad de las nanopartículas. La interacción de las nanopartículas, tanto frescas como recuperadas a partir de las microsferas, con lisozima a una concentración de 0.2 mg/mL que corresponde a la cantidad máxima de enzima detectada en secreciones traqueobronquiales humanas (Konstan y col., 1981), dio lugar a una disminución del tamaño de partícula situada entorno a los 100 nm, en el tiempo que duró el estudio (90 minutos); probablemente como resultado de la hidrólisis parcial de moléculas de quitosano presentes en la superficie de las nanopartículas (***Art. 2, Fig. 5***). No obstante, esta disminución de tamaño no compromete el objetivo inicial, pudiendo incluso facilitar la liberación *in vivo* de la macromolécula encapsulada en el sistema.

Considerando el conjunto de los resultados obtenidos en esta primera etapa, parece evidente que el sistema de administración microparticular

propuesto es adecuado, desde el punto de vista de su comportamiento *in vitro*, como vehículo transportador capaz de hacer llegar a las nanopartículas hasta la parte más distal del pulmón. Sin embargo, es preciso conocer la estructura del sistema, es decir, como se distribuyen sus distintos componentes (manitol y nanopartículas), cual es su estructura interna (si se trata de microsferas huecas o, si por el contrario, son partículas sólidas compactas). Este tipo de información podría resultar de gran importancia, por ejemplo, a la hora de interpretar los resultados que se puedan obtener *in vivo*. La visualización de las microsferas utilizando microscopía electrónica de barrido (SEM), informa acerca de las características superficiales de las partículas (esfericidad, textura, etc.), pero sin embargo no nos permite saber cual es su composición superficial, y tampoco nos da información relativa a la estructura interna de las microsferas. Por lo tanto, hemos decidido recurrir a la técnica de microscopia confocal (CLSM), para lo cual previamente se ha asociado a las nanopartículas una proteína con etiqueta fluorescente (FITC-BSA), y se ha marcado el manitol con otra etiqueta fluorescente (Bodipy®). La observación por CLSM del material pulverulento obtenido tras la atomización, nos ha permitido comprobar que las nanopartículas están homogéneamente distribuidas en las microsferas de manitol (**Figura 3**).

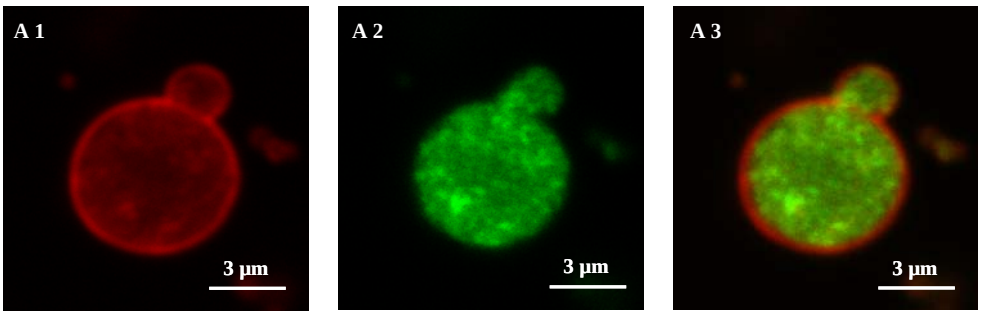

Figura 3. Imágenes obtenidas por microscopía confocal de las microsferas preparadas con una relación manitol/nanopartículas = 80/20; el manitol está marcado fue Bodipy® (rojo) y las nanopartículas con FITC-BSA (verde). A1: canal rojo, A2: canal verde, A3: superposición de los dos canales.

Previamente, el análisis realizado por SEM de las microsferas conteniendo nanopartículas, había indicado la presencia de algunas microsferas fragmentadas que eran huecas (***Art. 2, Fig. 3***). Dado que esta técnica (SEM) solo permite visualizar la superficie de las partículas, como previamente comentado, no era posible distinguir si todas las partículas eran huecas o no. El estudio realizado por microscopía confocal permitió obtener más información en relación a esta característica, y así hemos podido comprobar la existencia, aunque muy puntual, de algunas partículas huecas, que en casi todos los casos son partículas con tamaño muy superior a la media, que presentan algún tipo de brecha o hueco en su estructura (***Art. 3, Fig. 5***). Esta fragmentación puede haberse producido como consecuencia de la presión ejercida al preparar la muestra, sobre la capa externa de algunas microsferas, lo que provoca su colapso (Raula y col., 2004).

La observación de las imágenes A1 y A3 de la **Figura 3**, sugiere que el manitol forma una capa alrededor de toda la microsfera que, asimismo, parece evidenciar la ausencia de nanopartículas en la superficie de las mismas. Para confirmar este dato, se ha llevado a cabo un análisis minucioso de la superficie de las microsferas, empleando para ello dos técnicas específicas de análisis de superficie especialmente sensibles, la espectroscopia de fotoelectrones de Rayos X (XPS) y la espectrometría de masas de iones secundarios por tiempo de vuelo (TOF-SIMS). Estas técnicas (ver introducción del ***Art. 3*** para aclarar los principios teóricos de las mismas) permiten detectar, respectivamente, el porcentaje de los distintos elementos químicos y las masas de los iones que están presentes en la superficie de la muestra analizada. Para la realización de estos análisis, fueron utilizados dos controles, el manitol y las nanopartículas, de forma individual. Los resultados obtenidos por XPS confirman la existencia de nanopartículas en la superficie de las microsferas, ya que se detectaron elementos específicos de las nanopartículas que, obviamente, no aparecen en el manitol, como por ejemplo el nitrógeno (**Tabla 1**).

A su vez, el análisis realizado por TOF-SIMS ha corroborado los resultados obtenidos por XPS, detectando igualmente en la superficie de las microsferas no sólo señales característicos del manitol, sino también señales procedentes de las

nanopartículas, como es el caso del ión molecular correspondiente al grupo N-acetilglucosamina, que es la unidad básica del quitosano (***Art. 3, Fig. 6***).

Tabla 1. Composición superficial (porcentajes atómicos) de las nanopartículas CS/TPP, del manitol y de las microsferas (manitol/nanopartículas = 80/20), determinada por XPS

Elemento	**Nanopartículas CS/TPP (%)**	**Manitol (%)**	**Microsferas (%)**
C	53.8	56.2	54.9
O	33.8	43.8	43.3
N	4.5	0	0.6
P	2.7	0	0
Si	5.2	0	1.2
Relación N/C	0.084	0	0.011
Relación C/O	1.592	1.283	1.268

Estos resultados permiten confirmar que, efectivamente, las nanopartículas están distribuidas de forma homogénea en la estructura de las microsferas, aparentemente sin formar agregados y están presentes tanto en el interior como en la parte más externa de la partícula. Esta estructura puede explicar la eficaz recuperación de las nanopartúculas a partir de las microsferas tras su incubación en un medio acuoso, sin alteraciones morfológicas y físico-químicas. Asimismo, también puede justificar la ausencia de diferencias significativas en los perfiles de liberación obtenidos a partir de las nanopartículas recién preparadas o microencapsuladas, ya que al disolverse el manitol, las nanopartículas permanecerían aisladas en el medio de liberación.

II. Preparación y caracterización de las microsferas conteniendo sistemas complejos lípidos/nanopartículas de quitosano

La segunda etapa del trabajo experimental consistió en la elaboración de un segundo sistema de administración bastante similar al anterior, si bien es un poco más complejo en cuanto a su diseño, ya que se incluye un componente lipídico. La presencia de lípidos de tipo endógeno en las formulaciones para administración pulmonar, viene justificada por su capacidad para reducir la captura de los sistemas por parte de los macrófagos (Evora y col., 1998), habiéndose observado además la capacidad de los lípidos para actuar como promotores de la absorción de fármacos por esta vía (Liu y col., 1993; McAllister y col., 1996; Mitra y col., 2001). Por otro lado, la incorporación de lípidos en el sistema, podría contribuir a conseguir una liberación controlada del fármaco encapsulado.

El sistema de administración que se ha desarrollado consiste en microsferas de manitol conteniendo complejos entre nanopartículas de quitosano y lípidos; siendo el papel de las microsferas, al igual que en el caso anterior, actuar simplemente como vehículos transportadores inertes capaces de hacer llegar los complejos a la superficie del epitelio pulmonar. Para la formación de los complejos, previamente se preparan por separado una suspensión de nanopartículas de quitosano y una fina película o film de fosfolípidos seco que, a continuación, se hidrata con la suspensión de nanopartículas. Una vez obtenida la suspensión de los complejos, se mezcla de inmediato con una disolución acuosa de manitol, y se procede a la atomización, que conduce a la obtención del sistema final (***Art. 4, Materiales y métodos***). Para formar la cubierta lipídica se han seleccionado dos fosfolípidos endógenos del pulmón, la dipalmitoilfosfatidilcolina (DPPC) y el dimiristoilfosfatidilglicerol (DMPG), que son componentes fundamentales del surfactante pulmonar, y presentan, respectivamente, carga superficial neutra y negativa (Wright y Clements, 1987; Fattal y col., 1993; McAllister y col., 1996). Por lo tanto, se han obtenido dos formulaciones de complejos distintas, una en la que el film lipídico se compone solamente de DPPC y otra en la que ha sido formado por DPPC y DMPG (en una relación de masa de 10:1) que han sido caracterizados individualmente en cuanto a sus propiedades morfológicas y físico-químicas (***Art. 4***). En lo que se refiere a los complejos,

presentan todos ellos una morfología similar, independientemente de la composición del film lipídico utilizado para formarlos. La **Figura 4** es una imagen obtenida por microscopía electrónica de transmisión (TEM), que muestra el aspecto de estos sistemas complejos, sugiriendo que una parte importante de las nanopartículas, que corresponden a las zonas negras y densas de tamaño reducido que se aprecian en la imagen, se encuentran atrapadas o asociadas de alguna manera a otras estructuras de aspecto membranoso que probablemente corresponden a las bicapas fosfolipídicas, observándose además la existencia de nanopartículas aisladas, que aparentemente no presentan recubrimiento lipídico alguno, como las que se señalan en la figura mediante flechas.

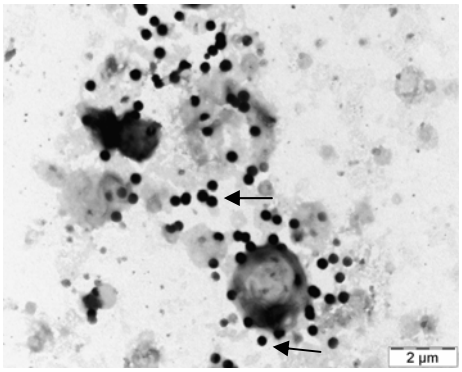

Figura 4. Microfotografía obtenida por TEM de los complejos lípido,/nanopartículas de quitosano (lípido/nanopartículas = 3:1; nanopartículas CS/TPP = 6:1). Las flechas señalan nanopartículas aparentemente aisladas.

Las características físico-químicas de los sistemas en los que se incluye al recubrimiento lipídico, fueron comparadas con las de las nanopartículas, así como con las de las correspondientes vesículas lipídicas utilizadas como control, y que fueron preparadas hidratando el film lipídico con agua, en lugar de con la suspensión de nanopartículas. El tamaño que presentan los complejos es de aproximadamente 2 µm, siendo el potencial zeta neutro (0.2 mV) en el caso de los complejos obtenidos utilizando DPPC; mientras que resulta negativo (alrededor de - 36 mV) para aquellos complejos formados utlizando una mezcla de DPPC y

DMPG (**Tabla 2**). No se han observado diferencias entre los tamaños de los complejos y los de las correspondientes vesículas control. Sin embargo, la comparación del tamaño de los complejos con el de las nanopartículas, permite constatar que hay una diferencia suficientemente grande (de 400 nm a más de 2 µm) como para sugerir el recubrimiento de las nanopartículas por los lípidos (***Art. 4, Tabla 1;*** **Tabla 2**).

Tabla 2. Tamaños y potenciales zeta de las vesículas control y de los complejos lípido/ nanopartículas (media ± D.E.; n = 3)

Sistema	Tamaño (nm)	Potencial Zeta (mV)
Vesículas control DPPC	2.2 ± 1.8	- 7.1 ± 4.6
Complejos DPPC/CS-NP	1.8 ± 1.8	0.2 ± 1.9
Vesículas control DPPC-DMPG	1.8 ± 1.7	- 54.0 ± 4.2
Complejos DPPC-DMPG/CS-NP	2.5 ± 1.6	- 36.2 ± 1.6

CS: quitosano; DPPC: dipalmitoilfosfatidilcolina; DMPG: dimiristoilfosfatidilglicerol; NP: nanopartículas

Comparando los resultados de potencial zeta, se puede comprobar que, tal y como cabía esperar, la presencia de DPPC dio lugar a vesículas con una carga superficial próxima a la neutralidad, mientras que la incorporación de DMPG se reflejó en la obtención de valores negativos de carga superficial (Fattal y col., 1993). A partir de la comparación de los valores de potencial zeta de los complejos con las correspondientes vesículas control y nanopartículas, se puede afirmar que hay claros indicios de que se ha producido una asociación y/o recubrimiento de las nanopartículas con el film lipídico. Este proceso parece más acentuado cuando en la composición de dicho film se incluye DMPG, que confiere una carga superficial fuertemente negativa, que contribuye a que se produzca una interacción más efectiva de la película lipídica con las nanopartículas de quitosano que, como ya se ha comentado anteriormente, presentan un potencial zeta marcadamente positivo. Así, cuando se utiliza el film compuesto por DPPC y DMPG, se produce una disminución del carácter negativo del potencial zeta, desde - 54 mV (vesículas

control) a - 36 mV (complejos), observándose una inversión completa en relación a las nanopartículas, cuyo valor de potencial zeta es de + 44 mV. Cuando el film lipídico está compuesto únicamente por DPPC, el potencial de los complejos (0 mV) resultó ser prácticamente igual al de las vesículas control (-7 mV), si bien significativamente distinto del correspondiente a las nanopartículas (+ 44 mV) (**Tabla 2**).

La incorporación de insulina en los complejos, se llevó a cabo por asociación previa a las nanopartículas de quitosano (***Art. 4, Materiales y métodos***). Las nanopartículas cargadas con insulina (eficacia de asociación = 70%, contenido en insulina (carga) = 36%), se utilizaron para hidratar el film lipídico previamente formado, de la misma manera descrita para preparar los complejos sin proteína (***Art. 4, Tabla 1***).

La formación de un sistema de administración que pudiera vehiculizar los complejos obtenidos hacía el pulmón, se consiguió recurriendo a la técnica de atomización utilizando manitol como excipiente, al igual que se mostró para las nanopartículas de quitosano sin recubrimiento lipídico. Considerando que en el caso del sistema desarrollado en la primera etapa (microsferas conteniendo nanopartículas de quitosano), la formulación que presentó propiedades más adecuadas desde el punto de vista morfológico y aerodinámico, fue aquella obtenida a partir de una relación manitol/nanopartículas = 80/20, se tomó la decisión de preparar el segundo sistema (microsferas conteniendo complejos lípido/nanopartículas) utilizando la misma relación (80% de manitol y 20% de complejos lípido/nanopartículas). La caracterización morfológica de las microsferas conteniendo complejos lípido/nanopartículas (***Art. 4, Fig. 3***), permitió comprobar que éstas son morfológicamente muy similares a las ya descritas anteriormente (***Art. 2, Fig. 2***), resultando ser partículas esféricas, de forma muy bien definida. Además, presentan propiedades adecuadas para una administración por vía pulmonar, ya que exhiben una baja densidad aparente (0.4 – 0.5 g/cm^3) y un diámetro aerodinámico comprendido entre 2.1 y 2.7 µm (***Art. 4, Tabla 3***).

Al igual que en el caso anterior, se ha procedido a comprobar que la técnica de atomización no inducía alteraciones en las características morfológicas

y físico-químicas de los complejos, que pudieran resultar comprometedoras para nuestros objetivos. Con tal motivo, se procedió a la caracterización de los complejos recuperados tras la incubación de las microsferas en un medio acuoso (PBS pH 7.4). Dicha caracterización reveló que sus propiedades eran similares a las que presentaban los complejos recién preparados, tanto desde el punto de vista morfológico como físico-químico (***Art. 4, Fig. 4*** *y* ***Tabla 4***), lo que confirma que la atomización es una técnica adecuada para lograr los objetivos propuestos. Además, como ya se ha comentado anteriormente, se descarta la posible degradación de la proteína asociada al sistema a causa del proceso de atomización, teniendo en cuenta el reducido período de tiempo en que la macromolécula contacta con las elevadas temperaturas generadas (Broadhead y col., 1992).

Una de las razones que nos ha llevado a incorporar lípidos en la formulación ha sido, tal y como se indica al inicio de esta sección, la posibilidad de que éstos contribuyeron a lograr una liberación controlada de la molécula encapsulada, en este caso la insulina; ya que, como se había comprobado para el sistema anterior, su liberación se produce de forma casi inmediata (**Figura 2**). Por ello, se evaluó la liberación del péptido a partir de cada una de las formulaciones de complejos (DPPC/nanopartículas y DPPC-DMPG/nanopartículas) en PBS pH 7.4 a 37ºC. Como se refleja en las curvas recogidas en la **Figura 5**, la liberación de la insulina a partir de las dos formulaciones de complejos es significativamente diferente de la observada para las nanopartículas. Estos resultados se atribuyen a la presencia de lípidos en los complejos, los cuales es probable que, en el proceso de constitución del sistema en un entorno acuoso, se organicen a modo de estructuras de tipo lamelar o membranoso, que han de ser traspasadas por la proteína en el proceso de liberación (Chupin y col., 2004).

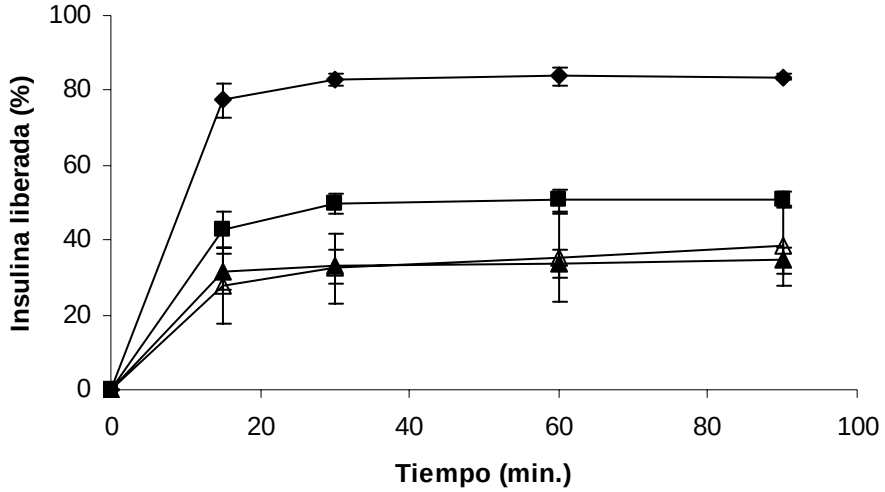

Figura 5. Perfiles de liberación de la insulina a partir de (♦) nanopartículas de quitosano, (■) complejos DPPC/nanopartículas, (▲) complejos DPPC-DMPG/nanopartículas, y (Δ) microsferas conteniendo complejos DPPC-DMPG/nanopartículas, en PBS pH 7.4 a 37ºC (30% de insulina p/p con relación al CS; media ± D.E., n = 3).

Además, se han observado diferencias en la liberación entre las dos formulaciones de complejos, de tal manera que la formulación en la que está presente un único lípido (DPPC) libera un 43% de la insulina al cabo de 90 minutos, mientras que la formulación en la que se incluyen los dos lípidos (DDPC y DMPG) libera el 30% del contenido en péptido en el mismo período de tiempo. Estas diferencias entre ambas formulaciones se deben, posiblemente, a la diferente interacción que se produce entre las nanopartículas y los fosfolípidos y, en consecuencia, al distinto recubrimeinto en cada uno de los casos, tal y como se había sugerido a partir de los resultados de la caracterización físico-química del sistema. Así, la formulación en la que se produce una mayor interacción entre nanopartículas y lípidos (la que contiene DPPC y DMPG), es la que proporciona una liberación más controlada de la proteína, lo que puede ser atribuido a un recubrimiento lípidico de las nanopartículas más homogéneo y eficaz.

Además hemos evaluado el perfil de liberación de la insulina a partir de las microsferas que contienen los complejos lípido/nanopartículas, utilizando

únicamente la formulación en la que están presentes los dos lípidos, teniendo en cuenta que lo que se trata de evaluar en este caso es el efecto de la microencapsulación en presencia de manitol. Como se observa en la **Figura 5**, el procedimiento de atomización utilizado para formar las microsferas, no ha tenido ninguna influencia sobre el perfil de liberación de la insulina a partir de los complejos microencapsulados. Así, pues, al igual que sucedería para el primer sistema, el manitol se disuelve tras la incubación del sistema en el medio acuoso, dejando libres los complejos y, en consecuencia, permitiendo la liberación del péptido encapsulado en las nanopartículas de quitosano.

El análisis de los datos de caracterización físico-química, así como de los obtenidos en el estudio de liberación realizado a partir de las dos formulaciones de complejos, sugiere, como ya se ha indicado, que la adsorción de los fosfolípidos en la superficie de las nanopartículas es más eficaz cuando el film lipidico se obtiene a partir de la mezcla de dos fosfolípidos, uno de ellos cargado negativamente. No obstante, la confirmación real de que la interacción se produce de verdad en esos términos, sólo es posible si se lleva a cabo un análisis estructural detallado de los dos sistemas. Nuestra hipótesis es que las nanopartículas estarían completamente recubiertas por los lípidos, en el caso de la formulación que incluye DPPC y DMPG; siendo el recubrimiento únicamente parcial cuando el sistema se forma utilizando sólo DPPC. Para corroborar esta hipótesis, hemos realizado un estudio exhaustivo de la composición superficial de los sistemas, utilizando dos técnicas específicas de análisis de superficies, como son la espectroscopia de fotoelectrones de Rayos X (XPS) y la espectrometría de masas de iones secundarios por tiempo de vuelo (TOF-SIMS); tal y como ya se hizo con anterioridad, en la sección I, para caracterizar la superficie de las microsferas que contienen las nanopartículas encapsuladas. Para poder establecer comparaciones, al igual que se ha hecho en el caso de la caracterización físico-química de los complejos, se han utilizado como controles las nanopartículas de quitosano y las vesículas obtenidas hidratando el film lipídico formado previamente a partir de las mismas mezclas lipídicas que se utilizan en cada formulación de complejos, con agua. El análisis efectuado por XPS de la superficie de los complejos, ha revelado que las señales a que dan lugar éstos, son muy similares a aquellas detectadas en las correspondientes vesículas

lipídicas control, siendo, por el contrario, muy diferentes de las señales correspondientes a las nanopartículas de quitosano (**Tabla 3**). Dichas observaciones lo que ponen de manifiesto es que los lípidos dominan la composición superficial de los complejos formados. Además, las relaciones N/C y C/O de los complejos y de las correspondientes vesículas control, presentan valores más próximos en el caso de la formulación que contiene DPPC y DMPG, lo que sugiere una vez más que, en este caso, el recubrimiento lipídico es más efectivo.

Tabla 3. Composición superficial (porcentajes atómicos) de nanopartículas de quitosano (CS-NP), vesículas control de DPPC, vesículas control DPPC-DMPG, complejos DPPC/NP y complejos DPPC-DMPG/NP, determinados por XPS

Elemento	**CS-NP (%)**	**Vesículas DPPC (%)**	**Complejos DPPC/NP**	**Vesículas DPPC-DMPG (%)**	**Complejos DPPC-DMPG/NP (%)**
C	53.8	81.7	80.2	78.1	78.8
O	33.8	14.0	15.4	16.9	16.3
N	4.5	2.0	1.8	1.8	1.8
P	2.7	2.3	2.0	2.2	2.2
Si	5.2	0	0.6	1.0	0.9
Relación N/C	0.084	0.025	0.022	0.023	0.023
Relación C/O	1.592	5.836	5.208	4.618	4.834

Los resultados obtenidos aplicando la técnica de TOF-SIMS han corroborado aquellos obtenidos por XPS. Mientras que el análisis de los complejos que incorporan DPPC ha revelado la existencia de zonas con señales característias únicamente del componente lipídico, así como otras zonas en las que las señales corresponden claramente a las nanopartículas, si bien se perciben con menor

intensidad que en el caso de los lípidos; en los complejos que incluyen DPPC y DMPG, solamente se han detectado en la superficie señales características de los lípidos y en ningún caso una señal que pueda ser atribuida a las nanopartículas (***Art. 5, Fig. 3*** *y* ***Fig. 4***). Teniendo en cuenta que el área de muestreo ha sido muy grande (***Art. 5, Materiales y métodos***), parece claro que la superficie de los complejos que contienen DPPC y DMPG está completamente constituida por fosfolípidos, mientras que la de los que incluyen sólo DPPC presenta una cantidad reducida de nanopartículas. Así pues, si analizamos en conjunto todos estos resultados, podemos concluir que el recubrimiento lipídico de las nanopartículas es más efectivo cuando el film lipídico está constituído por los dos lípidos, DPPC y DMPG, y presenta una carga fuertemente negativa, lo que apunta a que el mecanismo de interacción entre las nanopartículas de quitosano y los lípidos está basado fundamentalmente en las fuerzas electrostáticas. Además, como se ha comentado anteriormente, estos datos están en perfecta concordancia con los obtenidos en el estudio de liberación.

III. Estudio del comportamiento *in vitro* de las microsferas de manitol conteniendo nanopartículas de quitosano en cultivos de células respiratorias

Con el fin de establecer las posibilidades reales de administración pulmonar de las formulaciones desarrolladas en humanos, un aspecto de gran interés es el estudio de su comportamiento tras entrar en contacto con la superficie del epitelio pulmonar; principalmente si en las formulaciones se incluye algún componente polimérico que pueda, de alguna manera, causar daño en las mucosas. En ese sentido, además del estudio del comportamiento *in vivo* de los sistemas, están adquiriendo una gran relevancia los estudios realizados utilizando líneas celulares que mimeticen las características de los epitelios. Así, en esta fase del trabajo, se consideró interesante evaluar la biocompatibilidad de los sistemas desarrollados, seleccionando para ello el primer sistema descrito en esta memoria, es decir, las microsferas conteniendo nanopartículas de quitosano, precisamente por parecer muy importante la evaluación de este polímero. Dicha evaluación se realizó tras poner el sistema en contacto con células de origen humano, concretamente dos líneas celulares representativas de los epitelios bronquial

(Calu-3) y alveolar (A549), utilizando estudios de toxicidad y permeabilidad (***Art. 6***).

El estudio de toxicidad (realizado con metiltiazoltetrazolium – MTT), ha revelado la ausencia de toxicidad significativa de las formulaciones, tanto sobre las células Calu-3 como sobre las A549, para valores de concentración de nanopartículas hasta 1.3 mg/mL, durante 48 horas. En la **Figura 6**, se muestran a modo de ejemplo, los resultados de viabilidad celular de las células Calu-3, obtenidos tras 24 horas de incubación en presencia de las formulaciones de microsferas conteniendo nanopartículas de quitosano, en diferentes proporciones. Los resultados correspondientes a las 48 horas fueron muy similares, siendo igualmente parecidos a los observados en las células A549.

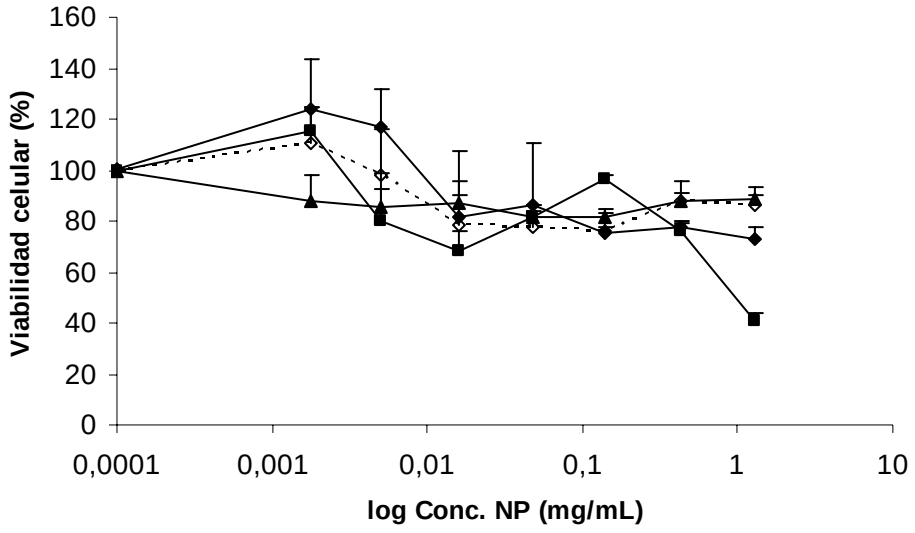

Figura 6. Viabilidad de las células Calu-3 evaluada por el ensayo de citotoxicidad MTT tras 24h de exposición de las células a las formulaciones de microsferas conteniendo nanopartículas de quitosano, con distintas relaciones manitol/nanopartículas (Ma/NP), en medio de cultivo celular: (◊) control NP, (♦) Ma/NP = 90/10, (■) Ma/NP = 80/20, (▲) Ma/NP = 60/40 (media ± SEM; n= 3 × 6).

Además, se han llevado a cabo estudios de resistencia eléctrica transepitelial (TER) y de permeabilidad celular a la fluoresceína, utilizando para ello únicamente las células Calu-3, ya que las A549 no forman uniones íntimas y, por lo tanto, no son adecuadas para realizar ensayos que requieran la

constitución de una barrera fisiológica por parte de las células (Forbes y Ehrhardt, 2005). En estos estudios, se ha observado que, tras la incubación de las células con la formulación seleccionada (manitol/nanopartículas = 80/20) a una concentración de 1.3 mg nanopartículas/mL, éstas no sufren alteraciones en los valores de TER (***Art. 6, Fig. 4***) o de permeabilidad, si se comparan con los obtenidos en células que no han sido tratadas con las formulaciones.

Por otro lado, se ha realizado un estudio por microscopía confocal, de la captación del sistema por parte de las células (***Art. 6, Fig. 5***). De estos resultados se deduce que si bien en ninguna de las líneas celulares utilizadas se aprecia la internalización de las partículas en las células, sí se ha comprobado la existencia de fenómenos de mucoadhesión dado que, tras lavados vigorosos de las células, se siguen observando partículas adheridas a la superficie de las mismas.

Los resultados de este estudio apoyan el valor del sistema propuesto, como vehículo transportador para la administración de macromoléculas terapéuticas por vía pulmonar; teniendo en cuanta que presenta características aerodinámicas y morfológicas adecuadas y habiéndose comprobado también su biocompatibilidad.

IV. Evaluación *in vivo* preliminar de las microsferas conteniendo nanopartículas de quitosano

Por último, para corroborar la eficacia de las nanopartículas de quitosano encapsuladas en microsferas de manitol, cuya biocompatibilidad había sido demostrada en dos líneas celulares respiratorias, se procedió a investigar de forma preliminar su comportamiento *in vivo*. Para ello, se llevó a cabo un ensayo de distribución cualitativa de las formulaciones en el pulmón, tras la administración por vía intratraqueal a ratas, de la formulación de microsferas conteniendo nanopartículas de quitosano marcadas con una etiqueta fluorescente (FITC-BSA) en forma de polvo seco. Las imágenes obtenidas permitieron verificar que las microsferas llegaban a alcanzar los alvéolos, presentando además una cierta tendencia a acumularse en el interior de los macrófagos. El hecho de que se visualicen las partículas en el espacio alveolar, constituye un punto de especial

relevancia de cara a lograr los objetivos propuestos en el planteamiento inicial del trabajo, ya que la administración sistémica de un fármaco por vía pulmonar supone que éste pueda pasar a la circulación sistémica y, en el pulmón, el lugar privilegiado para lograr una absorción sistémica son precisamente los alvéolos (***Sección IV, Fig. 4***).

Para la segunda parte de esta evaluación *in vivo* preliminar, se utilizó como péptido modelo la insulina, procediéndose a la determinación del efecto hipoglucémico de las microsferas conteniendo nanopartículas de quitosano cargadas con insulina. Tras su administración en forma de polvo seco por vía intratraqueal, se determinaron los niveles de glucemia de los animales a distintos tiempos. Como se muestra en la **Figura 7**, se ha verificado que las microsferas conteniendo nanopartículas de quitosano cargadas con insulina, producen una reducción en los niveles de glucosa mayor que la que se produce en el caso de la disolución de insulina utilizada como control. Más concretamente, se observa una reducción de aproximadamente 60% a los 60 minutos en el caso de la disolución, mientras que las microsferas provocan un descenso de los niveles de glucosa de aproximadamente el 90%, en el mismo período de tiempo.

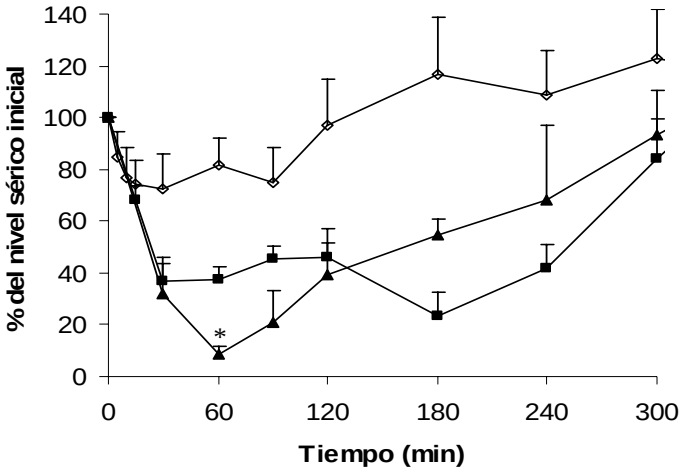

Figura 7. Efecto hipoglucémico tras administración intratraqueal de (◊) una disolución de PBS pH 7.4; (■) una disolución control de insulina (dosis = 17.9 U/kg) en PBS pH 7.4; y (▲) microsferas conteniendo insulina (manitol/nanopartículas=80/20; dosis = 16.7 U/kg) (n≥3).

Aunque estos resultados han sido obtenidos utilizando un número reducido de animales, creemos que pueden ser representativos para mostrar el potencial real del sistema desarrollado (nanopartículas de quitosano encapsuladas en microsferas de manitol), ya que ponen de manifiesto una vez más su eficacia.

Referencias bibliográficas

Broadhead, J., Edmond-Rouan, S.K., Rhodes, C.T., 1992. The spray drying of pharmaceuticals. Drug. Develop. Ind. Pharm. 18, 1169-1206.

Chupin, V., de Kroon, A.I.P.M., de Kruijff, B., 2004. Molecular architecture of nanocapsules, bilayer-enclosed solid particles of cisplatin. JACS. 126, 13816-13821.

Courrier, H.M., Butz, N., Vandamme, T.F., 2002. Pulmonary drug delivery systems: recent developments and prospects. Crit. Rev. Ther. Drug Carr. Syst. 19, 425-498.

Evora, C., Soriano, I., Rogers, R.A., Shakesheff, K.M., Hanes, J., Langer, R., 1998. Relating the phagocytosis of microparticles by alveolar macrophages to surface chemistry: the effect of 1,2-dipalmitoylphosphatidylcholine. J. Control. Release. 51, 143-152.

Fattal, E., Couvreur, P., Puisieux, F., 1993. Méthodes de préparation des liposomes. In: Delattre, J., Couvreur, P., Puisieux, F., Philippot, J. R., Schuber, F. (Eds.), Les liposomes: aspects technologiques, biologiques et pharmacologiques. Editions Inserm, Paris, pp. 43-52.

Fernandez-Urrusuno, R., Calvo, P., Remuñan-Lopez, C., Vila-Jato, J.L., Alonso, M.J., 1999. Enhancement of nasal absorption of insulin using chitosan nanoparticles. Pharm. Res. 16, 1576-1581.

Forbes, B., Ehrhardt, C., 2005. Human respiratory epithelial cell culture for drug delivery applications. Eur. J. Pharm. Biopharm. 60, 193-205.

Heyder, J., Gebhart, J., Rudolf, G., Schiller, C. F., Stahlhofen, W., 1986. Deposition of particles in the human respiratory tract in the size range 0.005-15 mm. J. Aerosol Sci. 17, 811-825.

Konstan, M.W., Chen, P.W., Sherman, J.M., Thomassen, M.J., Woodm, R.E., Boat, T.F., 1981. Human lung lysozyme: sources and properties. Am. Rev. Respir. Dis. 123, 120-124.

Kyle, H., Ward, J.P., Widdicombe, J.G., 1990. Control of pH of airway surface liquid of the ferret trachea in vitro. J. Appl. Physiol. 68, 135-140.

Liu, F., Shao, Z., Kildsig, D.O., Mitra, A.K., 1993. Pulmonary delivery of free and liposomal insulin. Pharm. Res. 10, 228-232.

McAllister, S.M., Alpar, H.O., Teitelbaum, Z., Bennett, D.B., 1996. Do interactions with phospholipids contribute to the prolonged retention of polypeptides within the lung? Adv. Drug Deliv. Rev. 19, 89-110.

Mitra, R., Pezron, I., Li, Y., Mitra, A.K., 2001. Enhanced pulmonary delivery of insulin by lung lavage fluid and phospholipids. Int. J. Pharm. 217, 25-31.

Raula, J., Eerikäinen, H., Kauppinen, E.I., 2004. Influence of the solvent composition on the aerosol synthesis of pharmaceutical polymer nanoparticles. Int. J. Pharm. 284, 13-21.

Walters, D.V., 2002. Lung lining liquid - The hidden depths. Biol. Neonate. 81, 2-5.

Wright, J.R., Clements, J.A., 1987. Metabolism and turnover of lung surfactant. Am. Rev. Respir. Dis. 135, 426-444.

Conclusiones

CONCLUSIONES

Los resultados fruto del trabajo experimental recogido en esta memoria, ponen de manifiesto el potencial de los sistemas microparticulares desarrollados como vehículos transportadores de nanopartículas de quitosano conteniendo macromoléculas terapéuticas hacia el pulmón, con fines sistémicos. Es esperable que, tras alcanzar la zona alveolar, el manitol que compone las microsferas se disuelva, liberando el sistema microencapsulado (nanopartículas de quitosano o complejos lípido/nanopartículas de quitosano) y, consecuentemente, la macromolécula asociada a ello.

De un modo más detallado, los resultados descritos nos han permitido extraer las siguientes conclusiones:

1. Se han preparado microsferas de manitol conteniendo nanopartículas de quitosano y complejos lípido/nanopartículas de quitosano, con características morfológicas y aerodinámicas adecuadas (diámetros aerodinámicos entre 1 y 5 μm) para administración por vía pulmonar, utilizando una técnica de atomización. Además, los sistemas microencapsulados están homogéneamente distribuidos por toda la microsfera, sin formar agregados en su interior, tal y como se comprobó utilizando técnicas específicas de microscopía y de análisis de superficie.

2. En lo que respecta a los complejos lípido/nanopartículas de quitosano, la composición fosfolipídica afecta a las características físico-químicas de los mismos, obteniéndose un recubrimiento lipídico de las nanopartículas más completo y, en consecuencia, un sistema más adecuado para nuestros propósitos, cuando el film lipídico contiene un fosfolípido cargado negativamente (DMPG), tal y como se ha comprobado aplicando las técnicas de análisis de superficie. Además, la presencia de este fosfolípido da lugar a una liberación más controlada del péptido encapsulado.

3. La relación de masas entre el manitol y el sistema incorporado en las microsferas, influye en las propiedades morfológicas y aerodinámicas de

las mismas, siendo la relación manitol/sistema microencapsulado = 80/20 la más adecuada.

4. El proceso de atomización con manitol no introduce alteraciones significativas ni en las características físico-químicas del sistema microencapsulado, ni en el perfil de liberación del péptido asociado. Así pues, el manitol actúa únicamente como soporte inerte para transportar las nanopartículas conteniendo la proteína terapéutica hacía la región alveolar, que es donde se produce mayoritariamente la absorción a nivel pulmonar.

5. Las microsferas conteniendo nanopartículas de quitosano han revelado ser biocompatibles con las células respiratorias de origen humano (líneas Calu-3 y A549), evidenciando además un carácter mucoadhesivo. Asimismo, la utilización de una técnica de microscopia, permitió confirmar que las microsferas alcanzan y se depositan en la región alveolar. Además, los estudios preliminares *in vivo* realizados, han puesto de manifiesto que las microsferas desarrolladas conteniendo insulina dan lugar a una respuesta hipoglucémica satisfactoria.

Bibliografía

BIBLIOGRAFÍA

Agnihotri, S.A., Mallikarjuna, N.N., Aminabhavi, T.M., **2004**. Recent advances in chitosan-based micro-and nanoparticles in drug delivery. *J. Control. Release.* 100, 5-28.

Ahsan, F., Rivas, I.P., Khan, M.A., Suárez-Torres, A.I., **2002**. Targeting to macrophages: role of physicochemical properties of particulate carriers – liposomes and microspheres – on the phagocytosis by macrophages. *J. Control. Release.* 79, 29-40.

Akhtar, S., Lewis, K.J., **1997**. Antisense oligonucleotide delivery to cultured macrophages is improved by incorporation into sustained-release biodegradable polymer microspheres. *Int. J. Pharm.* 151, 57-67.

Alcock, R., Blair, J.A., O'Mahony, D.J., Raoof, A., Quirk, A.V., **2002**. Modifying the release of leuprolide from spray dried OED microparticles. *J. Control. Release.* 82, 429-440.

Alonso, M.J., **1996**. Nanoparticulate drug carrier technology. In: Cohen, S., Bernstein, H. (Eds.), Microparticulate systems for the delivery of proteins and vaccines. Marcel Dekker, New York. pp. 203-242.

Alonso, M.J., **2004**. Nanomedicines for overcoming biological barriers. *Biomed. Pharmacother.* 58, 168-172.

Alonso, M.J., Sanchez, A., **2004**. Biodegradable nanoparticles as new transmucosal drug carriers. In: Svenson, S. (Ed.), Carrier-based drug delivery. American Chemical Society, New York, pp. 283-295.

Alonso-Sande, M., Cuña, M., Remuñán-López, C., Teijeiro-Osorio, D., Alonso-Lebrero, J.L., Alonso, M.J., **2006**. Formation of new glucomannan-chitosan nanoparticles and study of their ability to associate and deliver proteins. *Macromolecules.* 39, 4152-4158.

Alpar, H.O., Somavarapu, S., Atuah, K.N., Bramwell, V.W., **2005**. Biodegradable mucoadhesive particulates for nasal and pulmonary antigen and DNA delivery. *Adv. Drug Deliv. Rev.* 57, 411-430.

Alvarez-Román, R., Naik, A., Kalia, Y.N., Fessi, H., Guy, R.H., **2004**. Visualisation of skin penetration using confocal laser scanning microscopy. *Eur. J. Pharm. Biopharm.* 58, 301-316.

Amidi, M., Romeijn, S.G., Borchard, G., Junginger, H.E., Hennink, W.E., Jiskoot, W., **2006**. Preparation and characterisation of protein loaded N-trimethyl chitosan nanoparticles as nasal delivery system. *J. Control. Release.* 111, 107-116.

Antimisiaris, S.G., Jayasekera, P., Gregoriadis, G., **1993**. Liposomes as vaccine carriers. Incorporation of soluble and particulate antigens in giant vesicles. *J. Immunol. Methods.* 166, 271-280.

Arrault, J., Grand, C., Poon, W.C.K., Cates, M.E., **1997**. Stuffed onions: Particles in multilamellar vesicles. *Europhys. Lett.* 38, 625-630.

Artursson, P., Lindmark, T., Davisa, S.S., Illum, L., **1994**. Effect of chitosan on the permeability of monolayers of intestinal epithelial cells (Caco-2). *Pharm. Res.* 11, 1358-1361.

Bandi, N., Ayalasomayajula, S.P., Dhanda, D.S., Iwakawa, J., Cheng, P.-W., Kompella, U.B., **2005**. Intratracheal budesonide-poly(lactide-co-glycolide) microparticles reduce oxidative stress, VEGF expression, and vascular leakage in a benzo(a)pyrene-fed mouse model. *J. Pharm. Pharmacol.* 57, 851-860.

Beaulac, C., Sachetelli, S., Lagacé, J., **1999**. Aerosolization of low phase transition temperature liposomal tobramycin as dry powder in an animal model of chronic pulmonary infection caused by *Pseudomonas aeruginosa*. *J. Drug Target.* 7, 33-41.

Behrens, I., Vila-Pena, A.I., Alonso, M.J., Kissel, T., **2002**. Comparative uptake studies of bioadhesive and non-bioadhesive nanoparticles in human intestinal cell lines and rats: the effect of mucus on particle adsorption and transport. *Pharm. Res.* 19, 1185-1193.

Biesinger, M.C., Paepegaey, P.-Y., McIntyre, N.S., Harbottle, R.R., Petersen, N.O., **2002**. Principal component analysis of TOF-SIMS images of organic monolayers. *Anal. Chem.* 74, 5711-5716.

Belu, A.M., Graham, D.J., Castner, D.G., **2003**. Time-of-flight secondary ion mass spectrometry: techniques and applications for the characterization of biomaterial surfaces. *Biomaterials*. 24, 3635-3653.

Ben-Jebria, A., Chen, D., Eskew, M.L., Vanbever, R., Langer, R., Edwards, D.A., **1999**. Large porous particles for sustained protection from carbacol-induced bronchoconstriction in guinea pigs. *Pharm. Res.* 16, 555-561.

Berg, M.M., Kim, K.J., Lubman, R.L., Crandall, E.D., **1989**. Hydrophilic solute transport across rat alveolar epitehlium. *J. Appl. Physiol.* 66, 2320-2327.

Bivas-Benita, M., van Meijgaarden, K.E., Franken, K.L., Junginger, H.E., Borchard, G., Ottenhoff, T.H., Geluk, A., **2004**. Pulmonary delivery of chitosan-DNA nanoparticles enhances the immunogenicity of a DNA vaccine encoding HLA-A0201-restricted T-cell epitopes of *Mycobacterium tuberculosis*. *Vaccine.* 22, 1609-1615.

Bivas-Benita, M., Romrijn, S., Junginger, H.E., Borchard, G., **2004**. PLGA-PEI nanoparticles for gene delivery to pulmonary epithelium. *Eur. J. Pharm. Biopharm.* 28, 1-6.

Borchard, G., Luβen, H.L., De Boer, G.A., Verhoef, J.C., Lehr, C.M., Junginger, H.E., **1996**. The potential of mucoadhesive polymers in enhancing intestinal peptide drug absorption III: Effects of chitosan glutamate and carbomer on epithelial tight junctions in vitro. *J. Control. Release.* 39, 131-138.

Bosquillon, C., Lombry, C., Préat, V., Vanbever, R., **2001**. Influence of formulation excipients and physical characteristics of inhalation dry powders on their aerosolization performance. *J. Control. Release.* 70, 329-339.

Bosquillon, C., Lombry, C., Préat, V., Vanbever, R., **2001**. Comparison of particle sizing techniques in the case of inhalation dry powders. *J. Pharm. Sci.* 90, 2032-2041.

Bosquillon, C., Rouxhet, P.G., Ahimou, F., Simon, D., Culot, C., Préat, V., Vanbever, R., **2004**. Aerosolization properties, surface composition and physical state of spray-dried protein powders. *J. Control. Release.* 99, 357-367.

Bot, A.I., Tarara, T.E., Smith, D.J., Bot, S.R., Woods, C.M., Weers, J.G., **2000**. Novel lipid-based hollow-porous microparticles as a platform for immunoglobulin delivery to the respiratory tract. *Pharm. Res.* 17, 275-283.

Bot, A.I., Smith, D.J., Bot, S.R., Dellamary, L., Tarara, T.E., Harders, S., Phillips, W., Weers, J.G., Woods, C.M., **2001**. Receptor-mediated targeting of spray-dried lipid particles coformulated with immunoglobulin and loaded with a prototype vaccine. *Pharm. Res.* 18, 971-979.

Bourdos, N., Kollmer, F., Benninghoven, A., Ross, M., Sieber, M., Galla, H.-J., **2000**. Analysis of lung surfactant model systems with time-of-flight secondary ion mass spectrometry. *Biophys. J.* 79, 357-369.

Bourdos, N., Kollmer, F., Benninghoven, A., Sieber, M., Galla, H.-J., **2000**. Imaging of domain structures in a one-component lipid monolayer by time-of-flight secondary ion mass spectrometry. *Langmuir.* 16, 1481-1484.

Bozkir, A., Saka, O.M., **2004**. Chitosan nanoparticles for plasmid DNA delivery: effect of chitosan molecular structure on formulation and release characteristics. *Drug Deliv.* 11, 107-112.

Broadhead, J., Edmond-Rouan, S.K., Rhodes, C.T., **1992**. The spray drying of pharmaceuticals. *Drug. Develop. Ind. Pharm.* 18, 1169-1206.

Brzoska, M., Langer, K., Coester, C., Loitsch, S., Wagner, T.O.F., Mallinckrodt, C.V., **2004**. Incorporation of biodegradable nanoparticles into human airway epithelium cells - in vitro study of the suitability as a vehicle for drug or gene delivery in pulmonary diseases. *Biochem. Biophys. Res. Commun.* 318, 562-570.

Burger, K.N.J., Staffhorst, R.W.H.M., Vijlder, H.C., Velinova, M.J., Bomans, P.H., Frederik, P.M., Kruijff, B., **2002**. Nanocapsules: lipid-coated aggregates of cisplatin with high cytotoxicity. *Nat. Med.* 8, 81-84.

Burkitt, H.G., Young, B., Heath, J.W., **1993**. Histología funcional Wheater. Churchill Livingstone, Madrid.

Calvo, P., Remuñán-López, C., Vila-Jato, J.L., Alonso, M.J., **1997**. Novel hydrophilic Chitosan-Polyethylene Oxide nanoparticles as protein carriers. *J. Appl. Polym. Sci.* 63, 125-132.

Calvo, P., Remuñan-Lopez, C., Vila-Jato, J.L., Alonso, M.J., **1997**. Chitosan and Chitosan/Ethylene Oxide-Propylene Oxide block copolymer nanoparticles as novel carriers for proteins and vaccines. *Pharm. Res.* 14, 1431-1436.

Calvo, P., Vila-Jato, J.L., Alonso, M.J., **1997**. Effect of lysozyme on the stability of polyester nanocapsules and nanoparticles: stabilization approaches. *Biomaterials.* 18, 1305-1310.

Campbell, A., Taylor, P., Cayre, O.J., Paunov, V.N., **2004**. Preparation of aqueous gel beads coated by lipid bilayers. *Chem. Commun.* 21, 2378-2379.

Cannon, D.M., Pacholski, M.L., Winograd, N., Ewing, A.G., **2000**. Molecule specific imaging of freeze-fractured, frozen-hydrated model membrane systems using mass spectrometry. *J. Am. Chem. Soc.* 122, 603-610.

Carlesso, G., Kozlov, E., Prokop, A., Unutmaz, D., Davidson, J.M., **2005**. Nanoparticulate system for efficient gene transfer into refractory cell targets. *Biomacromolecules*. 6, 1185-1192.

Carvalho, E.L.S., Seijo, B., Alonso, M.J., Lipid-chitosan nanoparticle complexes (L/CS-Np) for oral insulin delivery: preparation, characterization and in vivo evaluation. *Int. J. Pharm.* (submitted)

Chidavaenzi, O.C., Buckton, G., Koosha, F., Pathak, R., **1997**. The use of thermal techniques to assess the impact of feed concentration on the amorphous content and polymorphic forms present in spray dried lactose. *Int. J. Pharm.* 159, 67-74.

Chidavaenzi, O.C., Buckton, G., Koosha, F., **2001**. The effect of co-spray drying with polyethyleneglycol 4000 on the cristallinity and physical form of lactose. *Int. J. Pharm.* 216, 43-49.

Chupin, V., de Kroon, A.I.P.M., de Kruijff, B., **2004**. Molecular architecture of nanocapsules, bilayer-enclosed solid particles of cisplatin. *J. Am. Chem. Soc.* 126, 13816-13821.

Clark, A., **2002**. Formulation of proteins and peptides for inhalation. *Drug Deliv. Syst. Sci.* 2, 73-77.

Clark, A.R., **2004**. Pulmonary delivery technology: recent advances and potential for the new millenium. In: Hickey, A.J. (Ed.), Pharmaceutical inhalation aerosol technology. Marcel Dekker, New York, pp. 571-591.

Cleland, J.L., Daugherty A., Mrsny, R., **2001**. Emerging protein delivery methods. *Curr. Opin. Biotech.* 12, 212-219.

Cliff, B., Lockyer, N.P., Corlett, C., Vickerman, J.C., **2003**. Development of instrumentation for routine TOF-SIMS imaging analysis of biological material. *Appl. Surf. Sci.* 203-204, 730-733.

Codrons, V., Vanderbist, F., Ucakar, B., Préat, V., Vanbever, R., **2004**. Impact of formulations and methods of pulmonary delivery on absorption of parathyroid hormone (1-34) from rat lungs. *J. Pharm. Sci.* 93, 1241-1252.

Codrons, V., Vanderbist, F., Verbeeck, R.K., Arras, M., Lison, D., Préat, V., Vanbever, R., **2003**. Systemic delivery of parathyroid hormone (1-34) using inhalation dry powders in rats. *J. Pharm. Sci.* 92, 938-950.

Cook, R.O., Pannu, R.K., Kellaway, I.W., **2005**. Novel sustained release microspheres for pulmonary drug delivery. *J. Control. Release.* 104, 79-90.

Cooney, D., Kazantseva, M., Hickey, A.J., **2004**. Development of a size-dependent aerosol deposition model utilising human airway epithelial cells for evaluating aerosol drug delivery. *ATLA, Altern. Lab. Anim.* 32, 581-590.

Correia, F.M., Petri, D.F.S., Carmona-Ribeiro, A.M., **2004**. Colloid stability of lipid/polyelectrolyte decorated latex. *Langmuir.* 20, 9535-9540.

Courrier, H.M., Butz, N., Vandamme, T.F., **2002**. Pulmonary drug delivery systems: recent developments and prospects. *Crit. Rev. Ther. Drug Carr. Syst.* 19, 425-498.

Cryan, S.-A., **2005**. Carrier-based strategies for targeting protein and peptide drugs to the lungs. *AAPS Journal.* 7, E20-E41.

Cuña, M., Alonso-Sande, M., Remuñan-Lopez, C., Pivel, J.P., Alonso-Lebrero, J.L., Alonso, M.J., **2006**. Development of phosphorylated glucomannan-coated chitosan nanoparticles as nanocarriers for protein delivery. *J. Nanosci. Nanotechnol.* 6, 2887-2895.

Dailey, L.A., Kleemann, E., Wittmar, M., Gessler, T., Schmehl, T., Roberts, C., Seeger, W., Kissel, T., **2003**. Surfactant-free, biodegradable nanoparticles for aerosol therapy based on the branched polyesters, DEAPA-PVAL-g-PLGA. *Pharm. Res.* 20, 2011-2020.

Dailey, L.A., Schmehl, T., Gessler, T., Wittmar, M., Grimminger, F., Seeger, W., Kissel, T., 2003. Nebulization of biodegradable nanoparticles: impact of nebulizer technology and nanoparticle characteristics on aerosol features. J. Control. Release. 86, 131-144.

Darwis, Y., Kellaway, I.W., **2002**. The lyophilization and aerosolisation of liposomes for pulmonary drug administration. *S.T.P. Pharm. Sci.* 12, 91-96.

Davies, M.C., Brown, A., Newton, J.M., Chapman, S.R., **1988**. SSIMS and SIMS imaging analysis of a drug delivery system. *Surf. Interface Anal.* 11, 591-595.

De Campos, A.M., Diebold, Y., Carvalho, E.L.S., Sánchez, A., Alonso, M.J., **2004**. Chitosan nanoparticles as new ocular drug delivery systems: in vitro stability, in vivo fate, and cellular toxicity. *Pharm. Res.* 21, 803-810.

De Campos, A., Sánchez, A., Alonso, M.J., **2001**. Chitosan nanoparticles : a new vehicle for the improvement of the delivery of drugs to the ocular surface. Application to cylosporin A. *Int. J. Pharm.* 224, 159-168.

Deleu, M., Paquot, M., Jacques, P., Thonart, P., Adriaensen, Y., Dufrêne, Y.F., **1999**. Nanometer scale organization of mixed surfactin/phosphatidylcholine monolayers. *Biophys. J.* 77, 2304-2310.

Dellamary, L., Smith, D.J., Bloom, A., Bot, S.R., Guo, G.R, Deshmuk, H., Costello, M., Bot, A.I., **2004**. Rational design of solid aerosols for immunoglobulin delivery by modulation of aerodynamic and release characteristics. *J. Control. Release.* 95, 489-500.

Dellamary, L., Tarara, T.E., Smith, D.J., Woelk, C.H., Adractas, A., Costello, M.L., Gill, H., Weers, J.G., **2000**. Hollow porous particles in metered dose inhalers. *Pharm. Res.* 17, 168-174.

Desai, M.P., Labhasetwar, V., Amidon, G.L., Levy, R.J., **1996**. Gastrointestinal uptake of biodegradable microparticles: effect of particle size. *Pharm. Res.* 13, 1838-1845.

Desai, T.R., Hancock, R.E.W., Finlay, W.H., **2003**. Delivery of liposomes in dry powder form: aerodynamic dispersion properties. *Eur. J. Pharm. Sci.* 20, 459-467.

Dickinson, P.A., Howells, S.W., Kellaway, I.W., **2001**. Novel nanoparticles for pulmonary drug administration. *J. Drug Target.* 9, 295-302.

Dittgen, M., Durrani, M., Lehmann, K., **1997**. Acrylic polymers. A review of pharmaceutical applications. *S. T. P. Pharm. Sci.* 7, 403-437.

Dong, Y., Feng, S., **2004**. Methoxy poly(ethylene glycol)-poly(lactide) (MPEG-PLA) nanoparticles for controlled delivery of anticancer drugs. *Biomaterials.* 25, 2843-2849.

Dornish, M., Hagen, A., Hansson, E., Peucheur, C., Vedier, F., Skaugrud, O., **1997**. Safety of Protasan™: Ultrapure chitosan salts for biomedical and pharmaceutical use. In: Domard, A., Roberts, G.A.F., Varum, K.M. (Eds.), Advances in chitin science. Jacques Andre publisher, Lyon, pp. 664-670.

Duarte, A.R.C., Costa, M.S., Simplício, A.L., Cardoso, M.M., Duarte, C.M., **2006**. Preparation of controlled release microspheres using supercritical fluid technology for delivery of anti-inflammatory drugs. *Int. J. Pharm.* 308, 168-174.

Dunbar, C., Scheuch, G., Sommerer, K., DeLong, M., Verma A., Batycky, R., **2002**. In vitro and in vivo dose delivery characteristics of large porous particles for inhalation. *Int. J. Pharm.* 245, 179-189.

Duszyk, M., **2001**. CFTR and lysozyme secretion in human airway epithelial cells. *Eur. J. Physiol.* 443, S45-S49.

Edwards, D. A., Ben-Jebria, A., Langer, R., **1998**. Recent advances in pulmonary drug delivery using large, porous inhaled particles. *J. Appl. Physiol.* 84, 379-385.

Edwards, D.A., Hanes, J., Caponetti, G., Hrkach, J., Ben-Jebria, A., Eskew, M.L., Mintzes, J., Deaver, D., Lotan N., Langer, R., **1997**. Large porous particles for pulmonary drug delivery. *Science.* 276, 1868-1871.

Eerikäinen, H., Kauppinen, E.I., **2003**. Preparation of polymeric nanoparticles containing corticosteroid by a novel aerosol flow reactor method. *Int. J. Pharm.* 263, 69-83.

Ehrhardt, C., Fiegel, J., Fuchs, S., Abu-Dahab, R., Schaefer, U.F., Hanes, J., Lehr, C.M., **2002**. Drug absorption by the respiratory mucosa: cell culture models and particulate drug carriers. *J. Aerosol Med.* 15, 131-139.

El-Baseir, M.M., Kellaway, I.W., **1998**. Poly(L-lactic acid) microspheres for pulmonary drug delivery: release kinetics and aerosolization studies. *Int. J. Pharm.* 175, 135-145.

El-Gibaly, I., **2002**. Development and in vitro evaluation of novel floating chitosan microcapsules for oral use: comparison with non-floating chitosan microspheres. *Int. J. Pharm.* 294, 7-21.

Elvira, C., Fanovich, A., Fernández, M., Fraile, J., San Román, J., Domingo, C., **2004**. Evaluation of drug delivery characteristics of microspheres of PMMA-PCL-cholesterol obtained by supercritical-CO_2 impregnation and by dissolution -evaporation techniques. *J. Control. Release.* 99, 231-240.

Evora, C., Soriano, I., Rogers, R.A., Shakesheff, K.M., Hanes, J. Langer, R., **1998**. Relating the phagocytosis of microparticles by alveolar macrophages to surface chemistry: the effect of 1,2-dipalmitoylphosphatidylcholine. *J. Control. Release.* 51, 143-152.

Fattal, E., Peracchia, M.T., Couvreur, P., **1997**. Poly (alkylcyanoacrylates). In: Domb, A.J., Kost, J., Wiseman, D.M. (Eds.), Handbook of biodegradable polymers. Harwood Academic Publishers, New York, pp. 183-201.

Fawcett, B., Fawcett, D.W., **1995**. Tratado de Histología. Interamericana McGraw-Hill, Madrid.

Feng, S., Huang, G., **2001**. Effects of emulsifiers on the controlled release of paclitaxel (Taxol®) from nanospheres of biodegradable polymers. *J. Control. Release.* 71, 53-69.

Fernández-Urrusuno, R., Calvo, P., Remuñán-López, C., Vila-Jato, J.L., Alonso, M.J., **1999**. Enhancement of nasal absorption of insulin using chitosan nanoparticles. *Pharm. Res.* 16, 1576-1581.

Fernández-Urrusuno, R., Romani, D., Calvo, P., Vila-Jato, J.L., Alonso, M.J., **1999**. Development of a freeze-dried formulation of insulin-loaded chitosan nanoparticles intended for nasal administration. *S.T.P. Pharm. Sci.* 9, 429-436.

Fery, A., Moya, S., Puech, P.-H., Brochard-Wyart, F., Mohwald, H., **2003**. Interaction of polyelectrolyte coated beads with phospholipid vesicles. *C. R. Phys.* 4, 259-264.

Fiegel, J., Ehrhardt, C., Schaefer, U.F., Lehr, C-M., Hanes, J., **2003**. Large porous particle impingement on lung epithelial cell monolayers – toward improved particle characterisation in the lung, *Pharm. Res.* 20, 788-796.

Finlay, W.H., Gehmlich, M.G., **2000**. Inertial sizing of aerosol inhaled from two dry powder inhalers with realistic breath patterns versus constant flow rates. *Int. J. Pharm.* 210, 83-95.

Finlay, W.H., Stapleton, K.W., Zuberbuhler, P., **1997**. Fine particle fraction as a measure of mass depositing in the lung during inhalation of nearly isotonic nebulized aerosols. *J. Aerosol Sci.* 28, 1301-1309.

Florea, B. I., Thanou, M., Junginger, H. E., Borchard, G., **2005**. Enhancement of bronchial octreotide absorption by chitosan and N-trimethylchitosan shows linear in vitro/in vivo correlation. *J. Control. Release.* 110, 353-361.

Folkesson, H.G., Matthey, M.A., Westrom, B.R., Kim, K.J., Karlsson, B.W., Hastings, R.H., **1996**. Alveolar epithelial clearance of protein. *J. Appl. Physiol.* 80, 1431-1445.

Forbes, B., Ehrhardt, C., **2005**. Human respiratory epithelial cell culture for drug delivery applications. *Eur. J. Pharm. Sci.* 60, 193-205.

Forbes, B., Martin, G.P., Lansley, A.B., **2000**. Formulation of inhaled medicines: effect of delivery vehicle on 16HBE14o- bronchial epithelial cells. *J. Aerosol Med.* 13, 281-288.

Forbes, B., Montoro-Garcia, A.M., Lansley, A.B., **1997**. [14C]-mannitol fluxes across human bronchial epithelial cells following apical exposure to EDTA, lactose, altered pH and anisotonicity. *Pharm. Res.* 14, S138.

Foster, K.A., Yazdanian, M., Audus, K.L., **2001**. Microparticulate uptake mechanisms of in vitro cell culture models of the respiratory epithelium. *J. Pharm. Pharmacol.* 53, 57-66.

Freitas, C., Müller, R.H., **1998**. Spray-drying of solid lipid nanoparticles (SLN™). *Eur. J. Pharm. Biopharm.* 46, 145-151.

Garcia-Contreras, L., Morçöl, T., Bell, S.J.D., Hickey, A.J., **2003**. Evaluation of novel particles as pulmonary delivery systems for insulin in rats. *AAPS Pharmsci.* 5, 1-11.

Gartner, L.P., Hiatt, J.L., **1997**. Histología: Texto y Atlas. Interamericana McGraw-Hill, Madrid.

Gehr, P., Green, F.H.Y., Geiser, M., Hof, V.I., Lee, M.M., Schurch, S., **1996**. Airway surfactant, a primary defence barrier: mechanical and immunological aspects. *J. Aerosol Med.* 9, 163-181.

Geneser, F. **2000**. Histología: Sobre bases biomoleculares. Editorial Medica Panamericana, Madrid.

Geys, J., Coenegrachts, L., Vercammen, J., Engelborghs, Y., Nemmar, A., Nemery, B., Hoet, P.H.M., **2006**. In vitro study of the pulmonary translocation of nanoparticles. A preliminary study. *Toxicol. Lett.* 160, 218-226.

Gerin, P.A., Dengis, P.B., Rouxhet, P.G., **1995**. Performance of XPS analysis of model biochemical compounds. *J. Chim. Phys.* 92, 1043-1065.

Gilani, K., Najafabadi, A.R., Barghi, M., Rafiee-Tehrani, M., **2004**. Aerosolisation of beclomethasone dipropionate using spray dried lactose/polyethylene glycol carriers. *Eur. J. Pharm. Biopharm.* 58, 595-606.

Gill, D.R., Davies, L.A., Pringle, I.A., Hyde, S.C., **2004**. The development of gene therapy for diseases of the lung. *Cell. Mol. Life Sci.* 61 355-368.

Goldbach, P., Brochart, H., Stamm, A., **1993**. Spray-drying of liposomes for a pulmonary administration. I. Chemical stability of phospholipids. *Drug Dev. Ind. Pharm.* 19, 2611-2622.

Grainger, C., Greenwell, L.L., Lockley, D.J., Martin, G.P., Forbes, B., **2006**. Culture of Calu-3 cells at the air-liquid interface provides a representative model of the airway epithelial barrier. *Pharm. Res.* 23, 1482-1490.

Grenha, A., Carrión-Recio, D., Seijo, B., Vila-Jato, J.L., Remuñán-López, C., **2005**. Microencapsulated chitosan nanoparticles for insulin lung delivery. *Proc. 32nd Ann. Meeting Control. Rel. Soc.* 59-59.

Grenha, A., Grainger, C.I., Dailey, L.A., Seijo, B., Martin, G.P., Remuñán-López, C., Forbes, B. Chitosan nanoparticle-containing microspheres are compatible with respiratory epithelial cells in vitro. *Biomaterials.* (submitted).

Grenha, A., Seijo, B., Remuñan-Lopez, C., **2005**. Microencapsulated chitosan nanoparticles for lung protein delivery. *Eur. J. Pharm. Sci.* 25, 427-437.

Grenha, A., Seijo, B., Serra, C., Remuñán-López, C. Chitosan nanoparticle-loaded microspheres: structure and surface characterisation. *Macromolecules*. (submitted).

Hagenhoff, B., **2000**. High resolution surface analysis by TOF-SIMS. *Mikrochimica Acta.* 132, 259-271.

Hanes, J., Dawson, M., Har-el, Y., Suh, J., Fiegel, J., **2004**. Gene delivery to the lung. In: Hickey, A.J. (Ed.), Pharmaceutical inhalation aerosol technology. Marcel Dekker, New York, pp. 489-539.

Heinemann, L., Klappoth, W., Rave, K., Hompesch, B., Linkeschowa, R., Heise, T., **2000**. Intra-individual variability of the metabolic effect of inhaled insulin together with an absorption enhancer. *Diabetes Care.* 23, 1343-1347.

Heyder, J., Gebhart, J., Rudolf, G., Schiller, C.F., Stahlhofen, W., **1986**. Deposition of particles in the human respiratory tract in the size range 0.005 – 15 μm. *J. Aerosol Sci.* 17, 811-825.

Hirano, S., Seino, H., Akiyama, Y., Nonaka, I., **1988**. Biocompatibility of chitosan by oral and intravenous administrations. *Polym. Mater. Sci. Eng.* 59, 897-901.

Huang, M., Khor, E., Lim, L.-Y. **2004**. Uptake and cytotoxicity of chitosan molecules and nanoparticles: effects of molecular weight and degree of deacetylation. *Pharm. Res.* 21, 344-353.

Huang, M., Zengshuan, M., Khor, E., Lim, L.-Y. **2002**. Uptake of FITC-chitosan nanoparticles by A549 cells. *Pharm. Res.* 19, 1488-1494.

Huang, Y.C., Vieira, A., Huang, K.L., Yeh, M.K., Chiang, C.H., **2005**. Pulmonary inflammation caused by chitosan microparticles. *J. Biomed. Mater. Res.* 75A, 283-287.

Huang, Y.C., Yeh, M.K., Cheng, S.-N., Chiang, C.H., **2003**. The characteristics of betamethasone-loaded chitosan microparticles by spray-drying method. *J. Microencap.* 20, 459-472.

Huang, Y.C., Yeh, M.K., Chiang, C.H., **2002**. Formulation factors in preparing BTM-chitosan microspheres by spray drying method. *Int. J. Pharm.* 242, 239-242.

Hussain, A., Arnold, J.J., Khan, M.A., Ahsan, F., **2004**. Absorption enhancers in pulmonary protein delivery. *J. Control. Release.* 94, 15-24.

Jacobs, E.R., DeCoursey, T.E., **1994**. Ion channels in lower respiratory tract cells. In: Effros, R.M., Chang, H.K. (Eds.), Fluid and solute transport in the airspaces of the lungs. Marcel Dekker, New York, pp. 151-177.

Jain, S., Sharma, R.K., Vyas, S.P., **2006**. Chitosan nanoparticles encapsulated vesicular systems for oral immunization: preparation, in-vitro and in-vivo characterization. *J. Pharm. Pharmacol.* 58, 303-310.

Janes, K.A., Calvo, P., Alonso, M.J., **2001**. Polysaccharide colloidal particles as delivery systems for macromolecules. *Adv. Drug Deliv. Rev.* 47, 83-97.

Jani, P., Halbert, G.W., Langridge, J., Florence, A.T., **1990**. Nanoparticle uptake by the art grastrointestinal mucosa: quantitation and particle size dependency. *J. Pharm. Pharmacol.* 42, 821-826.

John, C.M., Odom, R.W., Salvati, L., Annapragada, A.V., Lu, M.Y.F., **2005**. XPS and TOF-SIMS microanalysis of a peptide/polymer drug delivery device. *Anal. Chem.* 67, 3871-3878.

Jones, B.G., Dickinson, P.A., Gumbleton, M., Kellaway, I.W., **2002**. Lung surfactant phospholipids inhibit the uptake of respirable microspheres by the alveolar macrophage NR8383. *J. Pharm. Pharmacol.* 54, 1065-1072.

Kawashima, Y., Serigano, T., Hino, T., Yamamoto, H., Takeuchi, H., **1998**. A new powder design method to improve inhalation efficiency of pranlukast hydrate dry powder aerosols by surface modification with hydroxypropylmethylcellulose phthalate nanospheres. *Pharm. Res.* 15, 1748-1752.

Kawashima, Y., Yamamoto, H., Takeuchi, H., Fujioka, S., Hino, T., **1999**. Pulmonary delivery of insulin with nebulized DL-lactide/glycolide copolymer (PLGA) nanospheres to prolong hypoglycemic effect. *J. Control. Release.* 62, 279-287.

Kikuchi, H., Yamauchi, H., Hirota, S., **1991**. A spray-drying method for mass production of liposomes. *Chem. Pharm. Bull.* 39, 1522-1527.

Kirby, C.J., Gregoriadis, G., Liposomes, **1999**. Liposomes. In: Mathiowitz, E. (Ed.), Encyclopedia of Controlled Drug Delivery. John Wiley & Sons, New York, pp. 461-492.

Kobayashi, S., Kondo, S., Juni, K., **1994**. Study on pulmonary delivery of salmon calcitonin in rats: effects of protease inhibitors and absorption enhancers. *Pharm. Res.* 11, 1239-1243.

Konstan, M.W., Chen, P.W., Sherman, J.M., Thomassen, M.J., Woodm, R.E., Boat, T.F., **1981**. Human lung lysozyme: sources and properties. *Am. Rev. Resp. Dis.* 123, 120-124.

Köping-Hóggard, M., Csaba, N., Alonso, M.J. (submitted)

Koping-Hoggard, M., Varum, K.M., Issa, M., Danielsen, S., Christensen, B.E., Stokke, B.T., Artursson, P., **2004**. Improved chitosan-mediated gene delivery based on easily dissociated chitosan polyplexes of highly defined chitosan oligomers. *Gene Ther.* 11, 1441-1452.

Koping-Hoggard, M., Tubulekas, I., Guan, C.Y., Edwards, K., Nilsson, M., Varum, K.M., Artursson, P., **2001**. Chitosan as a nonviral gene delivery system. Structure□property relationships and characteristics compared with polyethylenimine in vitro and after lung administration in vivo. *Gene Ther.* 8, 1108-1121.

Koushik, K., Kompella, U.B., **2004**. Particle & device engineering for inhalation drug delivery. *Drug Deliv. Technol.* 4, 40-50.

Kreuter, J., **1991**. Liposomes and nanoparticles as vehicles for antibiotics. *Infection.* 19, S224-S228.

Kubota, Y., Takahashi, S., Matsuoka, O., **1983**. Dependence on particle size in the phagocytosis of latex particles by rabbit alveolar macrophages cultured in vitro. *J. Toxicol. Sci.* 8, 189-195.

Kumar, M., Behera, A.K., Lockey, R.F., Zhang, J., Bhullar, G., De la Cruz, C.P., Chen, L.C., Leong, K.W., **2002**. Intranasal gene transfer by chitosan-DNA nanospheres protects BALB/c mice against acute respiratory syncytial virus infection. *Hum. Gene Ther.* 13, 1415-1425.

Kumar, M., Kong, X., Behera, A.K., Hellermann, G.R., Lockey, R.F., Mohapatra, S.S. **2003**. Chitosan IFN-□-pDNA nanoparticle (CIN) therapy for allergic asthma. *Genet. Vaccines Ther.* 1, 3.

Kyle, H., Ward, J.P., Widdicombe, J.G., **1990**. Control of pH of airway surface liquid of the ferret trachea in vitro. *J. Appl. Physiol.* 68, 135-140.

Labiris, N.R., Dolovich, M.B., **2003**. Pulmonary drug delivery. Part I: Physiological factors affecting therapeutic effectiveness of aerosolized medications. *Br. J. Clin. Pharmacol.* 56, 588-599.

Lamprecht, A., Schäfer, U.F., Lehr, C.M., **2000**. Visualization and quantification of polymer distribution in microcapsules by confocal laser scanning microscopy (CLSM). *Int. J. Pharm.* 196, 223-226.

Lee, K.Y., Kwon, I.C., Jo, Y.H., Jeong, S.Y., **1998**. Preparation of chitosan self-aggregates as a gene delivery system. *J. Control. Release.* 51, 213-220.

Lehr, C.M., Bouwstra, J.A., Schacht, E.H., Junginger, H.E., **1992**. In vitro evaluation of mucoadhesive properties of chitosan and some other natural polymers. *Int. J. Pharm.* 78, 43-48.

Leong, K.W., Mao, H.Q., Truong-Le, V.L., Roy, K., Walsh, S.M., August, J.T., **1998**. DNA-polycation nanospheres as non-viral gene delivery vehicles. *J. Control. Release.* 53, 183-193.

Lim, S.T., Forbes, B., Martin, G.P., Brown, M.B., **2001**. In vivo and in vitro characterization of novel microparticulates based on hyaluronan and chitosan hydroglutamate. *AAPS PharmsciTech.* 2, 1-14.

Lin, W.-C., Tseng, C.-H., Yang, M.-C., **2005**. In-vitro hemocompatibility evaluation of a thermoplastic polyurethane membrane with surface-immobilized water-soluble chitosan and heparin. *Macromol. Biosci.* 5, 1013-1021.

Linstrom, P.J., Mallard, W.G., **2005**, NIST Chemistry Webbook, NIST Standard Reference Database, National Institute of Standards and Technology: Gaithersburg, MD, (http://webbook.nist.gov).

Liu, F., Shao, Z., Kildsig, D.O., Mitra, A.K., **1993**. Pulmonary delivery of free and liposomal insulin. *Pharm. Res.* 10, 228-232.

Lombry, C., Bosquillon, C., Préat, V., Vanbever, R., **2002**. Confocal imaging of rat lungs following intratracheal delivery of dry powders or solution of fluorescent probes. *J. Control. Release.* 83, 331-341.

Maa, Y.F., Nguyen, P.A., Sweeney, T., Shire, S.J., Hsu, C.C., **1999**. Protein inhalation powders: spray-drying vs spray freeze drying. *Pharm. Res.* 16, 249-254.

Maa, Y.F., Prestrelski, S.J., **2000**. Biopharmaceutical powders: particle formation and formulation considerations. *Current Pharm. Biotechnol.* 1, 283-302.

MacLaughlin, F.C., Mumper, R.J., Wang, J., Tagliaferri, J.M., Gill, I., Hinchcliffe, M., Rolland, A.P., **1998**. Chitosan and depolymerized chitosan oligomers as condensing carriers for in vivo plasmid delivery. *J. Control. Release.* 56, 259-272.

Makino, K., Yamamoto, N., Higuchi, K., Harada, N., Ohshima, H., Terada, H., **2003**. Phagocytic uptake of polystyrene microspheres by alveolar macrophages: effects of the size and surface properties of the microspheres. *Colloid. Surf. B-Biointerfaces.* 27, 33-39.

Makino, K., Yamada, T., Kimura, M., Oka, T., Oshima, H., Kondo, T., **1991**. Temperature and ionic strenght induced conformational changes in the lipid head group region of liposomes as suggested by zeta potential data. *Biophys. Chem.* 41, 175-183.

Marier, J.-F., Lavigne, J., Ducharme, M.P., **2002**. Pharmacokinetics and efficacies of liposomal and conventional formulations of tobramycin after intratracheal administration in rats with pulmonary Burkholderia cepacia infection. *Antimicrob. Agents Chemother.* 46, 3776-3781.

Matienzo, L.J., Winnacker, S.K., **2002**. Dry processes for surface modification of a biopolymer: chitosan. *Macromol. Mat. Eng.* 287, 871-880.

Matter, K., Balda, M.S., **2003**. Functional analysis of tight junctions. *Methods.* 30, 228-234.

McAllister, S.M., Alpar, H.O., Teitelbaum, Z., Bennett, D.B., **1996**. Do interactions with phospholipids contribute to the prolonged retention of polypeptides within the lung? *Adv. Drug Deliv. Rev.* 19, 89-110.

McCallion, O.N.M., Taylor, K.M.G., Thomas, M., Taylor, A.J., **1996**. Nebulization of monodisperse latex sphere suspensions in air-jet and ultrasonic nebulisers. *Int. J. Pharm.* 133, 203-214.

McDonald, K., Martin, G., **2000**. Transition to CFC-free metered dose inhalers - into the new millennium. *Int. J. Pharm.* 201, 89-107.

McMahon, J.M., Short, R.T., McCandlish, C.A., **1996**. Identification and mapping of phosphocholine in animal tissue by static secondary ion mass spectrometry and Tandem mass spectrometry. *Rapid Commun. Mass Spectrom.* 10, 335-340.

McPhail, D., Tetley, L., Dufes, C., Uchegbu, I.F., **2000**. Liposomes encapsulating polymeric chitosan based vesicles - a vesicle in vesicle system for drug delivery. *Int. J. Pharm.* 200, 73-86.

Mezei, M., **1988**. Liposomes in the topical application of drugs: a review. In: Gregoriadis, G. (Ed.), Liposomes as drug carriers: recent trends and progress. John Wiley & Sons, Chichester, pp. 663-677.

Mihalko, P.J., Schreier, H., Abra, R.M., **1988**. Liposomes: a pulmonary perspective. In: Gregoriadis, G. (Ed.), Liposomes as drug carriers: recent trends and progress. John Wiley & Sons, Chichester,pp. 679-694.

Mitra, R., Pezron, I., Li, Y., Mitra, A.K., **2001**. Enhanced pulmonary delivery of insulin by lung lavage fluid and phospholipids. *Int. J. Pharm.* 217, 25-31.

Mo, Y., Lim, L.-Y., **2004**. Mechanistic study of the uptake of wheat germ agglutinin-conjugated PLGA nanoparticles by A549 cells. *J. Pharm. Sci.* 93, 20-28.

Mo, Y., Lim, L.-Y. **2005**. Preparation and in vitro anticancer activity of wheat germ agglutinin (WGA).conjugated PLGA nanoparticles loaded with paclitaxel and isopropyl myristate. *J. Control. Release.* 107, 30-42.

Morimoto, K., Katsumata, H., Yabuta, T., Iwanaga, K., Kakemi, M., Tabata, Y., Ikada, Y., **2000**. Gelatin microspheres as a pulmonary delivery system:evaluation of salmon calcitonin absorption. *J. Pharm. Pharmacol.* 52, 611-617.

Moya, S., Donath, E., Sukhorukov, G.B., Auch, M., Bäumler, H., Lichtenfeld, H., Möhwald, H., **2000**. Lipid coating on polyelectrolyte surface modified colloidal particles and polyelectrolyte capsules. *Macromolecules.* 33, 4538-4544.

Müller, R.H., Mäder, K., Gohla, S., **2000**. Solid lipid nanoparticles (SLN) for controlled drug delivery - a review of the state of the art. *Eur. J. Pharm. Biopharm.* 50, 161-177.

Muzzarelli, R.A.A., **1985**. Chitin. In: Aspinall, G.O. (Ed.), The polysaccharides (Vol.3). Academic Press, Orlando, pp. 417-450.

Muzzarelli, R.A.A., **1997**. Human enzymatic activities related to the therapeutic administration of chitin derivatives. *Cell. Mol. Life Sci.* 53, 131-140.

Myers, M.A., Thomas, D.A., Stranb, L., **1993**. Pulmonary effects of chronic exposure to liposome aerosold in mice. *Exp. Lung Res.* 19, 1-19.

Nagai, T., Machida, Y., **1990**. Bioadhesive dosage forms for nasal administration. In: Lenaerts, V., Gurny, R. (Eds.), Bioadhesive drug delivery systems, CRC Press, Boca Raton, pp. 169-178.

Nygren, H., Börner, K., Hagenhoff, B., Malmberg, P., Månsson, J.-E., **2005**. Localization of cholesterol, phosphocholine and galactosylceramide in rat cerebellar cortex with imaging TOF-SIMS equipped with a bismuth cluster ion source. *Biochim. Biophys. Acta.* 1737, 102-110.

O'Hara, P., Hickey, A.J., **2000**. Respirable PLGA microspheres containing rifampicin for the treatment of tuberculosis: manufacture and characterization. *Pharm. Res.* 17, 955-961.

Okamoto, H., Aoki, M., Danjo, D., **2000**. A novel apparatus for rat in vivo evaluation of dry powder formulations for pulmonary administration. *J. Pharm. Sci.* 89, 1028-1035.

Okamoto, H., Nishida, S., Todo, H., Sakakura, Y., Iida, K., Danjo, K., **2003**. Pulmonary gene delivery by chitosan-pDNA complex powder prepared by a supercritical carbon dioxide process. *J. Pharm. Sci.* 92, 371-380.

Okamoto, H., Todo, H.,Iida K., Danjo, K., **2002**. Dry powders for pulmonary delivery of peptides and proteins. *Kona.* 20, 71-83.

Ostrowski, S.G., Szakal, C., Kozole, J., Roddy, T.P., Xu, J., Ewing, A.G., Winograd, N., **2005**. Secondary ion MS imaging of lipids in picoliter vials with a Buckminsterfullerene ion source. *Anal. Chem.* 77, 6190-6196.

Pandey, R., Sharma, A., Zahoor, A., Sharma, S., Khuller, G.K., Prasad, B., **2003**. Poly (DL-lactide-co-glycolide) nanoparticle-based inhalable sustained drug delivery system for experimental tuberculosis. *J. Antimicrob. Chemother.* 52, 981-986.

Pandit, S., Martin, C., Alpar, H.O., **2005**. Positively charged rifampicin-loaded microspheres for lung delivery. *J. Drug Deliv. Sci. Technol.* 15, 281-287.

Patton, J.S., **1996**. Mechanisms of macromolecule absorption by the lungs. *Adv. Drug. Deliv. Rev.* 19, 3-36.

Patton, J.S., Platz, R.M., **1992**. Pulmonary delivery of peptides and proteins for systemic action. *Adv. Drug Deliv. Rev.* 8, 179-196.

Peppas, N.A., **1997**. Hydrogels and drug delivery. *Colloid. Interface Sci.* 2, 531-537.

Perrin, D.E., English, J.P., **1997**. Polyglycolide and polylactide. In: Domb, A.J., Kost, J., Wiseman, D.M. (Eds.), Handbook of biodegradable polymers. Harwood Academic Publishers, New York, pp. 3-27.

Pfützner, A., Mann, A.E., Steiner, S.S., **2002**. Technosphere™/Insulin - a new approach for effective delivery of human insulin via the pulmonary route. *Diabetes Tech. Ther.* 4, 589-594.

Philip, V.A., Mehta, R.C., Mazumder, M.K., DeLuca, P.P., **1997**. Effect of surface treatment on the respirable fractions of PLGA microspheres formulated for dry powder inhalers. *Int. J. Pharm.* 151, 165-174.

Pohl, R., Kramer, P.A., Thrall, R.S., **1998**. Confocal laser scanning fluorescence microscopy of intact unfixed rat lungs. *Int. J. Pharm.* 168, 69-77.

Pohlmann, A.R., Weiss, V., Mertins, O., Silveira, N.P., Guterres, S.S., **2002**. Spray-dried indomethacin-loaded polyester nanocapsules and nanospheres: development, stability evaluation and nanostructure models. *Eur. J. Pharm. Sci.* 16, 305-312.

Polson, A., **1950**. Some aspects of diffusion in solution and a definition of a colloidal particle. *J. Phys. Colloid. Chem.* 54, 169-174.

Portero, A., Remuñán-López, C., Nielsen, H.M., **2002**. The potencial of chitosan in enhancing peptide and protein absorption across the TR146 cell culture model – an in vitro model of the bucal epithelium. *Pharm. Res.* 19, 169-174.

Prego, C., Garcia-Fuentes, M., Torres, D., Alonso, M.J., **2005**. Transmucosal molecular drug delivery. *J. Control. Release.* 101, 151-162.

Ranaldi, G., Marigliano, I., Vespignani, I., Perozzi, G., Sambuy, Y., **2002**. The effect of chitosan and other polycations on tight junction permeability in the human intestinal Caco-2 cell line. *J. Nutr. Biochem.* 13, 157-167.

Raula, J., Eerikäinen, H., Kauppinen, E.I., **2004**. Influence of the solvent composition on the aerosol synthesis of pharmaceutical polymer nanoparticles. *Int. J. Pharm.* 284, 13-21.

Rennard, S.I., Basset, G., Lecossier, D., O'Donnell, K.M., Pinkston, P., Martin, G.P., Crystal, R.G., **1986**. Estimation of of volume of epithelial lining fluid recovered by lavage using urea as marker of dilution. *J. Appl. Physiol.* 60, 532-538.

Rios, A., Gordillo, M.E., Bocanegra, C., Maldonado, J.A., **1994**. Administración nasal e inhalatoria. In: Ramos, B.S., Aznar, M.D. (Eds.), Administración de medicamentos: Teoria y práctica. Diaz de Santos, Madrid, pp. 131-149.

Roddy, T.P., Cannon, D.M., Ostrowski, S.G., Ewing, A.G., Winograd, N., **2003**. Proton transfer in time-of-flight secondaru ion mass spectrometry studies of frozen-hydrated dipalmitoylphosphatidylcholine. *Anal. Chem.* 75, 4087-4094.

Roos, Y.H., **2002**. Importance of glass transition and water activity to spray drying and stability of dairy powders. *Lait.* 82, 475-484.

Ross, M., Steinem, C., Galla, H.-J., Janshoff, A., **2001**. Visualization of chemical and physical properties of calcium-induced domains in DPPC/DPPS Langmuir-Blodgett layers. *Langmuir.* 17, 2437-2445.

Rudt, S., Müller, R.H., **1992**. In vitro phagocytosis of nano- and microparticles by chemiluminescence. I. Effect of analytical parameters, particle size and particle concentration. *J. Control. Release.* 22, 263-272.

Sakagami, M., Byron, P.R., **2005**. Respirable microspheres for inhalation. The potential of manipulating pulmonary disposition for improved therapeutic efficacy. *Clin. Pharmacok.* 44, 263-277.

Sakagami, M., Kinoshita, W., Sakon, K., Sato, J., Makino, Y., **2002**. Mucoadhesive beclomethasone microspheres for powder inhalation: their pharmacokinetics and pharmacodynamics evaluation. *J. Control. Release.* 80, 207-218.

Sakagami, M., Sakon, K., Kinoshita, W., Makino, Y., **2001**. Enhanced pulmonary absorption following aerosol adimistration of mucoadhesive powder microspheres. *J. Control. Release.* 77, 117-129.

Sanna, V., Kirschvink, N., Gustin, P., Gavini, E., Roland, I., Delattre, L., Evrard, B., **2003**. Preparation and in vivo toxicity study of solid lipid microparticles as carrier for pulmonary administration. *AAPS PharmsciTech.* 5, 1-7.

Schiavone, H., Palakodaty, S., Clark, A., York, P., Tzannis, S.T., **2004**. Evaluation of SCF-engineered particle-based lactose blends in passive dry powders inhalers. *Int. J. Pharm.* 281, 55-66.

Schnabelrauch, M., Vogt, S., Larcher, Y., Wilke, I., **2002**. Biodegradable polymer networks based on oligolactide macromers: synthesis, properties and biomedical applications. *Biomol. Eng.* 19, 295-298.

Schneeberger, E.E., Lynch, R.D. **1994**. Ultrastructure of the distal pulmonary epithelium. In: Effros, R.M., Chang, H.K. (Eds.), Fluid and solute transport in the airspaces of the lungs. Marcel Dekker, New York, pp. 1-25.

Schulz, H., **1998**. Mechanisms and factors affecting intrapulmonary particle deposition: implications for efficient inhalation therapies. *Pharm. Sci. Technol. Today.* 1, 336-344.

Schurch, S., Gehr, P., Im Hof, V., Geiser, M., Green, F., **1990**. Surfactant displaces particles toward the epithelium in airways and alveoli. *Resp. Physiol.* 80, 17-32.

Schwarz, C., Mehnert, W., Lucks, J.S., Müller, R.H., **1994**. Solid lipid nanoparticles (SLN) for controlled drug delivery I. Production, characterization and sterilization. *J. Control. Release.* 30, 83-96.

Seagrave, J., Nikula, K.J., **2000**. Multiple modes of responses to air pollution particulate materials in A549 alveolar type II cells. *Inhal. Toxicol.* 12, 247-260.

Seijo, B., Fattal, E., Roblot-Treupel, L., Couvreur, P., **1990**. Design of nanoparticles of less than 50 nm diameter: preparation, characterization and drug loading. *Int. J. Pharm.* 62, 1-7.

Sham, J.O., Zhang, Y., Finlay, W.H., Roa, W.H., Löbenberg, R., **2004**. Formulation and characterization of spray-dried powders containing nanoparticles for aerosol delivery to the lung. *Int. J. Pharm.* 269, 457-467.

Sharma, A., Sharma, U.S., **1997**. Liposomes in drug delivery: progress and limitations. *Int. J. Pharm.* 154, 123-140.

Sharma, R., Saxena, D., Dwivedi, A.K., Misra, A., **2001**. Inhalable microparticles containing drug combinations to target alveolar macrophages for treatment of pulmonary tuberculosis. *Pharm. Res.* 18, 1405-1410.

Shen, Z., Zhang, Q., Wei, S., Nagai, T., **1999**. Proteolytic enzymes as a limitation for pulmonary absorption of insulin: in vitro and in vivo investigations. *Int. J. Pharm.* 192, 115-121.

Skiba, M., Bounoure, F., Barbot, C., Arnaud, P., Skiba, M., **2005**. Development of cyclodextrin microspheres for pulmonary drug delivery. *J. Pharm. Pharm. Sci.* 8, 409-418.

Smith, I.J., **2002**. Developments in inhalation technology. *Drug Deliv. Syst. Sci.* 2, 63-65.

Smith, I.J., Parry-Billings, M., **2003**. The inhalers of the future? A review of dry powder devices on the market today. *Pulmon. Pharmacol. Ther.* 16, 79-95.

Smith, J., Wood, E., Dornish, M., **2004**. Effect of chitosan on epithelial cell tight junctions. *Pharm. Res.* 21, 43-49.

Smith, P. L., **1997**. Peptide delivery via the pulmonary route: a valid approach for local and systemic delivery. *J. Control. Release.* 46, 99-106.

Sostarecz, A.G., Cannon, D.M., McQuaw, C.M., Sun, S., Ewing, A.G., Winograd, N., **2004**. Influence of molecular environment on the analysis of phospholipids by time-of-flight secondary ion mass spectrometry. *Langmuir.* 20, 4926-4932.

Stearns, R.C., Paulauskis, J.D., Godaleski, J.J., **2001**. Endocytosis of ultrafines by A549 cells. *Am. J. Respir. Cell Mol. Biol.* 24, 108-115.

Steckel, H., Brandes, H.G., **2004**. A novel spray-drying technique to produce low density particles for pulmonary delivery. *Int. J. Pharm.* 278, 187-195.

Steiner, S., Pfützner, A., Wilson, B.R., Harzer, O., Heinemann, L., Rave, K., **2002**. Technosphere™/Insulin - proof of concept study with a new insulin formulation for pulmonary delivery. *Exp. Clin. Endocrinol. Diabetes.* 110, 10-16.

Stone, V., Shaw, J., Brown, D.M., MacNee, W., Faux, S.P., Donaldson, K., **1998**. The role of oxidative stress in the prolonged inhibitory effect of ultrafine carbon black on epithelial cell function. *Toxicol. In Vitro.* 12, 649-659.

Suarez, S., O'Hara, P., Kazantseva, M., Newcomer, C.E., Hopfer, R., McMurray, D.N., Hickey, A.J., **2001**. Airways delivery of rifampicin microparticles for the treatment of tuberculosis. *J. Antimicrob. Chemother.* 48, 431-434.

Suarez, S., O'Hara, P., Kazantseva, M., Newcomer, C.E., Hopfer, R., McMurray, D.N., Hickey, A.J., **2001**. Respirable PLGA microspheres containing rifampicin for the treatment of tuberculosis: screening in an infectious disease model. *Pharm. Res.* 18, 1315-1319.

Surendrakumar, K., Martin, G.P., Hodgers, E.C.M., Jansen, M., Blair, J.A., **2003**. Sustained release of insulin from sodium hyaluronate based dry powder formulations after pulmonary delivery to beagle dogs. *J. Control. Release.* 91, 385-394.

Suzuki,M., Machida, M., Adachi, K., Otabe, K., Sugimoto, T., Hayashi, M., Awazu, S., **2000**. Histopathological study of the effects of a single intratracheal instillation of surface active agents on lung in rats. *J. Toxicol. Sci.* 25, 49-55.

Tabata, Y., Ikada, I., **1998**. Effect of the size and surface charge of polymer microspheres on their phagocytosis by macrophage. *Biomaterials.* 9, 356-362.

Takeuchi, H., Yamamoto H., Kawashima, Y., **2001**. Mucoadhesive nanoparticulate systems for peptide drug delivery. *Adv. Drug Deliv. Rev.* 47, 39-54.

Taylor, G., Kellaway, I., **2001**. Pulmonary drug delivery. In: Hillery, A., Lloyd, A., Swarbrick, J. (Eds.), Drug delivery and targeting. For pharmacists and pharmaceutical scientists. Taylor & Francis, New York, pp. 269-300.

Taylor, K.M.G., Craig, D.Q.M., **2003**. Physical methods of study: differential scanning calorimetry. In: Torchilin, V.P., Weissig, V. (Eds.), Liposomes. Oxford University Press, Oxford, pp. 70-103.

Tee, S.K., Forbes, B., Larhrib, H., Marriott, C., Martin, G.P., **2001**. Development of an in vitro dissolution-absorption model to evaluate the delivery of aerosolised drug from dry powder inhaler formulations, *Drug Deliv. Lung.* 12, 115-118.

Teijeiro-Osório, D., Remuñán-López, C., Nielsen, H.M., **2005**. Comparative studies of chitosan nanoparticles and molecules in Calu-3 and TR146 cells. *Proc. 32 Ann. Meet. Exp. Control. Release Soc.* Miami, FL , #378.

Todo, H., Okamoto, H., Iida, K., Danjo, K., **2001**. Effect of additives on insulin absorption from intratracheally administered dry powders in rats. *Int. J. Pharm.* 220, 101-110.

Todo, H., Okamoto, H., Iida, K., Danjo, K., **2004**. Improvement of stability and absorbability of dry insulin powder for inhalation by powder-combination technique. *Int. J. Pharm.* 271, 41-52.

Tomoda, K., Kojima, S., Kajimoto, M., Watanabe, D., Nakajima, T., Makino, K., **2005**. Effects of pulmonary surfactant system on rifampicin release from rifampicin-loaded PLGA microspheres. *Coll. Surf. B - Biointerfaces.* 45, 1-6.

Troutier, A.-L., Delair, T., Pichot, C., Ladavière, C., **2005**. Physicochemical and interfacial investigation of lipid/polymer particle assemblies. *Langmuir.* 21, 1305-1313.

Troutier, A.-L., Véron, L., Delair, T., Pichot, C., Ladavière, C., **2005**. New insights into self-organization of a model lipid mixture and quantification of its adsorption on spherical polymer particles. *Langmuir.* 21, 9901-9910.

Tsapis, N., Bennett, D., Jackson, B., Weitz, D.A., Edwards, D.A., **2002**. Trojan particles: large porous carriers of nanoparticles for drug delivery. *Proc. Nat. Acad. Sci.* 99, 12001-12005.

Turner, N.H., Schreifels, J.A., **1998**. Surface analysis: X-ray photoelectron spectroscopy and auger electron spectroscopy. *Anal. Chem.* 70, 229R-250R.

Vanbever, R., Ben-Jebria, A., Mintzes, J., Langer, R., Edwards, D. A., **1999**. Sustained release of insulin from insoluble inhaled particles. *Drug Develop. Res.* 48, 178-185.

Vanbever, R., Mintzes, J., Wang, J., Nice, J., Chen, D., Batycky, R., Langer, R., Edwards, D.A., **1999**. Formulation and physical characterization of large porous particles for inhalation. *Pharm. Res.* 16, 1735-1742.

Velinova, M.J., Staffhorst, R.W.H.M., Mulder, W.J.M., Dries, A.S., Jansen, B.A.J., Kruijff, B., Kroon, A.I.P.M., **2004**. Preparation and stability of lipid-coated nanocapsules of cisplatin: anionic phospholipid specificity. *Biochim. Biophys. Acta.* 1663, 135-142.

Videira, M.A., Botelho, M.F., Santos, A.C., Gouveia, L.F., Lima, J.J.P., Almeida, A.J., **2002**. Lymphatic uptake of pulmonary delivered radiolabelled solid lipid nanoparticles. *J. Drug Target.* 10, 607-613.

Vila, A., Sanchez, A., Perez, C., Alonso, M.J., **2002**. PLA-PEG nanospheres: new carriers for transmucosal delivery of proteins and plasmid DNA. *Polym. Adv. Technol.* 13, 851-858.

Vila, A., Sánchez, A., Tobío, M., Calvo, P., Alonso, M. J., **2002**. Design of biodegradable particles for protein delivery. *J. Control. Release.* 78, 15-24.

Vyas, S.P., Singh, A., Sihorkar, V., **2001**. Ligand-receptor-mediated drug delivery: an emerging paradigm in cellular drug targeting. *Crit. Rev. Ther. Drug Carr. Syst.* 18, 1-76.

Walters, D.V., **2002**. Lung lining liquid – The hidden depths. Biol. Neonate. 81, S2-S5.

Weiner, A.L., **1989**. Liposomes as carriers for polypeptides. *Adv. Drug Deliv. Rev.* 3, 307-341.

Westmoreland, C., Walker, T., Matthews, J., Murdock, J., **1999**. Preliminary investigations into the use of a human bronchial cell line (16HBE14o-) to screen for respiratory toxins in vitro. *Toxicol. In Vitro.* 13, 761-764.

White, N.S., Errington, R.J., **2004**. Fluorescence techniques for drug delivery research: theory and practice. *Adv. Drug Deliv. Rev.* 57, 17-42.

Williams, R.O., Barron, M.K., Alonso, M.J., Remuñán-López, C., **1998**. Investigation of a pMDI system containing chitosan microspheres and P134a. *Int. J. Pharm.* 174, 209-222.

Winton, H.L., Wan, H., Cannell, M.B., Gruenert, D.C., Thompson, P.J., Garrod, D.R., Stewart, G.A., Robinson, C., **1998**. Cell lines of pulmonary and non-pulmonary origin as tools to study the effects of house dust mite proteinases on the regulation of epithelial permeability. *Clin. Exp. Allergy.* 28, 1273-1285.

Witschi, C., Mrsny, R., **1999**. In vitro evaluation of microparticles and polymer gels for use as nasal platforms for protein delivery. *Pharm. Res.* 16, 382-390.

Wolkers, W.F., Oldenhof, H., Tablin, F., Crowe, J.H., **2004**. Preservation of dried liposomes in the presence of sugar and phosphate. *Biochim. Biophys. Acta.* 1661, 125-134.

Wright, J.R., Clements, J.A., **1987**. Metabolism and turnover of lung surfactant. *Am. Rev. Respir. Disease.* 135, 426-444.

Yamada, K., Odomi, M., Okada, N., Fujita, T., Yamamoto, A., **2005**. Chitosan oligomers as potential and safe absorption enhancers for improving the pulmonary absorption of Interferon-α in rats. *J. Pharm. Sci.* 94, 2432-2440.

Yamamoto, H., Kuno, Y., Sugimoto, S., Takeuchi, H., Kawashima, Y., **2005**. Surface-modified PLGA nanosphere with chitosan improved pulmonary delivery of calcitonin by mucoadhesion and opening of the intercellular tight junctions. *J. Control. Release.* 102, 373-381.

Yamamoto, A., Okumura, S., Fukuda, Y., Fukui, M., Takahashi, K., Muranishi, S., **1997**. Improvement of the pulmonary absorption of (Asul,7)-eel calcitonin by various absorption enhancers and their pulmonary toxicity in rats. *J. Pharm. Sci.* 86, 1144-1147.

Yang, X., Joseph, K.A., Malanga, C.J., Rojanasakul, Y., **2000**. Characterization of proteolytic activities of pulmonary alveolar epithelium. *Int. J. Pharm.* 195, 93-101.

Yoo, H.S., Lee, J.E., Chung, H., Kwon, I.C., Jeong, S.Y., **2005**. Self-assembled nanoparticles containing hydrophobically modified glycol chitosan for gene delivery. *J. Control. Release.* 103, 235-243.

Zhang, Q., Shen, Z., Nagai, T., **2001**. Prolonged hypoglycemic effect of insulin-loaded polybutylcyanoacrylate nanoparticles after pulmonary administration to normal rats. *Int. J. Pharm.* 218, 75-80.

Zhang, W., Yang, H., Kong, X., Mohapatra, S., San Juan-Vergara, H., Hellermann, G., Behera, S., Singam, R., Lockey, R.F., Mohapatra, S.S., **2005**. Inhibition of respiratory syncytial virus infection with intranasal siRNA nanoparticles targeting the viral NS1 gene. *Nat. Med.* 11, 56-62.

Zhou, H., Zhang, Y., Biggs, D.L., Manning, M.C., Randolph, T.W., Christians, U., Hybertson, B.M., Ng, K., **2005**. Microparticle-based lung delivery of INH decreases INH metabolism and targets alveolar macrophages. *J. Control. Release.* 107, 288-299.

Zhu, A.P., Fang, N., Chan-Park, M.B., Chan, V., **2006**. Adhesion contact dynamics of 3T3 fibroblasts on poly (lactide-co-glycolide acid) surface modified by photochemical immobilization of biomacromolecules. *Biomaterials.* 27, 2566-2576.